

University of Alberta

ATP and central respiratory control: a three-part signaling system

by

Jennifer Dawn Zwicker

A thesis submitted to the Faculty of Graduate Studies and Research
in partial fulfillment of the requirements for the degree of

Doctor of Philosophy

Department of Physiology

©Jennifer Dawn Zwicker

Fall 2012

Edmonton, Alberta

Permission is hereby granted to the University of Alberta Libraries to reproduce single copies of this thesis and to lend or sell such copies for private, scholarly or scientific research purposes only. Where the thesis is converted to, or otherwise made available in digital form, the University of Alberta will advise potential users of the thesis of these terms.

The author reserves all other publication and other rights in association with the copyright in the thesis and, except as herein before provided, neither the thesis nor any substantial portion thereof may be printed or otherwise reproduced in any material form whatsoever without the author's prior written permission.

Abstract

ATP actions on central inspiratory networks are determined by a three-part signaling system comprising: i) excitatory actions of ATP at P2 receptors (Rs) ii) ectonucleotidases that degrade ATP into adenosine (ADO), and iii) inhibitory actions of ADO at P1Rs. During hypoxia, an initial increase in ventilation is followed by a secondary depression that is life threatening in premature infants. The release of ATP in respiratory networks, including the preBötzinger Complex (preBötC, inspiratory rhythm generation site) attenuates this secondary ventilatory depression. However, subsequent degradation of ATP to ADO may exacerbate the depression. The objective of my thesis research is to explore the significance of this three-part signaling system for preBötC networks in rodents using rhythmically active medullary slices from rats and mice, primary cultures of preBötC glia, and anesthetized adult rats. In neonatal rats *in vitro*, injection of ATP into the preBötC evokes an increase in inspiratory breathing frequency via a P2Y₁R mechanism that involves both neurons and glia. Analysis of cultured preBötC glia suggests that P2Y₁R stimulation evokes an increase in Ca²⁺ and release of glutamate, which excites inspiratory neurons. In contrast, injection of ATP into the preBötC of rhythmic slices from neonatal mice evokes a P2Y₁R-mediated frequency increase if A1 ADORs are blocked. In contrast to rats, neonatal mice are sensitive to ADO inhibition of preBötC frequency and have higher expression of the ectonucleotidase TNAP (an enzyme that degrades ATP to ADO). A delicate balance between P2R actions and P1R actions modulates the preBötC network of neonatal rodents. Purinergic signaling also influences the activity of mature preBötC networks in adult rats. Injection of a P2Y₁R agonist into the preBötC evoked a 40% increase in respiratory frequency while ADO injection had no effect. As predicted based on the proposed role of ATP in attenuating the

secondary hypoxic ventilatory depression, the increase of endogenous ectonucleotidase activity in the preBötC (via injection of a lentivirus controlling expression of the enzyme TMPAP) produced a greater secondary hypoxic ventilatory depression compared to control. This work lays the foundation for future research examining the importance of glia and purinergic modulation within the rhythmogenic inspiratory network.

Acknowledgements

This thesis would not have been possible without the tremendous support of the many amazing people in my life. I would like to express my gratitude to my supervisor, Dr. Greg Funk. His attention to detail, constructive criticism and commitment to teaching his students has challenged me to become a better scientist. I am fortunate to have had many amazing opportunities and experiences throughout grad school and this is largely attributed to the guidance and support Greg has provided along the way, it has been a privilege to have him as an advisor. Deepest gratitude is also due to the members of my supervisory committee, Dr. Klaus Ballanyi, Dr. Po-Yin Cheung and Dr. Elena Posse de Chaves for their guidance throughout my studies. I am grateful to members of my examining committee: I appreciate Dr. John Greer's perspective, advice and support throughout grad school and thank Dr. Chris Wilson for being a part of the thesis defense process. I would also like to thank Dr. Alex Gourine and his lab at the University College London (specifically Dr. Nephtali Marina) for their teaching and technical advice. I appreciated their hospitality and great sense of humor and after much debate I feel we have concluded the future is bright.

A big thank you is also due to my colleagues in the Funk, Greer and Gosgnach labs, both past and present, for the technical support and training along the way (Jason, Adrienne, Silvia, Sheena, Tuca, Matt, Amanda, Vishaal, Ann, Yong). There is always laughter and enthusiasm in the lab thanks to these people. A specific thanks is due to Dr. Adrienne Huxtable who has an amazing commitment to teaching in the lab; I owe many of my 'good' lab habits to the lessons instilled by Adrienne early on and appreciate the great friendship, encouragement, and support she always provides. Tremendous gratitude also goes to Dr. Silvia Pagliardini who patiently taught me the *in vivo* procedure and whose positive attitude, work ethic and enthusiasm in the lab are infectious. Thanks to Dr. Jason Dyck for getting me through the highs and lows of grad school, be it athletic adventures, conference adventures or lab life, his friendship has been invaluable along the way.

Finally, I would like to express my love and gratitude to my family and friends for their understanding and endless love and support through this and all aspects of my life; they have shaped who I am and I could not have done this without them. Thanks to my family, Donna, Terry and John Zwicker, who provide an unwavering source of support, love, understanding and encouragement. I have many amazing friends in my life and to acknowledge everyone who has made an impact on me, both personally and professionally would require a very long list. Thanks to Sarah, Carolyn, Adam, Sandra, Jill, Lauren, Joanna, Vanessa, Erin, Shayla, Lindsay, Jason, Adrienne, Chris, Brendan, Ashlyn and many more great friends, I am so lucky to have you all in my life.

Table of Contents

Abstract.....	ii
Acknowledgements.....	iv
Table of Contents	v
List of Figures.....	xi
List Abbreviations	xiv
Chapter 1: Introduction.....	1
1.1 Introduction	2
1.2 Central respiratory network and rhythm generation.....	2
1.2.1 PreBötC	6
1.2.2 RTN/pFRG.....	10
1.3 Central respiratory rhythm generation	12
1.3.1 Three-phase network hypothesis and hybrid pacemaker hypothesis.....	13
1.3.2 Emergent network group pacemaker hypothesis.....	14
1.3.3 Dual oscillators	15
1.3.4 Hierarchy of rhythm generation	17
1.4 Purinergic signaling and respiratory control	17
1.4.1 P2 Receptors	18
1.4.2 Ectonucleotidases.....	19
1.4.3 P1 Receptors	20
1.5 Glia and the central respiratory network.....	22
1.5.1 Astrocyte function	23
1.5.2 Astrocytes and neural networks	26

1.6 Chemoreception.....	27
1.6.1 Peripheral chemoreception.....	28
1.6.2 Central chemoreception	29
1.6.3 Hypoxic ventilatory response	31
1.7 Thesis objectives.....	36
1.8 References.....	38

Chapter 2: Glia contribute to the purinergic modulation of inspiratory rhythm generating networks **64**

2.1 Introduction	65
2.2 Methods.....	66
2.2.1 Electrophysiology	66
2.2.1.1 Drugs and their application	67
2.2.1.2 Whole-cell recording.....	68
2.2.2 Ca ²⁺ imaging of preBötC cells in rhythmic medullary slices	69
2.2.3 Primary cultures of glia from the ventral medulla at the level of the preBötC.....	70
2.2.3.1 Culture preparation.....	70
2.2.3.2 Ca ²⁺ imaging of glial cultures.....	71
2.2.3.3 High Performance Liquid Chromatography (HPLC)	72
2.2.3.4 Immunohistochemistry	72
2.2.4 Data and statistical analysis	73
2.3 Results	74
2.3.1 Contribution of glia to the ATP-evoked increase in inspiratory frequency	74
2.3.2 Involvement of VRACs in the ATP-evoked frequency increase	78
2.3.3 ATP sensitivity of preBötC glia	78
2.3.4 Release of glutamate from primary glia cultures.....	93

2.4 Discussion	95
2.5 References.....	100
Chapter 3: Purinergic modulation of preBötzinger Complex inspiratory rhythm in rodents: the interaction between ATP and adenosine.....	107
 3.1 Introduction	108
 3.2 Methods.....	110
3.2.1 Rhythmic medullary slices.....	110
3.2.2 Electrophysiological recordings.....	111
3.2.3 Drugs and their application.....	111
3.2.4 Mapping studies	114
3.2.5 Real Time-PCR	115
3.2.6 Data analysis.....	116
 3.3 Results	117
3.3.1 Effects of ATP on preBötC rhythm differ between mouse and rat.....	117
3.3.2 PreBötC of mouse is directly sensitive to modulation by P2Y ₁ R	118
3.3.3 The site of maximum P2Y ₁ R sensitivity corresponds to the site of maximum SP sensitivity	121
3.3.4 P2 and P1R interactions mediate the effects of ATP in mouse preBötC.....	123
3.3.5 ADO differentially affects preBötC rhythm in mouse and rat	128
3.3.6 Ectonucleotidase isoform expression in the preBötC differs between mouse and rat	
128	
 3.4 Discussion	132
3.4.1 Differential sensitivity of rat and mouse preBötC networks to ATP	132
3.4.2 P2Y ₁ receptor sensitivity.....	133

3.4.3 Differential sensitivity of mouse and rat preBötC to ATP reflects differential sensitivity to the ATP metabolite ADO	135
3.4.4 Differential ectonucleotidase expression.....	139
3.4.5 Physiological significance	143
3.5 References.....	144

Chapter 4: Exogenous and endogenous purinergic modulation of central respiratory networks *in vivo* **155**

4.1 Introduction	156
4.2 Methods.....	158
4.2.1 Virus injection	158
4.2.2 <i>In vivo</i> gene transfer.....	159
4.2.3 Whole body plethysmography.....	159
4.2.4 MRS 2365/ADO injection experiments.....	161
4.2.5 Histology.....	162
4.2.6 Drugs	162
4.2.7 Data analysis and statistics.....	163
4.3 Results	164
4.3.1 The hypoxic ventilatory response in control rats and those with TMPAP injections into the preBötC.....	164
4.3.2 The hypercapnic ventilatory response in control rats and those with TMPAP injections into the preBötC	170
4.3.3 PreBötC of adult rat is directly sensitive to modulation by P2Y ₁ R	172
4.3.4 PreBötC of adult rat is not sensitive to modulation by ADO	177
4.3.5 ATP and ADO microinjection: histology	182
4.3.6 Viral injection: histology.....	182

4.4 Discussion	185
4.4.1 The role of ATP in the hypoxic ventilatory response.....	185
4.4.2 Validation of TMPAP as a model to study purinergic signaling.....	187
4.4.3 Effects of TMPAP on the hypoxic ventilatory response reflect loss of ATP excitation	
190	
4.4.4 Significance of carotid-body denervation	192

4.5 References.....	194
----------------------------	------------

Chapter 5: Microglia TLR4 signaling does not contribute to the opioid-induced depression of respiration **203**

5.1 Introduction	204
5.2 Methods.....	206
5.2.1 Rhythmic medullary slices.....	206
5.2.2 Electrophysiological recordings.....	207
5.2.3 Drugs and their application.....	208
5.2.4 Plethysmographic recording	210
5.2.5 Data analysis and statistics.....	211
5.3 Results	211
5.3.1 TLR antagonism does not affect the DAMGO-mediated respiratory inhibition <i>in vitro</i>	211
5.3.2 Effects of LPS on preBötC rhythm	213
5.3.3 Microglia and opioid-induced respiratory depression.....	216
5.3.4 (+) Naloxone, has no effect on the opioid-evoked depression of frequency <i>in vivo</i>	
217	
5.4 Discussion	222

5.4.1	Neither TLR4 signaling nor microglia contribute to opioid respiratory depression	
	222	
5.4.2	Acute TLR4 activation in the preBötC does not modulate rhythm	229
5.5	References.....	231
Chapter 6: General Discussion		245
6.1	Introduction	246
6.2	Purinergic modulation of the central respiratory network by glia.....	247
6.3	Purinergic modulation maintains homeostasis in the hypoxic ventilatory response	256
6.4	Conclusions	263
6.5	References.....	264

List of Figures

Figure 1.1 Respiratory-related regions of the brainstem of the rat shown in horizontal (A) and sagittal (B) views.	8
Figure 2.1 The influence of the glial toxin MSO (0.1mM) on frequency increases evoked by ATP and SP in rhythmic medullary slice preparations.	76
Figure 2.2 The influence of the glial toxin FA (5mM) on the ATP and SP-evoked frequency increases in rhythmic medullary slice preparations.	77
Figure 2.3 Multi-photon imaging of fluo-4 Ca^{2+} fluorescence showing sensitivity of preBötC cells at a single optical plain to bath-applied ATP.....	82
Figure 2.4 Multi-photon imaging of fluo-4 Ca^{2+} fluorescence showing sensitivity of preBötC cells at a single optical plain to locally-applied ATP.....	83
Figure 2.5 Whole-cell voltage-clamp recordings from glia in the preBötC.	86
Figure 2.6 Glia cultured from the ventrolateral medulla respond to locally-applied ATP (0.01 mM, 10 s) with an increase in fluo-4 Ca^{2+} fluorescence.....	87
Figure 2.7 Glia cultured from the ventrolateral medulla express immunolabeling for the P2Y ₁ R	89
Figure 2.8 Glia cultured from preBötC punches respond to ATP with an increase in fluo-4 Ca^{2+} fluorescence.	92
Figure 2.9 ATP evokes glutamate release from ventrolateral medulla glia cultures.....	94
Figure 3.1 Differential effects of ATP on preBötC rhythm in mouse and rat.	119
Figure 3.2 P2Y ₁ R activation in the preBötC increases frequency in mouse and rat.	120
Figure 3.3 P2Y ₁ R potentiation of frequency in mouse is spatially restricted to the preBötC.	122

Figure 3.4 DPCPX in the preBötC of mouse unmasks an ATP-mediated frequency increase.

124

Figure 3.5 A₁R antagonism in the preBötC of mouse unmasks an ATP-mediated frequency increase.

126

Figure 3.6 P2Y₁Rs contribute to the ATP-evoked frequency increase in mouse.

127

Figure 3.7 Differential effects of ADO on preBötC rhythm in mouse and rat.

129

Figure 3.8 Real-time PCR analysis reveals differential expression of ectonucleotidase isoforms in preBötC tissue punches from mouse and rat.

131

Figure 3.9 Schematic diagram of purinergic signaling in the preBötC illustrating that the balance between the excitatory effects of ATP at P2Y₁Rs and the inhibitory effects of ADO at A₁Rs is tipped in favour of excitation in rats

142

Figure 4.1 Effects of LVV-SW-EF1a-TMPAP-EGFP or LVV-SW-EF1a-EGFP lentivirus injection in the preBötC on the minute ventilation (V_E), tidal volume (V_T), and breathing frequency (f) responses to hypoxia in carotid body intact rats.

167

Figure 4.2 Effects of LVV-SW-EF1a-TMPAP-EGFP or LVV-SW-EF1a-EGFP lentivirus injection in the preBötC on the minute ventilation (V_E), tidal volume (V_T), and breathing frequency (f) responses to hypoxia in carotid body denervated rats.

169

Figure 4.3 Effects of LVV-SW-EF1a-TMPAP-EGFP or LVV-SW-EF1a-EGFP lentivirus injection in the preBötC on the minute ventilation (V_E), tidal volume (V_T), and breathing frequency (f) responses to hypercapnia in carotid body intact rats.

174

Figure 4.4 Effects of LVV-SW-EF1a-TMPAP-EGFP or LVV-SW-EF1a-EGFP lentivirus injection in the preBötC on the minute ventilation (V_E), tidal volume (V_T), and breathing frequency (f) responses to hypercapnia in carotid body denervated rats.

176

Figure 4.5 Activation of P2Y ₁ R in preBötC of adult rat <i>in vivo</i> with MRS 2365 (1 mM) evokes an increase in respiratory frequency (f) and a decrease in tidal volume (V _T)	179
Figure 4.6 Activation of A1 R in preBötC of adult rat <i>in vivo</i> with ADO (500 μM) evokes no effect on respiratory frequency (f) or tidal volume (V _T).	180
Figure 4.7 ADO (500 μM) in the preBötC of adult rat <i>in vivo</i> has no effect on respiratory frequency (f) or tidal volume (V _T).	181
Figure 4.8 GFP expression 2 weeks after LVV-SW-EF1a-TMPAP-EGFP lentivirus injected in rat preBötC.....	184
Figure 5.1 Preapplication of TLR4 antagonist LPS-RS has no effect on the DAMGO-mediated inhibition of frequency.	214
Figure 5.2 Bath application of the TLR4-selective antagonist, (+) naloxone, has no effect on the opioid-evoked depression of frequency.	215
Figure 5.3 Local application of the TLR4 agonist LPS has no effect on respiratory frequency.	219
Figure 5.4 Microglia activation is not required for the opioid-induced respiratory depression	220
Figure 5.5 (-)-naloxone, but not (+)-naloxone counters fentanyl-induced depression of respiratory activity.	221
Figure 6.1 Schematic illustrating the mechanisms through which purinergic signaling is hypothesized to modulate activity at the glutamatergic inspiratory synapse and contribute to the hypoxic ventilatory response.	249

List Abbreviations

<u>Abbreviation</u>	<u>Definition</u>
Ach	Acetylcholine
aCSF	Artificial Cerebral Spinal Fluid
ADO	Adenosine
ADP	Adenosine Diphosphate
AMP	Adenosine Monophosphate
ATP	Adenosine Triphosphate
BDNF	Brain derived neurotrophic factor
BME	Basal Medium Eagle
BötC	Botzinger Complex
BSSC	Brainstem Spinal Cord
cAMP	Cyclic Adenosine Monophosphate
CCHS	Congenital Central Hypoventilation Syndrome
CNS	Central Nervous System
CNT	Concentrative Nucleoside Transporters
CRG	Central Rhythm Generator
Cx	Connexin
DIA	Diaphragm
DMSO	Dimethyl Sulfoxide
DRG	Dorsal Respiratory Group
E-NPP	Ectonucleotide Pyrophosphatase
E-NTPDase	Diphosphohydrolase
EMG	Electromyogram
ENT	Equilibriative Nucleoside Transporters
f	Frequency
FFA	Flufenamic Acid
GABA	Gamma-aminobutyric acid
GFAP	Glial Fibrillary Acidic Protein
GFP	Green Flourescent Protein
GG	Genioglossus
GLAST	Glutamate Aspartate Transporter
GLN	Glutamine
GLT1	Glutamate Transporter
GPCR	G Protein Coupled Receptor
HPLC	High Performance Lipid Chromatography
HVR	Hypoxic Ventilatory Response
i.p.	Interperitoneal
ICW	Intercellular Calcium Wave
IL	Interleukin
IO	Inferior Olive
LPS	Lipopolysacharide

Abbreviation	Definition
MN	Motor Neuron
NA	Nucleus Ambiguus
NDS	Normal Donkey Serum
NK1	Neurokinin 1
NTS	Nucleus Tractus Solitarius
P1R	Adenosine Receptor
P2XR	Purinergic Receptor
P2YR	Purinergic Receptor
PBS	Phosphate Buffered Saline
PCR	Polymerase Chain Reaction
pFRG	Parafacial Respiratory Group
PLC	Phospholipase C
PNS	Peripheral Nervous System
preBötC	Pre-Botzinger Complex
PRG	Pontine Respiratory Group
REM	Rapid Eye Movement
ROI	Region of Interest
RS	Rat Serum
RTN	Retrotrapezioid Nucleus
SD	Sprague Dawley
SP	Substance P
SP-SAP	Substance P conjugated to saporin toxin
SST	Somatostatin
TCA	Tricarboxylic Acid Cycle
T _i	Time of Inspiration
T _i /T _{tot}	Duty Cycle
TLR	Toll Like Receptor
TNAP	Tissue-nonspecific Alkaline Phosphatase
TNF	Tumor Necrosis Factor
Trk	Tyrosine Kinase
TTX	Terodotoxin
V _E	Minute Ventilation
VLM	Ventrolateral Medulla
VRAC	Volume Regulated Anion Channel
VRC	Ventral Respiratory Column
V _T	Tidal Volume

Chapter 1: Introduction

1.1 Introduction

Breathing appears to be a simple rhythmic movement of air through airways and into and out of the lungs, however, there is an incredibly complex, robust neuronal network that controls this behavior. This network must coordinate the interaction between neurons, motoneurons, muscles, chest wall, lung, airways and multiple sensory elements to produce spontaneous, rhythmic breathing movements that maintain blood gas levels to match metabolic demand.

This thesis examines the central inspiratory network involved in controlling respiratory rhythm and how purinergic modulation contributes to the dynamic adaptability of this robust network. The central inspiratory network consists of both neurons and glia cells, and this thesis will specifically examine the importance of glia and three-part purinergic signaling system in modulating the central inspiratory rhythm-generating network using cell culture, *in vitro* and *in vivo* techniques. The first chapter of this thesis will review the central inspiratory network, and discuss areas of the central nervous system (CNS) involved in central respiratory control and current theories of rhythm generation. This will be followed by an overview of purinergic signaling in respiratory control, which will then be discussed in the context of purinergic modulation in important physiological responses such as the hypoxic ventilatory response.

1.2 Central respiratory network and rhythm generation

Breathing is necessary for life in all mammals and is controlled by the brain as a rhythmic behavior. The respiratory system has the important function of maintaining oxygen, carbon dioxide and hydrogen ion concentrations within the body. To continuously maintain this homeostasis the central neural network must be both robust and highly adaptable. The core rhythm-generating center is in the brainstem and modulation of this network affects motor output to change the timing and pattern of contraction of muscles driving the respiratory pump from birth. Breathing must be integrated with a variety of behaviors such as

changes in state (sleep vs wakefulness), locomotion, speech, swallowing and chewing. This integration occurs largely due to modulation of the central inspiratory network by neurotransmitters and neuromodulators. Understanding the networks controlling breathing is critical for development of rational therapeutic approaches for a variety of diseases with disordered breathing.

The central respiratory network located in the medulla oblongata and pons is responsible for generation of the respiratory rhythm. There are three interconnected primary regions which are classified based on the phase of the respiratory cycle in which neurons fire (inspiratory, expiratory and phase-spanning) and their firing pattern. These regions include the pontine respiratory group (PRG), the dorsal respiratory group (DRG) and the ventral respiratory column (VRC). Each of these three groups will be described below.

The PRG is in the dorsolateral pons and contains neurons that fire during inspiration and expiration. This was first determined in vagotimized, anesthetized cats where transections caudal to this pontine region disrupted the timing of the normal breathing pattern (Lumsden, 1923). The parabrachialis medialis and Kölliker-Fuse nuclei has been identified as the PRG (Dutschmann and Herbert, 2006; Segers et al., 2008). Reciprocal connections exist between the PRG and the medullary respiratory regions (Bianchi and St John, 1981, 1982). *In vivo* and *in situ* experiments have shown the PRG controls the duration of the respiratory cycle and, more specifically, the post-inspiratory phase (Dutschmann and Herbert, 2006; Smith et al., 2007). The PRG is thought to be important in phase switching between inspiration and expiration (Foutz et al., 1988; Borday et al., 1998).

The DRG is located in the dorsal medulla in the nucleus of the solitary tract (NTS) and contains neurons that primarily fire during inspiration. This region is an important relay station for information regarding peripheral mechanoreflexes and chemoreflexes (Nattie, 1999). The primary afferent inputs into the central respiratory network are chemoreceptor and pulmonary stretch receptors. These pulmonary stretch receptors provide information about the mechanical status of the lungs and chest wall. They monosynaptically transmit

information about lung volume to second order relay neurons in the NTS (Bonham and McCrimmon, 1990; Kubin et al., 2006; Gourine et al., 2008) and mediate a host of reflexes referred to as the Breuer-Herring reflexes which have a variety of effects on respiratory pattern depending on when during the respiratory cycle the afferent information arrives. Most common is that the lungs are inflating during inspiration and as afferent feedback increases with increasing lung volume this activity suppresses inspiratory activity and helps terminate inspiration. This is the inspiratory termination reflex. In anesthetized animals, vagotomy uniformly abolishes entrainment to mechanical ventilation (Petrillo et al., 1983). However in conscious human lung transplant patients it has been shown that there is no absolute requirement for vagal feedback to induce entrainment to mechanical ventilation, suggesting there may be additional entraining stimuli present during wakefulness or cortical influences (Simon et al., 2000). If something delays emptying of the lung during expiration, pulmonary stretch receptor feedback will prolong expiration via the expiratory prolonging reflex.

The NTS is also an important relay station for chemoreception, as it receives peripheral carotid body chemoreceptor inputs. Peripheral and central inputs converge primarily on a chemosensitive/integrating region in the retrotrapezoid nucleus (RTN) characterized by chemosensitive glutamatergic interneurons which strongly express Phox2b (Mulkey et al., 2004; Stornetta et al., 2006; Guyenet et al., 2008). Phox2b has been shown to mark an “uninterrupted chain of sensors and neurons” involved in the integration of peripheral and central chemoreception (Dauger et al., 2003; Stornetta et al., 2006). The circuit includes peripheral chemoreceptors on the carotid bodies, chemoreceptor afferents relay in the NTS and chemoresponsive NTS projections extend to the VLM and RTN central chemoreceptors. RTN neurons have been shown to receive a strong excitatory input from carotid chemoreceptor afferents that have a glutamatergic synapse in the NTS (Takakura et al., 2006). These findings suggest that RTN neurons have the capability of detecting brain P_{CO_2} directly and respond to changes in arterial blood gas via direct neural inputs from peripheral chemoreceptors. The RTN also regulates central chemosensitivity in a state-

dependent manner, and its acidification increases breathing (reviewed in (Nattie, 2001)). The RTN is thought to have bidirectional connections with the ventral respiratory column and these connections have been suggested as providing an anatomical framework for reciprocal integration of information between the central chemoreflex mechanism and the central regulation of respiratory and other autonomic functions (Rosin et al., 2006) Projections to the VLM allow this integrated peripheral and central chemoreceptor drive to influence the respiratory circuitry.

The inability to permanently disrupt rhythm with discrete lesions throughout the network led to the view that respiratory rhythm derived from a highly distributed network (Lumsden, 1923). The DRG was thought to play more important role in rhythm generation than ventral respiratory nuclei, but none had been shown to be necessary or sufficient to the generation and transmission of rhythm (Speck and Beck, 1989). In 1984 a landmark paper was published (Suzue, 1984) describing the isolated brainstem spinal cord (BSSC) preparation that generated breathing rhythm in 0–4 day neonatal rats and with increasing immunohistochemistry, genetics and molecular biology work being done in rodents, the rat became an increasingly popular model for studying the central inspiratory network. This preparation enabled the careful dissection of rostral and caudal respiratory groups while monitoring respiratory rhythm for any disruption. It was found that removing both the PRG and the DRG did not impair the ability of the preparation to generate stable rhythm, suggesting that the VRC was likely the region generating basic respiratory rhythm.

The ventral respiratory column (VRC) extends from the facial nucleus to the spinomedullary junction and specifically contains the parafacial respiratory group/retrotrapezoid nucleus complex (pFRG/RTN), the Bötzinger complex, the preBötzinger complex (preBötC), rostral ventral respiratory group (rVRG), and the caudal ventral respiratory group (cVRG) (Nattie, 1999; Feldman et al., 2003). The BötC, contains predominately expiratory neurons and is thought to be a major source of expiratory activity during eupnea (Jiang and Lipski, 1990; Tian et al., 1999) and coordination of inspiratory and

expiratory activities. However it has been proposed that a separate active expiratory oscillator, located rostral the BötC in the parafacial respiratory group (pFRG), interacts with the preBötC to generate coordinated patterns of inspiratory and expiratory activity (Feldman and Del Negro, 2006; Janczewski and Feldman, 2006). The BötC neurons extend inhibitory synapses to other respiratory related neurons in the medulla and have extensive connections to the preBötC (Feldman and Del Negro, 2006). The rVRG and cVRG both have premotor neurons that connect to respiratory motor neuron pools; the rVRG and cVRG have primarily inspiratory and expiratory premotor neurons, respectively (Nattie, 1999). While the pFRG/RTN, BötC, preBötC, rVRG and cVRG are all interconnected and important in the production of a normal eupneic breathing pattern (Fig 1.1), the pFRG/RTN and preBötC are believed to be of critical importance to rhythm generation and will be reviewed below.

1.2.1 PreBötC

The VRG receives input from higher brain centers, peripheral and central chemoreceptors and other brainstem regions involved in respiratory rhythm generation. By serially sectioning the BSSC preparation along the rostral caudal axis of the VRC, it was determined that there is a small 200 µm region of the VRC called the preBötC that is essential for generating breathing rhythm(Ruangkittisakul et al., 2008). Moreover, it was shown that this region is sufficient for generating a respiratory-related rhythm. A medullary slice of tissue extending from the caudal margin of the BötC caudally to a region rostral to obex that contained the preBötC (slice located ventral to the semi-compact division of the nucleus ambiguus (NA), caudal to the compact division of the NA and rostral to the lateral reticular nucleus) generates robust inspiratory-related activity *in vitro* (Smith et al., 1991). The preBötC contains propriobulbar interneurons necessary for generation of respiratory rhythm. The development of the slice preparation enabled the study of a functionally active rhythm generating circuit *in vitro* and resulted in a major advancement in the analysis

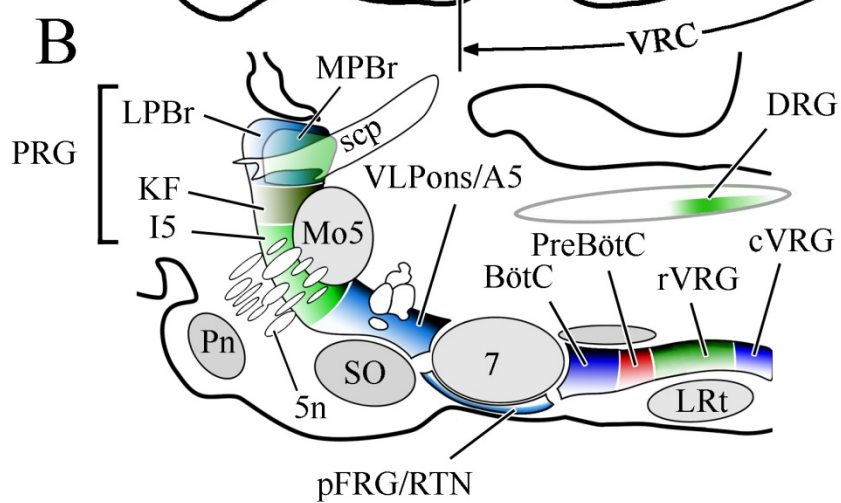
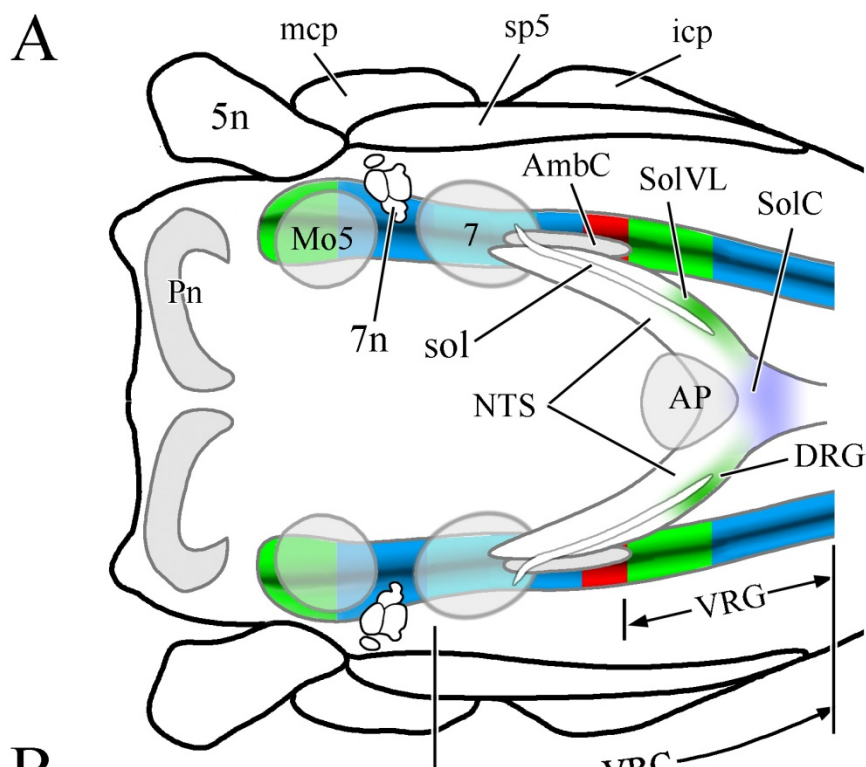


Figure 1.1 Respiratory-related regions of the brainstem of the rat shown in horizontal (A) and sagittal (B) views.

Respiratory-related regions comprise a nearly continuous column in the lateral brainstem. The boundaries depicted between the various brainstem compartments reflect functional distinctions between adjacent regions relative to their impact on breathing. *Abbreviations:* 5n, trigeminal nerve; 7, facial nucleus; 7n, facial nerve; A5, A5 noradrenergic neuronal group; AmbC, compact part of nucleus ambiguus; AP, area postrema; BötC, Bötzinger complex; cVRG, caudal division of ventral respiratory group; DRG, dorsal respiratory group; I5, intertrigeminal area; icp, inferior cerebellar peduncle; KF, Kölliker-Fuse nucleus; LPBr, lateral parabrachial region; LRt, lateral reticular nucleus; mcp, medial cerebellar peduncle; Mo5, motor nucleus of the trigeminal nerve; MPBr, medial parabrachial region; NTS, nucleus of the solitary tract; pFRG, parafacial respiratory group; Pn, basilar pontine nuclei; preBötC, preBötzinger complex; PRG, pontine respiratory group; RTN, retrotrapezoid nucleus; rVRG, rostral division of ventral respiratory group; scp, superior cerebellar peduncle; SO, superior olive; sol, solitary tract; SolC, commissural subdivision of the nucleus of the solitary tract; SolVL, ventrolateral subdivision of the nucleus of the solitary tract; sp5, spinal trigeminal tract; vlPons, ventrolateral pontine region; VRC, ventral respiratory column of the medulla; VRG, ventral respiratory group. Adapted from Alheid and McCrimmon (2008) *Respir Physiol Neurobiol*. 64:3-11

of mechanisms underlying the generation and transmission of respiratory oscillations in neonatal mammals. The preBötC is both necessary and sufficient for respiratory rhythm generation (Smith et al., 1991; Ruangkittisakul et al., 2008) and several reviews have discussed its importance in respiratory rhythm generation (Feldman et al., 2003; Feldman and Del Negro, 2006; Feldman and Janczewski, 2006). Precise anatomic delineation of the preBötC greatly facilitated the exploration of the functional role of these neurons and the putative mechanisms of respiratory rhythrogenesis and frequency modulation. PreBötC neurons were found to co-express neurokinin-1 receptor (NK1R) and μ -opioid receptors (Gray et al., 1999) providing the first opportunity for targeted molecular manipulation of the preBötC. The specific bilateral lesion of > 80% NK1R neurons (using substance P conjugated to the toxin saporin (SP-SAP)) showed that destruction of preBötC NK1R neurons first disrupted breathing during sleep, especially rapid eye movement (REM) sleep when apnea occurred (McKay et al., 2005). With further loss of these preBötC neurons, breathing during wakefulness became ataxic (Gray et al., 2001). It was subsequently demonstrated that NK1R neurons are not confined to the preBötC area (Guyenet et al., 2002). NK1R expression remains a reasonable marker for the preBötC since it contains the highest density of NK1R immunolabeling, but NK1R expressing neurons can be found along the VRC (Gray et al., 1999; Gray et al., 2001). The search for definitive markers of preBötC neurons has therefore continued. More recently, somatostatin (SST) has emerged as a useful marker of a subgroup of glutamatergic preBötC interneurons (Stornetta et al., 2003). That these preBötC neurons are critical for rhythm generation *in vivo* was demonstrated by expressing the allatostatin receptor in SST expressing neurons of the preBötC (using a novel adeno-associated virus). Silencing these neurons via perfusion of allatostatin into the cerebrospinal fluid produced a reversible, repeatable apnea (Tan et al., 2008), further validating the *in vitro* work characterizing the preBötC as a key site in rhythm generation. Ultimately, the preBötC can now be anatomically defined in adult and juvenile rodents as a region containing neurons expressing the NK1R, μ -opioid receptor, tyrosine kinase B

receptor (TrkB), somatostatin (SST), and the type 2 vesicular glutamate transporter VGlut2 (Gray et al., 1999; Stornetta et al., 2002; Thoby-Brisson et al., 2003). Two recent studies have now determined the developmental lineage of preBötC neurons using transgenic mice. These studies found that Dbx1-expressing progenitor cells give rise to preBötC neurons (Bouvier et al., 2010; Gray et al., 2010). Respiratory activity in Dbx1-null mutants is absent *in vivo* and *in vitro*. Additionally, mice deficient in MafB, an important transcription factor for neuronal specification of rhombomeres 5-6, demonstrate ataxic breathing *in vitro* and lethal central apnea *in vivo*, due to loss of preBötC neurons (Blanchi et al., 2003). These studies suggest that a genetically definable population in the preBötC generates breathing and that a mammalian central rhythm generator can be generated from a single developmental precursor population. A variety of studies in other animal models have also demonstrated the presence of the preBötC. These include the demonstration that lesions of the preBötC in goats can eliminate eupnea (Wenninger et al., 2004) and the identification of electrophysiological properties of the adult preBötC in the cat (Schwarzacher et al., 1995) and dog (Krolo et al., 2005), however other *in vivo* studies don't support the idea that the preBötC is important (Zuperku et al., 2008). The human correlate of the preBötC has been identified as a group of NK1 expressing neurons that corresponds with the rodent preBötC (Lavezzi and Matturri, 2008; Schwarzacher et al., 2011).

1.2.2 RTN/pFRG

The preBötC is no longer thought to be the only respiratory rhythm generator. Respiratory rhythm has been demonstrated to arise out of two distinct but functionally interacting, rhythmogenic networks: the RTN/pFRG (Onimaru and Homma, 2003) and the preBötC (Smith et al., 1991). These oscillatory networks are thought to control a different respiratory phase with the preBötC driving inspiration and the RTN/pFRG controlling active expiration as well as being important in central chemosensitivity (Janczewski and Feldman, 2006; Guyenet et al., 2008). The RTN/pFRG is a heterogeneous group of neurons ventral and

slightly caudal to the VII motor nucleus, located rostral to the preBötC (Feldman and Smith, 1989; Onimaru and Homma, 2003). There are two overlapping neuron populations comprising the rhythmogenic pFRG neurons and the chemosensitive RTN neurons. Voltage sensitive dyes were used to visualize the phasic activity in the RTN/pFRG and bilateral lesioning reduced respiratory frequency (Onimaru and Homma, 2003). The RTN/pFRG plays a critical role in the development of respiratory rhythms (Thoby-Brisson et al., 2009) however its significance is still under debate. Several *in vitro* studies have shown that there are a group of respiratory neurons ventrolateral to the facial nucleus that fire before inspiration (Onimaru and Homma, 2003; Onimaru et al., 2006) and when this region is transected away *in vivo* (leaving the preBötC intact) active expiration is abolished while inspiration remains (Janczewski and Feldman, 2006). This suggests that the pFRG is critical in embryonic development of rhythmic networks but transitions into mediating active expiration later in development. It was originally proposed that the pFRG was in fact the primary rhythmic excitatory drive that entrains the preBötC inspiratory oscillator (Onimaru and Homma, 2003). However this was problematic as removal of the pFRG did not abolish inspiratory rhythm and this region did not show rhythmicity during resting conditions or anesthesia. One current theory is that the pFRG develops from a primary inspiratory oscillator to an immature version of the RTN that later plays a key role in central chemoreception (Guyenet et al., 2009; Guyenet and Mulkey, 2010). In contrast, the pFRG is proposed to be a conditional oscillator that is responsible for active expiration later in development as part of the “two oscillator hypothesis” (Feldman and Del Negro, 2006; Janczewski and Feldman, 2006; Pagliardini et al., 2011). The role of the pFRG remains controversial.

Optogenetic stimulation *in vivo* selectively stimulating Phox2B chemosensitive neurons of the RTN/pFRG or all neurons in a region lateral to the chemosensory region suggest that the RTN and pFRG (the active expiratory oscillator) may be functionally distinct, partially overlapping regions. Optogenetic activation of Phox2B RTN chemosensory

neurons increases inspiratory frequency but does not appear to reset inspiratory rhythm (Abbott et al., 2009; Kanbar et al., 2010). Optogenetic activation of neurons just lateral to the RTN increases inspiratory frequency, evokes active expiration and resets inspiratory rhythm (Pagliardini et al., 2011). This active expiration is functional but silenced by endogenous GABA and glycine inhibition. These findings suggest that the pFRG is turned on (or disinhibited) in situations when active expiration is necessary to increase ventilation, such as exercise. Similar to the preBötC, the RTN/pFRG oscillator originates from rhombomere 5, however it is specified by a number of well-defined transcription factors different from the preBötC. Specifically, Phox2b-expressing and Egr2-expressing progenitor derived neurons are thought to correspond to the adult pFRG as they generate a respiratory-related rhythmic activity in the embryonic hindbrain (Thoby-Brisson et al., 2009).

1.3 Central respiratory rhythm generation

Advancements in our understanding of the neural mechanisms of breathing have been due to an interdisciplinary framework for characterizing how breathing is centrally controlled, including detailed knowledge of the developmental lineage of respiratory networks, accumulating experimental *in vivo* and *in vitro* data, and computational models. While this multidisciplinary approach has brought the field a long way from the initial discovery of the primary site of respiratory rhythm generation, there still remains much to learn regarding network organization in the neural control of breathing. Here I will outline the mechanisms by which the preBötC is proposed to generate respiratory rhythm and discuss the integration of the dual oscillator hypothesis in this mechanism. Recent findings suggest that the mechanism underlying respiratory rhythm generation is controlled by multiple drives from more rostral brainstem components, which regulate the dynamic behaviour of the core circuitry and I will discuss how this enables the network to adapt to different physiological and metabolic conditions.

1.3.1 Three-phase network hypothesis and hybrid pacemaker hypothesis

The finding that respiratory rhythm persists in thin brainstem slices that contain the preBötC, led to the hypothesis that the preBötC was the source of respiratory rhythm (Smith et al., 1991; Rekling and Feldman, 1998; Smith et al., 2000). However, our model of the mechanisms of rhythm generation has evolved over the last 3 decades from a three-phase network hypothesis (Richter, 1982) to a hybrid pacemaker network hypothesis (Koshiya and Smith, 1999) to the current emergent network or group pacemaker hypothesis (Feldman and Del Negro, 2006). The initial three-phase network hypothesis was based on the theory that inspiration and expiration occur as a result of reciprocal inhibition between two key groups of neurons within the central respiratory neuronal network, the early-inspiratory and post-inspiratory (or early-expiratory) neurons (Richter, 1982; Ogilvie et al., 1992). The motor pattern during normal breathing is considered to consist of three phases: inspiration, post-inspiration (post-I) and the later stage 2 (E-2) of expiration.

However the observation that rhythm persists *en bloc* (Feldman et al., 1990) and in slices (Onimaru et al., 1990; Gray et al., 1999) after the attenuation of postsynaptic inhibition, combined with the discovery of conditional pacemaker neurons in the preBötC (Smith et al., 1991) led to the hybrid pacemaker network hypothesis that intrinsically rhythmic pacemaker neurons drive the respiratory rhythm (Onimaru et al., 1989; Smith et al., 1991; Gray et al., 1999; Smith et al., 2000). This hypothesis involves synaptically coupled pacemaker cells forming the basic oscillator in the preBötC. This hypothesis is supported by the fact that cells with pacemaker properties have been identified in the preBötC (Smith et al., 1991; Rekling and Feldman, 1998; Del Negro et al., 2001) and the pFRG (Onimaru et al., 1989, 1997; Ballanyi et al., 1999). In the preBötC about 20% of neurons have endogenous bursting properties (Mellen and Thoby-Brisson, 2012). Two types of pacemaker neurons have been identified in the preBötC (reviewed in (Feldman and Del Negro, 2006)): pacemakers that depend on the persistent sodium current (I_{NaP}) and a second group that is dependent on the Ca^{2+} -dependent, non-specific cationic current (I_{CAN}). The I_{NaP} pacemaker neurons are present

throughout development, are insensitive to Cd^+ , show voltage-dependent changes in bursting frequency and are inhibited by the I_{NaP} antagonist riluzole (Del Negro et al., 2002). Surprisingly, eliminating this pacemaker population did not affect respiratory rhythm (Del Negro et al., 2002) suggesting that voltage-dependent bursting in pacemaker neurons is not essential for respiratory rhythmogenesis *in vitro*. The other group of pacemaker preBötC neurons emerge during development and are driven by I_{CAN} , are sensitive to Cd^+ , show voltage-independent bursting behaviour, and are inhibited by the I_{CAN} antagonist flufenamic acid (FFA)(Pace et al., 2007). Like the rizazole experiments showing that rhythm is not dependent on I_{NaP} , application of I_{CAN} antagonists to the rhythmic slice preparation had no effect on the rhythmogenesis of the slice (Pena et al., 2004). In normoxia, respiratory rhythm generation could only be abolished with the application of both riluzole and FFA (Pena et al., 2004). Initially this was interpreted as suggesting that rhythm generation is dependent on a heterogeneous population of pacemaker neurons. Subsequent experiments, however, have shown that once rhythm is blocked via riluzole and FFA, it can be restored with agents that simply increase excitability, which questions the importance of pacemaker properties (Del Negro et al., 2005).

1.3.2 Emergent network group pacemaker hypothesis

While it is clear there are cells in the preBötC with pacemaker properties, the group pacemaker hypothesis, first proposed in 1998 by Rekling and Feldman, gained considerable support with the observation that excitatory modulators can revive network activity after blockade of I_{NaP} and I_{CAN} in the transverse slice (Del Negro et al., 2005). *In vitro* when pacemaker properties of the preBötC are eliminated, respiratory rhythm can continue as long as pharmacological excitation is provided to compensate for the significant reduction of I_{NaP} and I_{CAN} . PreBötC network excitability and rhythmicity can be restored by Substance P or AMPA ((2-amino-3-(5-methyl-3-oxo-1,2- oxazol-4-yl)propanoic acid)) (Morgado-Valle and Feldman, 2004; Pena et al., 2004). With the emergent network or group pacemaker hypothesis, pacemaker neurons are not necessary for rhythm generation under normal

conditions, however their rhythmogenic properties may be more important in conditions of stress such as hypoxia or reduced input such as the slice preparation. It has been shown both *in situ* and *in vitro* that a type of respiratory-related activity generated under extreme hypoxic conditions, gasping, relies on the activity of I_{NaP} -dependent pacemaker neurons (Pena et al., 2004; Paton et al., 2006).

This emergent network hypothesis suggests there are two types of pacemaker neurons embedded in a respiratory neuron network. Eupnea is driven primarily by recurrent excitation between I_{NaP} and I_{CAN} pacemaker neurons while under conditions of stress the pacemaker properties of this network are emergent. The pacemaker cells are important in that they initiate positive feedback to the network through recurrent glutamatergic excitation, ultimately amplifying the synaptic depolarization. The subset of inspiratory neurons that are pacemakers participate in network activity but their pacemaker properties are not necessary – the inspiratory discharge is induced by excitatory synaptic input which is amplified by I_{NaP} or I_{CAN} (Feldman and Del Negro, 2006; Del Negro et al., 2010). However, recently inspiratory-modulated glycinergic pacemaker neurons in the preBötC have been identified, challenging the idea that pacemaker neurons are exclusively excitatory (Morgado-Valle et al., 2010). Burst termination is thought to occur via activity dependent outward currents and synaptic inhibition (Feldman and Del Negro, 2006). These glycinergic pacemakers may contribute to burst synchronization within the preBötC, and coordination between the preBötC and the pFRG. In the current emergent network hypothesis, robust functioning of the respiratory network likely is due to the interdependence of the network where cells have specific functions, yet none are essential for a functioning network.

1.3.3 Dual oscillators

The central respiratory rhythm generation model has become more complicated with evidence of the pFRG as a second oscillator. The RTN/pFRG is rhythmic in the embryonic hindbrain and is in-phase with the preBötC when it becomes active as an oscillator (Thoby-

Brisson et al., 2009), firing just before the inspiratory oscillator. The RTN/pFRG oscillator rhythmic activity persists when the preBötC is blocked pharmacologically by opioids, demonstrating the independence of this oscillator from the preBötC (Thoby-Brisson et al., 2005). These pacemaker cells have I_{NaP} properties and the hyperpolarization-activated I_h current is important in modulating burst duration, while gap junctions synchronize cell firing within the network (Mellen et al., 2003; Thoby-Brisson et al., 2009).

Difference in opinions on the importance of the RTN/pFRG as an oscillator can be attributed to the changes that occur during development. Transgenic studies have shown that disruption of either network in neonatal animals is lethal (Blanchi et al., 2003; Thoby-Brisson et al., 2009; Bouvier et al., 2010; Gray et al., 2010), however in older animals this type of disruption is survivable. This robust characteristic of the network is thought to be due to the plasticity of the respiratory network. Connections between RTN/pFRG network and the preBötC rely on complex reciprocal glutamatergic/GABAergic synapses (gamma-aminobutyric acid) (Thoby-Brisson et al., 2009; Bochorishvili et al., 2012). The phase locking between these two oscillators is thought to be due to these reciprocal connections. The difference between the slice and *en bloc* preparation and their response to low concentration DAMGO ([D-Ala², NMe-Phe⁴, Gly-ol⁵]-enkephalin) application illustrates this, as in slice which contains only the opioid-sensitive preBötC, DAMGO evokes a continuous increase in inspiratory period. In contrast in the *en bloc* preparation which contains both oscillators the slowing is quantal, resulting from one or more skipped inspiratory bursts (Mellen et al., 2003). The pFRG provides a timing signal so that when the opioid depressed preBötC oscillator discharges, it does so in phase with the pFRG whose oscillatory frequency does not change in the presence of opioids. As explained by the emergent network hypothesis, the network is dynamic in nature and cells within these two oscillators will participate in network activity under certain conditions, such as hypoxia or hypercapnea (Paton et al., 2006; Abdala et al., 2009), to maintain the robust nature of the respiratory rhythm generating network (Ramirez and Viemari, 2005).

1.3.4 Hierarchy of rhythm generation

While RTN/pFRG and preBötC have been shown to represent the core oscillators of rhythmic respiratory behaviors, a series of rostral to caudal transection experiments in the *in situ* arterially perfused rat brainstem-spinal cord preparation (Paton, 1996) show that there is a rostral-to-caudal stacking of network building blocks. The sequential removal of rostral pons and medullary regions progressively reorganizes network dynamics (Rybäk et al., 2007; Smith et al., 2007) (reviewed in (Smith et al., 2009)). These studies have shown that the three-phase rhythm seen *in vivo* (inspiration, post-inspiration (post-I or P-I) and expiration) requires the presence of the pons. When the pons is removed, a two-phase rhythm is generated by intrinsic reciprocal inhibitory synaptic connections between the BötC, preBötC and the RTN/pFRG. Subsequent removal of structures rostral to the preBötC will produce a one-phase inspiratory oscillation that is more reliant on the intrinsic pacemaker properties of preBötC neurons. These studies help emphasize the importance of the dynamic hierarchy of the interaction between the pontine, BötC and preBötC networks. The emergent network is likely robust due to its state dependent adaptability afforded by the complex rhythmogenic mechanisms and the neuromodulators that regulate them.

1.4 Purinergic signaling and respiratory control

In addition to being an energy molecule, ATP acts in the CNS as both a neurotransmitter through ionotropic P2XRs and as a neuromodulator through metabotropic P2YRs (Burnstock, 2006). Our understanding of the molecular biology of P2R has made great progress, however, the physiological significance of purinergic signaling in the CNS is less understood. Purinergic signaling appears to be important in the homeostatic functions of the respiratory network, specifically the ventilatory responses to CO₂ and hypoxia. An important point of this thesis, however, is that purinergic signaling needs to be considered as more than just ATP acting at P2Rs. It is more accurately viewed as a three-part system where

the overall effect is a reflection of the dynamic interaction between the actions of ATP (and ADP) at P2Rs, ectonucleotidases and ADO acting at P1Rs. This section will first briefly describe the different components of this three-part purinergic signaling system and then review what is currently known about the purinergic system within the central respiratory network. It is clear that ATP features prominently in the signaling that occurs between glia and neurons in multiple regions of the CNS (Koles et al., 2011), and I will review the role of glia within the central inspiratory network and how this relates to purinergic signaling.

1.4.1 P2 Receptors

ATP mediates the actions of P2Rs of which there are two major families, P2X and P2Y receptors. P2XRs are ligand-gated, ionotropic, non-selective cation channels with a significant Ca^{2+} permeability that mediate fast excitatory responses (Burnstock, 2007a). There are 7 P2XR receptor subunits (P2X_{1-7}) and a variety of splice variants that combine together as trimers to form functional P2XRs. P2Y receptors mediate slower responses to ATP and ADP via G-protein receptor coupled mechanisms. There are 8 different P2Y receptors that can be divided into different functional groups based on the second messenger systems to which they couple (Abbracchio and Ceruti, 2006). $\text{P2Y}_{1,2,4,6}$ couple to $\text{G}_{q/11}$; $\text{P2Y}_{12,13}$ couple to G_i and P2Y_{14} to G_i/G_o ; P2Y_{12} couples to both $\text{G}_{q/11}$ and G_s .

In the CNS, both neurons and glia express P2X and P2YRs (Abbracchio and Ceruti, 2006; Burnstock, 2007b; Burnstock et al., 2011; Illes et al., 2011; Song et al., 2011) with the exception of P2Y_{11} expression on glia and P2X_7 expression on neurons (Sim et al., 2004). Expression is subunit and region specific and the cellular mediators of the ATP response within the respiratory network still remain unclear. Within the ventral respiratory column, neurons are a candidate as they show immunoreactivity for P2X_{1-6} subunits and P2Y_1 subunits (Kanjhan et al., 1999; Yao et al., 2000; Thomas et al., 2001; Gourine et al., 2003; Yao et al., 2003). Populations of neurons within the ventral column have specific expression of some purinergic receptors. Pacemaker and non-pacemaker neurons within the preBötC are

activated and antagonized by P2Y₁R agonist 2MeSADP and antagonist MRS2179, although the weak excitation of this response compared to the robust network response questions whether these neurons are exclusively responsible (Lorier et al., 2007; Lorier et al., 2008). P2XRs are also likely to mediate some neuronal excitability, even though this may not contribute to the ATP-mediated frequency increase. There are also ambiguous motoneurons that show high sensitivity to P2X₃R activation postnatally that disappears by postnatal day 13 (Brosenitsch et al., 2005). Within the ventral medulla, P2R have an important role in chemosensitivity, which will be discussed later. Chemosensitive neurons in the RTN are sensitive to ATP modulation (Gourine et al., 2005a; Mulkey et al., 2006). ATP also modulates the excitability of raphe neurons (which provide tonic excitatory drive) that activate the respiratory network directly (Cao and Song, 2007) as well via its modulatory influence on the RTN (Mulkey et al., 2007; Depuy et al., 2011).

1.4.2 Ectonucleotidases

A family of enzymes called ectonucleotidases hydrolyzes ATP. These enzymes break ATP down into ADP (adenosine diphosphate), AMP (adenosine monophosphate) and ADO (adenosine). These enzymes are key element in the three-part purinergic signaling system that set the balance between levels of P2 and P1R agonists. Consequently there is increasing interest in better understanding the expression and function of these enzymes throughout the CNS as the different types have differential substrate affinities and end products. There are four main families of ectonucleotidases: ectonucleotidase triphosphate diphosphohydrolases (E-NTPDases); ectonucleotide pyrophosphatase/phosphodiesterase (E-NPP); alkaline phosphatases and ecto-5' nucleotidase. These ectonucleotidases have a heterogeneous distribution throughout the brain resulting in varying activity such as the higher activity observed in the cortex than the medulla (Kukulski et al., 2004). Each enzyme has different substrate affinity, although most require the presence of divalent cations (Ca^{2+} and Mg^{2+}) and alkaline pH in the tissue (7.5-8.5) is optimal (Ziganshin et al., 1994). Ectonucleotidases are

also affected by temperature with temperature dependence being both tissue and enzyme isoform specific (Ghildyal and Manchanda, 2004). However with all conditions equal, the difference in ATP hydrolysis rate is due to different expression and density of these enzymes and their ability to produce ATP by-products in the extracellular space. E-NTPDases are the major ectonucleotidases present in the CNS and hydrolyze ATP to AMP. ENTPDase1 and 2 are both expressed by neurons and astrocytes in the CNS and ENTPDase1 is also found on microglia (Braun et al., 2003; Robson et al., 2006; Zimmermann, 2006). Even within enzyme families there is a difference in substrate affinity as ENTPDase1 hydrolyzes ATP and ADP to AMP equally (Wang and Guidotti, 1996; Heine et al., 1999) whereas ENTPDase2 has a 100 fold greater affinity for ATP and will therefore preferentially produce ADP, the preferred agonist for P2Y₁R (Kegel et al., 1997; Mateo et al., 1999) if ATP is abundant. E-NPPs hydrolyze ATP to AMP and have a limited distribution in the brain (Robson et al., 2006; Zimmermann, 2006). Alkaline phosphatases degrade ATP all the way to ADO while Ecto-5' nucleotidase hydrolyses AMP to ADO and are distributed throughout the CNS (Zimmermann, 2006). The cellular actions of ectonucleotidases and their impact on functional networks, such as the respiratory network remain unclear. From limited work in the preBötC respiratory network, it appears that enzyme complement has a major impact on the purinergic modulation of the respiratory activity. While there is high expression of multiple ectonucleotidases isoforms in the medulla, including the preBötC (Huxtable et al., 2009), the expression in specific respiratory cells is unclear (Langer et al., 2008). The role of ectonucleotidases and their role in setting the balance between the excitatory actions of ATP and inhibitory actions of ADO in the respiratory network are critical to our understanding of purinergic modulation. The specific expression of these enzymes within respiratory regions, and specifically within respiratory synapses at sites of ATP release needs to be determined.

1.4.3 P1 Receptors

There are 4 subtypes of G-protein coupled receptors: A1, high affinity A2a and low

affinity A2bRs, and A3Rs (Burnstock, 2007a). ADO binds to all 4 types of receptors, although A1R and A2aR are most potently activated by ADO (Fields and Burnstock, 2006; Burnstock, 2007b). The predominant subtypes in the CNS are A1, A2a and A3Rs, which have both pre- and postsynaptic mechanisms. The most abundant P1R subtypes in the brain are the A1Rs, which couple through pertussis toxin (PTX)-sensitive G proteins to inhibit adenylyl cyclase and decrease cAMP production. These effects of P1R are inhibitory via either presynaptic inhibition of neurotransmitter release by inhibiting voltage-gated Ca^{2+} channels and activating K^+ channels or postsynaptically by increasing voltage- or Ca^{2+} dependent K^+ conductances (Burnstock, 2007a; Burnstock et al., 2011). In contrast, A2aR and A2bRs are typically excitatory on neurons activated through a Gs protein coupled mechanism that stimulates adenylyl cyclase and formation of cAMP (Ralevic and Burnstock, 1998) and this has variable effects on neuronal excitability. The significance of A3Rs in the CNS is unclear although it is known that these receptors couple to Gai-2, Gai-3, and Gq-like proteins, and either increase intracellular Ca^{2+} by stimulating IP3 or decrease cAMP by inhibiting adenylyl cyclase (Burnstock, 2007a). The expression of P1R changes throughout development with A1Rs first detected at E14 in the cortex, hypoglossal nucleus and spinal cord and increasing in expression from birth until P21 where it reaches a constant expression level (Weaver, 1996). Expression of A2aRs also increases after birth, reaches a peak between P14 – 21 and expression begins to decrease at P90 (Zaidi et al., 2006). The dynamic state of these receptors throughout development has an effect on the action of ADO in the central respiratory network. The implications of ADO on respiratory frequency and hypoxic ventilatory depression will be discussed in a later section.

Since ADO is the end product of ATP breakdown, purinergic signaling is terminated when ADO is moved from the extracellular to intracellular space by nucleoside transporters in the plasma membrane (Thorn and Jarvis, 1996). There are two types of nucleoside transporters: equilibrative nucleoside transporters (ENTs) which transport ADO down its concentration gradient and concentrative nucleoside transporters (CNTs) which require

energy to transport ADO against its concentration gradient (Kong et al., 2004). CNTs have a limited distribution in the CNS and are concentrated in other tissues such as the small intestine, heart, bone marrow, placenta, macrophages, splenocytes, kidney and liver (reviewed in (Podgorska et al., 2005)). ENTs are expressed throughout the body, including the brain although the expression of these transporters in the medulla is not known. These transporters could be significant in purinergic signaling, as conditions that elevate intracellular ADO such as hypoxia will result in the transport of ADO out of the cell, elevating extracellular ADO levels and increasing the activation of P1Rs, which in many areas of the brain is considered neuroprotective (Lutz, 1992; Lutz and Prentice, 2002).

1.5 Glia and the central respiratory network

Neurons have traditionally been viewed to be the primary cellular element involved in the processing of information within the brain. The electrical excitability of neurons, attributed by the expression of ligand and voltage gated ion channels that underlie input-dependent changes in membrane potential and large amplitude, regenerative action potentials, are critical for the processing of information within the nervous system. Due to their lack of electrical excitability, glia have conventionally been viewed as playing a supportive role, acting as the “glue” for the neuronal networks of the CNS (Verkhratsky and Steinhauser, 2000). Glia make up 90% of cells in the brain tissue and have important roles in trophic and metabolic support for neurons, neuronal survival and differentiation, neuronal guidance, neurite outgrowth and synaptogenesis, immune and inflammatory responses, controlling cerebral blood flow and maintaining brain homeostasis by buffering of K^+ and neurotransmitters within the extracellular space (Porter and McCarthy, 1995; Deitmer et al., 1998; Allen and Barres, 2005; Fiacco and McCarthy, 2006; Haydon and Carmignoto, 2006; He and Sun, 2007; Iadecola and Nedergaard, 2007; Barres, 2008). More recently, however, due to advanced imaging and genetic techniques, this view is changing and growing evidence suggests that astrocytes possess Ca^{2+} excitability, release and respond to transmitters and

may actually play an active role in information processing in the brain (Giaume et al., 2010; Gourine and Kasparov, 2011).

There are many types of glia cells such as Schwann cells, oligodendrocytes, astrocytes, radial glia, microglia, ependymal cells and polydendrocytes and each cell has specialized functions within the CNS (He and Sun, 2007). Glia vary greatly in cell morphology and location, however, this diverse group of cells can be classified based on function, immunoreactivity and electrophysiology into four subpopulations: microglia, oligodendrocytes, polydendrocytes and astrocytes (see recent review for criteria (Mulkey et al., 2010)). Oligodendrocytes and Schwann cells are myelin producing cells which myelinate neurons in the CNS and PNS, respectively. Polydendrocytes are NG2-expressing, glial precursor cells present throughout life (Nishiyama et al., 2009). Radial glia are one type of polydendrocyte that function as scaffolding for migrating, developing neurons, and can also be neural stem cells. Microglia are immune cells of non-neuronal origin and are involved in mediating immune and inflammatory responses in the central nervous system. They can be ‘activated’ by injury/toxicity, which produces morphological and receptor expression changes that result in the release of pro-inflammatory factors that activate and mediate inflammatory processes in the CNS. Astrocytes are the largest class of glial cells and the main glia cell involved in cell signaling. In addition they help to establish the blood brain barrier, as they are highly associated with the surrounding vasculature(Attwell et al., 2010). As a subpopulation, astrocytes can be divided further based on location into protoplasmic and fibrous astrocytes in the gray and white matter respectively. Three types of astrocytes have been identified within the preBötC, however, their functional role remains unclear (Grass et al., 2004). In this thesis, I explore the role of astrocytes and microglia in the modulation of central respiratory networks.

1.5.1 Astrocyte function

Some important functions of astrocytes include maintaining extracellular K⁺ levels

and low extracellular glutamate levels. Astrocytes have a very high resting K⁺ conductance, which includes inwardly rectifying K⁺ channels (Kir4.1), and give them a negative resting membrane potential very near the equilibrium potential for K⁺ (Kuffler and Nicholls, 1966; Kettenmann et al., 1983; Butt and Kalsi, 2006). The ability for astrocytes to maintain low extracellular glutamate is important for preventing excitotoxic related neuronal death (Danbolt, 2001). Glia located near synaptic terminals have high affinity glutamate transporters GLAST/EAAT1 and GLT1/EAAT2 (Gegelashvili et al., 1997) that remove glutamate from the synaptic cleft. The glutamate taken up by astrocytes is used to produce glutamine via glutamine synthetase or lactate and aspartate depending on low glutamate or high glutamate concentrations, respectively (McKenna, 2007). Glutamine released from astrocytes is taken up by neurons that use this as a substrate to synthesize glutamate (Kvamme et al., 2001). Glutamate may also be metabolized as an energy substrate in astrocytes through the tricarboxylic acid cycle (McKenna, 2007).

Astrocytes are of great interest in the modulation of neural networks. The use of Ca²⁺-sensitive fluorescent dyes has revealed that astrocytes, while not electrically excitable, exhibit cellular excitability based on changes in cytosolic Ca²⁺ that can give rise to intracellular calcium waves that propagate between astrocytes, in part through purinergic signaling (Cornell-Bell et al., 1990; Perea and Araque, 2005). The functional significance of this intracellular and intercellular Ca²⁺ mediated signal *in vivo* remains controversial, however, it may stimulate responses with important implication for neuronal function. There is interaction between neurons and astrocytes as neuron activity can trigger these Ca²⁺ waves in culture and slice preparations, and in turn these waves can modulate neuronal activity (Dani et al., 1992; Nedergaard, 1994; Parpura et al., 1994; Kang et al., 1998; Parri et al., 2001). Astrocytes express a wide variety of G protein-coupled receptors (GPCRs) in culture, *in situ* and *in vivo* in several regions of the brain, which can evoke an increase in intracellular Ca²⁺ (Porter and McCarthy, 1995; Beck et al., 2004; Agulhon, 2008). These intercellular Ca²⁺ waves are thought to propagate via a variable combination of at least two mechanisms.

They are initiated via a second messenger cascade that mobilizes intracellular Ca^{2+} . The wave propagates between cells in part by passing through gap junctions (Finkbeiner, 1992; Nedergaard, 1994; Suadicani et al., 2006). It is also regenerated “de novo” by ATP, which is released from the astrocyte in response to the intracellular Ca^{2+} wave, activating P2Rs on neighboring cells, which activates second messenger cascades increasing intracellular Ca^{2+} (Guthrie et al., 1999; Fumagalli et al., 2003). The extracellular ATP may also cause increases in intracellular Ca^{2+} by activating P2X₇Rs on the astrocyte surface that can transform into a macrochannel if ATP concentrations are high enough (Guthrie et al., 1999; Fumagalli et al., 2003). The most common second messenger cascade underlying increases in intracellular Ca^{2+} in astrocytes (in culture and slices *in vitro*) is the phospholipase C (PLC)/ inositol 1,4,5-triphosphate (IP₃) pathway, which ultimately causes Ca^{2+} release from the endoplasmic reticulum (Agulhon, 2008).

Knowledge about the bidirectional exchange between astrocytes and neuronal function has expanded dramatically suggesting that astrocytes are actively involved in processing, storage and transfer of information by the nervous system (for review see (Volterra and Meldolesi, 2005; Haydon and Carmignoto, 2006; Hamilton and Attwell, 2010)). Astrocytes express receptors and respond to a variety of neurotransmitters (glutamate, norepinephrine, acetylcholine, GABA, histamine, ADO and ATP) (Haydon and Carmignoto, 2006) with increases in intracellular Ca^{2+} . In turn this increase in intracellular Ca^{2+} appears in some brain regions, especially when examined *in vitro*, to evoke the release of gliotransmitters (ATP, D-serine and glutamate) (Agulhon, 2008) which can influence neuron excitability and synaptic transmission (Haydon, 2001). These gliotransmitters may be released by a variety of mechanisms including Ca-dependent exocytosis, opening of hemichannels (Ye et al., 2003), volume-regulated anion channels (Kamelberg et al., 1990), reversal of transporters (Szatkowski et al., 1990) and diffusion through ionotropic purinergic receptors, especially the P2X₇ receptors (Duan et al., 2003). In some brain regions, especially the hippocampus, astrocytes and the transmitters they release are considered to play an

integral role in information transfer across the synapse. In fact the conventional view of the synapse as a two part structure comprising pre- and postsynaptic neuronal elements has been replaced by the concept of a tripartite synapse in which astrocytic processes are intimately associated with both pre and postsynaptic neuronal elements, respond to neurotransmitters and in turn release gliotransmitters that influence pre-and postsynaptic processes and information flow across the synapse (Araque et al., 1999). Whether the tripartite synapse is unique to hippocampus or ubiquitous throughout the brain, as well as the function of glia within the synapse *in vivo* remains to be determined.

1.5.2 Astrocytes and neural networks

The role of astrocytes within the central respiratory network remains unclear. Functioning glia are necessary for maintenance of respiratory rhythm *in vitro* (Hulsmann et al., 2000), but these data primarily emphasize the importance of astrocytes as a critical source of glutamine, which is required by the excitatory inspiratory neurons to produce glutamate. In fact, when inspiratory rhythm fails in the presence of glial-toxins, rhythm can be restored by adding glutamine to the bathing media (Hulsmann et al., 2000). There are at least three populations of astrocytes in the ventral medulla (Grass et al., 2004). The first two populations have an important role buffering excess glutamate and K⁺ buffering with non-rectifying, symmetrical, voltage-independent K⁺ currents or A-type K⁺ currents. The third group was an NG-2 like glia progenitor cell that has outward rectifying K⁺ currents. The function of these types of glia cells within the medulla remains unclear.

Despite evidence that astrocytes influence neuronal excitability *in situ*, understanding the role of gliotransmission in controlling the activity of neural networks underlying complex behaviors remains limited (Zhang et al., 2003; Haydon and Carmignoto, 2006; Halassa et al., 2009; Halassa and Haydon) and controversial (Agulhon et al., 2008; Agulhon et al., 2010; Kirchhoff, 2010). In this thesis I will look at the role of glia and gliotransmission in purinergic signaling as it relates to the control of breathing. Glia in many brain regions express P2 receptors (Verkhratsky et al., 2009; Halassa and Haydon, 2010; Koles et al.,

2011) and consequently we hypothesize that glia within the preBötC do as well. Whether gliotransmission occurs in the preBötC and influences preBötC activity remains to be determined (Ballanyi et al., 2010). There is growing evidence that gliotransmission modulates neuronal activity and may have a role in regulating physiological processes. Gliotransmission, via Ca-dependent exocytotic mechanisms, appears to play an important role in sleep homeostasis (Halassa et al., 2010) and basal mechanical nociception (Foley et al., 2011). Due to the difficulty of manipulating neurotransmission versus gliotransmission the physiological significance of gliotransmission in modulating activity of functionally behaving, mammalian neural networks remains poorly understood.

1.6 Chemoreception

The responsiveness of central respiratory network chemosensory afferent feedback is key to its primary physiological function of maintaining homeostatic control over CO₂, pH and O₂ levels in the blood and brain. There are two groups of chemoreceptors, which use CO₂/pH signals as a measure of the acid-base status of the blood and brain and reflect the adequacy of breathing relative to metabolism. The peripheral chemoreceptors, located in the carotid bodies and aortic bodies (in some species) are the primary oxygen sensors of the body but also respond to changes in CO₂/pH in the arterial blood. Changes in arterial PO₂, PCO₂ and pH are transduced into increased action potential discharge in the carotid sinus nerve to the NTS and ultimately to central respiratory networks that respond with changes in ventilation appropriate to restore O₂ or CO₂/pH homeostasis (Nattie, 2001; Guyenet et al., 2008).

Central chemoreceptors respond to CO₂/pH and are believed to be located at a variety of locations in the brainstem. Central chemosensitive neurons are hypothesized to express a variety of acid-sensitive ion channels that underlie their depolarization and increased discharge when brain pH decreases (Guyenet, 2008). The increased discharge excites the respiratory controller causing an homeostatic increase in ventilation and compensatory

decrease in CO₂ and increase in pH. New data point to the existence of O₂ sensors in the brain that contribute to the hypoxic ventilatory response but the site of these sensors, their mechanism of detection and influence on breathing are poorly understood. This is one area that will be explored in this thesis - specifically the role of central purinergic signaling in the hypoxic ventilatory response.

1.6.1 Peripheral chemoreception

Peripheral chemoreceptors are neurosecretory glomus cells located in the carotid bodies of all mammalian species and in the aortic arch of some species (i.e. present in man and cat, but not in rabbit, rat or mouse) (Spyer and Gourine, 2009). The peripheral chemoreceptors are thought to primarily be oxygen-sensing organs, however they contribute to about a third of the overall CO₂/pH response (Forster et al., 2008; Smith et al., 2010). CO₂ detection occurs by acid-sensitive K⁺ channels in glomus cells, which release ATP and ACh to activate the carotid sinus afferents (Rong et al., 2003). The glossopharyngeal nerve relays info to the NTS, where the information is processed and distributed causing changes in respiratory activity graded with stimulus intensity. In contrast the O₂ sensing mechanism in peripheral chemoreceptors is not well understood (for review see (Kemp, 2006; Kumar and Prabhakar, 2007). Hypoxia is thought to result in the rapid inhibition of K⁺ channels in the glomus cells leading to cell depolarization, induction of ATP and ACh release followed by the activation of afferent terminals in the carotid sinus nerve, and increased discharge. This feedback synapses in the NTS and radiating from there somehow influences brainstem respiratory networks to increase ventilation (Zec and Kinney, 2003). There may be several mechanisms involved in transducing the hypoxic stimulus into increased carotid sinus nerve activity (Blain et al., 2010; Smith et al., 2010). Hypoxia-evoked ATP release has been detected from carotid body cultures, slices and whole-mounts *in vitro* (Buttigieg and Nurse, 2004). The hypoxic ventilatory response and hypoxic sensitivity of the isolated carotid body and whole-animal response is severely blunted in P2X₂ knockout mice suggesting ATP

binds primarily to P2X₂ but also P2X₃Rs on the carotid sinus nerve afferent fibers (Rong et al., 2003).

1.6.2 Central chemoreception

There are several sites in the brainstem contributing to central chemoreception including the caudal NTS, dorsal motor nucleus of the vagus, rostroventrolateral medulla, preBötC, medullary raphe, locus coeruleus, and RTN (Nattie, 1999; Guyenet, 2008). There are two main theories describing the organization of central chemoreceptive networks. One describes a distributed network of multiple chemosensitive areas that each feed separately into the respiratory controller to evoke respiratory responses in accordance with CO₂/pH levels in the respective area. This arrangement would result in a network with multiple redundancies such that failure in one area alone would not have a devastating impact.

Consistent with this organization, lesions of RTN (glutamatergic), raphe (serotonergic), locus ceruleus (noradrenergic) or medullary neurons (NK1) all produce reductions in CO₂ chemosensitivity (Nattie and Li, 2009), but none abolishes central CO₂ chemosensitivity. However, it still remains unclear whether all these regions are functional respiratory chemoreceptors. For example, reduced CO₂ sensitivity following raphe lesions could reflect that raphe neurons provide excitatory drive to chemosensory cells, but are not chemosensors themselves.

The second leading hypothesis is that the RTN acid sensitive neurons are the primary chemoreceptor cells, which detect changes in CO₂ and pH in the CNS. Through direct inputs to the respiratory network, adjust breathing accordingly and maintain the stability of arterial PCO₂ (Guyenet, 2008). In this model, the RTN is also a key integrative site into which all other central chemosensitive regions feed. In the context of CO₂/pH, RTN output to the respiratory controller therefore represents the key homeostatic signal to the respiratory controller. Whether the RTN serves this key integrating function or is simply one of several chemosensory sites, however, remains unclear (Guyenet, 2008; Nattie and Li, 2009; Dean

and Putnam, 2010; Gargaglioni et al., 2010). Compelling evidence that the RTN is a key chemosensitive region is the discovery that CCHS patients who lack CO₂ sensitivity lack Phox2b neurons and the chemosensory cells in the RTN are Phox2b neurons (Guyenet et al., 2010).

In the context of this thesis, there is some evidence for the involvement of both purinergic modulation and glia cells in central chemoreception. ATP is implicated in the central hypercapnic response, as elevated CO₂ evokes ATP release from chemosensitive areas of the ventral surface of the medulla, specifically the RTN and raphe, and this ATP release contributes to the CO₂-evoked increase in phrenic nerve discharge; i.e. application of PPADS reduces the ventilatory response to CO₂ (Gourine et al., 2005a). The cellular source of ATP evoked by CO₂ has recently been addressed using adenoviral vectors with a GFAP promoter, which allowed the expression of a genetically encoded calcium indicator (*Case12*) specifically within glia in the RTN (Gourine et al., 2010). This transgenic approach revealed that astrocytes in the ventral surface chemoreceptor areas respond to decreases in pH by increasing Ca²⁺ and releasing ATP via an exocytotic mechanism. Furthermore, the ATP release activated phox2b positive RTN chemoreceptor neurons, ultimately increasing breathing frequency. Using optogenetics, photoactivation of channel rhodopsin 2-expressing astrocytes activated phox2b positive chemoreceptor neurons through an ATP dependent mechanism. Complimentary experiments showed that photoactivation of these glial cells also increased respiration *in vivo*. This study illustrates the important role of astrocytes and purinergic signaling in the hypercapnic ventilatory response. Astrocytes on the ventral surface also appear to release ATP in response to CO₂ through a Ca²⁺-independent mechanism (Huckstepp et al., 2010a; Huckstepp et al., 2010b). Using slices containing the ventral surface of the medulla, this study found that CO₂ dependent ATP release occurs without acidification and may occur via opening of a connexin 26 (Cx26) gap junction hemichannel. Genetically tagged glia limitans cells in the ventral medulla expressing Cx26 were shown to exhibit a large fluorescent signal in response to elevated CO₂, suggesting the

involvement of large diameter channel like hemichannels. *In vivo* pharmacological block of hemichannels dramatically reduced ATP release and attenuated the hypoxic ventilatory response (Huckstepp et al., 2010b) by ~25%, suggesting that Cx26 contributes to the release of ATP in response to CO₂. The importance of these pH and CO₂ detection mechanisms and the contribution of ATP release to the hypercapnic ventilatory response still remains to be determined.

The release of ATP from the RTN during the hypercapnic response does not fall within the area of specific interest to this thesis, the preBötC. In contrast, analysis of horizontal medullary slices show that during hypoxia ATP is released from deeper regions including the ventral respiratory column and the preBötC during the early stages of the secondary hypoxic ventilatory depression (Gourine et al., 2005b). Consequently, I next discuss the hypoxic ventilatory response and current evidence supporting a role for glia and ATP in this response.

1.6.3 Hypoxic ventilatory response

The ventilatory response to hypoxia is biphasic, consisting of an initial increase in ventilation (augmentation phase) followed by a secondary respiratory depression (depression phase). This depression phase is often accompanied by a decrease in temperature and metabolism and can be fatal in premature and newborn infants (Mortola, 1996; Mortola and Saiki, 1996; Waters and Gozal, 2003). This is because the depressive phase can produce fatal apneas when ventilation falls below baseline levels in premature and neonatal infants (Bissonnette, 2000). The depressive phase in moderate hypoxia (~10%) changes developmentally such that in more mature animals ventilation no longer falls below baseline during the depressive phase (Richter et al., 1991; Bissonnette, 2000). The initial increase in ventilation in the augmentation phase is largely due to peripheral chemoreceptors detecting the low O₂ and increasing synaptic drive to the central respiratory network (Guyenet et al., 2010). Centrally acting ATP does not appear to play a role in the hypoxia-induced increase in

frequency, however without ATP peripherally at P2X₂Rs there is no hypoxic ventilatory response (Rong et al., 2003).

ATP may have a role in shaping the secondary hypoxic ventilatory depression. The use of ATP biosensors in anesthetized adult rats suggests that ATP is released on the ventral surface of the brainstem during systemic hypoxia (10% oxygen in the inspired air) (Gourine et al., 2005b). This increase in ATP increased ~25 seconds after the onset of the hypoxic ventilatory response and occurred even after sinoaortic denervation and vagotomy. When P2 receptors were blocked the secondary hypoxic ventilatory depression was increased, further implicating ATP in offsetting the magnitude of the hypoxic ventilatory depression.

Given that ATP appears to be released in the brainstem during hypoxia and is implicated in shaping the hypoxic ventilatory response (Gourine et al., 2005b), our lab has investigated the mechanism of ATP action within the preBötC (Lorier et al., 2007; Lorier et al., 2008; Huxtable et al., 2009). The cellular mediators of ATP actions in the medulla are unknown. Neurons in the ventral respiratory column have immunoreactivity for P2X₁₋₆ and P2Y₁Rs (Kanjhan et al., 1999; Yao et al., 2000; Lorier et al., 2004). Our lab had found that there is a potent P2Y₁R-mediated excitatory mechanism in the preBötC of neonatal rats as ATP is excitatory when applied via bath application to the medulla (Lorier et al., 2004) or locally to the preBötC *in vitro* (Lorier et al., 2007). ATP weakly excites the majority of preBötC pacemaker inspiratory neurons. The ATP-evoked frequency increase in the preBötC is P2Y₁R mediated as there are P2Y₁R on preBötC neurons and the response is abolished with the P2Y₁R antagonist MRS 2179. The preBötC appears to be particularly sensitive to P2Y₁R modulation as it is ~ 100 fold and ~1000 more sensitive than the XII MN pool (Funk et al., 1997) and phrenic MN pool respectively (Miles et al., 2002; Funk et al., 2008). The weak excitation exhibited by neurons in the preBötC suggests that the ATP evoked frequency increase in the preBötC inspiratory network is not exclusively mediated by P2Y₁R actions of neurons. *In vivo*, local application of ATP to the ventral surface of the medulla of anaesthetized ventilated adult rats increases the activity of expiratory and inspiratory neurons

in the medulla (Gourine et al., 2003). These respiratory neurons expressed P2XR and the ATP mediated response was abolished with suramin suggesting that P2XR (and P2YR) may have a role in the ATP response. However, the ability to block the ATP-evoked response *in vitro* with a specific P2Y₁R antagonist, suggests that P2XR do not have a prominent role. In contrast, another study found that injection of ATP into the ventral medulla produced apnea (Thomas et al., 2001). However, the effects of ATP *in vitro* are specific to the preBötC *in vitro* (Lorier et al., 2007); Thomas et al. 2001 did not identify the site of ATP application *in vivo*. A study by Gourine et al. 2005 showed that exogenous application of ATP into the ventral medulla rostral to the preBötC produced apnea however the site of injection was not confirmed (Gourine et al., 2005a). Given the inconsistency between individual neuronal responses, that the sites from which most network responses were evoked were not anatomically identified, and that ATP activates glia (Zhang et al., 2003; Gordon et al., 2005; Espallergues et al., 2007) this thesis will examine the involvement of glia cells in the preBötC network response to ATP.

Application of ATP to the preBötC of the neonatal rat *in vitro* prep produces a 2-4 fold increase in inspiratory burst frequency followed by a brief 20% frequency decrease which appears to be dependent on ATP hydrolysis in that the depression is not evoked by the hydrolysis-resistant ATP analogue ATPγS (Lorier et al., 2007). It is possible that the lack of an inhibition with ATPγS reflects the slightly different P2R agonist profiles of ATP and ATPγS. A role for ADO in the inhibition is further supported by the observation in embryonic rats that ADO antagonists enhance the ATP-evoked frequency increase and on their own cause a significant increase in frequency, consistent with a basal inhibitory ADO tone (Huxtable et al., 2009). Importantly, this ADO-mediated inhibition is developmentally regulated, as it is only apparent in rhythmically active slices from embryonic but not postnatal rats (Huxtable et al., 2009). Similarly, in brainstem spinal cord preparations from rat it is not observed beyond postnatal day 3 (Lagercrantz et al., 1984). However, species variability must be considered because ADO inhibits the activity of preBötC inspiratory

neurons in the mouse via an A1 receptor-, cAMP-dependent mechanism up to at least postnatal day 14 (Mironov et al., 1999).

Extracellular ADO, derived from ATP hydrolysis or transport from intracellular stores via the equilibrative nucleoside transporter may also be an important contributor to the secondary hypoxic ventilatory depression (for review see (Ballanyi, 2004; Herlenius and Lagercrantz, 2004)). ADO depresses respiration in fetal (Bissonnette et al., 1990; Koos et al., 1994), newborn (Lagercrantz et al., 1984) and adult mammals (Yamamoto et al., 1994). More importantly, ADO antagonists can reduce or eliminate the hypoxia-induced respiratory depression in fetal and newborn preparations (Runold et al., 1989; Bissonnette et al., 1990; Koos et al., 2005). While multiple studies suggest that ADO plays an important role in the secondary hypoxic respiratory depression, there is great variability in species response to ADO antagonists (reviewed in (Ballanyi, 2004; Funk et al., 2008)). Thus, it is unlikely that ADO is the sole mediator of the depressive phase. Indeed, GABA may be a significant contributor (Ballanyi et al., 1999; Ballanyi, 2004; Mayer et al., 2006; Funk et al., 2008). It is clear that respiratory depression is most pronounced in fetal/newborn mammals, which also holds true for premature or newborn human infants.

While ADO appears to have a role in the hypoxia-induced secondary respiratory depression, the mechanism and site of action of ADO remain unclear. Two mechanisms may be involved; an A2aR-mediated excitation of GABAergic neurons that inhibit respiratory networks via GABA_ARs and an A1R-mediated inhibition that appears to have both pre and postsynaptic components. However the importance of these two mechanisms to the ADO-mediated inhibition of breathing is not clear, and is likely both species- and developmentally-dependent. An A2 or A2aR agonist-evoked respiratory inhibition is primarily detected under *in vivo* conditions when systemic or cerebroventricular administration provides drug access throughout the central nervous system (Wilson et al., 2004; Koos et al., 2005; Mayer et al., 2006). Reduced brainstem spinal cord preparations in neonatal rodents have failed to show A2aR-mediated inhibition (Herlenius et al., 1997; Mironov et al., 1999) suggesting this

inhibition may be outside the brainstem network or may emerge later in development. A1R appear to be involved in the inhibition of breathing by ADO as vascular or central administration of A1R agonists produce inhibition of breathing (Hedner et al., 1985; Runold et al., 1986). In anesthetized cats *in vivo* (Schmidt et al., 1995) the use of an A1R antagonist to increase or reduce the hypoxic depression, suggest a role for A1Rs. However in fetal and newborn sheep there may be a different mechanism as A2a antagonist application throughout the CNS blocked respiratory depression (Koos et al., 2005). The site of the inhibitory effects of ADO during hypoxia also remains unclear, but multiple sites may contribute.

Identification of the site of ADO action is a challenge (Bissonnette, 2000). A reduction in the frequency of rhythmic bursts generated by preBötC islands and an inhibition of preBötC inspiratory neurons by A1Rs in mice (Mironov et al., 1999; Vandam et al., 2008) both suggest that A1Rs in the preBötC contribute to the ADO-mediated frequency inhibition however the effects on frequency have not been established. ADO has been reported to have no effect on brainstem rhythm in rat (Brockhaus and Ballanyi, 2000; Ballanyi, 2004; Ruangkittisakul and Ballanyi, 2010) suggesting a possible species difference. Some transection experiments have suggested that sites rostral to the medulla may be implicated in the ADO actions on the central respiratory network (reviewed in (Bissonnette, 2000)), however, the VRC remains a candidate based on the respiratory inhibition evoked by ADO in this region in some species (see (Funk et al., 2008) for review). *In vitro* and *in vivo* experiments have mixed findings where some show inhibition of respiratory frequency (Mironov et al., 1999; Wang et al., 2005) while others do not see inhibition (Ballanyi et al., 1999). Ultimately, the mechanism and site of action of the secondary hypoxic ventilatory depression mediated by ADO within the central respiratory network needs to be determined. The entire three part signaling system should be examined as the source of extracellular ADO within respiratory regions, and the balance between the excitatory actions of ATP and the inhibitory actions of ADO within the medulla will determine the outcome of the hypoxic ventilatory response. Ectonucleotidases and regionally specific receptor expression will have

a critical role in regulating this balance. In this light, ectonucleotidase-mediated degradation of ATP can occur via neurons or glia. Equilibrative nucleoside transport of ADO or release of ADO by glia into the extracellular space may also significantly influence extracellular ADO levels (Martin et al., 2007). Consequently, in this thesis I will look at the ectonucleotidase activity, receptor sensitivity and the role of glia within the preBötC to better understand the mechanisms via which purinergic signaling contributes the hypoxic ventilatory response.

1.7 Thesis objectives

This introduction has provided a brief review of the central respiratory network, the components in the brainstem involved in respiratory rhythm generation, the components involved in the three part purinergic signaling system and our understanding of glia cells within the CNS. Purinergic signaling, potentially involving glia cells, has an important role in the homeostatic chemoreceptor functions of the central respiratory network. The overall objective of this thesis is to examine the influence of purinergic signaling on preBötC activity and its potential involvement in the hypoxic ventilatory response. I will examine how glia cells may contribute to this purinergic modulation, the dynamics of the three-part purinergic signaling system, purinergic signaling in the hypoxic ventilatory response *in vivo* and the influence of inflammatory processes on the central respiratory network.

Specific objectives were to test the hypothesis that:

- 1) Glia contribute to the excitatory action of ATP on preBötC inspiratory networks

This will be done by:

- a. Determining if glia from the preBötC respond to ATP
- b. Determining if glia release excitatory amino acids in response to ATP

2) Purinergic signaling mechanisms in the preBötC of rat and mouse are conserved

This will be done by:

- a. Determining if P2Y₁R excitatory mechanism is common to mouse and rat
- b. Determining if the PreBötC network of neonatal mouse but not rat is sensitive to adenosine inhibition
- c. Determining if ectonucleotidases expression in the preBötC is conserved across species

3) Sensitivity of the preBötC network to purinergic modulation extends beyond the perinatal period and has a role in the secondary hypoxic ventilatory depression

This will be done by:

- a. Determining if P2Y₁R modulation occurs in the preBötC of adult rat *in vivo*
- b. Determining if ADO modulation occurs in the preBötC of adult rat *in vivo*
- c. Determining if increased ATP breakdown affects the hypoxic ventilatory response of adult rat *in vivo*

4) TLR4 signaling cascades and microglia contribute to the opioid-induced respiratory depression

This will be done by:

- d. Determining if TLR4 activation modulates the activity of preBötC inspiratory rhythm generating networks *in vitro*
- e. Determining if TLR4- mediated glial mechanisms contribute to the opioid-induced depression of preBötC respiratory activity *in vitro* and *in vivo*
- f. Determining if microglia activation is required for the opioid-induced respiratory depression *in vitro*

1.8 References

- Abbott SB, Stornetta RL, Fortuna MG, Depuy SD, West GH, Harris TE, Guyenet PG (2009) Photostimulation of retrotrapezoid nucleus phox2b-expressing neurons in vivo produces long-lasting activation of breathing in rats. *J Neurosci* 29:5806-5819.
- Abbracchio MP, Ceruti S (2006) Roles of P2 receptors in glial cells: focus on astrocytes. *Purinergic Signal* 2:595-604.
- Abdala AP, Rybak IA, Smith JC, Paton JF (2009) Abdominal expiratory activity in the rat brainstem-spinal cord in situ: patterns, origins and implications for respiratory rhythm generation. *J Physiol* 587:3539-3559.
- Agulhon C, Fiacco TA, McCarthy KD (2010) Hippocampal short- and long-term plasticity are not modulated by astrocyte Ca²⁺ signaling. *Science* 327:1250-1254.
- Agulhon C, Petracic J, McMullen AB, Sweger EJ, Minton SK, Taves SR, Casper KB, Fiacco TA, McCarthy KD (2008) What is the role of astrocyte calcium in neurophysiology? *Neuron* 59:932-946.
- Agulhon C, Petracic, J., McMullen, A.B., Sweger, E.J., Minton, S.K., Taves, S.R., Casper, K.B., Fiacco, T.A., McCarthy, K.D. (2008) What is the role of astrocyte calcium in neurophysiology? *Neuron* 59:932-946.
- Allen NJ, Barres BA (2005) Signaling between glia and neurons: focus on synaptic plasticity. *Curr Opin Neurobiol* 15:542-548.
- Araque A, Parpura V, Sanzgiri RP, Haydon PG (1999) Tripartite synapses: glia, the unacknowledged partner. *Trends Neurosci* 22:208-215.
- Attwell D, Buchan AM, Charpak S, Lauritzen M, Macvicar BA, Newman EA (2010) Glial and neuronal control of brain blood flow. *Nature* 468:232-243.

- Ballanyi K (2004) Neuromodulation of the perinatal respiratory network. Current Neuropharmacology 2:221-243.
- Ballanyi K, Onimaru H, Homma I (1999) Respiratory network function in the isolated brainstem-spinal cord of newborn rats. Prog Neurobiol 59:583-634.
- Ballanyi K, Panaiteescu B, Ruangkittisakul A (2010) Control of breathing by "nerve glue". Sci Signal 3:pe41.
- Barres BA (2008) The mystery and magic of glia: a perspective on their roles in health and disease. Neuron 60:430-440.
- Beck A, Nieden RZ, Schneider HP, Deitmer JW (2004) Calcium release from intracellular stores in rodent astrocytes and neurons *in situ*. Cell Calcium 35:47-58.
- Bianchi AL, St John WM (1981) Pontile axonal projections of medullary respiratory neurons. Respir Physiol 45:167-183.
- Bianchi AL, St John WM (1982) Medullary axonal projections of respiratory neurons of pontile pneumotaxic center. Respir Physiol 48:357-373.
- Bissonnette JM (2000) Mechanisms regulating hypoxic respiratory depression during fetal and postnatal life. Am J Physiol Regul Integr Comp Physiol 278:R1391-1400.
- Bissonnette JM, Hohimer AR, Chao CR, Knopp SJ, Notoroberto NF (1990) Theophylline stimulates fetal breathing movements during hypoxia. Pediatr Res 28:83-86.
- Blain GM, Smith CA, Henderson KS, Dempsey JA (2010) Peripheral chemoreceptors determine the respiratory sensitivity of central chemoreceptors to CO₂. J Physiol 588:2455-2471.

- Blanchi B, Kelly LM, Viemari JC, Lafon I, Burnet H, Bevengut M, Tillmanns S, Daniel L, Graf T, Hilaire G, Sieweke MH (2003) MafB deficiency causes defective respiratory rhythmogenesis and fatal central apnea at birth. *Nat Neurosci* 6:1091-1100.
- Bochorishvili G, Stornetta RL, Coates MB, Guyenet PG (2012) Pre-Botzinger complex receives glutamatergic innervation from galaninergic and other retrotrapezoid nucleus neurons. *J Comp Neurol* 520:1047-1061.
- Bonham AC, McCrimmon DR (1990) Neurones in a discrete region of the nucleus tractus solitarius are required for the Breuer-Hering reflex in rat. *J Physiol* 427:261-280.
- Borday V, Foutz AS, Nordholm L, Denavit-Saubie M (1998) Respiratory effects of glutamate receptor antagonists in neonate and adult mammals. *Eur J Pharmacol* 348:235-246.
- Bouvier J, Thoby-Brisson M, Renier N, Dubreuil V, Ericson J, Champagnat J, Pierani A, Chedotal A, Fortin G (2010) Hindbrain interneurons and axon guidance signaling critical for breathing. *Nat Neurosci* 13:1066-1074.
- Braun N, Sevigny J, Mishra SK, Robson SC, Barth SW, Gerstberger R, Hammer K, Zimmermann H (2003) Expression of the ecto-ATPase NTPDase2 in the germinal zones of the developing and adult rat brain. *Eur J Neurosci* 17:1355-1364.
- Brockhaus J, Ballanyi K (2000) Anticonvulsant A(1) receptor-mediated adenosine action on neuronal networks in the brainstem-spinal cord of newborn rats. *Neuroscience* 96:359-371.
- Brosenitsch TA, Adachi T, Lipski J, Housley GD, Funk GD (2005) Developmental downregulation of P2X3 receptors in motoneurons of the compact formation of the nucleus ambiguus. *Eur J Neurosci* 22:809-824.

- Burnstock G (2006) Historical review: ATP as a neurotransmitter. *Trends Pharmacol Sci* 27:166-176.
- Burnstock G (2007a) Physiology and pathophysiology of purinergic neurotransmission. *Physiol Rev* 87:659-797.
- Burnstock G (2007b) Purine and pyrimidine receptors. *Cellular and molecular life sciences : CMLS* 64:1471-1483.
- Burnstock G, Fredholm BB, Verkhratsky A (2011) Adenosine and ATP receptors in the brain. *Curr Top Med Chem* 11:973-1011.
- Butt AM, Kalsi A (2006) Inwardly rectifying potassium channels (Kir) in central nervous system glia: a special role for Kir4.1 in glial functions. *J Cell Mol Med* 10:33-44.
- Buttigieg J, Nurse CA (2004) Detection of hypoxia-evoked ATP release from chemoreceptor cells of the rat carotid body. *Biochemical and biophysical research communications* 322:82-87.
- Cao Y, Song G (2007) Purinergic modulation of respiration via medullary raphe nuclei in rats. *Respir Physiol Neurobiol* 155:114-120.
- Cornell-Bell AH, Finkbeiner SM, Cooper MS, Smith SJ (1990) Glutamate induces calcium waves in cultured astrocytes: long-range glial signaling. *Science* 247:470-473.
- Danbolt NC (2001) Glutamate uptake. *Prog Neurobiol* 65:1-105.
- Dani JW, Chernjavsky A, Smith SJ (1992) Neuronal activity triggers calcium waves in hippocampal astrocyte networks. *Neuron* 8:429-440.
- Dauger S, Pattyn A, Lofaso F, Gaultier C, Goridis C, Gallego J, Brunet JF (2003) Phox2b controls the development of peripheral chemoreceptors and afferent visceral pathways. *Development* 130:6635-6642.

- Dean JB, Putnam RW (2010) The caudal solitary complex is a site of central CO₂ chemoreception and integration of multiple systems that regulate expired CO₂. *Respir Physiol Neurobiol* 173:274-287.
- Deitmer JW, Verkhratsky AJ, Lohr C (1998) Calcium signalling in glial cells. *Cell Calcium* 24:405-416.
- Del Negro CA, Morgado-Valle C, Feldman JL (2002) Respiratory rhythm: an emergent network property? *Neuron* 34:821-830.
- Del Negro CA, Johnson SM, Butera RJ, Smith JC (2001) Models of respiratory rhythm generation in the pre-Botzinger complex. III. Experimental tests of model predictions. *J Neurophysiol* 86:59-74.
- Del Negro CA, Hayes JA, Pace RW, Brush BR, Teruyama R, Feldman JL (2010) Synaptically activated burst-generating conductances may underlie a group-pacemaker mechanism for respiratory rhythm generation in mammals. *Prog Brain Res* 187:111-136.
- Del Negro CA, Morgado-Valle C, Hayes JA, Mackay DD, Pace RW, Crowder EA, Feldman JL (2005) Sodium and calcium current-mediated pacemaker neurons and respiratory rhythm generation. *J Neurosci* 25:446-453.
- Depuy SD, Kanbar R, Coates MB, Stornetta RL, Guyenet PG (2011) Control of breathing by raphe obscurus serotonergic neurons in mice. *J Neurosci* 31:1981-1990.
- Duan S, Anderson CM, Keung EC, Chen Y, Swanson RA (2003) P2X7 receptor-mediated release of excitatory amino acids from astrocytes. *J Neurosci* 23:1320-1328.

Dutschmann M, Herbert H (2006) The Kolliker-Fuse nucleus gates the postinspiratory phase of the respiratory cycle to control inspiratory off-switch and upper airway resistance in rat. *Eur J Neurosci* 24:1071-1084.

Espallergues J, Solovieva O, Techer V, Bauer K, Alonso G, Vincent A, Hussy N (2007) Synergistic activation of astrocytes by ATP and norepinephrine in the rat supraoptic nucleus. *Neuroscience* 148:712-723.

Feldman JL, Smith JC (1989) Cellular mechanisms underlying modulation of breathing pattern in mammals. *Ann N Y Acad Sci* 563:114-130.

Feldman JL, Del Negro CA (2006) Looking for inspiration: new perspectives on respiratory rhythm. *Nat Rev Neurosci* 7:232-242.

Feldman JL, Janczewski WA (2006) Point:Counterpoint: The parafacial respiratory group (pFRG)/pre-Botzinger complex (preBotC) is the primary site of respiratory rhythm generation in the mammal. Counterpoint: the preBotC is the primary site of respiratory rhythm generation in the mammal. *J Appl Physiol* 100:2096-2097; discussion 2097-2099, 2103-2098.

Feldman JL, Mitchell GS, Nattie EE (2003) Breathing: rhythmicity, plasticity, chemosensitivity. *Annu Rev Neurosci* 26:239-266.

Feldman JL, Smith JC, Ellenberger HH, Connelly CA, Liu GS, Greer JJ, Lindsay AD, Otto MR (1990) Neurogenesis of respiratory rhythm and pattern: emerging concepts. *Am J Physiol* 259:R879-886.

Fiacco TA, McCarthy KD (2006) Astrocyte calcium elevations: properties, propagation, and effects on brain signaling. *Glia* 54:676-690.

- Fields RD, Burnstock G (2006) Purinergic signalling in neuron-glia interactions. *Nat Rev Neurosci* 7:423-436.
- Finkbeiner S (1992) Calcium waves in astrocytes-filling in the gaps. *Neuron* 8:1101-1108.
- Foley JC, McIver SR, Haydon PG (2011) Gliotransmission modulates baseline mechanical nociception. *Mol Pain* 7:93.
- Forster HV, Martino P, Hodges M, Krause K, Bonis J, Davis S, Pan L (2008) The carotid chemoreceptors are a major determinant of ventilatory CO₂ sensitivity and of PaCO₂ during eupneic breathing. *Adv Exp Med Biol* 605:322-326.
- Foutz AS, Champagnat J, Denavit-Saubie M (1988) N-methyl-D-aspartate (NMDA) receptors control respiratory off-switch in cat. *Neurosci Lett* 87:221-226.
- Fumagalli M, Brambilla R, D'Ambrosi N, Volonte C, Matteoli M, Verderio C, Abbracchio MP (2003) Nucleotide-mediated calcium signaling in rat cortical astrocytes: Role of P2X and P2Y receptors. *Glia* 43:218-203.
- Funk GD, Huxtable AG, Lorier AR (2008) ATP in central respiratory control: A three-part signaling system. *Respir Physiol Neurobiol*.
- Funk GD, Kanjhan R, Walsh C, Lipski J, Comer AM, Parkis MA, Housley GD (1997) P2 receptor excitation of rodent hypoglossal motoneuron activity in vitro and in vivo: a molecular physiological analysis. *J Neurosci* 17:6325-6337.
- Gargaglioli LH, Hartzler LK, Putnam RW (2010) The locus coeruleus and central chemosensitivity. *Respir Physiol Neurobiol* 173:264-273.
- Gegelashvili G, Danbolt NC, Schousboe A (1997) Neuronal soluble factors differentially regulate the expression of the GLT1 and GLAST glutamate transporters in cultured astroglia. *J Neurochem* 69:2612-2615.

- Ghildyal P, Manchanda R (2004) Effects of cooling and ARL 67156 on synaptic ecto-ATPase activity in guinea pig and mouse vas deferens. Autonomic neuroscience : basic & clinical 115:28-34.
- Giaume C, Koulakoff A, Roux L, Holcman D, Rouach N (2010) Astroglial networks: a step further in neuroglial and gliovascular interactions. Nat Rev Neurosci 11:87-99.
- Gordon GR, Baimoukhamedova DV, Hewitt SA, Rajapaksha WR, Fisher TE, Bains JS (2005) Norepinephrine triggers release of glial ATP to increase postsynaptic efficacy. Nat Neurosci 8:1078-1086.
- Gourine AV, Kasparov S (2011) Astrocytes as brain interoceptors. Exp Physiol 96:411-416.
- Gourine AV, Atkinson L, Deuchars J, Spyer KM (2003) Purinergic signalling in the medullary mechanisms of respiratory control in the rat: respiratory neurones express the P2X2 receptor subunit. J Physiol 552:197-211.
- Gourine AV, Llaudet E, Dale N, Spyker KM (2005a) ATP is a mediator of chemosensory transduction in the central nervous system. Nature 436:108-111.
- Gourine AV, Llaudet E, Dale N, Spyker KM (2005b) Release of ATP in the ventral medulla during hypoxia in rats: role in hypoxic ventilatory response. J Neurosci 25:1211-1218.
- Gourine AV, Dale N, Korsak A, Llaudet E, Tian F, Huckstepp R, Spyker KM (2008) Release of ATP and glutamate in the nucleus tractus solitarius mediate pulmonary stretch receptor (Breuer-Hering) reflex pathway. J Physiol 586:3963-3978.
- Gourine AV, Kasymov V, Marina N, Tang F, Figueiredo MF, Lane S, Teschemacher AG, Spyker KM, Deisseroth K, Kasparov S (2010) Astrocytes control breathing through pH-dependent release of ATP. Science 329:571-575.

Grass D, Pawlowski PG, Hirrlinger J, Papadopoulos N, Richter DW, Kirchhoff F, Hulsmann S (2004) Diversity of functional astroglial properties in the respiratory network. *J Neurosci* 24:1358-1365.

Gray PA, Rekling JC, Bocchiaro CM, Feldman JL (1999) Modulation of respiratory frequency by peptidergic input to rhythmogenic neurons in the preBotzinger complex. *Science* 286:1566-1568.

Gray PA, Janczewski WA, Mellen N, McCrimmon DR, Feldman JL (2001) Normal breathing requires preBotzinger complex neurokinin-1 receptor-expressing neurons. *Nat Neurosci* 4:927-930.

Gray PA, Hayes JA, Ling GY, Llona I, Tupal S, Picardo MC, Ross SE, Hirata T, Corbin JG, Eugenin J, Del Negro CA (2010) Developmental origin of preBotzinger complex respiratory neurons. *J Neurosci* 30:14883-14895.

Guthrie PB, Knappenberger J, Segal M, Bennett MV, Charles AC, Kater SB (1999) ATP released from astrocytes mediates glial calcium waves. *J Neurosci* 19:520-528.

Guyenet PG (2008) The 2008 Carl Ludwig Lecture: retrotrapezoid nucleus, CO₂ homeostasis, and breathing automaticity. *J Appl Physiol* 105:404-416.

Guyenet PG, Mulkey DK (2010) Retrotrapezoid nucleus and parafacial respiratory group. *Respir Physiol Neurobiol* 173:244-255.

Guyenet PG, Stornetta RL, Bayliss DA (2008) Retrotrapezoid nucleus and central chemoreception. *J Physiol* 586:2043-2048.

Guyenet PG, Stornetta RL, Bayliss DA (2010) Central respiratory chemoreception. *J Comp Neurol* 518:3883-3906.

Guyenet PG, Sevigny CP, Weston MC, Stornetta RL (2002) Neurokinin-1 receptor-expressing cells of the ventral respiratory group are functionally heterogeneous and predominantly glutamatergic. *J Neurosci* 22:3806-3816.

Guyenet PG, Bayliss DA, Stornetta RL, Fortuna MG, Abbott SB, DePuy SD (2009) Retrotrapezoid nucleus, respiratory chemosensitivity and breathing automaticity. *Respir Physiol Neurobiol* 168:59-68.

Halassa MM, Haydon PG (2010) Integrated brain circuits: astrocytic networks modulate neuronal activity and behavior. *Annu Rev Physiol* 72:335-355.

Halassa MM, Fellin T, Haydon PG (2009) Tripartite synapses: roles for astrocytic purines in the control of synaptic physiology and behavior. *Neuropharmacology* 57:343-346.

Halassa MM, Dal Maschio M, Beltramo R, Haydon PG, Benfenati F, Fellin T (2010) Integrated brain circuits: neuron-astrocyte interaction in sleep-related rhythmogenesis. *ScientificWorldJournal* 10:1634-1645.

Hamilton NB, Attwell D (2010) Do astrocytes really exocytose neurotransmitters? *Nat Rev Neurosci* 11:227-238.

Haydon PG (2001) GLIA: listening and talking to the synapse. *Nat Rev Neurosci* 2:185-193.

Haydon PG, Carmignoto G (2006) Astrocyte control of synaptic transmission and neurovascular coupling. *Physiol Rev* 86:1009-1031.

He F, Sun YE (2007) Glial cells more than support cells? *Int J Biochem Cell Biol* 39:661-665.

Hedner T, Hedner J, Bergman B, Mueller RA, Jonason J (1985) Characterization of adenosine-induced respiratory depression in the preterm rabbit. *Biology of the neonate* 47:323-332.

- Heine P, Braun N, Heilbronn A, Zimmermann H (1999) Functional characterization of rat ecto-ATPase and ecto-ATP diphosphohydrolase after heterologous expression in CHO cells. *Eur J Biochem* 262:102-107.
- Herlenius E, Lagercrantz H (2004) Development of neurotransmitter systems during critical periods. *Exp Neurol* 190 Suppl 1:S8-21.
- Herlenius E, Lagercrantz H, Yamamoto Y (1997) Adenosine modulates inspiratory neurons and the respiratory pattern in the brainstem of neonatal rats. *Pediatr Res* 42:46-53.
- Huckstepp RT, Eason R, Sachdev A, Dale N (2010a) CO₂-dependent opening of connexin 26 and related beta connexins. *J Physiol* 588:3921-3931.
- Huckstepp RT, id Bihi R, Eason R, Spyer KM, Dicke N, Willecke K, Marina N, Gourine AV, Dale N (2010b) Connexin hemichannel-mediated CO₂-dependent release of ATP in the medulla oblongata contributes to central respiratory chemosensitivity. *J Physiol* 588:3901-3920.
- Hulsmann S, Oku Y, Zhang W, Richter DW (2000) Metabolic coupling between glia and neurons is necessary for maintaining respiratory activity in transverse medullary slices of neonatal mouse. *Eur J Neurosci* 12:856-862.
- Huxtable AG, Zwicker JD, Poon BY, Pagliardini S, Vrouwe SQ, Greer JJ, Funk GD (2009) Tripartite purinergic modulation of central respiratory networks during perinatal development: the influence of ATP, ectonucleotidases, and ATP metabolites. *J Neurosci* 29:14713-14725.
- Iadecola C, Nedergaard M (2007) Glial regulation of the cerebral microvasculature. *Nat Neurosci* 10:1369-1376.

- Illes P, Verkhratsky A, Burnstock G, Franke H (2011) P2X Receptors and Their Roles in Astroglia in the Central and Peripheral Nervous System. *The Neuroscientist* : a review journal bringing neurobiology, neurology and psychiatry.
- Janczewski WA, Feldman JL (2006) Distinct rhythm generators for inspiration and expiration in the juvenile rat. *J Physiol* 570:407-420.
- Jiang C, Lipski J (1990) Extensive monosynaptic inhibition of ventral respiratory group neurons by augmenting neurons in the Botzinger complex in the cat. *Exp Brain Res* 81:639-648.
- Kanbar R, Stornetta RL, Cash DR, Lewis SJ, Guyenet PG (2010) Photostimulation of Phox2b medullary neurons activates cardiorespiratory function in conscious rats. *Am J Respir Crit Care Med* 182:1184-1194.
- Kang J, Jiang L, Goldman SA, Nedergaard M (1998) Astrocyte-mediated potentiation of inhibitory synaptic transmission. *Nat Neurosci* 1:683-692.
- Kanjhan R, Housley GD, Burton LD, Christie DL, Kippenberger A, Thorne PR, Luo L, Ryan AF (1999) Distribution of the P2X2 receptor subunit of the ATP-gated ion channels in the rat central nervous system. *J Comp Neurol* 407:11-32.
- Kegel B, Braun N, Heine P, Maliszewski CR, Zimmermann H (1997) An ecto-ATPase and an ecto-ATP diphosphohydrolase are expressed in rat brain. *Neuropharmacology* 36:1189-1200.
- Kemp PJ (2006) Detecting acute changes in oxygen: will the real sensor please stand up? *Exp Physiol* 91:829-834.
- Kettenmann H, Sonnhof U, Schachner M (1983) Exclusive potassium dependence of the membrane potential in cultured mouse oligodendrocytes. *J Neurosci* 3:500-505.

- Kimelberg HK, Goderie SK, Higman S, Pang S, Waniewski RA (1990) Swelling-induced release of glutamate, aspartate, and taurine from astrocyte cultures. *J Neurosci* 10:1583-1591.
- Kirchhoff F (2010) Neuroscience. Questionable calcium. *Science* 327:1212-1213.
- Koles L, Leichsenring A, Rubini P, Illes P (2011) P2 receptor signaling in neurons and glial cells of the central nervous system. *Adv Pharmacol* 61:441-493.
- Kong W, Engel K, Wang J (2004) Mammalian nucleoside transporters. *Curr Drug Metab* 5:63-84.
- Koos BJ, Mason BA, Punla O, Adinolfi AM (1994) Hypoxic inhibition of breathing in fetal sheep: relationship to brain adenosine concentrations. *J Appl Physiol* 77:2734-2739.
- Koos BJ, Kawasaki Y, Kim YH, Bohorquez F (2005) Adenosine A2A-receptor blockade abolishes the roll-off respiratory response to hypoxia in awake lambs. *Am J Physiol Regul Integr Comp Physiol* 288:R1185-1194.
- Koshiya N, Smith JC (1999) Neuronal pacemaker for breathing visualized in vitro. *Nature* 400:360-363.
- Krolo M, Tonkovic-Capin V, Stucke AG, Stuth EA, Hopp FA, Dean C, Zuperku EJ (2005) Subtype composition and responses of respiratory neurons in the pre-botzinger region to pulmonary afferent inputs in dogs. *J Neurophysiol* 93:2674-2687.
- Kubin L, Alheid GF, Zuperku EJ, McCrimmon DR (2006) Central pathways of pulmonary and lower airway vagal afferents. *J Appl Physiol* 101:618-627.
- Kuffler SW, Nicholls JG (1966) The physiology of neuroglial cells. *Ergeb Physiol* 57:1-90.

- Kukulski F, Sevigny J, Komoszynski M (2004) Comparative hydrolysis of extracellular adenine nucleotides and adenosine in synaptic membranes from porcine brain cortex, hippocampus, cerebellum and medulla oblongata. *Brain Res* 1030:49-56.
- Kumar P, Prabhakar N (2007) Sensing hypoxia: carotid body mechanisms and reflexes in health and disease. *Respir Physiol Neurobiol* 157:1-3.
- Kvamme E, Torgner IA, Roberg B (2001) Kinetics and localization of brain phosphate activated glutaminase. *J Neurosci Res* 66:951-958.
- Lagercrantz H, Yamamoto Y, Fredholm BB, Prabhakar NR, von Euler C (1984) Adenosine analogues depress ventilation in rabbit neonates. Theophylline stimulation of respiration via adenosine receptors? *Pediatr Res* 18:387-390.
- Langer D, Hammer K, Koszalka P, Schrader J, Robson S, Zimmermann H (2008) Distribution of ectonucleotidases in the rodent brain revisited. *Cell Tissue Res* 334:199-217.
- Lavezzi AM, Matturri L (2008) Functional neuroanatomy of the human pre-Botzinger complex with particular reference to sudden unexplained perinatal and infant death. *Neuropathology : official journal of the Japanese Society of Neuropathology* 28:10-16.
- Lorier AR, Lipski J, Housley GD, Greer JJ, Funk GD (2008) ATP sensitivity of preBotzinger complex neurones in neonatal rat in vitro: mechanism underlying a P2 receptor-mediated increase in inspiratory frequency. *J Physiol* 586:1429-1446.
- Lorier AR, Peebles K, Brosenitsch T, Robinson DM, Housley GD, Funk GD (2004) P2 receptors modulate respiratory rhythm but do not contribute to central CO₂ sensitivity in vitro. *Respir Physiol Neurobiol* 142:27-42.

- Lorier AR, Huxtable AG, Robinson DM, Lipski J, Housley GD, Funk GD (2007) P2Y1 receptor modulation of the pre-Botzinger complex inspiratory rhythm generating network in vitro. *J Neurosci* 27:993-1005.
- Lumsden T (1923) Observations on the respiratory centres in the cat. *J Physiol* 57:153-160.
- Lutz PL (1992) Mechanisms for anoxic survival in the vertebrate brain. *Annu Rev Physiol* 54:601-618.
- Lutz PL, Prentice HM (2002) Sensing and responding to hypoxia, molecular and physiological mechanisms. *Integr Comp Biol* 42:463-468.
- Martin ED, Fernandez M, Perea G, Pascual O, Haydon PG, Araque A, Cena V (2007) Adenosine released by astrocytes contributes to hypoxia-induced modulation of synaptic transmission. *Glia* 55:36-45.
- Mateo J, Harden TK, Boyer JL (1999) Functional expression of a cDNA encoding a human ecto-ATPase. *Br J Pharmacol* 128:396-402.
- Mayer CA, Haxhiu MA, Martin RJ, Wilson CG (2006) Adenosine A2A receptors mediate GABAergic inhibition of respiration in immature rats. *J Appl Physiol* 100:91-97.
- McKay LC, Janczewski WA, Feldman JL (2005) Sleep-disordered breathing after targeted ablation of preBotzinger complex neurons. *Nat Neurosci* 8:1142-1144.
- McKenna MC (2007) The glutamate-glutamine cycle is not stoichiometric: fates of glutamate in brain. *J Neurosci Res* 85:3347-3358.
- Mellen NM, Thoby-Brisson M (2012) Respiratory circuits: development, function and models. *Curr Opin Neurobiol*.
- Mellen NM, Janczewski WA, Bocchiaro CM, Feldman JL (2003) Opioid-induced quantal slowing reveals dual networks for respiratory rhythm generation. *Neuron* 37:821-826.

- Miles GB, Parkis MA, Lipski J, Funk GD (2002) Modulation of phrenic motoneuron excitability by ATP: consequences for respiratory-related output in vitro. *J Appl Physiol* 92:1899-1910.
- Mironov SL, Langohr K, Richter DW (1999) A1 adenosine receptors modulate respiratory activity of the neonatal mouse via the cAMP-mediated signaling pathway. *J Neurophysiol* 81:247-255.
- Morgado-Valle C, Feldman JL (2004) Depletion of substance P and glutamate by capsaicin blocks respiratory rhythm in neonatal rat in vitro. *J Physiol* 555:783-792.
- Morgado-Valle C, Baca SM, Feldman JL (2010) Glycinergic pacemaker neurons in preBotzinger complex of neonatal mouse. *J Neurosci* 30:3634-3639.
- Mortola JP (1996) Ventilatory responses to hypoxia in mammals. In: *In Tissue Oxygen Deprevention* (Haddad GGaL, G., ed), pp 433-477. New York, NY: Marcel Dekker.
- Mortola JP, Saiki C (1996) Ventilatory response to hypoxia in rats: gender differences. *Respir Physiol* 106:21-34.
- Mulkey DK, Wenker IC, Kreneisz O (2010) Current ideas on central chemoreception by neurons and glial cells in the retrotrapezoid nucleus. *J Appl Physiol* 108:1433-1439.
- Mulkey DK, Mistry AM, Guyenet PG, Bayliss DA (2006) Purinergic P2 receptors modulate excitability but do not mediate pH sensitivity of RTN respiratory chemoreceptors. *J Neurosci* 26:7230-7233.
- Mulkey DK, Stornetta RL, Weston MC, Simmons JR, Parker A, Bayliss DA, Guyenet PG (2004) Respiratory control by ventral surface chemoreceptor neurons in rats. *Nat Neurosci* 7:1360-1369.

- Mulkey DK, Rosin DL, West G, Takakura AC, Moreira TS, Bayliss DA, Guyenet PG (2007) Serotonergic neurons activate chemosensitive retrotrapezoid nucleus neurons by a pH-independent mechanism. *J Neurosci* 27:14128-14138.
- Nattie E (1999) CO₂, brainstem chemoreceptors and breathing. *Prog Neurobiol* 59:299-331.
- Nattie E, Li A (2009) Central chemoreception is a complex system function that involves multiple brain stem sites. *J Appl Physiol* 106:1464-1466.
- Nattie EE (2001) Central chemosensitivity, sleep, and wakefulness. *Respir Physiol* 129:257-268.
- Nedergaard M (1994) Direct signaling from astrocytes to neurons in cultures of mammalian brain cells. *Science* 263:1768-1771.
- Nishiyama A, Komitova M, Suzuki R, Zhu X (2009) Polydendrocytes (NG2 cells): multifunctional cells with lineage plasticity. *Nat Rev Neurosci* 10:9-22.
- Ogilvie MD, Gottschalk A, Anders K, Richter DW, Pack AI (1992) A network model of respiratory rhythmogenesis. *Am J Physiol* 263:R962-975.
- Onimaru H, Homma I (2003) A novel functional neuron group for respiratory rhythm generation in the ventral medulla. *J Neurosci* 23:1478-1486.
- Onimaru H, Arata A, Homma I (1989) Firing properties of respiratory rhythm generating neurons in the absence of synaptic transmission in rat medulla in vitro. *Exp Brain Res* 76:530-536.
- Onimaru H, Arata A, Homma I (1990) Inhibitory synaptic inputs to the respiratory rhythm generator in the medulla isolated from newborn rats. *Pflugers Arch* 417:425-432.
- Onimaru H, Arata A, Homma I (1997) Neuronal mechanisms of respiratory rhythm generation: an approach using in vitro preparation. *Jpn J Physiol* 47:385-403.

- Onimaru H, Kumagawa Y, Homma I (2006) Respiration-related rhythmic activity in the rostral medulla of newborn rats. *J Neurophysiol* 96:55-61.
- Pace RW, Mackay DD, Feldman JL, Del Negro CA (2007) Inspiratory bursts in the preBotzinger complex depend on a calcium-activated non-specific cation current linked to glutamate receptors in neonatal mice. *J Physiol* 582:113-125.
- Pagliardini S, Janczewski WA, Tan W, Dickson CT, Deisseroth K, Feldman JL (2011) Active expiration induced by excitation of ventral medulla in adult anesthetized rats. *J Neurosci* 31:2895-2905.
- Parpura V, Basarsky TA, Liu F, Jeftinija K, Jeftinija S, Haydon PG (1994) Glutamate-mediated astrocyte-neuron signalling. *Nature* 369:744-747.
- Parri HR, Gould TM, Crunelli V (2001) Spontaneous astrocytic Ca²⁺ oscillations in situ drive NMDAR-mediated neuronal excitation. *Nat Neurosci* 4:803-812.
- Paton JF (1996) The ventral medullary respiratory network of the mature mouse studied in a working heart-brainstem preparation. *J Physiol* 493 (Pt 3):819-831.
- Paton JF, Abdala AP, Koizumi H, Smith JC, St-John WM (2006) Respiratory rhythm generation during gasping depends on persistent sodium current. *Nat Neurosci* 9:311-313.
- Pena F, Parkis MA, Tryba AK, Ramirez JM (2004) Differential contribution of pacemaker properties to the generation of respiratory rhythms during normoxia and hypoxia. *Neuron* 43:105-117.
- Perea G, Araque A (2005) Glial calcium signaling and neuron-glia communication. *Cell Calcium* 38:375-382.

- Petrillo GA, Glass L, Trippenbach T (1983) Phase locking of the respiratory rhythm in cats to a mechanical ventilator. *Can J Physiol Pharmacol* 61:599-607.
- Podgorska M, Kocbuch K, Pawelczyk T (2005) Recent advances in studies on biochemical and structural properties of equilibrative and concentrative nucleoside transporters. *Acta Biochim Pol* 52:749-758.
- Porter JT, McCarthy KD (1995) GFAP-positive hippocampal astrocytes in situ respond to glutamatergic neuroligands with increases in $[Ca^{2+}]_i$. *Glia* 13:101-112.
- Ralevic V, Burnstock G (1998) Receptors for purines and pyrimidines. *Pharmacol Rev* 50:413-492.
- Ramirez JM, Viemari JC (2005) Determinants of inspiratory activity. *Respir Physiol Neurobiol* 147:145-157.
- Rekling JC, Feldman JL (1998) PreBotzinger complex and pacemaker neurons: hypothesized site and kernel for respiratory rhythm generation. *Annu Rev Physiol* 60:385-405.
- Richter DW (1982) Generation and maintenance of the respiratory rhythm. *The Journal of experimental biology* 100:93-107.
- Richter DW, Bischoff A, Anders K, Bellingham M, Windhorst U (1991) Response of the medullary respiratory network of the cat to hypoxia. *J Physiol* 443:231-256.
- Robson SC, Sevigny J, Zimmermann H (2006) The E-NTPDase family of ectonucleotidases: Structure function relationships and pathophysiological significance. *Purinergic Signal* 2:409-430.
- Rong W, Gourine AV, Cockayne DA, Xiang Z, Ford AP, Spyer KM, Burnstock G (2003) Pivotal role of nucleotide P2X2 receptor subunit of the ATP-gated ion channel mediating ventilatory responses to hypoxia. *J Neurosci* 23:11315-11321.

- Rosin DL, Chang DA, Guyenet PG (2006) Afferent and efferent connections of the rat retrotrapezoid nucleus. *J Comp Neurol* 499:64-89.
- Ruangkittisakul A, Ballanyi K (2010) Methylxanthine reversal of opioid-evoked inspiratory depression via phosphodiesterase-4 blockade. *Respir Physiol Neurobiol* 172:94-105.
- Ruangkittisakul A, Schwarzacher SW, Secchia L, Ma Y, Bobocea N, Poon BY, Funk GD, Ballanyi K (2008) Generation of eupnea and sighs by a spatiochemically organized inspiratory network. *J Neurosci* 28:2447-2458.
- Runold M, Lagercrantz H, Fredholm BB (1986) Ventilatory effect of an adenosine analogue in unanesthetized rabbits during development. *J Appl Physiol* 61:255-259.
- Runold M, Lagercrantz H, Prabhakar NR, Fredholm BB (1989) Role of adenosine in hypoxic ventilatory depression. *J Appl Physiol* 67:541-546.
- Rybäk IA, Abdala AP, Markin SN, Paton JF, Smith JC (2007) Spatial organization and state-dependent mechanisms for respiratory rhythm and pattern generation. *Prog Brain Res* 165:201-220.
- Schmidt C, Bellingham MC, Richter DW (1995) Adenosinergic modulation of respiratory neurones and hypoxic responses in the anaesthetized cat. *J Physiol* 483 (Pt 3):769-781.
- Schwarzacher SW, Smith JC, Richter DW (1995) Pre-Botzinger complex in the cat. *J Neurophysiol* 73:1452-1461.
- Schwarzacher SW, Rub U, Deller T (2011) Neuroanatomical characteristics of the human pre-Botzinger complex and its involvement in neurodegenerative brainstem diseases. *Brain* 134:24-35.

- Segers LS, Nuding SC, Dick TE, Shannon R, Baekey DM, Solomon IC, Morris KF, Lindsey BG (2008) Functional connectivity in the pontomedullary respiratory network. *J Neurophysiol* 100:1749-1769.
- Sim JA, Young MT, Sung HY, North RA, Surprenant A (2004) Reanalysis of P2X7 receptor expression in rodent brain. *J Neurosci* 24:6307-6314.
- Simon PM, Habel AM, Daubenspeck JA, Leiter JC (2000) Vagal feedback in the entrainment of respiration to mechanical ventilation in sleeping humans. *J Appl Physiol* 89:760-769.
- Smith CA, Forster HV, Blain GM, Dempsey JA (2010) An interdependent model of central/peripheral chemoreception: evidence and implications for ventilatory control. *Respir Physiol Neurobiol* 173:288-297.
- Smith JC, Abdala AP, Rybak IA, Paton JF (2009) Structural and functional architecture of respiratory networks in the mammalian brainstem. *Philos Trans R Soc Lond B Biol Sci* 364:2577-2587.
- Smith JC, Ellenberger HH, Ballanyi K, Richter DW, Feldman JL (1991) Pre-Botzinger complex: a brainstem region that may generate respiratory rhythm in mammals. *Science* 254:726-729.
- Smith JC, Abdala AP, Koizumi H, Rybak IA, Paton JF (2007) Spatial and functional architecture of the mammalian brain stem respiratory network: a hierarchy of three oscillatory mechanisms. *J Neurophysiol* 98:3370-3387.
- Smith JC, Butera RJ, Koshiya N, Del Negro C, Wilson CG, Johnson SM (2000) Respiratory rhythm generation in neonatal and adult mammals: the hybrid pacemaker-network model. *Respir Physiol* 122:131-147.

- Song X, Guo W, Yu Q, Liu X, Xiang Z, He C, Burnstock G (2011) Regional expression of P2Y(4) receptors in the rat central nervous system. *Purinergic Signal* 7:469-488.
- Speck DF, Beck ER (1989) Respiratory rhythmicity after extensive lesions of the dorsal and ventral respiratory groups in the decerebrate cat. *Brain Res* 482:387-392.
- Spyer KM, Gourine AV (2009) Chemosensory pathways in the brainstem controlling cardiorespiratory activity. *Philos Trans R Soc Lond B Biol Sci* 364:2603-2610.
- Stornetta RL, Sevigny CP, Guyenet PG (2002) Vesicular glutamate transporter DNPI/VGLUT2 mRNA is present in C1 and several other groups of brainstem catecholaminergic neurons. *J Comp Neurol* 444:191-206.
- Stornetta RL, Rosin DL, Wang H, Sevigny CP, Weston MC, Guyenet PG (2003) A group of glutamatergic interneurons expressing high levels of both neurokinin-1 receptors and somatostatin identifies the region of the pre-Botzinger complex. *J Comp Neurol* 455:499-512.
- Stornetta RL, Moreira TS, Takakura AC, Kang BJ, Chang DA, West GH, Brunet JF, Mulkey DK, Bayliss DA, Guyenet PG (2006) Expression of Phox2b by brainstem neurons involved in chemosensory integration in the adult rat. *J Neurosci* 26:10305-10314.
- Suadicani SO, Brosnan CF, Scemes E (2006) P2X7 receptors mediate ATP release and amplification of astrocytic intercellular Ca²⁺ signaling. *J Neurosci* 26:1378-1385.
- Suzue T (1984) Respiratory rhythm generation in the in vitro brain stem-spinal cord preparation of the neonatal rat. *J Physiol* 354:173-183.
- Szatkowski M, Barbour B, Attwell D (1990) Non-vesicular release of glutamate from glial cells by reversed electrogenic glutamate uptake. *Nature* 348:443-446.

- Takakura AC, Moreira TS, Colombari E, West GH, Stornetta RL, Guyenet PG (2006) Peripheral chemoreceptor inputs to retrotrapezoid nucleus (RTN) CO₂-sensitive neurons in rats. *J Physiol* 572:503-523.
- Tan W, Janczewski WA, Yang P, Shao XM, Callaway EM, Feldman JL (2008) Silencing preBotzinger complex somatostatin-expressing neurons induces persistent apnea in awake rat. *Nat Neurosci* 11:538-540.
- Thoby-Brisson M, Trinh JB, Champagnat J, Fortin G (2005) Emergence of the pre-Botzinger respiratory rhythm generator in the mouse embryo. *J Neurosci* 25:4307-4318.
- Thoby-Brisson M, Cauli B, Champagnat J, Fortin G, Katz DM (2003) Expression of functional tyrosine kinase B receptors by rhythmically active respiratory neurons in the pre-Botzinger complex of neonatal mice. *J Neurosci* 23:7685-7689.
- Thoby-Brisson M, Karlen M, Wu N, Charnay P, Champagnat J, Fortin G (2009) Genetic identification of an embryonic parafacial oscillator coupling to the preBotzinger complex. *Nat Neurosci* 12:1028-1035.
- Thomas T, Ralevic V, Bardini M, Burnstock G, Spyer KM (2001) Evidence for the involvement of purinergic signalling in the control of respiration. *Neuroscience* 107:481-490.
- Thorn JA, Jarvis SM (1996) Adenosine transporters. *Gen Pharmacol* 27:613-620.
- Tian GF, Peever JH, Duffin J (1999) Botzinger-complex, bulbospinal expiratory neurones monosynaptically inhibit ventral-group respiratory neurones in the decerebrate rat. *Exp Brain Res* 124:173-180.

Vandam RJ, Shields EJ, Kelty JD (2008) Rhythm generation by the pre-Botzinger complex in medullary slice and island preparations: effects of adenosine A(1) receptor activation. *BMC Neurosci* 9:95.

Verkhratsky A, Steinhauser C (2000) Ion channels in glial cells. *Brain Res Brain Res Rev* 32:380-412.

Verkhratsky A, Krishtal OA, Burnstock G (2009) Purinoceptors on neuroglia. *Mol Neurobiol* 39:190-208.

Volterra A, Meldolesi J (2005) Astrocytes, from brain glue to communication elements: the revolution continues. *Nat Rev Neurosci* 6:626-640.

Wang JL, Wu ZH, Pan BX, Li J (2005) Adenosine A1 receptors modulate the discharge activities of inspiratory and biphasic expiratory neurons in the medial region of Nucleus Retrofacialis of neonatal rat in vitro. *Neurosci Lett* 379:27-31.

Wang TF, Guidotti G (1996) CD39 is an ecto-(Ca²⁺,Mg²⁺)-apyrase. *J Biol Chem* 271:9898-9901.

Waters KA, Gozal D (2003) Responses to hypoxia during early development. *Respir Physiol Neurobiol* 136:115-129.

Weaver DR (1996) A1-adenosine receptor gene expression in fetal rat brain. *Brain Res Dev Brain Res* 94:205-223.

Wenninger JM, Pan LG, Klum L, Leekley T, Bastastic J, Hodges MR, Feroah TR, Davis S, Forster HV (2004) Large lesions in the pre-Botzinger complex area eliminate eupneic respiratory rhythm in awake goats. *J Appl Physiol* 97:1629-1636.

- Wilson CG, Martin RJ, Jaber M, Abu-Shaweeesh J, Jafri A, Haxhiu MA, Zaidi S (2004) Adenosine A_{2A} receptors interact with GABAergic pathways to modulate respiration in neonatal piglets. *Respir Physiol Neurobiol* 141:201-211.
- Yamamoto M, Nishimura M, Kobayashi S, Akiyama Y, Miyamoto K, Kawakami Y (1994) Role of endogenous adenosine in hypoxic ventilatory response in humans: a study with dipyridamole. *J Appl Physiol* 76:196-203.
- Yao ST, Barden JA, Finkelstein DI, Bennett MR, Lawrence AJ (2000) Comparative study on the distribution patterns of P2X(1)-P2X(6) receptor immunoreactivity in the brainstem of the rat and the common marmoset (*Callithrix jacchus*): association with catecholamine cell groups. *J Comp Neurol* 427:485-507.
- Yao ST, Gourine AV, Spyer KM, Barden JA, Lawrence AJ (2003) Localisation of P2X2 receptor subunit immunoreactivity on nitric oxide synthase expressing neurones in the brain stem and hypothalamus of the rat: a fluorescence immunohistochemical study. *Neuroscience* 121:411-419.
- Ye ZC, Wyeth MS, Baltan-Tekkok S, Ransom BR (2003) Functional hemichannels in astrocytes: a novel mechanism of glutamate release. *J Neurosci* 23:3588-3596.
- Zaidi SI, Jafri A, Martin RJ, Haxhiu MA (2006) Adenosine A_{2A} receptors are expressed by GABAergic neurons of medulla oblongata in developing rat. *Brain Res* 1071:42-53.
- Zec N, Kinney HC (2003) Anatomic relationships of the human nucleus of the solitary tract in the medulla oblongata: a DiI labeling study. *Autonomic neuroscience : basic & clinical* 105:131-144.

- Zhang JM, Wang HK, Ye CQ, Ge W, Chen Y, Jiang ZL, Wu CP, Poo MM, Duan S (2003) ATP released by astrocytes mediates glutamatergic activity-dependent heterosynaptic suppression. *Neuron* 40:971-982.
- Ziganshin AU, Hoyle CHV, Burnstock G (1994) Ecto-enzymes and metabolism of extracellular ATP. *Drug Development Research* 32:134-146.
- Zimmermann H (2006) Ectonucleotidases in the nervous system. *Novartis Found Symp* 276:113-128; discussion 128-130, 233-117, 275-181.
- Zuperku EJ, Brandes IF, Stucke AG, Sanchez A, Hopp FA, Stuth EA (2008) Major components of endogenous neurotransmission underlying the discharge activity of hypoglossal motoneurons *in vivo*. *Adv Exp Med Biol* 605:279-284.

Chapter 2: Glia contribute to the purinergic modulation of inspiratory rhythm generating networks

A version of this chapter has been published as:

Huxtable AG*, Zwicker JD*, Alvares TS, Ruangkittisakul, A, Fang X, Hahn LB, Posse de Chaves E, Baker GB, Ballanyi K, Funk GD. (2010) Glia contribute to the purinergic modulation of inspiratory rhythm generating networks. J Neurosci, 30(11):3947-3958

*AGH and JDZ contributed equally to this work

Contribution:

I am co-first author of this paper. I performed all experiments and data analysis for all of figures 4.4, 4.6 and 4.7 and was involved in conceptualization of the manuscript. Figure 4.4 and 4.6 involved culturing glial cells from the ventral medulla and characterizing their sensitivity to ATP as well the contribution of P2Y₁R receptors to the ATP response using Ca²⁺-sensitive dyes and fluorescent-imaging techniques. Figure 7 involved developing a protocol and method to test whether cultured glia release glutamate in response to ATP. I also contributed to the manuscript writing and revisions of the methods, results and discussion sections. Overall, my contribution was ~45% of the total.

2.1 Introduction

Traditionally, glia have been recognized for their important roles in metabolically supporting neurons (Tsacopoulos, 2002), indirectly influencing neuronal activity by buffering extracellular K⁺ (Gardner-Medwin et al., 1981), and removing neurotransmitters from the extracellular space (Parpura et al., 1994). It is now clear that glia express receptors for a variety of neurotransmitters (including glutamate, GABA, norepinephrine, and acetylcholine), release a number of gliotransmitters (including glutamate, ATP, and D-serine), and directly modulate neuronal activity through gliotransmission (Haydon and Carmignoto, 2006; He and Sun, 2007). Despite growing evidence that gliotransmission modulates neuronal activity and the recent demonstration in mice that gliotransmission is important for sleep homeostasis (Halassa et al., 2009), understanding its role in controlling the activity of neural networks underlying complex behaviors is limited.

To further explore the role of glia in modulating network behavior, we examined a brainstem network that generates breathing (Feldman and Del Negro, 2006), a vital rhythmic motor behavior that controls homeostasis, to understand the involvement of glia in the modulation of this behavior by ATP. ATP acts by binding to seven subtypes of ionotropic P2X receptors (P2X₁₋₇Rs) (North, 2002) and 8 subtypes of metabotropic P2YRs (P2Y_{1, 2, 4, 6, 11-14}) (Abbraccchio et al., 2003). Seminal studies (Edwards et al., 1992; Evans et al., 1992; Silinsky et al., 1992) that established ATP as a neurotransmitter contributing to fast synaptic transmission in the CNS are now supported by extensive literature showing multiple pre- and postsynaptic actions of P2XRs and P2YRs on neuronal excitability (Gourine, 2005; Gourine et al., 2005; Lorier et al., 2007). ATP is also a gliotransmitter that modulates synaptic efficacy on multiple time scales at glutamatergic synapses (Zhang et al., 2003; Gordon et al., 2005), inhibits and excites neurons (Newman, 2003; Burnstock, 2007), and stimulates hormone release from hypothalamic neurons (Espallergues et al., 2007). In addition to releasing ATP, glia express multiple P2R subtypes that when activated can initiate self-

propagating calcium waves that are proposed to influence local network excitability (Fiacco and McCarthy, 2006).

Within respiratory networks, ATP and P2R signaling contribute to homeostatic ventilatory responses (Gourine et al., 2003; Gourine et al., 2005). During hypoxia, for example, a delayed release of ATP from respiratory regions of the medulla activates P2Rs and attenuates the secondary hypoxic ventilatory depression (Gourine et al., 2005), which can be life-threatening in premature/newborn infants. This excitation is likely to involve a potent P2Y₁R-mediated excitation of the preBötzinger complex (preBötC) (Lorier et al., 2007), the proposed site of inspiratory rhythm generation (Smith et al., 1991). The cellular mediators of this ATP-evoked excitation are not known. The majority of neurons in the preBötC are weakly excited by ATP (Lorier et al., 2008) and likely contribute to the frequency response; however, based on the emerging role of glia in ATP signaling (Newman, 2003; Zhang et al., 2003; Gordon et al., 2005; Burnstock, 2007; Espallergues et al., 2007), the aim of this study is to test the hypothesis that glia are important contributors to the modulatory actions of ATP on preBötC inspiratory rhythm generating networks. These data will provide insight into the general roles of glia and ATP in modulating the activity of neural networks involved in generating rhythmic motor behaviors.

2.2 Methods

All experiments were conducted in accordance with the guidelines of the Canadian Council on Animal Care and were approved by the University of Alberta Animal Ethics Committee.

2.2.1 Electrophysiology

Rhythmic, transverse, 700 µm thick slices of the medulla from Sprague Dawley rats (postnatal day 0-4, P0-4) were cut with the preBötC at the rostral surface of the slice (-0.35 mm caudal to the caudal aspect of the facial nucleus) (Smith et al., 1991; Ruangkittisakul et

al., 2006; Lorier et al., 2007). Slices were perfused (8 ml/min, 28°C) with artificial cerebrospinal fluid (aCSF) containing (mM): 120 NaCl, 3KCl, 1.0 CaCl₂, 2.0 MgSO₄, 26 NaHCO₃, 1.25 NaH₂PO₄, and 20 D-glucose, and equilibrated with 95% O₂/5%CO₂ to pH 7.45. Rhythmic inspiratory-related motor output was recorded through suction electrodes placed on the hypoglossal (XII) nerve rootlets and the site on the rostral surface overlying the preBötC that generated the largest amplitude rhythmic signal. Signals were amplified, filtered (300 Hz-1K), rectified and integrated. Data were acquired using Axoscope 9.2 and a Digidata 1322 A/D (Molecular Devices, Union City, CA).

2.2.1.1 Drugs and their application

Adenosine 5'-triphosphate (ATP, 0.1 mM, P2R agonist), fluoroacetate (FA, 5 mM, glial aconitase enzyme inhibitor), methionine sulfoximine (MSO, 0.1 mM, glial glutamine synthetase enzyme inhibitor), glutamine (GLN, 1.5 mM), 4-(2-butyl-6,7-dichloro-2-cyclopentylindan-1-on-5-yl)oxybutyric acid (DCPIB, 0.02 mM, volume-regulated anion channels inhibitor), tetrodotoxin (TTX, 0.5 μM), 6-cyano-7-nitroquinoxaline-2,3-dione (CNQX, 0.1 mM), DL-2-Amino-5-phosphonopentanoic acid (APV, 0.05 mM), glutamate (1 mM), suramin (0.5 mM), and pyridoxal phosphate-6-azo(benzene-2,4-disulfonic acid) tetrasodium salt (PPADS 0.1 mM) were obtained from Sigma-Aldrich (St Louis, MO). Substance-P (SP, 1 μM), MRS 2365 (0.001 mM, P2Y₁R agonist, and MRS 2279 (0.5 mM, P2Y₁R antagonist) were obtained from Tocris (Ellisville, MO). Drugs were prepared as stock solutions in aCSF and frozen in aliquots. ATP was made fresh each day.

Drugs were bath-applied (FA, MSO, GLN, and DCPIB) and given 15 min to equilibrate, or were microinjected (ATP and SP) using triple-barreled glass micropipettes (5-6 μm outer diameter per barrel) lowered into the preBötC with a micromanipulator. Injections were made with a controlled pressure source into the site where ATP (0.1 mM, 10

s) produced the maximum frequency increase, which was previously established to be the preBötC (Lorier et al., 2007). Consecutive agonist applications were at 15 min intervals.

2.2.1.2 Whole-cell recording

For whole-cell recording of inspiratory neurons, 700 μm rhythmic medullary slice preparations were used as described above. For whole-cell recording of glia, brainstems were sectioned to the vicinity of the preBötC and three, 300 μm sections were taken. Sections were then visually inspected and those corresponding to the preBötC (1-2 per animal) were used for recording. It is therefore possible that some cells were located just rostral or caudal to the preBötC. Cells located near the surface were visualized in an 800 μl chamber (27°C, flow rate of 2 ml/min) with differential interference contrast and infrared video microscopy. Glass micropipettes (3.5-4.5 M Ω) were filled with solution containing (mM): 140 potassium-gluconate, 5 NaCl, 1 CaCl₂, 1 MgCl₂, 10 EGTA, 10 HEPES, and 1 glucose. pH was adjusted to 7.25-7.30 by 5 M KOH. Glia were targeted based on published anatomical features (Grass et al., 2004), such as being half the diameter of neurons in the region (~10 μm), ovoid, with small processes, and close to blood vessels. Glia were distinguished from neurons electrophysiologically under current clamp by delivering an incrementing series of rectangular current steps (8 steps, 1 s) from a holding potential of -60 mV until the cell fired action potentials or membrane potential was depolarized above -10 mV. Cells that did not fire action potentials (presumptive glia) were tested for agonist sensitivity under voltage-clamp conditions at a holding potential of -60 mV by microinjecting drugs from triple-barreled glass micropipettes (as above) placed 5-10 μm above the slice surface. Negative voltage pulses (-3 to -30 mV, 0.5 s duration, 0.5 Hz) or ramps (-80 to -30 mV over 2 s during control, drug, or washout) were applied to monitor input resistance (R_N). Membrane current or voltage signals, obtained using a Multiclamp 700Aa amplifier (Molecular Devices, Sunnyvale, CA), were low-pass filtered (Bessel 5 kHz), acquired, and controlled using

Digidata 1322A A/D board with Axoscope 9.2 and Clampex 9.2 (pClamp, Molecular Devices, Union City, CA). Liquid junction potentials for potassium-gluconate solution (13 mV) were corrected off-line.

2.2.2 Ca^{2+} imaging of preBötC cells in rhythmic medullary slices

Rhythmic, 700 μm slices were placed in a recording chamber (1.5 ml), perfused with aCSF (5 ml/min) and rhythm monitored from the XII nerve rootlets. Fluo-4-AM (0.5 mM, Sigma-Aldrich, Oakville, ON) was pressure injected (0.7-1 psi) into the preBötC for 10 min using a single barrel pipette (5-10 μm) (Ruangkittisakul and Ballanyi, 2006; Ruangkittisakul et al., 2006; Ruangkittisakul et al., 2008). Fluorescence signals evoked by bath-applied agonists/antagonists were monitored through a multi-photon confocal microscope (Olympus FV300, Fluoview software; Carsen Group, Markham, ON) connected to a Ti:Sa laser (Coherent, Santa Clara, CA) using a 20X objective and 3X digital zoom with scan rates of 1.08 s/frame. ATP was bath-applied in the majority of experiments by pumping 0.1 mM ATP through the chamber at a flow rate of 5 ml/min and monitoring the time course of fluorescence changes. Other bath-applied drugs, including TTX (0.5 μM) to block action potentials, CNQX (10 μM) and APV (50 μM) to block AMPA and NMDA receptors respectively were added to the perfusion solution and were allowed to equilibrate for 15 min prior to the application of ATP. ATP (0.1 mM, 30 s) was also applied locally in some experiments using methods described for slices above. Consecutive ATP applications were separated by 15 min. While it is typical that the concentration of drug must be ~10-fold higher during local compared to bath application in order to produce the same effect, this is not the case with ATP. Bath-applied ATP has poor access to the preBötC because it is degraded by ectonucleotidases (Funk et al., 2008). This is supported by our demonstration with ATP biosensors, where to obtain concentrations of 10 μM ATP below the slice surface, the bath concentration must be raised 100-fold to 1 mM (Funk et al., 2008). Also, ATP

diffuses small distances in tissue due to an active process that we attribute to enzymatic breakdown (Huxtable et al., 2009). Second, with bath application, drug concentration rises slowly and can lead to receptor desensitization/internalization, which will greatly attenuate responses.

2.2.3 Primary cultures of glia from the ventral medulla at the level of the preBötC

2.2.3.1 Culture preparation

Two types of cultures were prepared from 300 µm preBötC slices. First, the slice was cut into dorsal and ventral halves at the dorsal border of nucleus ambiguus and ventral tissue collected for ventral medulla cultures. Second, the preBötC region was collected using 21G tissue punches to produce preBötC cultures. All culture media were used at 37°C. Both types of tissues were transferred to separate 15 ml conical tubes, washed (2X) with Dulbecco's Phosphate Buffered Saline (PBS, 2ml) (Invitrogen, Burlington, ON), and centrifuged (1500g, 1 min). Ventral tissue was then incubated in digestion buffer (0.25% Trypsin-EDTA in PBS; Invitrogen) for 5 min. The supernatant was replaced with BME-glucose solution (2 ml) that was produced by adding to 1X Basal Medium Eagle solution (BME; Invitrogen): 3.3 mM glucose (final concentration of 8.8 m), 2 mM L-GLN (Sigma-Aldrich, Oakville, ON), penicillin/streptomycin (10,000 units of penicillin/10,000 µg of streptomycin per ml; Gibco, Invitrogen), and 10% rat serum (RS). The tissue was centrifuged (1500g, 3 min), the supernatant replaced with BME-glucose (1 ml), and tissue homogenized through titration and centrifuged with fresh BME-glucose at 1500g for 6 min and 3 min. Tissue was then re-suspended in BME-glucose and cells were plated on T25 flasks (Flask TC Vent 25 cm, Fisher Scientific). In contrast, preBötC punches were plated directly on Theromox plastic coverslips (NUNC Brand products, Rochester, NY) and placed in a T25 flask containing BME-glucose (1ml).

Ventral medullary cells and preBötC coverslips were incubated in 1 ml BME-glucose for the first 24 hrs and 1 ml BME-sorbitol (10% RS) thereafter. BME-sorbitol was equivalent to BME-glucose except that D-glucose was replaced with sorbitol (2.5 mM, Fisher Scientific) to select for glia. After 48 hrs, fresh media (with 2.5% RS) was added and changed every 3 days. Ventral tissue cultures were maintained for 2 weeks and then split, plated on glass coverslips (Electron Microscopy Sciences, Hatfield, PA) and studied (imaging and immunocytochemistry) 3-5 days later. PreBötC punches (on coverslips) were grown for 6 days, smeared, maintained in a 24-well plate for 2 weeks, and then imaged.

2.2.3.2 Ca²⁺ imaging of glial cultures

Cultures were loaded for 45 min (35°C) with the membrane-permeant Ca²⁺ sensitive dye, fluo-4-AM (0.01 mM) in aCSF, containing (mM): 117 NaCl, 5 KCl, 1 NaH₂PO₄, 2 CaCl₂, 1 MgSO₄, 26 NaHCO₃, and 6 glucose. Coverslips were then moved to the recording chamber (3 ml volume, 28°C, 6 ml/min flow rate) containing aCSF gassed with 20% O₂/5% CO₂/75% N₂.

Fluorescence intensity was measured using an upright microscope (Zeiss Axioskop2 FS Plus) fitted with a 40X water immersion objective (NA=0.8), xenon arc lamp (175W, Sutter Instruments, Novato, CA), and a SensiCam QE (Cooke Corporation, Romulus, MI). Imaging Workbench 6.0 (INDEC BioSystems, Mountain View, CA) was used to control a Lambda 10-2 shutter system (Sutter Instruments, Novato, CA). Images were acquired at 1 Hz (20 ms exposure). Drugs (ATP, 0.01 mM, MRS 2365, 0.001 mM; MRS 2279, 0.5 mM; suramin, 0.5 mM; PPADS, 0.1 mM) were applied from triple-barreled micropipettes using a controlled pressure source. Consecutive agonist applications were 10 min apart. Locally-applied ATP concentration was 10-fold lower in these experiments compared to slice experiments because of improved drug access to glial monolayers.

2.2.3.3 High Performance Liquid Chromatography (HPLC)

Ventral medulla cultures in 24-well plates were washed with aCSF (1 ml, 2X) and incubated for 1 min in 250 µl aCSF. A 50 µl sample was removed from each well to determine baseline glutamate levels and this was replaced with 50 µl of aCSF, ATP, or ATP and a P2 receptor antagonist cocktail. Final concentrations were: 50 µM ATP, 500 µM MRS 2279, 500 µM suramin, and 100 µM PPADS. After 5 min, a 250 µl sample was collected for HPLC.

Samples were centrifuged (12,000g, 5 min) and the supernatants analyzed blindly for glutamate by reverse-phase HPLC with fluorimetric detection after reacting with N-isobutyryl-L-cysteine and o-phthaldialdehyde (Grant et al., 2006). The fluorescence detector was set at an excitation wavelength of 344 nm and an emission wavelength of 433 nm. Glutamate levels in the 5 min samples are reported relative to baseline levels measured at time zero.

2.2.3.4 Immunohistochemistry

When cultured cells were re-suspended from T25 flasks, some cells were seeded in 24-well culture plates for immunocytochemistry. After two days, wells were washed (3X) with PBS (pH 7.2) and fixed with 4% paraformaldehyde in phosphate buffer (PB) for 20 min. Cells were treated with Triton X-100 (0.1%, 15 min at room temperature), washed with PBS (2X) and blocked with 2% bovine serum albumin in PBS for 2 hrs. Cells were then incubated in the primary antibodies in the blocking buffer for 2 hrs at room temperature. Primary antibodies included rabbit polyclonal anti-GFAP (1:500, Promega, Madison, WI), monoclonal anti-S-100 (β -subunit) (1:1000, Sigma Aldrich, Oakville, ON), rabbit anti-P2Y₁ (1:500, Alomone Labs, Jerusalem, Israel), monoclonal antibody anti-neurofilament 160 kDa, clone NN18 (Millipore, Jaffrey, New Hampshire), and polyclonal rabbit anti-neurofilament 150 kDa (Millipore, Temecula, CA). Monoclonal anti-S-100 (β -subunit) was used in

conjunction with either rabbit polyclonal anti-GFAP, rabbit anti-P2Y₁, or polyclonal anti-neurofilament 150. Monoclonal antibody anti-neurofilament 160 was used with rabbit polyclonal anti-GFAP. After three washes with PBS, cells were incubated with the secondary antibodies in the blocking buffer for 1 hr at room temperature. Secondary antibodies used include Alexa Fluor® 488 donkey anti-mouse IgG (H+L) (1:1000, Molecular Probes, Invitrogen, Burlington, ON) for the monoclonal anti-S-100 (β -subunit) or anti-neurofilament antibodies. Alexa Fluor® 594 donkey anti-rabbit IgG (H+L) (1:1000, Molecular Probes, Invitrogen, Burlington, ON) was used with the rabbit anti-P2Y₁ primary antibody. Cells were washed with PBS (3X), Hoechst solution (nuclear stain; Sigma Aldrich, Oakville, ON) applied and mounting medium added to the wells for imaging on a Nikon Eclipse TE300 fluorescent microscope equipped with a digital camera. Images were adjusted for brightness and contrast using Northern Eclipse Image analysis (Empix Imaging Inc., Mississauga, ON). All images within a series were adjusted identically.

2.2.4 Data and statistical analysis

Inspiratory frequency, cell holding current, and R_N were analyzed off-line using Clampfit 9.2 (pClamp, Molecular Devices, Union City, CA). Effects of bath-applied drugs on inspiratory frequency were assessed by comparing instantaneous frequencies ([1/burst period] x 60) averaged over 5 min during control and the steady-state drug response. For local drug applications, baseline frequency (2 min prior to drug application) was compared to the maximum frequency observed within the first minute of drug application, as determined from a moving average of three cycles.

For Ca²⁺ imaging of rhythmic slices, fluo-4 labeled cells were selected as regions of interest (ROIs). The area and fluorescence intensity of each ROI were determined using Fluoview V 5.0 (Markham, ON). Cells were grouped based on ROI size ($\leq 50 \mu\text{m}^2$, $50-100 \mu\text{m}^2$, $\geq 100 \mu\text{m}^2$). Raw fluorescence intensity, measured under control conditions and in

response to ATP, in the absence and presence of antagonists was compared within and between groups.

Ca^{2+} imaging data from glial cultures were analyzed offline using Imaging Workbench 6.0 (INDEC BioSystems, Mountain View, CA). ROIs were drawn around cell margins and baseline fluorescence for each ROI was calculated from the average intensity of three images taken prior to drug administration. Agonist effects were assessed by comparing the maximum agonist-evoked fluorescence value to the baseline fluorescence. Antagonist effects were assessed by comparing, relative to baseline (maximum fluorescence/baseline fluorescence) the maximum fluorescence evoked by the agonist in the absence and presence of the antagonist.

Differences between means were compared using raw data (except data relevant to Figure 2.6C-E) and either a t-test, One-Way, or Two-Way ANOVA with multiple comparison post tests (GraphPad Prism Version 4, GraphPad Software, Inc, San Diego, CA). $P<0.05$ was considered significant. Data are expressed as mean \pm SEM.

2.3 Results

2.3.1 Contribution of glia to the ATP-evoked increase in inspiratory frequency

The effects of bath-applied glial toxins on network behavior were assessed by monitoring changes in baseline inspiratory frequency generated by medullary slices. As reported previously (Hulsmann et al., 2000), FA (5 mM, n=10) and MSO (0.1 mM, n=7) significantly reduced baseline rhythm from 14.1 ± 1.0 to 10.6 ± 1.8 bursts/min and from 14.8 ± 2.0 to 11.8 ± 2.2 bursts/min after 30 min, respectively (data not shown, One-Way ANOVA, Tukey's Multiple Comparison Test). Baseline frequency fell further to 8.6 ± 1.5 bursts/min and 8.9 ± 2.0 bursts/min after 60 min. After 60-150 min in FA or MSO, inspiratory activity was reduced by at least 75% of control in all preparations. In four preparations (two with FA; two with MSO), rhythm stopped completely. At this time, application of GLN (1.5

mM) in the presence of the toxin returned rhythm to 10.9 ± 1.1 bursts/min in FA or 11.6 ± 1.7 bursts/min in MSO within 15 min.

To examine the contribution of glia to the effect of P2R activation on inspiratory frequency, we compared in the same slice network responses to local application of ATP and SP into the preBötC in control conditions and after restoration of toxin-disrupted rhythm with GLN. SP is a neuropeptide that evokes a potent increase in inspiratory frequency when applied into the preBötC (Gray et al., 1999; Gray et al., 2001) and was used as a control to assess the ability of the inspiratory network to respond to excitatory stimuli after toxin treatment. In control conditions, ATP (0.1 mM, 10 s) caused frequency to increase from 14.6 ± 2.5 to 34.8 ± 2.6 bursts/min; however, in the presence of MSO/GLN ATP no longer evoked a significant increase in frequency. Frequency was 9.6 ± 1.8 bursts/min in control and 18.4 ± 2.6 bursts/min in MSO/GLN (Fig 2.1A, B, n=7, One-Way ANOVA, Tukey's Multiple Comparison Test). In contrast, the SP (1 μ M, 10 s) response was not affected by MSO/GLN (Fig 2.1C, D). SP caused frequency to increase from 14.3 ± 2.3 to 31.2 ± 3.8 bursts/min in control conditions and from 11.5 ± 2.1 to 26.2 ± 5.3 bursts/min in MSO/GLN (Fig 2.1D, One-Way ANOVA, Tukey's Multiple Comparison Test).

These experiments were repeated using the FA toxin, instead of MSO. The ATP-evoked peak frequency response in control conditions (14.3 ± 1.0 bursts/min to 32.0 ± 3.3 bursts/min) was significantly reduced in FA/GLN (10.9 ± 1.0 to 22.8 ± 2.3 bursts/min) (Fig 2.2A, B). In contrast, the SP-evoked peak frequency response in control conditions (12.0 ± 2.3 to 34.2 ± 4.4 bursts/min) was unaffected by FA/GLN (11.2 ± 0.8 to 31.2 ± 4.2 bursts/min) (Fig 2.2C, D, n=10, One-Way ANOVA, Tukey's Multiple Comparison Test).

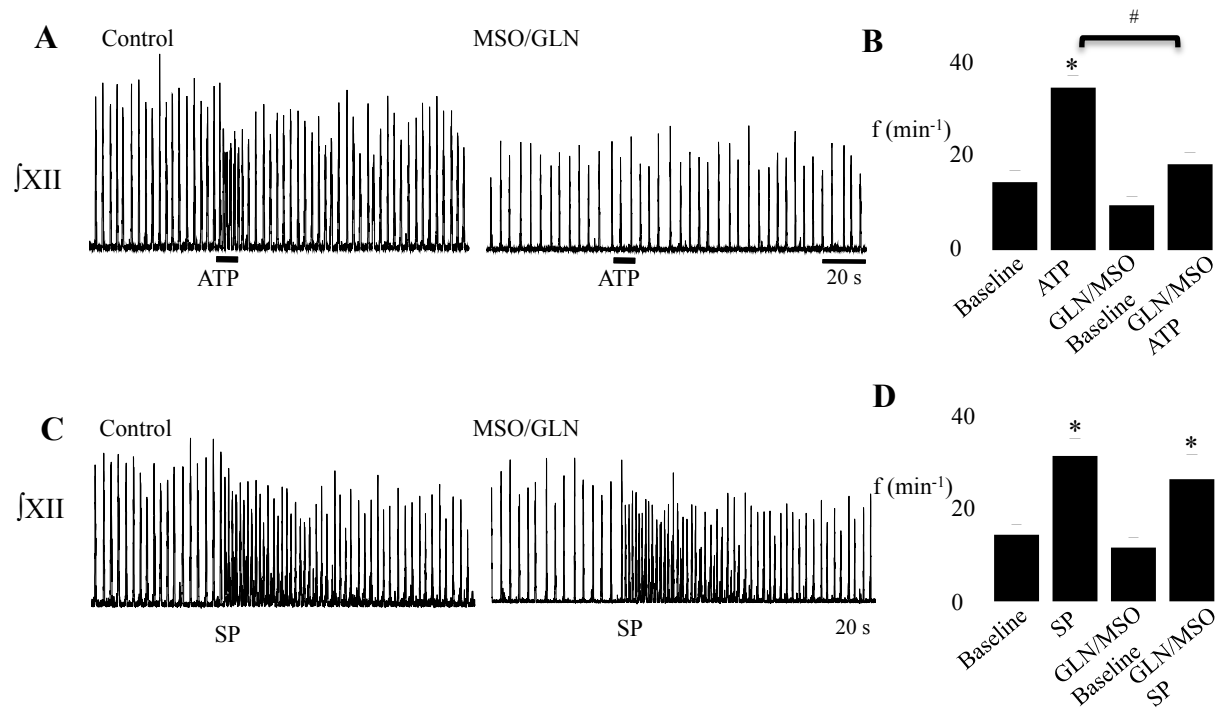


Figure 2.1 The influence of the glial toxin MSO (0.1mM) on frequency increases evoked by ATP and SP in rhythmic medullary slice preparations.

Local application of ATP (0.1 mM, 10 s, A) and SP (1 μM , 10 s, C) in the preBötC during control conditions (left panels) and in the presence of MSO and GLN (1.5 mM, middle panels). Group data ($n=7$) for the changes in frequency associated with ATP (B) and SP (D) applications. (* $p<0.001$ indicates significant difference from baseline or GLN/MSO baseline, # $p<0.001$ indicates significant difference between ATP responses.)

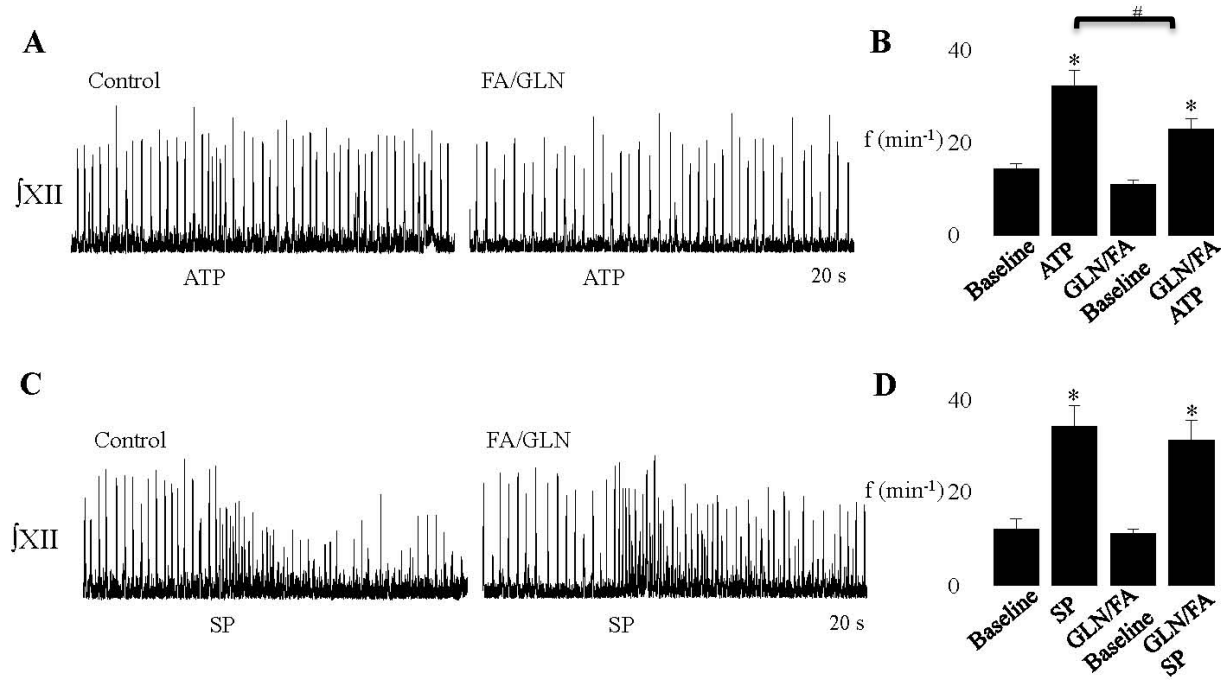


Figure 2.2 The influence of the glial toxin FA (5mM) on the ATP and SP-evoked frequency increases in rhythmic medullary slice preparations.

Integrated XII nerve recordings after local application of ATP (0.1 mM, 10 s, A) and SP (1 μ M, 10 s, C) into the preBötC during control (left panels) and FA and GLN (1.5 mM, middle panels). Group data (n=10) showing changes in the maximum frequency evoked in response to ATP (B) and SP (D) in control and FA/GLN. (* p<0.001 indicates significant difference from baseline or FA/GLN baseline, # p<0.01 indicates significant difference between ATP responses).

2.3.2 Involvement of VRACs in the ATP-evoked frequency increase

Extracellular ATP can influence glial function by activating glial volume-regulated anion channels (VRACs), which facilitate movement of gliotransmitters (ATP and excitatory amino acids) from intracellular to extracellular compartments (Mongin and Kimelberg, 2005). To test whether VRACs contribute to the ATP-evoked frequency increase, we compared ATP responses in control conditions and after bath-application of the VRAC inhibitor, DCPIB (20 µM).

DCPIB had no effect on baseline frequency or the ATP-evoked frequency increase. Baseline frequency was 19.7 ± 1.5 , 20.8 ± 1.2 , and 20.1 ± 1.8 bursts/min in control, DCPIB, and after 15 min of washout, respectively. The ATP-evoked peak frequencies were 43.7 ± 5.1 , 44.7 ± 4.0 , and 46.9 ± 4.8 bursts/min in control, DCPIB, and after DCPIB washout respectively (data not shown, n=9, One-Way ANOVA).

2.3.3 ATP sensitivity of preBötC glia

To further explore the involvement of glia in the ATP-evoked frequency increase, we tested whether glia in the region of the preBötC have the capacity to respond directly to ATP. This was addressed in three ways.

Firstly, multi-photon fluo-4 Ca⁺² imaging of the preBötC was used to examine the ATP sensitivity of glia. Dye injection into the preBötC labeled morphologically diverse cells over an area that was 200-300 µm in diameter and within which cells could be visualized to a depth of 80 µm (Ruangkittisakul et al., 2008). Our objective was to assess whether glia in respiratory regions in the brainstem are sensitive to ATP. Thus, the first step was to establish that we were recording from cells within the preBötC. This was accomplished by identifying cells with Ca⁺² oscillations in synchrony with inspiratory-related XII nerve bursts, like the three shown in Fig 2.3A. Once the inspiratory cell column was functionally identified, the plane of focus was adjusted to contain the largest number of small cells (putative glia). The

rhythmically-active, inspiratory-related neurons identified in the first stage of this protocol were typically amongst the largest cells ($146 \pm 28 \mu\text{m}^2$). However, they were not tested for their ATP-sensitivity because none were present in the focal plane containing the highest number of our target cells. In addition, we have previously established using whole-cell recording that most preBötC inspiratory neurons are sensitive to ATP (Lorier et al., 2008). While ATP is typically applied locally to the preBötC, it was bath-applied in these experiments to activate the largest number of cells possible and because minor movements of the tissue during local application changed the focal plan and confounded quantification of changes in fluorescence. Twenty-six to 34 cells per slice (Fig 2.3B) responded to bath-applied ATP with an increase in fluorescence intensity. Since neurons and glia in this region cannot be unequivocally distinguished based on visual inspection, cells showing any detectable change in fluorescence in response to ATP application were outlined as ROIs and divided into three groups based on cross-sectional area (Group 1, $\leq 50 \mu\text{m}^2$; Group 2, 50 to $100 \mu\text{m}^2$; Group 3, $\geq 100 \mu\text{m}^2$). Based on published whole-cell recording data (Grass et al., 2004) and our own whole-cell recordings from non-rhythmic, 300 μm thick slices (Fig 2.5), non-excitatory glia are $\leq 10 \mu\text{m}$ in diameter ($\sim 80 \mu\text{m}^2$), therefore, groups 1 and 2 were considered most likely to comprise glia.

Cells in the three cell groups had similar baseline fluorescence intensity but responded differently to bath-applied ATP (0.1 mM) (Fig 2.3B-D). Fluorescence in Group 1 ($n=77$, from 5 slices) and Group 2 cells ($n=49$, from 5 slices) increased significantly from 800 ± 41 to 1634 ± 79 (an increase of 857 ± 65) and 802 ± 41 to 1216 ± 72 (an increase of 418 ± 63) fluorescence units, respectively (Fig 2.3B-D). Fluorescence did not change significantly in Group 3 (730 ± 41 to 922 ± 67 ; $n=20$, from 5 slices; Fig 2.3B-D).

To address the possibility that these ATP responses were indirect, perhaps mediated through neuronal excitation and neurotransmitter release, ATP was applied again to the same cells but this time in the presence of a bath-applied antagonist cocktail of TTX (0.5 μM) to block action potentials, and CNQX (10 μM) and APV (50 μM) to block AMPA and NMDA

receptors, respectively. The antagonist cocktail abolished inspiratory rhythm within 3 min. The fluorescence increase (peak response-baseline) evoked by ATP after 5 min, while significantly lower than the original response, was still significant and averaged 393 ± 45 and 238 ± 41 fluorescence units for Group 1 and Group 2 cells, respectively (Fig 2.3D, Two-Way ANOVA, Bonferroni correction). ATP responses evoked at 15 min intervals during antagonist washout remained constant and were similar to those seen in the antagonist (Fig 2.3D).

The only unexpected result from these imaging experiments was that the largest cells (presumptive neurons) did not respond to ATP with a significant increase in Ca^{2+} fluorescence. Neurons, including inspiratory neurons, in the preBötC express P2X₂ and P2Y₁ receptors (Lorier et al., 2004; Lorier et al., 2007). The vast majority of inspiratory neurons also respond to ATP with inward currents under whole-cell recording conditions (Lorier et al., 2008). Neurons in this region would therefore be expected to respond to ATP; however, given the greater potential for ATP hydrolysis by ectonucleotidases with bath application (Funk et al., 2008; Huxtable et al., 2009) (i.e. ATP has to diffuse through tissue whereas with local application it is injected into the site of interest) and for receptor desensitization/internalization (as the ATP concentration gradually increases). In addition to enzymatic breakdown and receptor desensitization, the lack of neuronal calcium increase to bath-applied ATP can also be attributed to the fact that we're only measuring changes in intracellular calcium. ATP might be affecting the membrane potential without causing noticeable calcium change. As such, we measured the fluo-4 fluorescence evoked by locally-applied ATP to test the possibility that the non-responsiveness of large cells was associated with bath-application of ATP (1 mM). Given the smaller number of cells activated, they were grouped simply as large ($139\pm23 \mu\text{m}^2$, range $95\text{-}201 \mu\text{m}^2$, n=5) or small ($61.0\pm3.2 \mu\text{m}^2$, range $50\text{-}75 \mu\text{m}^2$, n=9). In this protocol, large and small cells responded to ATP with a significant increase in fluorescence, as shown for individual cells in Fig 2.4. This increase

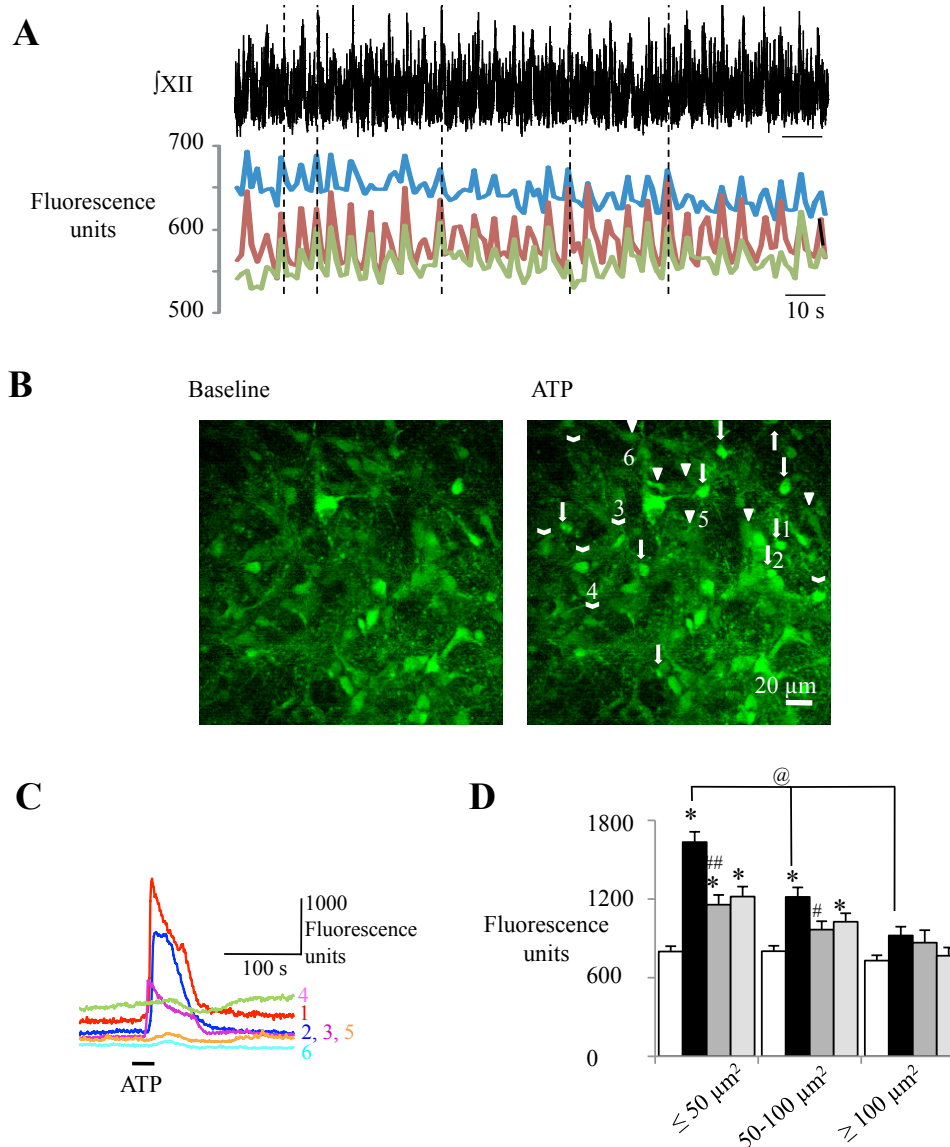


Figure 2.3 Multi-photon imaging of fluo-4 Ca^{2+} fluorescence showing sensitivity of preBötC cells at a single optical plain to bath-applied ATP.

A) Small fluorescence oscillations recorded from 3 cells in-phase with rhythmic bursts of activity recorded from the XII nerve in the same x-y plane as cells shown in B but slightly more superficial. B) Multi-photon images of the preBötC showing fluo-4 fluorescence under baseline conditions (left panel) and during bath application of ATP (0.1 mM, 30 s, right panel). C) Traces showing time course of fluo-4 fluorescence recorded from the 6 ROIs (numbered 1-6) in response to ATP application. Cells of different cross sectional areas are indicated with the following symbols: cells $\leq 50 \mu\text{m}^2$ (\downarrow), $50-100 \mu\text{m}^2$ (\vee), or $\geq 100 \mu\text{m}^2$ (Δ). D) Group data of cells ($n=77 \leq 50 \mu\text{m}^2$; $n=49 50-100 \mu\text{m}^2$; $n=20 \geq 100 \mu\text{m}^2$ from 5 slices) showing baseline fluorescence (white bars), peak fluorescence values evoked by ATP (black bars, 0.1 mM, 30 s), peak fluorescence values evoked by ATP in the presence of TTX, CNQX, and APV (dark gray bars, 0.5 μM , 0.1 mM, and 0.05 mM respectively), and the ATP response after antagonist washout (light gray bars) (* $p<0.001$ indicates significant difference from baseline; # $p<0.05$, ## $p<0.001$ indicate significant difference from ATP response, @ $p<0.001$ indicates significant difference from $\leq 50 \mu\text{m}^2$ cell ATP response).

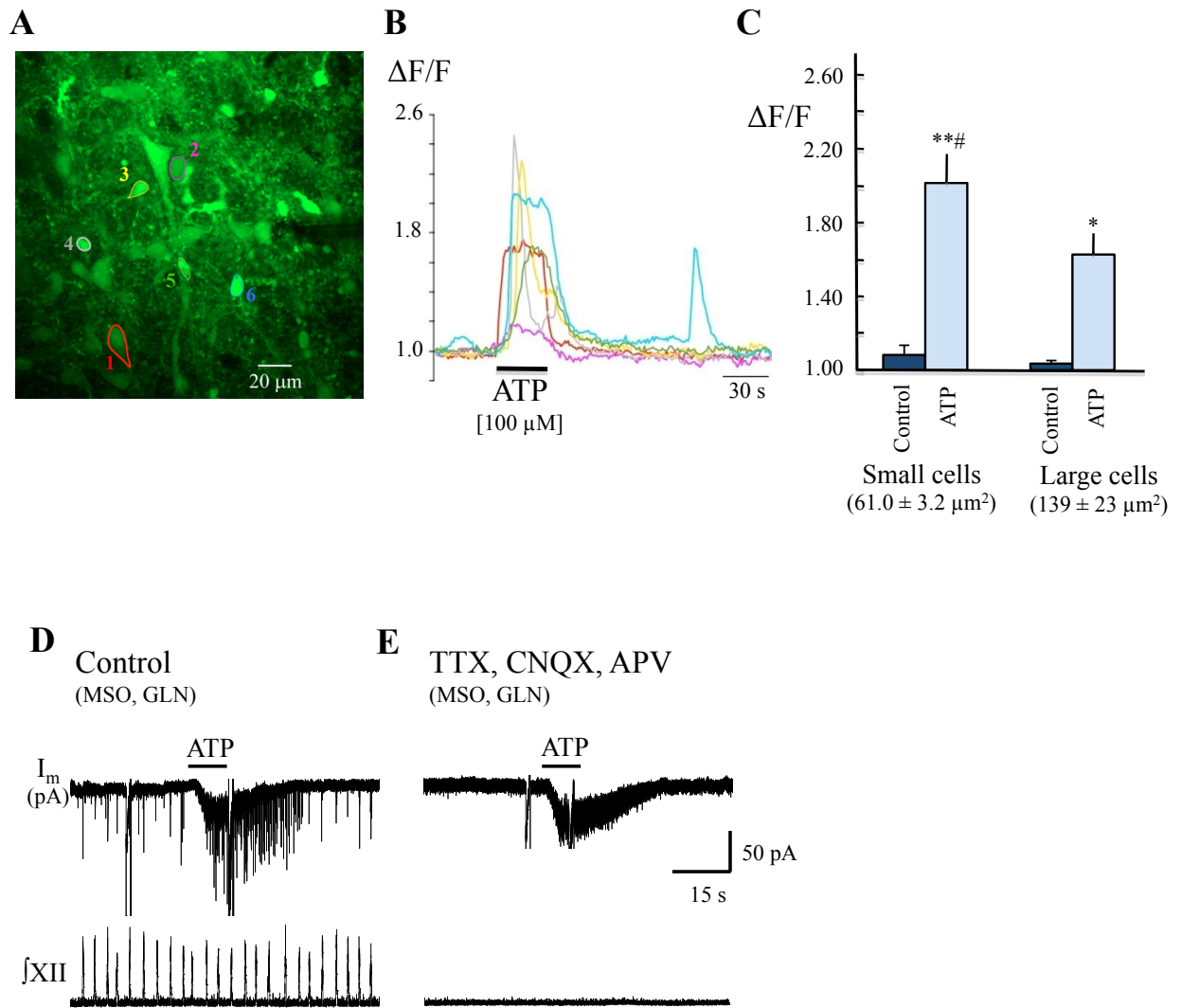


Figure 2.4 Multi-photon imaging of fluo-4 Ca^{2+} fluorescence showing sensitivity of preBötC cells at a single optical plain to locally-applied ATP.

A) Multi-photon image of the preBötC showing baseline fluo-4 fluorescence of multiple cells. Six cells are color-coded and the time course of their fluorescence responses to locally-applied ATP (100 μM , 30 s) are shown in B. Red and pink cells have areas $>100 \mu\text{m}^2$. C) Group data showing peak fluorescence responses to locally-applied aCSF (control) and ATP of small ($n=9$) and large ($n=5$) cells. D) Response of an inspiratory neuron to locally-applied ATP (1.0 mM, 10 s) after incubating the slice in MSO (0.1 mM) for 90 min and recovering rhythm with glutamine (GLN, 1.5 mM). E) Response of the same neuron 15 min later after bath application of TTX (0.5 μM), CNQX (10 μM), APV (100 μM). F) Group data showing mean peak ATP-evoked (10 mM) currents in inspiratory neurons in MSO/GLN and then after bath application of TTX, CNQX, and APV ($n=4$). (** $p<0.001$, * $p<0.01$ indicate significant difference between control [aCSF] and ATP; # $p<0.05$ indicates significant difference between small and large cells).

from 1140 ± 207 to 1838 ± 403 fluorescence units ($162 \pm 13\%$) and 1300 ± 142 to 2374 ± 203 fluorescence units ($201 \pm 14\%$) in large and small cells, respectively (Fig 2.4A-C).

To further establish that neuron sensitivity is not dependent on glia, we measured ATP currents of inspiratory and non-inspiratory neurons in rhythmic slices under two conditions. The first, after 90 min incubation in MSO (0.1 mM) and restoration of rhythm with GLN (1.5 mM) and the second, after adding TTX (0.5 μ M), CNQX (10 μ M), and APV (100 μ M) to the bath to block synaptic transmission and glutamatergic receptors. We demonstrated, as expected based on data from Lorier et al. (2008), that the neurons responded to ATP under both conditions, i.e. that neuronal ATP currents are not dependent on glutamate release from glia. As shown for a single inspiratory neuron (defined by the presence of synaptic currents in phase with rhythmic fXII activity) in Fig 2.4D and E, ATP (1 mM, 10 s) evoked a current in MSO/GLN that was similar following bath application of TTX, CNQX, and APV. Group data were similar. Currents evoked by 10 mM ATP averaged 30 ± 4.7 pA in MSO/GLN and 26 ± 7.2 pA after TTX, CNQX, and APV. These currents were associated with $14.3 \pm 6.2\%$ and $13.8 \pm 6.1\%$ decreases in R_N before and after TTX, CNQX, and APV respectively. Four non-inspiratory neurons tested only after addition of TTX, CNQX, and APV responded to ATP (10 mM) with currents of 30 ± 10 pA.

While ATP-evoked Ca^{2+} increases in Group 1 and 2 cells suggest direct activation of glia by ATP, size criteria alone do not unequivocally identify glia. Thus, to further test whether glia can respond directly to ATP, we used whole-cell recording to target nonexcitable cells (that could not fire action potentials) with morphology similar to that described previously (Grass et al., 2004). ATP (0.1 mM, 30 s) or the P2Y₁R agonist (0.1 mM MRS 2365, 30 s) was applied to 8 cells (<10 μ m diameter) in total (ATP to 7 cells and MRS 2365 to 5 cells). ATP and MRS 2365 responses were pooled as P2R agonist-evoked currents because the ATP- and MRS 2365-evoked currents were similar and if a cell responded to ATP, it also responded to MRS 2365. Cells fell into two categories based on their ATP sensitivity, input resistance (R_N), and resting potential. The first group responded to P2R

agonists with average currents of 36 ± 6 pA ($n=4$), as shown for a single cell in Fig 2.5A. This group had low R_N values (23 ± 2 M Ω) and resting membrane potentials of -68 ± 0.8 mV, depolarized compared to other work (Grass et al., 2004) due to elevated extracellular K $^+$ used here. The second group of cells ($n=4$) did not respond to P2R agonists. These cells had higher R_N (289 ± 37 M Ω) and significantly more depolarized resting membrane potentials (-59 ± 2 mV). The relationship between P2R agonist-evoked current amplitude and cell R_N is plotted for each cell in Fig 2.5B ($n=8$) and reveals distinct groups. Amplitudes for the ATP currents in high and low input resistance cells are plotted in Fig 2.5C. Glutamate (1 mM, 200-500 ms) was applied as a control to assess cell viability. Low (-98 ± 13 pA, $n=2$) and high (-91 ± 48 pA, $n=2$) R_N cells responded similarly to glutamate.

Even with whole-cell recording, the possibility remains that glial responses in tissue slices are mediated indirectly through neuronal activation and neurotransmitter release. To eliminate the possibility of secondary activation, primary cultures of glia from the ventral medulla at the rostro-caudal level of the preBötC were produced to test the ATP sensitivity of these cells in isolation. We confirmed the glial composition of cultures using immunocytochemistry with antibodies against two common glial markers (S100 β and GFAP), a neuronal marker (NF-160), and Hoechst staining to label cell nuclei (data not shown). The majority (>90%) of cells cultured from the ventral medulla on 5 occasions were positive for both glial markers. These cultures were devoid of NF-160 staining, but 5-10% of cells identified by Hoechst staining did not stain for glial markers.

To determine the P2R sensitivity of ventral medullary glia, cells were loaded with fluo-4 AM and visualized under DIC optics (Fig 2.6A). The triple-barreled pipette was positioned 10-20 μ m above the coverslip, upstream of a cluster of cells (orientation shown in Fig 2.6A), and changes in fluorescence monitored following local drug application. Local application of ATP (0.01 mM, 10 s) caused a significant increase in fluorescence from a baseline of 91 ± 5 to an average peak of 196 ± 11 fluorescence units (Fig 2.6C, $n=98$, from 3 coverslips, Two-Way ANOVA, Bonferroni correction). SP (1 μ M, 10 s), on the other hand,

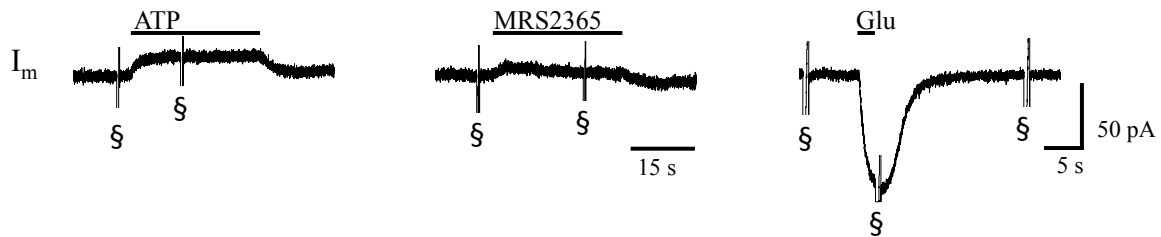
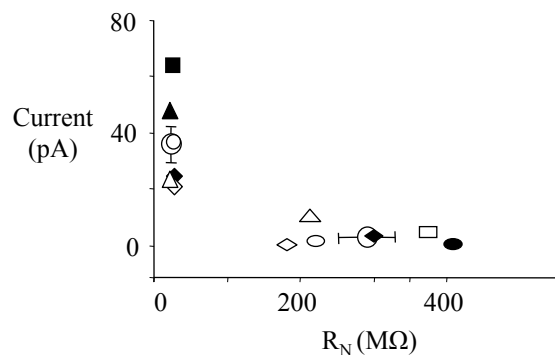
A**B**

Figure 2.5 Whole-cell voltage-clamp recordings from glia in the preBötC.

A) Membrane current responses of a single glial cell to local application of ATP (0.1 mM, 30 s, left), a P2Y₁R agonist (0.1 mM MRS 2365, 30 s, middle), and glutamate (1 mM, 2 s, right). B) Group data (n=8) showing the relationship between maximum agonist-evoked current and input resistance (R_N); each symbol type represents a different cell; open symbols represent ATP responses; closed symbols represent responses to MRS 2365 in the same cell; circles represent averaged data. C) Group data showing the current response produced by local ATP application on cells with high (n=4) and low input resistance (n=3). (* p<0.01 indicates significant difference, § indicates current response to a voltage ramp).

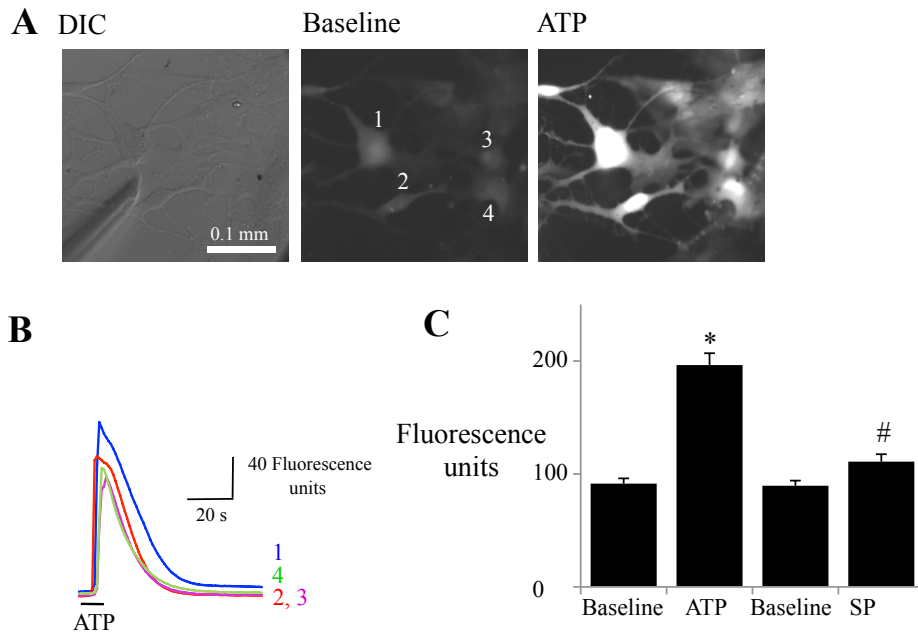


Figure 2.6 Glia cultured from the ventrolateral medulla respond to locally-applied ATP (0.01 mM, 10 s) with an increase in fluo-4 Ca^{2+} fluorescence.

A) DIC image of cultured glia and the position of the drug pipette (left panel). Epifluorescence image of cells in left panel showing baseline fluorescence (middle panel) after incubation with fluo-4 AM (10 μM) and during local application of ATP (right panel). B) Traces showing the time course of changes in intracellular calcium measured in 4 ROIs (numbered 1-4) in A. C) Group data ($n=98$) showing a significant increase in fluorescence in response to ATP, but not SP. (* $p<0.001$, indicates significant difference from baseline, # $p<0.001$ indicates significant difference from ATP response.)

evoked small fluorescent increases in some cells, but when averaged over the population these changes in fluorescence (90 ± 5 to 111 ± 7 fluorescence units) were not significant (Fig 2.6C, n=98, from 3 coverslips, Two-Way ANOVA, Bonferroni correction).

Given the potential for heterogeneity in glial properties between regions, we examined glia cultured specifically from preBötC punches. The occasional NF-150 immunolabeled, neuron-like cell could survive in these cultures, but had morphology (cell bodies of 20-25 μm with multiple processes) distinct from any cells used in the slice Ca^{2+} imaging. Imaged areas were devoid of this neuron-like cell type.

Since P2Y₁Rs are the main subtype underlying the frequency increase evoked by ATP in the preBötC (Lorier et al., 2007), we tested in both culture types the hypothesis that P2Y₁Rs contribute to the ATP-evoked increase in intracellular Ca^{2+} . In ventral medullary cultures, local application of ATP (0.01 mM, 10 s) evoked a 3.53 ± 0.29 fold increase in fluorescence (data not shown). When preceded by a 90 s application of the P2Y₁R antagonist (0.5 mM MRS 2279) the ATP-evoked change in Ca^{2+} was significantly reduced to a 2.79 ± 0.29 fold increase that recovered toward control levels (3.53 ± 0.031 fold increase) after 10 min of antagonist washout (data not shown, n=20, from 3 coverslips, One-Way ANOVA, Bonferroni correction). The P2Y₁R agonist, MRS 2365 (1 μM , 10 s) caused a significant 5.0 ± 0.5 fold fluorescence increase in glia (n=28, 5 coverslips, paired t-test) to a maximum of 177 ± 45 fluorescence units from a baseline level of 37 ± 9 fluorescence units (data not shown). This increase was significantly reduced to a 3.1 ± 0.4 fold increase by 90 s pre-application of MRS 2279 (0.5 mM, a P2Y₁R antagonist, n=28, from 5 coverslips). After 10 min of washout, the MRS 2365 response partially recovered to a 4.0 ± 0.4 fold increase (data not shown). P2Y₁R sensitivity was further supported with immunocytochemical analysis of fixed cultures, which demonstrated that cultured cells labeled for both S100 β and the P2Y₁R (Fig 2.7, n=4 coverslips). Local application of ATP (0.01 mM, 10 s) to the preBötC punches

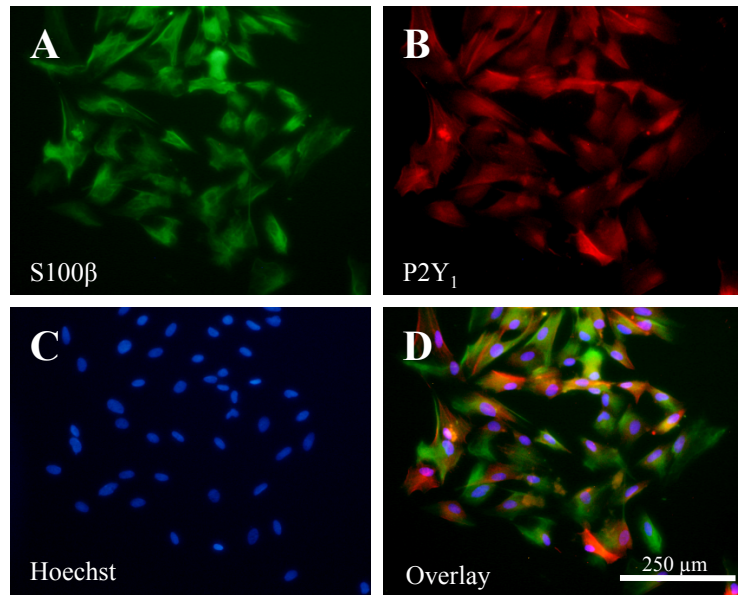


Figure 2.7 Glia cultured from the ventrolateral medulla express immunolabeling for the P2Y₁R

Epifluorescence images of a glial culture showing immunolabeling for the glial marker S100 β (monoclonal anti-S-100 β -subunit antibody with Alexa Fluor® 488 donkey anti-mouse IgG, A) and the P2Y₁R (rabbit anti-P2Y₁ with Alexa Fluor® 594 donkey anti-rabbit IgG, B). C) Hoechst staining of cell nuclei. D) The overlay of A-C.

caused a significant, 2.4 ± 0.1 fold increase, in cell fluorescence from 66 ± 3 to 154 ± 9 fluorescence units (Fig 2.6). In preBötC cultures, local application of ATP (0.01 mM, 10 s) caused a significant, 2.4 ± 0.1 fold, increase in cell fluorescence from 66 ± 3 to 154 ± 9 fluorescence units (Fig 2.8). However, this increase was significantly reduced by a 90 s pre-application of MRS 2279 (0.5 mM) to a 1.4 ± 0.1 fold increase (Fig 2.8). The antagonism was reversible, recovering to a 2.3 ± 0.1 fold increase 15 min after antagonist washout (Fig 2.8A-C, One-Way ANOVA, Bonferroni correction). Similarly, MRS 2365 (0.001 mM, 10 s) caused a 2.8 ± 0.1 fold fluorescence increase that was reduced to a 1.3 ± 0.03 fold increase by MRS 2279 and recovered to a 2.5 ± 0.1 fold increase after 15 min of antagonist washout (Fig 2.8D, One-Way ANOVA, Bonferroni correction).

The increase in fluorescence after MRS 2279 and either ATP or MRS 2365 in the preBötC cultures was not significantly different from baseline fluorescence (Fig 2.8C, D). This was not the case, however, with the ventral medullary cultures (described above) in which a significant fluorescence response persisted in the presence of MRS 2279. To assess whether this might reflect contribution of non-P2Y₁Rs to the ATP response in ventral medullary cultures, we compared the block produced by MRS 2279 alone and then in combination with PPADS (100 µM) and suramin (500 µM). ATP evoked a 2.45 ± 0.12 fold increase in fluorescence (Fig 2.8E). This was reduced to a 1.97 ± 0.08 fold increase by MRS 2279 in combination with PPADS and suramin, which was a bigger reduction than that produced by MRS 2279 alone (1.84 ± 0.07 , n=52 cells from 4 cultures).

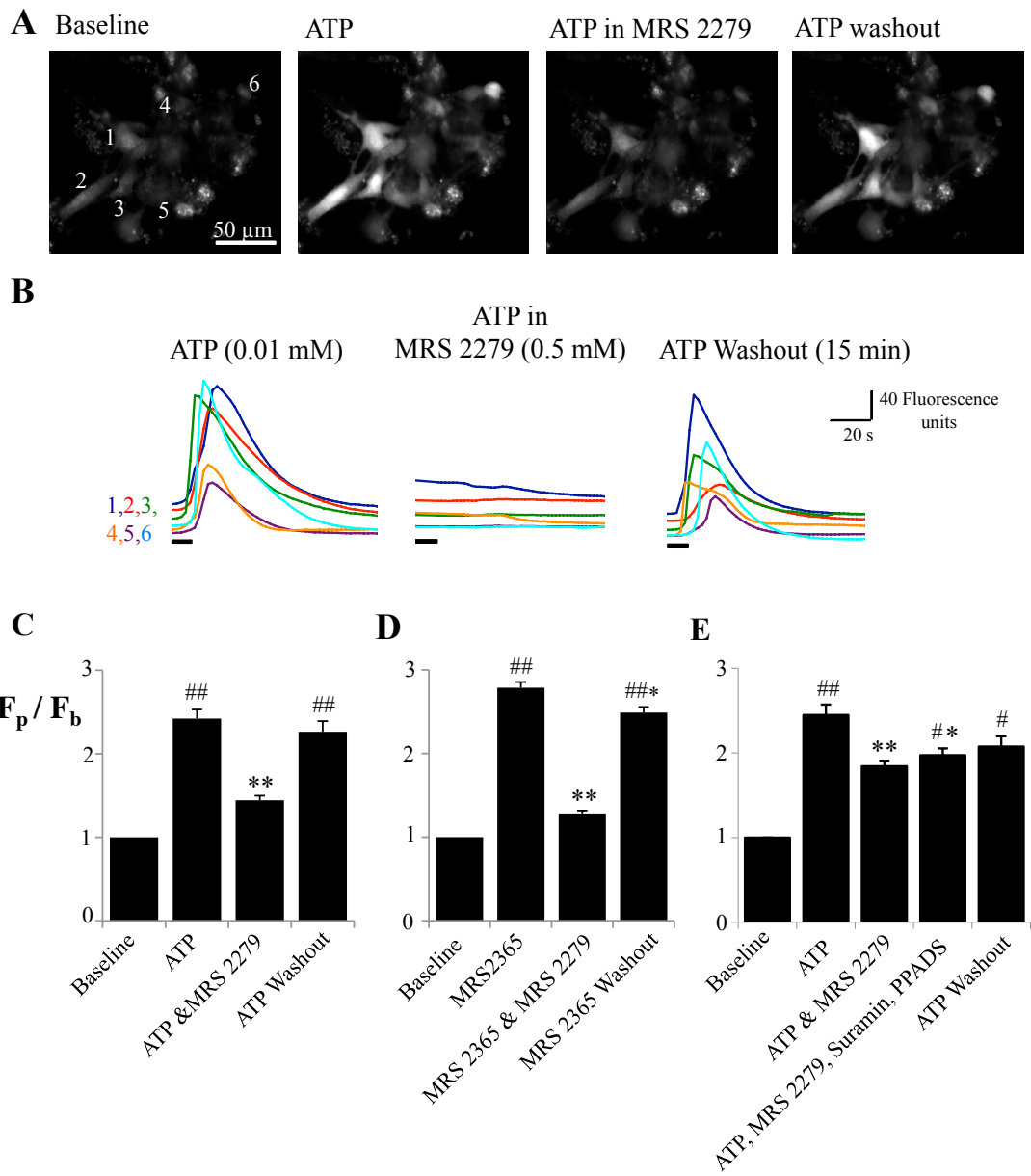


Figure 2.8 Glia cultured from preBötC punches respond to ATP with an increase in fluo-4 Ca^{2+} fluorescence.

A) Epifluorescence images showing the fluo-4 signal under baseline conditions (left panel), during local application of ATP (0.01 mM, 10 s,) during control conditions (second panel), after pre-application of P2Y₁R antagonist (0.5 mM MRS 2279, 90 s, third panel), and after washout of the antagonist (right panel). B) Time course of ATP-evoked fluorescence changes measured from 6 ROIs (numbered in A) in control (left), in MRS 2279 (middle), and during washout (right). C) Group data (n=63) showing relative changes in fluorescence in response to ATP and to ATP in the presence of MRS 2279. D) Group data (n=28) demonstrating the relative changes in fluorescence in response to the P2Y₁R agonist, MRS 2365 (0.001 mM, 10 s) and to MRS 2365 in the presence of MRS 2279. E) Group data from ventrolateral medulla cultures (n=52) showing the relative change in fluorescence evoked by ATP alone, in the presence of MRS 2279, in MRS2279 and PPADS (100 μM) and suramin (500 μM), and during washout. (# $p<0.001$, # $p<0.05$ indicates significant difference from baseline; * $p<0.01$, ** $p<0.001$, indicates significant difference from peak).

2.3.4 Release of glutamate from primary glia cultures

While the preceding data demonstrate that glia in, or cultured from, the preBötC respond to ATP with an outward current or an increase in intracellular Ca^{2+} , the glia need to release excitatory agents to influence inspiratory neurons, and in turn network activity. Given that ATP evokes glutamate release from glia (Parpura et al., 1994; Araque et al., 2000; Jeremic et al., 2001; Domercq et al., 2006) and that glutamate in the preBötC potently increases inspiratory frequency (Greer et al., 1991; Smith et al., 1991; Funk et al., 1993), we hypothesized that glia from the ventral medulla at the level of the preBötC release glutamate in response to ATP. To test this, we used HPLC to measure glutamate concentration in culture media at time zero and after 5 min incubation in either aCSF, ATP, or ATP and a P2R antagonist cocktail (0.5 mM suramin, 0.1 mM PPADS, 0.5 mM MRS 2279). At 5 min, glutamate levels in aCSF were at 0.92 ± 0.05 ($n=12$) of levels at time zero. In contrast, ATP evoked a 1.90 ± 0.26 fold increase (Fig 2.9, $n=12$, One-Way ANOVA, Tukey's Multiple Comparison) in glutamate concentration. Importantly, this ATP-evoked increase in glutamate was abolished (0.94 ± 0.16 of time zero levels) when ATP was co-applied with the P2R antagonist cocktail (Fig 2.9, $n=10$, One-Way ANOVA, Tukey's Multiple Comparison), indicating that the glutamate release was dependent on P2R activation.

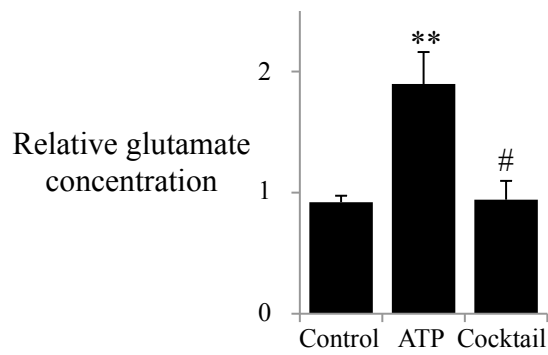


Figure 2.9 ATP evokes glutamate release from ventrolateral medulla glia cultures.

The glutamate concentration in the culture media was measured using high performance liquid chromatography at time zero and after 5 min incubation periods of either: aCSF (control, n=12), ATP (0.05 mM, n=12), or ATP with a cocktail of P2R antagonists (0.5 mM suramin, 0.1 mM PPADS, 0.5 mM MRS 2279, n=10). Levels are reported relative to values at time zero. (# p<0.01 indicates significant difference from ATP-evoked glutamate, * p<0.001 indicates significant difference from control).

2.4 Discussion

Glia are necessary for maintaining inspiratory network activity (Hulsmann et al., 2000), but until now the role of gliotransmission in modulating inspiratory network activity has not been examined. Abundant evidence indicate that glia influence neuronal excitability, but understanding how glia influence neuronal networks is limited and includes their involvement in synapse formation and elimination (Haydon and Carmignoto, 2006; He and Sun, 2007), changes in synaptic efficacy (Zhang et al., 2003; Gordon et al., 2005), and sleep regulation (Halassa et al., 2009). We present evidence that modulation of inspiratory network activity by ATP does not just occur through neurons (Lorier et al., 2008), but also through glia.

The block of the ATP-evoked frequency increase by the glial toxin MSO, and its significant attenuation by FA, strongly implicate glia in this response. Whether the actions of these toxins result exclusively from their actions on glia or through secondary mechanisms is controversial. The fact that MSO more effectively inhibits the ATP-evoked frequency response suggests that either MSO is more effective in blocking glia or that non-glial actions of MSO account for its greater efficacy. The toxins had similar effects on baseline rhythm in our experiments, but previous data in rhythmic slices showed that after 60 min FA reduced frequency to $47.4\pm7.1\%$ of control, while MSO reduced frequency to $5.3\pm5.3\%$ (Hulsmann et al., 2000). While these data suggest that MSO is more effective at blocking rhythm, and our data indicate that MSO is more effective at blocking the ATP response, they do not establish that MSO has a greater ability to disrupt glial function. The important point is that two glial toxins, operating through different mechanisms, both inhibit the ability of ATP to excite preBötC inspiratory networks, supporting a glial contribution to the network response.

Recent work suggests that the acute actions of MSO and FA are in fact mediated primarily through glia. First, FA induced inward currents or depolarizations in glia but had no effect on XII MNs (Hulsmann et al., 2000). Second, a side-effect of systemically-applied

MSO is glycogen deposition in cranial motoneurons of neonatal rat (Young et al., 2005).

While the impact of glycogen on neuron and network function is unclear, it is unlikely of significance as the deposition occurs on a time scale (days) much slower than relevant to our manipulations. Third, FA and MSO increase extracellular K⁺ (Largo et al., 1997). Again, however, this is unlikely a factor in our experiments as it would enhance inspiratory rhythm and motor output of rhythmic slices rather than impair it.

The most compelling evidence supporting involvement of glia in the ATP-evoked increase frequency inspiratory is that while glial toxins altered the effects of ATP on frequency, the sensitivity of preBötC networks to SP persisted; i.e., the toxins did not affect what is most likely a neuronally-mediated response. Supporting the neuronal nature of the SP response is that preBötC neurons critical for rhythm generation are excited by SP and express NK1Rs (Gray et al., 1999; Gray et al., 2001). In addition, glia cultured from the preBötC have minimal SP sensitivity (Fig. 2.6), and few glia respond to SP with small increases in intracellular Ca⁺² (Hartel et al., 2009). Furthermore, while cultured glia express NK1R mRNA (Too et al., 1994), glia in guinea pig (Yip and Chahl, 2001) and human brain (Tooney et al., 2000) do not express NK1R protein. Thus, while it remains possible that SP alters glial activity without changing intracellular Ca²⁺, the persistence of the neuronally-mediated SP response strongly supports the glial specificity of the toxins.

At the same time, the fact that one of the toxins (FA) only reduced the ATP-response raises the possibility that neurons contribute. In fact, the moderate and almost ubiquitous sensitivity of preBötC inspiratory neurons to ATP (Lorier et al., 2008) combined with the sensitivity of preBötC neurons to ATP in the presence of MSO, TTX, and glutamate receptor antagonists, suggest that the ATP response is most likely mediated through activation of both neurons and glia. Data also suggest that while glia are not required for all modulators (e.g., SP) to influence inspiratory rhythm, they are important to the ATP response.

Our hypothesis that glia contribute to the ATP response is further supported by numerous lines of evidence that preBötC glia show P2R-dependent ATP sensitivity. To

begin, ATP responses do not involve VRACs. From this point, delineating glial from neuronal drug actions in an intact network is difficult since glia and neurons release many of the same transmitters (e.g., glutamate and ATP) and express the same receptors (Porter and McCarthy, 1997; Deitmer et al., 1998). We, used multiple techniques to confirm ATP sensitivity of preBötC glia. Multi-photon Ca^{2+} imaging in rhythmic slices established that small preBötC cells respond to ATP with increased intracellular Ca^{2+} . As size criteria alone do not positively identify glia, whole-cell recording data were important as these demonstrated that small, non-excitatory preBötC cells with electrical properties similar to previously identified astrocytes (Grass et al., 2004), are sensitive to P2R modulation. Lack of a detectable ATP response in half of the nonexcitable cells supports heterogeneity of glia (Grass et al., 2004), but does not necessarily indicate that cells are insensitive to ATP, only that P2R stimulation did not evoke a change in membrane current. It is also possible that the ATP-insensitive cells are oligodendrocytes, as these also have high input resistance values (Chvatal et al., 2004; Karadottir et al., 2008). However, our data do not allow unequivocal discrimination because at the ages studied here (P0-4) astrocyte precursor cells, astrocytes, oligodendrocyte precursor cells, and oligodendrocytes all fit within the size range of recorded cells.

Since the multi-photon and whole-cell experiments were performed in brain slices, the possibility remains that responses reflect indirect activation of glia by ATP-evoked neurotransmitter release. The P2R sensitivity of glia cultures derived from the VLM and preBötC was therefore instrumental in establishing direct ATP sensitivity of glia. Culturing of cells can induce changes in gene transcription and receptor expression (Kimelberg et al., 1997). However, the properties of glial receptors (including P2Rs) measured *in vitro* are often unchanged in culture (Neary et al., 1988). Thus, while we cannot exclude the possibility that the responses in culture reflect altered P2R expression, the culture data are consistent with Ca^{2+} imaging and whole-cell electrophysiology data and strongly support that preBötC glia are sensitive to ATP, in part through P2Y₁Rs.

Involvement of glia in the ATP-evoked frequency increase is further supported by our demonstration of ATP-evoked, P2R-dependent glutamate release. Glutamate potently excites inspiratory rhythm (Greer et al., 1991; Funk et al., 1993; Funk et al., 1997). We therefore propose that activation of glial P2Rs increases intracellular Ca^{2+} (as shown using multi-photon imaging of slices and Ca^{2+} imaging in culture) and evokes glutamate release, which in turn activates preBötC neurons, causing a frequency increase. Changes in intracellular Ca^{2+} are associated with gliotransmitter release (including glutamate and ATP) in glia cultures from multiple brain regions (Araque et al., 2000; Coco et al., 2003; Fiacco and McCarthy, 2006). In addition to local release of glutamate from individual glia, ATP could also influence preBötC activity by inducing Ca^{2+} oscillations in glial networks; this could produce widespread glutamate release (Deitmer et al., 1998; Fiacco and McCarthy, 2006; Haydon and Carmignoto, 2006). While we have demonstrated that glia contribute to the respiratory network ATP response, directly respond to ATP, and release glutamate in response to ATP, this does not exclude a contribution from other gliotransmitters.

At present, hypoxia is the only physiological stimulus known to cause ATP release within the ventrolateral medulla, where it offsets the hypoxic ventilatory depression (Gourine et al., 2005). Based on previous data and those presented here, we propose that the increase in frequency associated with ATP and P2Y₁R activation in the preBötC is due to combined actions on neurons and glia. Direct P2R activation of preBötC neurons will cause membrane depolarization or increased excitability and a frequency increase (Lorier et al., 2007; Lorier et al., 2008). Direct activation of preBötC glia will evoke the release of glutamate (and perhaps other gliotransmitters), which will depolarize preBötC neurons causing frequency to increase. Both actions, neuronal and glial, may then attenuate the hypoxic ventilatory depression.

In summary, we demonstrate that glia contribute to the purinergic excitation of preBötC rhythm generating networks and propose that this contribution involves the direct activation of glial P2Rs and glutamate release. While it is widely accepted that glia play

significant and diverse roles in modulating the activity of neurons, the difficulty of discretely manipulating neuro- versus gliotransmission means that the physiological significance of gliotransmission in modulating activity of functionally identified, behaving, mammalian neural networks is poorly understood. Our data are significant in that they demonstrate a contribution of glia to the neurochemical modulation of the functioning mammalian brainstem network that generates inspiratory rhythm. This raises important questions about the potential involvement of glia in modulating activity of other motor behaviors. In addition, given the complement of receptors that glia express (Porter and McCarthy, 1997; Deitmer et al., 1998), glial modulation of network activity is likely to extend beyond purinergic signaling.

2.5 References

- Abbracchio MP, Boeynaems JM, Barnard EA, Boyer JL, Kennedy C, Miras-Portugal MT, King BF, Gachet C, Jacobson KA, Weisman GA, Burnstock G (2003) Characterization of the UDP-glucose receptor (re-named here the P2Y14 receptor) adds diversity to the P2Y receptor family. *Trends Pharmacol Sci* 24:52-55.
- Araque A, Li N, Doyle RT, Haydon PG (2000) SNARE protein-dependent glutamate release from astrocytes. *J Neurosci* 20:666-673.
- Burnstock G (2007) Physiology and pathophysiology of purinergic neurotransmission. *Physiol Rev* 87:659-797.
- Chvatal A, Anderova M, Sykova E (2004) Analysis of K⁺ accumulation reveals privileged extracellular region in the vicinity of glial cells *in situ*. *J Neurosci Res* 78:668-682.
- Coco S, Calegari F, Pravettoni E, Pozzi D, Taverna E, Rosa P, Matteoli M, Verderio C (2003) Storage and release of ATP from astrocytes in culture. *J Biol Chem* 278:1354-1362.
- Deitmer JW, Verkhratsky AJ, Lohr C (1998) Calcium signalling in glial cells. *Cell Calcium* 24:405-416.
- Domercq M, Brambilla L, Pilati E, Marchaland J, Volterra A, Bezzi P (2006) P2Y1 receptor-evoked glutamate exocytosis from astrocytes: control by tumor necrosis factor-alpha and prostaglandins. *J Biol Chem* 281:30684-30696.
- Edwards FA, Gibb AJ, Colquhoun D (1992) ATP receptor-mediated synaptic currents in the central nervous system. *Nature* 359:144-147.

- Espallergues J, Solovieva O, Techer V, Bauer K, Alonso G, Vincent A, Hussy N (2007) Synergistic activation of astrocytes by ATP and norepinephrine in the rat supraoptic nucleus. *Neuroscience* 148:712-723.
- Evans RJ, Derkach V, Surprenant A (1992) ATP mediates fast synaptic transmission in mammalian neurons. *Nature* 357:503-505.
- Feldman JL, Del Negro CA (2006) Looking for inspiration: new perspectives on respiratory rhythm. *Nat Rev Neurosci* 7:232-242.
- Fiacco TA, McCarthy KD (2006) Astrocyte calcium elevations: properties, propagation, and effects on brain signaling. *Glia* 54:676-690.
- Funk GD, Smith JC, Feldman JL (1993) Generation and transmission of respiratory oscillations in medullary slices: role of excitatory amino acids. *J Neurophysiol* 70:1497-1515.
- Funk GD, Huxtable AG, Lorier AR (2008) ATP in central respiratory control: A three-part signaling system. *Respir Physiol Neurobiol*.
- Funk GD, Johnson SM, Smith JC, Dong XW, Lai J, Feldman JL (1997) Functional respiratory rhythm generating networks in neonatal mice lacking NMDAR1 gene. *J Neurophysiol* 78:1414-1420.
- Gardner-Medwin AR, Coles JA, Tsacopoulos M (1981) Clearance of extracellular potassium: evidence for spatial buffering by glial cells in the retina of the drone. *Brain Res* 209:452-457.
- Gordon GR, Baimoukhamedova DV, Hewitt SA, Rajapaksha WR, Fisher TE, Bains JS (2005) Norepinephrine triggers release of glial ATP to increase postsynaptic efficacy. *Nat Neurosci* 8:1078-1086.

Gourine AV (2005) On the peripheral and central chemoreception and control of breathing: an emerging role of ATP. *J Physiol* 568:715-724.

Gourine AV, Atkinson L, Deuchars J, Spyer KM (2003) Purinergic signalling in the medullary mechanisms of respiratory control in the rat: respiratory neurones express the P2X2 receptor subunit. *J Physiol* 552:197-211.

Gourine AV, Llaudet E, Dale N, Spyer KM (2005) Release of ATP in the ventral medulla during hypoxia in rats: role in hypoxic ventilatory response. *J Neurosci* 25:1211-1218.

Grant SL, Shulman Y, Tibbo P, Hampson DR, Baker GB (2006) Determination of d-serine and related neuroactive amino acids in human plasma by high-performance liquid chromatography with fluorimetric detection. *J Chromatogr B Analyt Technol Biomed Life Sci* 844:278-282.

Grass D, Pawlowski PG, Hirrlinger J, Papadopoulos N, Richter DW, Kirchhoff F, Hulsmann S (2004) Diversity of functional astroglial properties in the respiratory network. *J Neurosci* 24:1358-1365.

Gray PA, Rekling JC, Bocchiaro CM, Feldman JL (1999) Modulation of respiratory frequency by peptidergic input to rhythmogenic neurons in the preBotzinger complex. *Science* 286:1566-1568.

Gray PA, Janczewski WA, Mellen N, McCrimmon DR, Feldman JL (2001) Normal breathing requires preBotzinger complex neurokinin-1 receptor-expressing neurons. *Nat Neurosci* 4:927-930.

Greer JJ, Smith JC, Feldman JL (1991) Role of excitatory amino acids in the generation and transmission of respiratory drive in neonatal rat. *J Physiol* 437:727-749.

- Halassa MM, Florian C, Fellin T, Munoz JR, Lee SY, Abel T, Haydon PG, Frank MG (2009) Astrocytic modulation of sleep homeostasis and cognitive consequences of sleep loss. *Neuron* 61:213-219.
- Hartel K, Schnell C, Hulsmann S (2009) Astrocytic calcium signals induced by neuromodulators via functional metabotropic receptors in the ventral respiratory group of neonatal mice. *Glia* 57:815-827.
- Haydon PG, Carmignoto G (2006) Astrocyte control of synaptic transmission and neurovascular coupling. *Physiol Rev* 86:1009-1031.
- He F, Sun YE (2007) Glial cells more than support cells? *Int J Biochem Cell Biol* 39:661-665.
- Hulsmann S, Oku Y, Zhang W, Richter DW (2000) Metabolic coupling between glia and neurons is necessary for maintaining respiratory activity in transverse medullary slices of neonatal mouse. *Eur J Neurosci* 12:856-862.
- Huxtable AG, Zwicker JD, Poon BY, Pagliardini S, Vrouwe SQ, Greer JJ, Funk GD (2009) Tripartite purinergic modulation of central respiratory networks during perinatal development: the influence of ATP, ectonucleotidases, and ATP metabolites. *J Neurosci* 29:14713-14725.
- Jeremic A, Jeftinija K, Stevanovic J, Glavaski A, Jeftinija S (2001) ATP stimulates calcium-dependent glutamate release from cultured astrocytes. *J Neurochem* 77:664-675.
- Karadottir R, Hamilton NB, Bakiri Y, Attwell D (2008) Spiking and nonspiking classes of oligodendrocyte precursor glia in CNS white matter. *Nat Neurosci* 11:450-456.

- Kimelberg HK, Cai Z, Rastogi P, Charniga CJ, Goderie S, Dave V, Jalonen TO (1997) Transmitter-induced calcium responses differ in astrocytes acutely isolated from rat brain and in culture. *J Neurochem* 68:1088-1098.
- Largo C, Ibarz JM, Herreras O (1997) Effects of the gliotoxin fluorocitrate on spreading depression and glial membrane potential in rat brain in situ. *J Neurophysiol* 78:295-307.
- Lorier AR, Lipski J, Housley GD, Greer JJ, Funk GD (2008) ATP sensitivity of preBotzinger complex neurones in neonatal rat in vitro: mechanism underlying a P2 receptor-mediated increase in inspiratory frequency. *J Physiol* 586:1429-1446.
- Lorier AR, Peebles K, Brosenitsch T, Robinson DM, Housley GD, Funk GD (2004) P2 receptors modulate respiratory rhythm but do not contribute to central CO₂ sensitivity in vitro. *Respir Physiol Neurobiol* 142:27-42.
- Lorier AR, Huxtable AG, Robinson DM, Lipski J, Housley GD, Funk GD (2007) P2Y1 receptor modulation of the pre-Botzinger complex inspiratory rhythm generating network in vitro. *J Neurosci* 27:993-1005.
- Mongin AA, Kimelberg HK (2005) ATP regulates anion channel-mediated organic osmolyte release from cultured rat astrocytes via multiple Ca²⁺-sensitive mechanisms. *American journal of physiology Cell physiology* 288:C204-213.
- Neary JT, van Breemen C, Forster E, Norenberg LO, Norenberg MD (1988) ATP stimulates calcium influx in primary astrocyte cultures. *Biochemical and biophysical research communications* 157:1410-1416.
- Newman EA (2003) Glial cell inhibition of neurons by release of ATP. *J Neurosci* 23:1659-1666.

- North RA (2002) Molecular physiology of P2X receptors. *Physiol Rev* 82:1013-1067.
- Parpura V, Basarsky TA, Liu F, Jeftinija K, Jeftinija S, Haydon PG (1994) Glutamate-mediated astrocyte-neuron signalling. *Nature* 369:744-747.
- Porter JT, McCarthy KD (1997) Astrocytic neurotransmitter receptors in situ and in vivo. *Prog Neurobiol* 51:439-455.
- Ruangkittisakul A, Ballanyi K (2006) Reversal by phosphodiesterase-4 blockers of in vitro apnea in the isolated brainstem-spinal cord preparation from newborn rats. *Neurosci Lett* 401:194-198.
- Ruangkittisakul A, Schwarzacher SW, Secchia L, Poon BY, Ma Y, Funk GD, Ballanyi K (2006) High sensitivity to neuromodulator-activated signaling pathways at physiological [K⁺] of confocally imaged respiratory center neurons in on-line-calibrated newborn rat brainstem slices. *J Neurosci* 26:11870-11880.
- Ruangkittisakul A, Schwarzacher SW, Secchia L, Ma Y, Bobocea N, Poon BY, Funk GD, Ballanyi K (2008) Generation of eupnea and sighs by a spatiochemically organized inspiratory network. *J Neurosci* 28:2447-2458.
- Silinsky EM, Gerzanich V, Vanner SM (1992) ATP mediates excitatory synaptic transmission in mammalian neurones. *Br J Pharmacol* 106:762-763.
- Smith JC, Ellenberger HH, Ballanyi K, Richter DW, Feldman JL (1991) Pre-Botzinger complex: a brainstem region that may generate respiratory rhythm in mammals. *Science* 254:726-729.
- Too HP, Marriott DR, Wilkin GP (1994) Preprotachykinin-A and substance P receptor (NK1) gene expression in rat astrocytes in vitro. *Neurosci Lett* 182:185-187.

- Tooney PA, Au GG, Chahl LA (2000) Tachykinin NK1 and NK3 receptors in the prefrontal cortex of the human brain. *Clin Exp Pharmacol Physiol* 27:947-949.
- Tsacopoulos M (2002) Metabolic signaling between neurons and glial cells: a short review. *J Physiol Paris* 96:283-288.
- Yip J, Chahl LA (2001) Localization of NK1 and NK3 receptors in guinea-pig brain. *Regul Pept* 98:55-62.
- Young JK, Dreshaj IA, Wilson CG, Martin RJ, Zaidi SI, Haxhiu MA (2005) An astrocyte toxin influences the pattern of breathing and the ventilatory response to hypercapnia in neonatal rats. *Respir Physiol Neurobiol* 147:19-30.
- Zhang JM, Wang HK, Ye CQ, Ge W, Chen Y, Jiang ZL, Wu CP, Poo MM, Duan S (2003) ATP released by astrocytes mediates glutamatergic activity-dependent heterosynaptic suppression. *Neuron* 40:971-982.

Chapter 3: Purinergic modulation of preBötzinger Complex inspiratory rhythm in rodents: the interaction between ATP and adenosine

A version of this chapter has been published as

Zwicker JD, Rajani V, Hahn LB, Funk GD Purinergic modulation of preBötzinger complex inspiratory rhythm in rodents: the interaction between ATP and adenosine. J Physiol 2011. 589:4583-4600.

I performed all experiments and data analysis procedures except those listed below. I also contributed to experimental design, article drafting and revision, and final approval. V Rajani performed and analyzed experiments associated with Fig 5, contributed relevant sections of text and participated in the final revision process. LB Hahn designed, performed and analyzed the RTPCR experiments that described ectonucleotidase expression in the preBötC of mouse and rat, contributed relevant sections to the manuscript and provided final approval. GD Funk oversaw all aspects of the study, from conception to final publication. Overall, my contribution was ~90% of the total.

3.1 Introduction

Extracellular ATP acts on seven subtypes of ionotropic P2X (North, 2002) and eight subtypes of metabotropic P2Y receptor (R) (Abbracchio et al., 2003) to support diverse signaling functions in the peripheral and central nervous systems. In central respiratory control, P2 receptor signaling is most strongly implicated in chemoreceptor reflexes that regulate arterial O₂, and CO₂ or pH (Gourine et al., 2005a). During hypoxia, an initial increase in ventilation is followed by a secondary depression that is most pronounced, and potentially life-threatening, in fetal animals and premature infants. ATP contributes to this ventilatory response. It is released from the ventral respiratory column after the initial increase in ventilation where it attenuates the secondary hypoxic ventilatory depression (Gourine, 2005). The ATP excitation likely involves a potent P2Y₁R-mediated excitation of preBötC inspiratory networks, which in turn is likely to have both neuronal and astrocytic components (Lorier et al., 2008; Huxtable et al., 2010).

It is also important to consider that the actions of ATP are not determined solely by its actions at P2Rs. ATP signaling is best considered as a three-part system whose effects are determined from a dynamic interaction between the signaling actions of ATP and ADP at P2 receptors, the spatial distribution of ectonucleotidases that differentially metabolize ATP into ADP, AMP and adenosine (ADO), and the signaling actions of ADO at P1 receptors. The dynamics of this interaction are highly relevant for respiratory control because ADO is implicated as a respiratory depressant in adult (Eldridge et al., 1984; Yamamoto et al., 1994), newborn (Runold et al., 1989; Herlenius et al., 1997) and especially fetal mammals (Bissonnette et al., 1990). It is also implicated in the hypoxia-induced depression of ventilation (Moss, 2000). The control of swimming onset and offset in tadpoles by a similar ATP-ADO interaction (Dale and Gilday, 1996) suggests that this control mechanism may not be unique to inspiratory networks but represent a more widespread property of rhythmic motor networks. To fully understand the significance of ATP signaling for respiratory control

requires the characterization of processes ongoing within each limb of this 3-part signaling system.

To this end, we will characterize the purinergic modulation of the preBötC network in mouse. Responses in rat will be simultaneously assessed as a positive control to ensure the validity of any differences between mouse and published responses in rat. The rationale for extending this analysis to mouse is three-fold. First, the sensitivity of preBötC networks to P2Y₁R excitation has only been reported in neonatal Wistar and Sprague-Dawley (SD) rat (Lorier et al., 2007; Lorier et al., 2008; Huxtable et al., 2009; Huxtable et al., 2010). Determining whether this mechanism is limited to rats is an important step in defining its potential significance in modulation of respiratory rhythm in mammals in general. We will also test whether ADO produced by degradation of ATP in the preBötC is sufficient to inhibit inspiratory rhythm. Reports in intact mammals of many species consistently show that ADO inhibits breathing (Lagercrantz et al., 1984; Eldridge et al., 1985; Burr and Sinclair, 1988; Koos and Matsuda, 1990; Bissonnette et al., 1991; Wilson et al., 2004). Despite this and the clinical significance of ADO signaling for the control of breathing, neither the mechanism(s) nor the site(s) mediating the inhibitory actions of ADO on breathing rhythm have been identified. Brainstem involvement is uncertain. An A1R-mediated inhibition is reported in some mouse studies (Mironov et al., 1999; Vandam et al., 2008) but ADO is often reported to have no effect on brainstem rhythm in rat (Brockhaus and Ballanyi, 2000; Ballanyi, 2004; Ruangkittisakul and Ballanyi, 2010), suggesting a possible species difference. Even in mouse the role of the preBötC in the ADO inhibition is also unknown. Some preBötC inspiratory neurons are inhibited by ADO (Mironov et al., 1999), but whether this is sufficient to inhibit frequency will be explored. Ectonucleotidase expression in the preBötC of mouse and rat will also be determined to gain insight into the degree to which differences in ATP response kinetics might be attributed to differential enzyme expression. Third, establishing the ATP sensitivity of murine networks will also be of value given that the modulation of preBötC rhythm by ATP appears to involve both neurons (Lorier et al.,

2008) and astrocytes (Huxtable et al., 2010). Transgenic tools for identifying, monitoring and manipulating astrocytes are available in mouse but not rat. Baseline data in mouse will facilitate the application of these tools in determining the role of astrocytes in the purinergic modulation of preBötC activity.

3.2 Methods

All experiments were conducted in accordance with the guidelines of the Canadian Council on Animal Care and were approved by the University of Alberta Animal Ethics Committee.

3.2.1 Rhythmic medullary slices

Animals were anesthetized through inhalation of isoflurane and decerebrated. The brainstem–spinal cord was then isolated in cold artificial cerebrospinal fluid (aCSF) containing the following (in mM): 120 NaCl, 3 KCl, 1.0 CaCl₂, 2.0 MgSO₄, 26 NaHCO₃, 1.25 NaH₂PO₄, 20 D-glucose, equilibrated with 95% O₂/5% CO₂. The brainstem–spinal cord was pinned to a wax chuck, and serial 100–200 µm sections were cut in the rostral-to-caudal direction using a vibratome (VT1000S, Leica, Nussloch, Germany) and transilluminated to identify anatomical landmarks. Rhythmic, transverse, 700 µm-thick slices of the medulla from SD rats [postnatal day 0–4 (P0–P4)] and Swiss CD mice [postnatal day 0–5 (P0–P5)] were cut with the preBötC at the rostral surface of the slice, -0.35 mm caudal to the caudal aspect of the facial nucleus in rat (Smith et al., 1991; Ruangkittisakul et al., 2006; Lorier et al., 2007) and -0.35 to -0.4 mm caudal to the caudal aspect of the facial nucleus in mouse paying particular attention to the structure of the inferior olive (Ruangkittisakul et al., 2011). Slices were pinned with the rostral surface up on Sylgard resin in a recording chamber (volume, 5 ml) and perfused with aCSF that was recirculated at a flow rate of 15 ml/min. The concentration of K⁺ in the aCSF ([K⁺]_e) was raised from 3 to 9 mM at least 30 min before the

start of data collection. Medullary slices from neonatal Swiss CD mice and SD rats generated stable rhythm in 3 mM K⁺ that then decayed. The majority of protocols in this study involved multiple interventions, and therefore required slices that produced stable inspiratory-related rhythm for extended periods (i.e., >5 h). Therefore, the [K⁺]_e was raised from 3 to 9 mM to produce prolonged, stable rhythm (Ruangkittisakul et al., 2011).

3.2.2 Electrophysiological recordings

Inspiratory activity was recorded, using glass suction electrodes (A-M Systems, Carlsborg, WA), from cut ends of XII (hypoglossal) nerve rootlets and directly from the ventrolateral surface of the slice. Surface field potentials were recorded using a four-axis manual manipulator to place a suction electrode (120 µm inside diameter) on the surface of the slice over the approximate region of the ventral respiratory cell column (Ramirez et al., 1997). The pipette was systematically moved in steps corresponding to one-half of the pipette diameter until the most robust signal was detected. Signals were amplified, bandpass filtered (100 Hz to 5 kHz), full-wave rectified, integrated using a leaky integrator ($\tau = 25$ or 50 msec), and displayed using Axoscope 9.2 (Molecular Devices, Union City, CA). Data were saved to computer using a Digidata 1322 A/D board and AxoScope 9.2 software (Molecular Devices) for off-line analysis. All recordings were conducted at room temperature (22–24°C).

3.2.3 Drugs and their application

Adenosine 5'-triphosphate disodium salt (ATP) (P2R agonist, 100 µM microinjected) and adenosine (A1,2,3R agonist, 500 µM microinjected) were obtained from Sigma-Aldrich. All other chemicals were obtained from Tocris Bioscience including: [Sar⁹-Met(O₂)¹¹]-substance P (SP) (NK1R agonist, 1 µM microinjected); MRS 2279 ((1R*,2S*)-4-[2-Chloro-6-(methylamino)-9H-purin-9-yl]-2-(phosphonooxy)bicyclo[3.1.0]hexane-1-methanol

dihydrogen phosphate ester diammonium salt, P2Y₁R antagonist, 500 μM microinjected); MRS 2365 ([[1R,2R,3S,4R,5S)-4-[6-amino-2-(methylthio)-9H-purin-9-yl]-2,3-dihydroxybicyclo[3.1.0]hex-1-yl]methyl]diphosphoric acid mono ester trisodium salt), P2Y₁R agonist, 100 μM microinjected); and DPCPX (8 cyclopentyl-1,3-dipropylxanthine), A₁R antagonist, 2 μM local microinjection and 0.5 μM bath application given 15 min to equilibrate). A P2X receptor antagonist cocktail was bath-applied and given 15 min to equilibrate. It consisted of: TNP-ATP (50 μM, selective for P2X₁, P2X₃ and P2X_{2/3} Rs in the nM range, but can also affect P2X₂, P2X₄, P2X₆, P2X_{1/5}, and P2X₇ Rs at concentrations several orders of magnitude higher (Lambrecht, 2000; Lorier et al., 2007)), NF023 (10 μM, selective for P2X₁) (Soto et al., 1999), 5-BDBD (50 μM, selective for P2X₄) (Donnelly-Roberts et al., 2008) and A740003 (10 μM, selective for P2X₇) (King, 2007).

Drugs were prepared as stock solutions in aCSF and frozen in aliquots. The final concentration of K⁺ in the drug solutions was matched to that of the aCSF. Exceptions were ATP and ADO, which were made fresh on the day of the experiment, and DPCPX, which was made up in DMSO and diluted such that the final concentration of DMSO never exceeded 0.01%. In slice preparations, drugs were unilaterally applied locally to the preBötC via triple-barreled pipettes (5–6 μm outer diameter per barrel) pulled from borosilicate glass capillaries (World Precision Instruments). Care was taken to ensure that the outer tip diameter was within this range because fluorescent imaging (40x objective) of Lucifer yellow-filled triple-barreled pipettes established that pipettes in this range did not leak, but they did leak if tip diameter exceeded 6.5 μm. Avoiding leakage was essential because of the potential for agonist evoked P2R desensitization or internalization. Drug microinjections were controlled by a programmable stimulator (Master-8; A.M.P.I. Instruments) connected to a picospritzer (Spritzer4 Pressure Micro-Injector, 18 psi). Consecutive agonist applications were separated by a minimum of 15 min. We did not systematically assess whether this was the minimum time interval required for consistent responses, but it was sufficient for reproducible responses. The concentrations of drugs used in the present study should not be

directly compared with those in experiments in which similar agents are applied in the bath or directly to isolated cells. The concentration of drug decreases exponentially with distance from the pipette tip, and previous experiments with this preparation have established that drug concentration in the pipette must be ~10-fold greater than the bath-applied concentration to produce similar effects (Liu et al., 1990).

The drug injection site was established by first placing a suction electrode on the rostral surface of the slice and moving in 50 μm increments in both the x and y planes to identify the region that gave the largest amplitude inspiratory signal in-phase with the XII nerve recording. This served as an initial reference point from which to begin functionally mapping the ventrolateral medulla for the site that produced the most rapid-onset frequency increase in response to locally injected SP. The rationale is that as distance from the site of maximum sensitivity decreases, the onset delay will also decrease since drug will have less distance to diffuse to its site of action. The NK1R agonist SP (1 μM) was locally injected under the surface electrode using a triple-barreled drug pipette. The drug pipette was then systematically moved in 50 μm steps along the dorsoventral axis and SP injections (1 μM , 10 sec) repeated at 15 min intervals. The pipette was then moved to the maximally-responsive position on the dorsoventral axis and injections continued on the mediolateral axis. Traces were immediately examined to identify the site of maximum SP sensitivity, the SP “hotspot”, where SP evoked a frequency increase that was at least two-fold greater than baseline and occurred in the first interburst interval following drug onset. Identifying the injection site in this manner was essential because our previous data in rat revealed that, while the sites of maximum SP sensitivity and maximum ATP sensitivity correspond very closely, ATP is rapidly hydrolyzed in the preBötC and undergoes limited diffusion compared to SP. In other words, if injection sites are outside the hotspot, it is possible to evoke a significant SP response but no ATP response. Based on these criteria, the established sensitivity of preBötC networks to SP (Johnson et al., 1996; Gray et al., 1999; Lorier et al., 2007; Huxtable et al., 2009; Huxtable et al., 2010), the close correspondence between the sites of maximum SP and

maximum ATP sensitivity (the ATP hotspot) (Lorier et al., 2007), and that the ATP hotspot has been identified via histological and immunohistochemical criteria as the preBötC (Lorier et al., 2007), we are confident that the SP hotspot corresponds to the preBötC. Similar criteria were applied to define the MRS 2365 (100 μ M) hotspot in mouse and ATP (100 μ M) hotspot in rat. We have previously demonstrated that ATP diffuses minimally through the medullary tissue (Funk et al., 2008a; Huxtable et al., 2009) and that to evoke a frequency increase the injection site must be very close to the ATP “hotspot,” which has been established previously using histological and immunohistochemically in postnatal animals as corresponding to the preBötC (Lorier et al., 2007).

3.2.4 Mapping studies

Previous mapping studies in rhythmic medullary slices from neonatal rat demonstrated that the maximum potentiation of frequency by locally microinjected ATP occurs in the preBötC (Lorier et al., 2007). This mapping procedure was performed here in mice using 10 sec applications of 100 μ M MRS 2365 to determine if the P2Y₁R sensitive-site was also spatially restricted. Mapping began with injection of MRS 2365 (10 sec, 100 μ M) into the SP hotspot. MRS 2365 responses were then mapped by moving the injection site in 100 μ m increments along the dorsoventral axis until the response diminished by at least 50% of maximum. The pipette was then moved to the maximally responsive position on the dorsoventral axis and injections continued on the mediolateral axis. Microinjections were repeated at 15 min intervals. At the end of the mapping procedure, the pipette was returned to the site of maximum MRS 2365 sensitivity (which in all cases corresponded to the SP hotspot) for a final injection. Physical interference between the surface extracellular electrode and the injection pipette prevented microinjections medial to the recording pipette.

3.2.5 Real Time-PCR

Brainstems from mice and rat were isolated and sectioned as described above for the rhythmic slice preparations. When landmarks for the rostral border of the preBötC were apparent, a single 300 µM section was isolated and pinned down on sylgard in sterile aCSF. PreBötC tissue from mice and rats was then removed bilaterally using a 21 gauge tissue punch. Two punches from each animal were put directly into lysis buffer (Dynabead mRNA DIRECT kit; Invitrogen Molecular Probes, Carlsbad, CA, USA) and stored at -80° C until needed. mRNA was extracted using the same Dynabead mRNA DIRECT kit (Invitrogen Molecular Probes). mRNA was used as the template to make cDNA using High Capacity Reverse Transcription kit (Applied Biosystems, Carlsbad, CA, USA) with oligo d(T) primers. The product of the reverse transcription reaction was then cleaned using MinElute PCR purification kit (Qiagen, Mississauga, Ontario, CAN) to obtain a pure and concentrated sample that was used directly in the real-time PCR reaction, which was run in triplicate. A standard curve was run in triplicate for each transcript of interest to obtain the relationship between starting copy number and threshold cycle number. The standard curve was generated using a plasmid containing the full cDNA of interest that was diluted to contain a specific copy number: 2×10^1 to 2×10^8 . Clones for NTPDase 1, 2 and 3 were generous gifts from H. Zimmerman (Institute of Cell Biology and Neuroscience, Goethe-University). Those for TNAP, ecto5' ectonucleotidase and cyclophilin A were obtained commercially (Open Biosystems). An icycler (BioRad, Mississauga, Ontario, CAN) and 2x SYBR Green master mix (Applied Biosystems) were used to run the PCR and the data was retrieved to show specific starting copy number in each sample. The housekeeping gene, cyclophilin A, was used as an internal control to facilitate comparison between runs and species cDNA. Genes of interest were NTPDase1, 2, and 3, TNAP and ecto5' ectonucleotidase. The following sense (s) and antisense (as) primer sequences for each transcript were used: ENTPDase-1(s 5'-GGAGCCTGAAGAGCTACCC, as 5'-GTCTGATTAGGGCACGAA, accession

number U81295); ENTPDase-2 (s 5'-CTTCGGGATGTACCCAGAGA, as 5'-CAGCAGGTAGTTGGCAGTCA, accession number Y11835); ENTPDase-3 (s 5'-ATGTGTATCAGTGGCCAGCA, as 5'-CTCATTGCAACCTCAGCA, accession number AJ437217); TNAP (s 5'-CCTTGAAAAATGCCCTGAA, as 5'-CTTGGAGAGAGCCACAAAGG, accession number BC088399); ECTO5'(s 5'-ATGCCTTGCAAATACCTG, as 5'-GGTTTCCCATGTTGCACTCT, accession number BC098665), and; CYCLA (s 5'-CACCGTGTCTTCGACATCAC, as 5'-CCAGTGCTCAGAGCACGAAAG). Temperature curves were run for each primer pair to establish conditions in which primer efficiencies were all >95%. Expression levels of the ectonucleotidase genes of interest were first measured as the ratio of the starting copy number relative to the starting copy number of cyclophilin A. From this, we assessed the total ectonucleotidase mRNA expression as the sum of all isoforms and then calculated the percentage of this total contributed by each isoform (eg. starting copy # for each isoform/(Σ starting copy number for TNAP, ENTPDase 1, 2, 3 and ecto5" ectonucleotidase) x 100).

3.2.6 Data analysis

The effects of a drug on frequency of integrated inspiratory bursts recorded via suction electrodes from XII nerve roots were assessed off-line using pClamp 9.2 (Clampfit) and Microsoft Excel software. Values of frequency during the drug were compared with the average value during the 2 min control period that immediately preceded drug application. The maximum effect of a drug on frequency was determined as the maximum (or minimum) value measured in the moving average of inspiratory frequency (calculation based on the average of three consecutive bursts) during the first min after injection. The time course of the response was obtained by averaging data points in 30 sec bins for the 1 min period immediately before drug application, in 10 sec bins for the first 60 sec after the onset of drug application (first 30 sec only for SP and MRS 2365), and in 30 sec bins for the remainder of

the time. Parameters are reported relative to control (predrug or prestimulus) levels, as mean \pm SE. Statistical comparison of means was performed on raw data unless otherwise stated using GraphPad Prism version 4 (GraphPad Software). Statistical comparison of relative data was performed only after verification of normality. Differences between means were identified using a one-way ANOVA with Dunnett's multiple comparison test or via two-way repeated measures ANOVA. The proportional contribution of mRNA for TNAP and ENTPDase2 isoforms to the total ectonucleotidase mRNA was then compared in mice vs rat using a one-way ANOVA with Bonferroni's correction for multiple comparisons. All values are reported as means \pm standard error of the mean (SEM), Values of $p < 0.05$ were assumed significant.

3.3 Results

3.3.1 Effects of ATP on preBötC rhythm differ between mouse and rat

To test whether ATP directly modulates preBötC rhythm generating networks of mouse, as seen previously in SD and Wistar rat (Lorier et al., 2004; Lorier et al., 2007; Huxtable et al., 2009), we locally applied ATP to the preBötC of rhythmically-active medullary slices of Swiss CD mice. The injection site for ATP within the preBötC was established using the mapping protocol developed previously (Lorier et al., 2007; Huxtable et al., 2009; Huxtable et al., 2010) based primarily on the functional criterion that activation of NK1Rs in the preBötC evokes a rapid-onset increase in burst frequency (Johnson et al., 1996; Gray et al., 1999). When injected into the site of maximum sensitivity (the SP hotspot), SP (1 μ M) produced a rapid-onset, 2.70 ± 0.43 - fold increase in burst frequency that peaked within 10 sec of SP application and remained significantly greater than baseline frequency until 90 sec after drug onset (Fig 3.1 A, B, $n = 10$, $p < 0.05$). Local injection of ATP (100 μ M) into the same site had no significant effect on inspiratory frequency. ATP caused only small, statistically insignificant fluctuations in frequency.

Given the surprising finding that ATP was without effect in the mouse preBötC, we performed parallel experiments in SD rat as a positive control and to verify previous data (Lorier et al., 2004; Lorier et al., 2007; Huxtable et al., 2009; Huxtable et al., 2010). SP responses in rat were similar to those in mouse. SP produced a rapid onset, 2.30 ± 0.23 - fold increase in frequency that remained significantly elevated above baseline for 90s (Fig 3.1 C, D, $n = 6$, $p < 0.05$). In contrast, ATP responses were markedly different between rat and mouse. As seen previously in SD and Wistar rats (Lorier et al., 2004; Lorier et al., 2007; Huxtable et al., 2009; Huxtable et al., 2010), local application of ATP (0.1 mM; 10 sec) produced a rapid-onset, short duration, 2.77 ± 0.05 - fold increase in burst frequency that was significantly greater (one-way ANOVA, Dunnett's multiple comparison, $n = 6$, $p < 0.01$) than baseline for 20 sec (Fig 3.1 C, D).

3.3.2 PreBötC of mouse is directly sensitive to modulation by P2Y₁R

The frequency effects of ATP in the preBötC of postnatal rat are mediated primarily by P2Y₁Rs (Lorier et al., 2007). However, because ATP has multiple signaling actions via activation of P2X and P2YRs, we hypothesized that the lack of an ATP-evoked frequency effect in mouse reflects that ATP is acting on other purinergic receptors to counteract a P2Y₁R-mediated frequency increase. As an initial test of this hypothesis, we assessed whether the preBötC rhythm generating networks in mice are sensitive to P2Y₁R modulation by locally applying a P2Y₁R agonist (MRS 2365) to the preBötC. As previously, parallel experiments in rat served as positive controls. Injection of MRS 2365 (0.1 mM, 10 sec) into the site of maximum SP sensitivity produced a significant 2.63 ± 0.20 - fold ($n = 10$, $p < 0.05$) and 2.01 ± 0.08 - fold ($n = 6$, $p < 0.01$) frequency increase in mouse (Fig 3.2A) and rat (Fig 3.2B) slice preparations respectively. Increases remained elevated above baseline

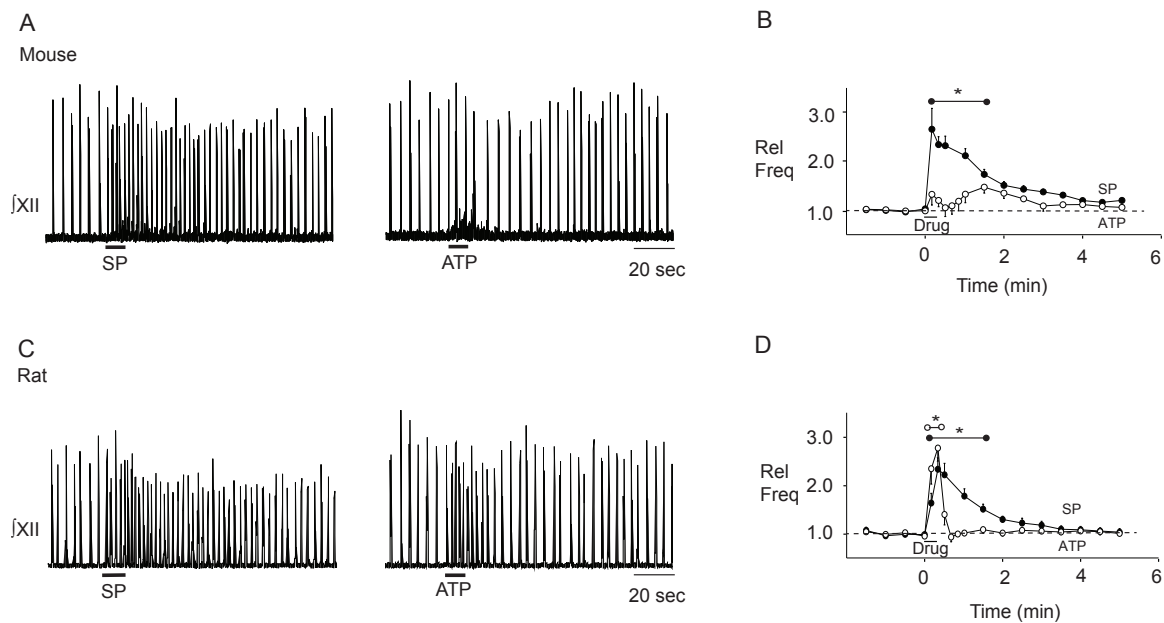


Figure 3.1 Differential effects of ATP on preBötC rhythm in mouse and rat.

Integrated XII nerve (XII) recordings from a medullary slice preparation after local application of ATP (0.1 mM, 10 sec, ○) and SP (1 μM, 10 sec, ●) in the preBötC of mouse (A) and rat (C). Group data illustrating the time course of the response evoked by each agonist in mouse (B, n = 10) and rat (D, n = 6). * indicates range over which values were significantly different from control. Error bars indicate SEM. Rel. Freq., relative frequency.

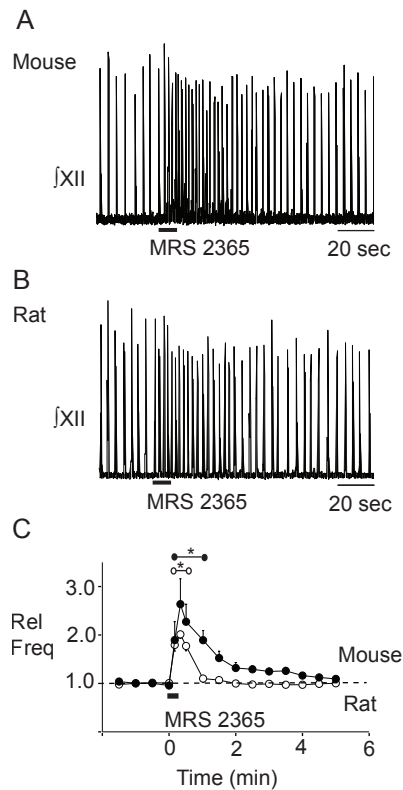


Figure 3.2 P2Y₁R activation in the preBötC increases frequency in mouse and rat.

Integrated XII nerve (fXII) recordings from a medullary slice preparation showing responses to local application of the P2Y₁R agonist MRS 2365 (0.1 mM, 10 sec) in the preBötC of mouse (A) and rat (B). Group data (C) illustrating the time course of the response evoked by MRS 2365 in mouse ($n = 10$, ●) and rat ($n = 6$, ○). * indicates range over which values were significantly different from control. Error bars indicate SEM. Rel. Freq., relative frequency.

frequency for 60 sec (mouse) and 30 sec (rat) (one-way ANOVA, Dunnetts multiple comparison) (Fig 3.2C).

3.3.3 The site of maximum P2Y₁R sensitivity corresponds to the site of maximum SP sensitivity

To establish in mouse that the site at which frequency is maximally-sensitivity to SP corresponds to the site of maximum P2Y₁R sensitivity, as well as the spatial selectivity of the P2Y₁R-mediated frequency increase, we injected MRS 2365 in a grid-like fashion around the SP hotspot and mapped the P2Y₁R evoked frequency increase (Lorier et al., 2007). The MRS 2365-mediated increase in frequency decreased when microinjection sites were moved away from the hotspot in any direction. This is shown for a series of injections applied progressively more ventral from the identified SP hotspot in a single rhythmic slice. The frequency increase evoked by MRS 2365 decreased progressively as the injection site was moved ventrally. At 300 μ m ventral, MRS 2365 had no effect (Fig 3.3A). Group data in Fig 3.3B are consistent with this and show that when MRS 2365 is microinjected 100 μ m lateral to the hotspot, responses decreased to 0.75 ± 0.1 of the response evoked at the SP hotspot. In the dorsoventral axis, responses decreased to 0.56 ± 0.05 , 0.51 ± 0.06 and 0.44 ± 0.07 of maximum when injections were made 100, 200 and 300 μ m dorsal to the SP hotspot (Fig 3.3B), and to 0.63 ± 0.1 , 0.49 ± 0.05 and 0.36 ± 0.05 of the maximum when injections were made 100, 200 and 300 μ m ventral to the hotspot (Fig 3.3. A, B). All frequency responses evoked by MRS 2365 outside the SP hotspot were significantly smaller than that induced at the SP hotspot ($n = 5$, $p < 0.01$, one-way ANOVA, Dunnetts multiple comparison). These data indicate that SP and MRS 2365 act within the same site to maximally excite inspiratory rhythm. Data also establish that P2Y₁R sensitivity of the inspiratory rhythm is not a general property of the ventrolateral medulla but a property that is restricted to a specific region.

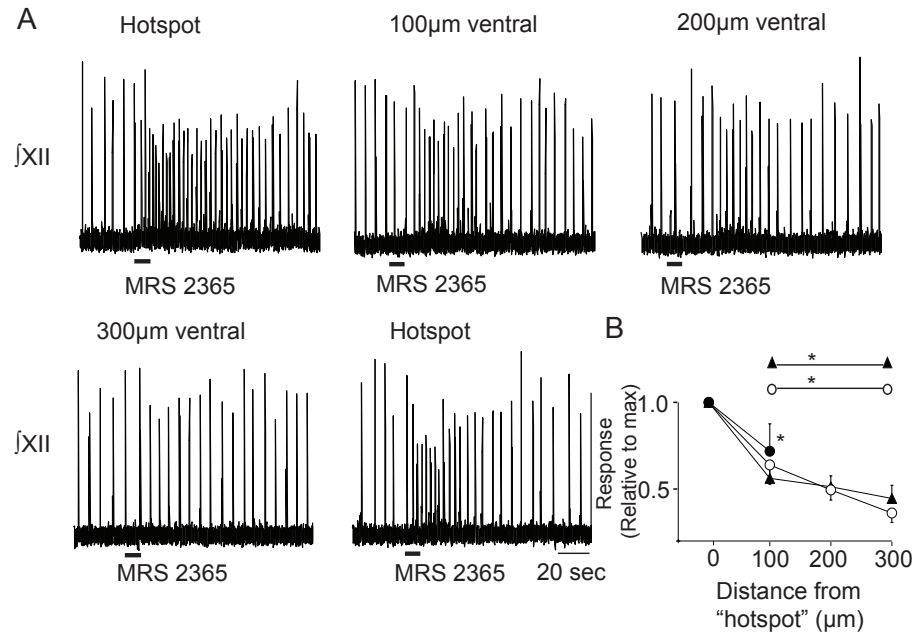


Figure 3.3 P2Y₁R potentiation of frequency in mouse is spatially restricted to the preBötC.

A, Integrated XII nerve (fXII) recordings from a mouse medullary slice preparation illustrating the effects on inspiratory-related output of locally applying 0.1 mM MRS 2365 (P2Y₁R agonist) at the site of maximum SP sensitivity (hotspot) in the VRC and at sites of varying distance from the hotspot. **B**, Group data illustrating P2Y₁R agonist responses evoked when injections were made at increasing distances from the hotspot in the ventral (n = 5, ○), dorsal (n = 5, ▲) and lateral (n = 5, ●) directions. Data are plotted relative to the maximum response evoked at the hotspot. * Significantly different from maximum response. Error bars indicate SEM.

3.3.4 P2 and P1R interactions mediate the effects of ATP in mouse preBötC

We hypothesized that the different effects of ATP and the hydrolysis-resistant P2Y₁R agonist MRS 2365 on frequency in the mouse reflected degradation of ATP to ADO and, in the case of ATP, coactivation of excitatory (P2Y₁) and inhibitory (P1) receptor mechanisms. We compared the effect of local application of ATP to the SP hotspot, before and after block of A₁Rs via local preapplication of the A₁R antagonist DPCPX (Fig 3.4A) into the preBötC. DPCPX was used because the inhibitory actions of ADO within the preBötC of mice are primarily mediated through A₁R (Mironov *et al.*, 1999).

As seen previously in Fig 3.1, although local application of ATP alone evoked minor fluctuations in mouse rhythm (Fig 3.4A), none of these changes was significant (Fig 3.4B). However, when applied after DPCPX (2 μM, 90 sec), ATP produced a significant 1.82 ± 0.08 - fold increase in frequency that became significantly greater than baseline 20 sec after the onset of the ATP application and remained elevated above control for the next 30 sec ($n = 6$, $p < 0.01$; one-way ANOVA, Dunnett's multiple comparison). In addition to demonstrating that ATP alone has no effect on baseline frequency (one-way ANOVA) and that it does increase frequency relative to baseline in the presence of DPCPX (one-way ANOVA), comparison of the ATP response in control with that in DPCPX revealed that the frequency response in DPCPX is significantly elevated compared to the control ATP response (two-way repeated measures ANOVA, time - drug interaction $p < 0.0005$, $df = 17$, $F = 2.73$). The unmasking of an ATP-evoked frequency increase by the A₁R antagonist DPCPX, suggests that ATP is ordinarily broken down to ADO, which acts via A₁Rs to counteract the effects of ATP at P2Y₁Rs. The caveat with this experiment is that the concentration of DPCPX produced in the tissue by local application of 2 μM DPCPX, which will be in the range of 0.2 μM due to diffusion and dilution from the point source of the pipette tip, has the potential to

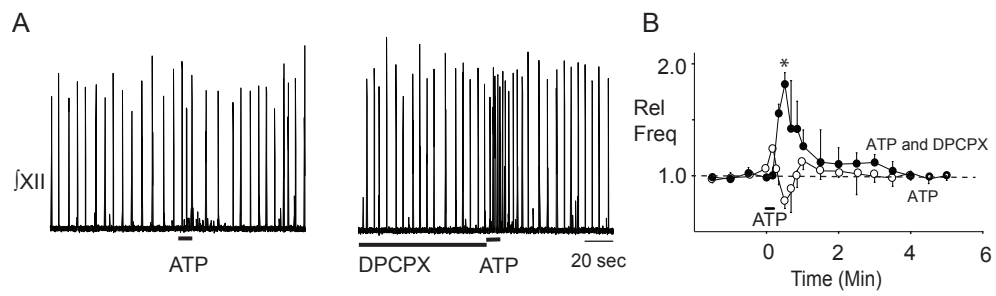


Figure 3.4 DPCPX in the preBötC of mouse unmasks an ATP-mediated frequency increase.

A, Integrated XII nerve (jXII) recordings from a mouse medullary slice preparation showing responses to local application of ATP (0.1 mM, 10 sec; left trace) under control conditions and after a 90s preapplication of an A₁R antagonist (2 μ M DPCPX; right trace). **B**) Group data illustrating the time course response evoked by ATP alone ($n = 6$, ○) and in the presence of DPCPX ($n = 6$, ●). * indicates range over which values were significantly different from control. Error bars indicate SEM. Rel. Freq., relative frequency.

affect A2ARs. We therefore repeated these experiments using a 20-fold lower concentration of DPCPX in the pipette ($0.1 \mu\text{M}$). The resulting tissue concentration of DPCPX of approximately $0.01 \mu\text{M}$ is 3-fold lower than the IC_{50} for A2ARs (Klotz, 2000) and should be selective for A1Rs. Under these conditions, DPCPX significantly enhanced the effects of ATP on inspiratory frequency from 1.74 ± 0.22 in control to 2.72 ± 0.62 (Fig 3.5, $n = 6$, $p = 0.004$; paired t-test) in DPCPX. These findings further support our hypothesis that when ATP is injected into the preBötC an A1R-mediated inhibition counteracts a P2Y₁R-mediated excitation.

To further explore this hypothesis, we tested whether P2Y₁R antagonists could block the excitatory effects of ATP once they are unmasked by DPCPX. We bath-applied DPCPX ($0.2 \mu\text{M}$) and then compared the effects on frequency of locally-applying ATP into the preBötC before and immediately after preapplication of the P2Y₁R antagonist (90 sec, $500 \mu\text{M}$). When applied alone (with DPCPX in the bath throughout the experiment), ATP evoked a significant 1.75 ± 0.13 - fold increase in frequency (Fig 3.6A, B, $n = 6$; one-way ANOVA, Dunnett's multiple comparison). When applied alone (with DPCPX in the bath throughout the experiment), ATP evoked a significant 1.75 ± 0.13 - fold increase in frequency compared to the control baseline frequency (Fig 3.5A, B, $n = 6$; one-way ANOVA, Dunnett's multiple comparison). Following preapplication of MRS 2279, ATP no longer had any effect on baseline frequency (Fig 3.5A, B; $n = 6$, $p < 0.01$; one-way ANOVA, Dunnett's multiple comparison). In addition to comparing frequency values during drug to those observed pre-drug, a comparison of the frequency responses evoked by ATP alone and following preapplication of MRS 2279, revealed that the frequency response following MRS 2279 was significantly smaller than control, (Fig 3.6A, B; $n = 6$; two-way repeated measures ANOVA, time - drug interaction $p < 0.0001$, $\text{df} = 34$, $F = 4.685$). The inhibitory actions of MRS 2279 were completely reversible. After 15 min of washout, ATP produced a 1.79 ± 0.22 - fold increase in frequency (Fig 3.6A, B).

While the excitatory effects of ATP appear to be completely mediated by P2Y₁Rs, there

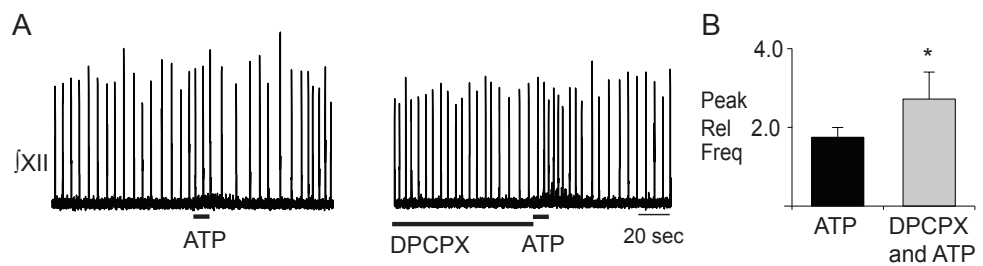


Figure 3.5 A₁R antagonism in the preBötC of mouse unmasks an ATP-mediated frequency increase.

A, Integrated XII nerve (\int XII) recordings from a mouse medullary slice preparation showing responses to local application of ATP (0.1 mM, 10 sec; left trace) under control conditions and after a 90s preapplication of an A₁R antagonist (0.2 μ M DPCPX; right trace). B) Group data illustrating the peak frequency effect evoked by ATP alone and in the presence of DPCPX (n = 6). * indicates significant difference from ATP alone. Error bars indicate SEM. Rel. Freq., relative frequency.

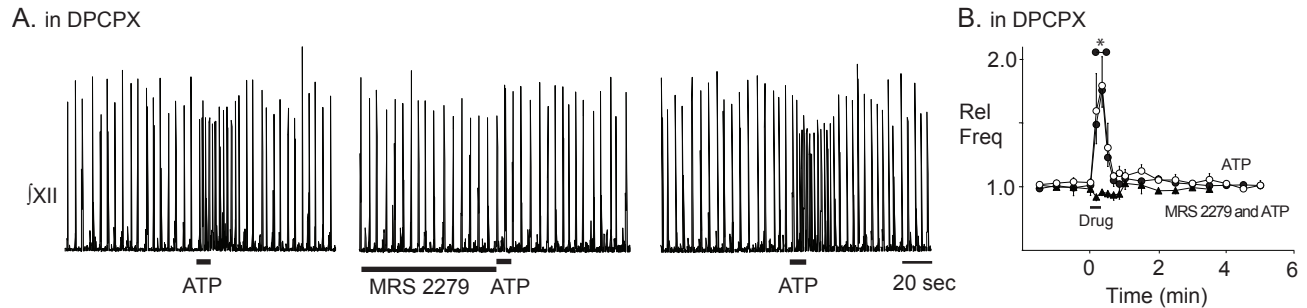


Figure 3.6 P2Y₁Rs contribute to the ATP-evoked frequency increase in mouse.

A. Integrated XII nerve (XII) recordings from a mouse medullary slice preparation illustrating the responses evoked by applying ATP (0.1 mM, 10 sec; left trace) under control conditions, after a 90 sec preapplication of P2Y₁R antagonist, MRS 2279 (0.5 mM; middle trace) and during recovery (0.1 mM; right trace). **B.** Group data illustrating the peak response evoked by ATP alone ($n = 6$) and in the presence of MRS 2279 ($n = 6$). * Significantly different from response evoked by ATP alone control. Error bars indicate SEM. Rel. Freq., relative frequency.

is immunohistochemical and electrophysiological evidence of P2XRs in the ventrolateral medulla (Thomas et al., 2001; Gourine et al., 2003). To determine if P2XRs counteract the P2Y₁R excitatory effects of ATP in the preBötC, a P2X antagonist cocktail consisting of TNP-ATP (50 μM), NF023 (10 μM), 5-BDBD (50 μM) and A740003 (10 μM) was bath applied. ATP was without effect before and after local preapplication of the P2XR antagonist cocktail (One-way ANOVA, n = 5; data not shown); i.e., preapplication of the P2X antagonist cocktail did not unmask a significant ATP excitation.

3.3.5 ADO differentially affects preBötC rhythm in mouse and rat

At least two factors could contribute to our observation that in the rat ATP alone is excitatory, while in the mouse ATP is only excitatory in the presence of an A1R antagonist. First, we hypothesized that preBötC rhythm generating networks of postnatal mice are more sensitive to ADO-mediated inhibition than rat. To test this, we compared in rhythmic slices from postnatal mouse and rat the effects on inspiratory rhythm of locally-applying ADO directly into the preBötC, as defined using the SP mapping protocol described previously. In mice, ADO (500 μM, 30 sec) reduced inspiratory frequency to 0.69 ± 0.06 of control. Frequency remained significantly below control for the interval between 30 and 60 sec after the onset of ADO application (Fig 3.7B, n = 6, p < 0.05; one-way ANOVA, Dunnett's multiple comparison). Similar injections in rat had no effect on baseline inspiratory frequency (Fig 3.7A, B, n = 6).

3.3.6 Ectonucleotidase isoform expression in the preBötC differs between mouse and rat

We also hypothesized that the differential ATP sensitivity in mouse and rat reflects differential expression of ectonucleotidases in the preBötC. Specifically, we hypothesized

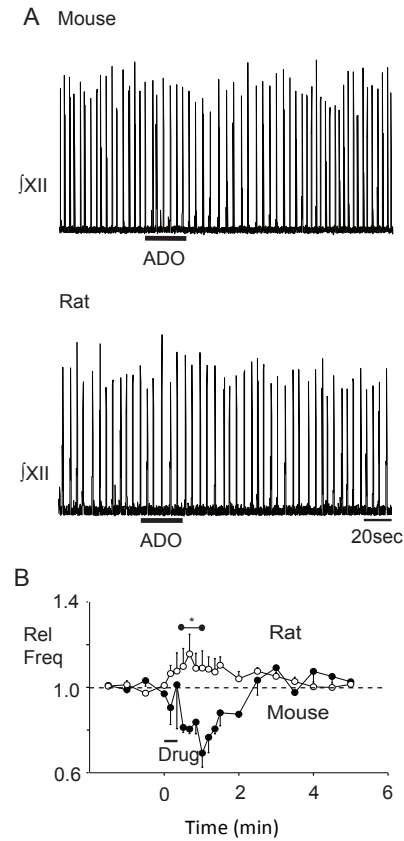


Figure 3.7 Differential effects of ADO on preBötC rhythm in mouse and rat.

Integrated XII nerve (IXII) recordings from a medullary slice preparation illustrating responses evoked by local application of ADO (500 μ M, 30 sec) into the preBötC of mouse (A, left) and rat (A, right). B. Group data illustrating the time course of the response evoked by ADO in mouse ($n = 6$, ●) and rat ($n = 6$, ○). * indicates range over which values were significantly different from control. Error bars indicate SEM. Rel. Freq., relative frequency.

that the complement of ectonucleotidase isoforms in the preBötC of mouse favours inhibition via rapid degradation of ATP directly to ADO, while in the rat it favours excitation through generation of ADP. This was based on the observations that ectonucleotidase-mediated degradation of ATP is a key determinant of ATP response kinetics in the preBötC of rat (Huxtable et al., 2009), and increasing evidence for spatial heterogeneity of ectonucleotidase expression between brain regions (Langer et al., 2008). To test this hypothesis we collected preBötC tissue punches from mouse and rat, extracted mRNA and used real-time PCR to compare levels of mRNA expression for the 5 major ectonucleotidase isoforms involved in ATP degradation. These included ENTPDase 1,2,3, tissue nonspecific alkaline phosphatase (TNAP) and ecto5'-ectonucleotidase. The ENTPDase isoforms 1, 2 and 3 all degrade ATP to AMP but with different affinities. ENTPDase2 is unique in that it has 100-fold higher affinity for ATP than ADP and will therefore lead to the accumulation of ADP in an environment with excess ATP as substrate. Importantly, ADP is a stronger P2Y₁R agonist than ATP. TNAP completely degrades ATP to ADO, while ecto5' ectonucleotidase degrades AMP to ADO. Based on our hypothesis, we predicted that TNAP would be prevalent in mice while ENTPDase 2 would be dominant in rat message RNA (mRNA) copy number for each enzyme isoform expressed relative to cyclophilin A (Fig 3.8). Since we cannot be certain that cyclophilin A expression levels are the same in preBötC punches from mouse and rat, we can not directly compare these ratios between mouse and rat. Instead, we simply compared the proportion that each isoform contributed to the total ectonucleotidase mRNA. As predicted, TNAP was the most highly-expressed isoform in the mouse preBötC, while ENTPDase 2 was the most highly expressed isoform in rat. TNAP comprised $79.7 \pm 3.8\%$ of the total ectonucleotidase mRNA in mouse (Fig 3.8, n = 6, p < 0.001), which was a significantly greater proportion than in rat ($17.7 \pm 0.8\%$, n = 4). In contrast, ENTPDase 2 comprised $54.6 \pm 1.3\%$ of the total ectonucleotidase mRNA in rat and this was significantly greater than its proportional expression in mouse ($7.3 \pm 1.8\%$) (One-way ANOVA, Bonferroni multiple comparison).

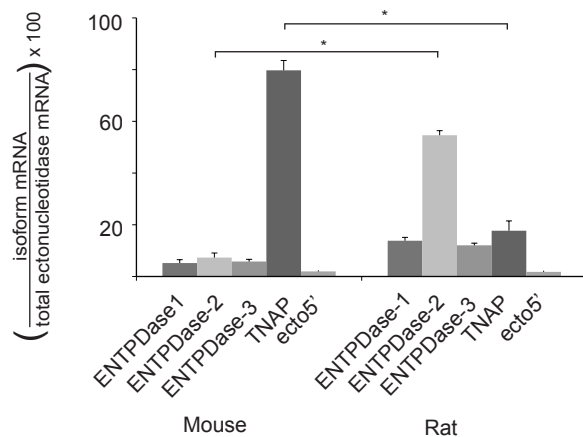


Figure 3.8 Real-time PCR analysis reveals differential expression of ectonucleotidase isoforms in preBötC tissue punches from mouse and rat.

The percentage contribution of each ectonucleotidase isoform to the total ectonucleotidase mRNA expressed in preBötC punches from mouse ($n = 6$) and rat ($n = 4$) (eg. starting copy # for each isoform/ $(\sum$ starting copy number for TNAP, ENTPDase 1, 2, 3 and ecto5' ectonucleotidase) $\times 100$). Error bars indicate SEM. * indicates significant difference between the compared columns.

3.4 Discussion

3.4.1 Differential sensitivity of rat and mouse preBötC networks to ATP

ATP in the preBötC of neonatal Wistar and SD rat evokes a biphasic response comprising a rapid, P2Y₁R-mediated increase that peaks within 10–20 sec, followed by a secondary inhibition that reaches a nadir ~30–40 sec after drug onset (Lorier et al., 2007; Huxtable et al., 2009). The kinetics of the frequency response in rat closely follow the concentration of ATP in the preBötC, which is in large part determined by ectonucleotidases that degrade ATP (Huxtable et al., 2009) ultimately to ADO. The source of the secondary frequency decrease in rats is not known. It is variable in magnitude, appears to be more prominent in Wistar rats and is dependent on ATP degradation since it is absent when nonhydrolyzable ATP agonists are used (Lorier et al., 2007). In fetal rats, an ADO contribution is likely since a basal ADO tone reduces frequency and blockade of ADO receptors enhances the ATP-evoked frequency increase (Huxtable et al., 2009). However in postnatal rats, neither of these effects are present and the secondary inhibition (Huxtable et al., 2009) cannot be blocked with ADO antagonists (Funk et al., 2008a). That this secondary inhibition is not obvious in Fig 3.1 likely reflects in part that we are using SD rats. Most significant, however, is that the inhibition is very brief (1–2 cycles) and that its timing varies between preparations. Thus, when group data are plotted as a time course relative to ATP onset as in Fig 3.1, this secondary decrease in frequency is often obscured (Lorier et al., 2007; Huxtable et al., 2009).

Given the potency of ATP in the rat preBötC, our demonstration that ATP does not significantly affect the activity preBötC inspiratory networks in postnatal mice was very surprising. Several factors could account for this differential sensitivity. PreBötC networks in mice may simply be insensitive to P2 and P1R modulation. Alternatively, preBötC networks of mice might be sensitive to ATP but the P2Y₁R-mediated excitation previously characterized in rat may be obscured by an opposing inhibitory mechanism including; the actions of ATP at other P2Rs; actions of the inhibitory ATP metabolite ADO at P1Rs; or

differential expression of ecotnucleotidases in the preBötC of mice that underlies a more rapid degradation of ATP to its inactive (eg. AMP) or inhibitory (ADO) metabolites.

3.4.2 P2Y₁ receptor sensitivity

Our data show conclusively that the preBötC networks of mice are highly sensitive to the excitatory effects of P2Y₁R activation. Application of a P2Y₁R selective agonist potently increased frequency when applied to the preBötC as defined by the SP hotspot. Several lines of evidence support the finding that the SP hotspot corresponds to the preBötC. First, it is well established that SP excites preBötC networks in mice and rat and this response has been used as a functional marker for the preBötC (Johnson et al., 1996; Gray et al., 1999; Lieske et al., 2000). NK1R immunoreactivity is the anatomical marker used most extensively for identifying the preBötC (Gray et al., 1999; Gray et al., 2001; Guyenet and Wang, 2001; Wang et al., 2001; Pagliardini et al., 2003; Pagliardini et al., 2005) and while NK1R expression is not limited to the preBötC, it is the most densely labeled region in the ventral medulla. Second, our previous mapping studies in rat revealed that the site of maximum ATP sensitivity corresponds closely with that of SP, and that this site corresponds to the preBötC based on anatomical and NK1R immunolabeling (Lorier et al., 2007). Our functional identification of the preBötC was based on the site at which SP evoked the maximum, most rapid-onset frequency increase; i.e. the frequency increase occurred in the first interburst interval following drug onset. The latter criteria was most useful based on the rationale that as distance to the site of maximum sensitivity decreases, the onset delay also decreases because less time is required for the drug to diffuse to its site of action. We are therefore confident that the lack of an ATP response in mice does not reflect that injection sites were outside the preBötC. This is corroborated by the fact that when A1Rs were blocked, ATP caused frequency to increase.

In addition, mapping experiments using the P2Y₁R agonist MRS 2365 confirmed that the site at which frequency is maximally-sensitive to SP corresponds to the site of maximum

P2Y₁R sensitivity. As seen for ATP responses in rat (Lorier et al., 2007), the MRS 2365 effect also decreases with distance from the hotspot. The ATP response in rat was more spatially restricted than the P2Y₁R effect in mouse, but this is expected since ATP is rapidly degraded in the preBötC and undergoes very limited diffusion. MRS 2365 is hydrolysis resistant and is expected to diffuse over greater distances.

The cellular mechanisms underlying the P2Y₁R excitation in mice are not known. In rat it most likely reflects activation of neurons and glia. ATP evokes inward currents in virtually all preBötC inspiratory neurons tested, including pacemaker neurons, via either the inhibition of a resting K⁺ channel or activation of a mixed cation current (Lorier et al., 2008). P2Y₁Rs primarily activate a mixed cation current in inspiratory neurons. Thus, it is the activation of this mixed cation current that most likely mediates the neuronal component of the ATP frequency increase. Additional possibilities are that P2Y₁Rs influence rhythm by modulating the persistent Na current (I_{NaP}) or the calcium-dependent, non-selective cation (I_{CaN}) current, which underlie pacemaker activity of preBötC inspiratory neurons (Feldman and Del Negro, 2006). I_{CaN} is of particular interest because metabotropic glutamate Rs act via phospho-lipase C (PLC) to enhance I_{CaN} and amplify glutamatergic inspiratory synaptic currents in preBötC neurons (Pace et al., 2007; Pace and Del Negro, 2008) P2Y₁Rs, like metabotropic glutamate Rs, signal through PLC (von Kugelgen and Wetter, 2000; Sak and Illes, 2005).

PreBötC glia also contribute to the P2Y₁R-mediated frequency increase (Huxtable et al., 2010). Glial toxins markedly attenuate the sensitivity of preBötC networks to ATP but not SP. The mechanisms via which glia contribute to the ATP-evoked frequency increase remain to be characterized. The working hypothesis is that P2Y₁R-mediated increases in Ca²⁺ concentration in the astrocytes evoke glutamate and ATP release which both act on respiratory neurons to increase frequency. Ca²⁺-dependent gliotransmitter release has been described in astrocytes from multiple brains regions, including the RTN (Gourine et al., 2010). Within the preBötC complex of rhythmic slices, ATP and MRS 2365 evoke whole-cell currents in electrophysiologically identified astrocytes and increases in intracellular Ca²⁺

in small, putative astrocytes. Astrocytes cultured specifically from the preBötC also respond to P2Y₁R activation with robust Ca²⁺ increases and glutamate release, which in turn may contribute to the ATP-evoked frequency increase (Huxtable et al., 2010). However, it remains to be determined whether the ATP-evoked frequency increase is dependent on increases in astrocytic Ca²⁺.

3.4.3 Differential sensitivity of mouse and rat preBötC to ATP reflects differential sensitivity to the ATP metabolite ADO

Given that the preBötC networks are sensitive to P2Y₁R-mediated excitation, the lack of an ATP effect in mice may reflect that ATP activates some other mechanism that obscures the P2Y₁ excitation. It is highly unlikely that an inhibitory P2XR mechanism obscures the P2Y₁R-mediated excitation because a P2XR antagonist cocktail delivered prior to ATP did not reveal any ATP excitation. We cannot exclude the possibility that our cocktail failed to block a critical P2X receptor subtype but this is unlikely. The cocktail included TNP-ATP, which selectively antagonizes P2X₁, P2X₃ and P2X_{2/3} receptors in the nanomolar range (Lambrecht, 2000; Lorier et al., 2007), as well as P2X₂, P2X₄, P2X₆, P2X_{1/5}, and P2X₇ receptors at concentrations used here (Lambrecht, 2000). It also included NF023, 5-BDBD and A740003 which selectively antagonize P2X₁, P2X₄ and P2X₇ receptors, respectively (Soto et al., 1999; King, 2007; Donnelly-Roberts et al., 2008).

Instead, the failure to observe an ATP-mediated frequency increase in mice appears to result completely from the degradation of ATP to ADO and the activation of an A1R-mediated inhibition that obscures the P2Y₁R excitation. This was apparent in that the block of A1Rs within the preBötC revealed a potent, P2Y₁R-mediated ATP excitation. ADO sensitivity of mouse preBötC networks was confirmed by significant frequency reductions following local injection of ADO directly into the preBötC. To be clear, we are not suggesting that all ATP is instantaneously converted to ADO upon injection into the

preBötC. In fact, the unmasking in mouse of an ATP-evoked excitation following block of A1Rs indicates that significant ATP remains in the preBötC. Rather, our data indicate that when ATP is applied in mouse, sufficient ADO is produced rapidly enough to counteract the P2Y₁R-mediated excitation.

The situation is very different in the neonatal rat in that blockade of A1Rs does not affect the ATP evoked excitation (Huxtable et al., 2009). This insensitivity in rat of the ATP response to A1R antagonists suggests that production of ADO from ATP either does not occur fast enough to counteract the initial ATP excitation or that ADO does not inhibit preBötC networks in rat. RTPCR analysis of ectonucleotidase expression reveals that the enzyme complement in mouse favours rapid degradation of ATP to adenosine while that in rat favours generation of ADP, which is excitatory at P2Y₁Rs (details discussed below). Moreover, even if ATP is degraded to ADO at the same rate in rat and mouse, ADO would not alter the P2Y₁R-mediated excitation in rat because the preBötC of postnatal rat is not sensitive to ADO (Fig 3.7).

Our definitive demonstration that mouse and rat preBötC networks are differentially sensitive to ADO is significant because it helps to resolve considerable confusion in the literature on the mechanisms and sites that mediate the inhibitory actions of ADO on breathing. To clarify, in intact animals when ADO is applied either systemically or via cerebroventricular administration where it can act throughout the CNS, data are consistent. First, ADO inhibits breathing in virtually all species examined (under anesthesia) including sheep, lambs, piglets, rabbits, cats and rats (Lagercrantz et al., 1984; Eldridge et al., 1985; Burr and Sinclair, 1988; Koos and Matsuda, 1990; Bissonnette et al., 1991; Schmidt et al., 1995; Wilson et al., 2004). The observation in conscious humans that adenosine stimulates breathing (Fuller et al., 1987; Griffiths et al., 1990; Reid et al., 1991; Griffiths et al., 1997) underlies the suggestion that anesthetic might enhance the inhibitory actions of adenosine. However, it appears more likely that the stimulatory action of adenosine in awake humans is dominated by its excitation of peripheral chemoreceptors (Fuller et al., 1987; Reid et al.,

1991; Kowaluk et al., 1998). Second, the ADO inhibition is greater in fetal/newborns (Eldridge et al., 1984; Wilson et al., 2004). Third, ADO antagonists are associated with an increase in baseline frequency implying the respiratory networks are under tonic ADO-mediated inhibition (Schmidt et al., 1995). At least two discrete mechanisms are involved in the inhibition of ventilation by ADO. An A2AR-mediated excitation of GABAergic neurons that ultimately inhibit brainstem respiratory networks is a major contributor to the ADO-mediated inhibition evoked *in vivo* in sheep (Koos et al., 2005), lambs (Koos and Chau, 1998), piglets (Wilson et al., 2004) and rat (Mayer et al., 2006). Neither the source of the A2A excitatory input to GABAergic neurons nor the GABAergic input to the brainstem is known, but both appear suprabulbar in origin and therefore unlikely contributors to the brainstem mechanisms under examination here. This is based on the observation that, although A2ARs are expressed in VRC regions containing GABAergic neurons (Wilson et al., 2004), an A2AR-mediated GABAergic inhibition has never been detected in reduced preparations that lack suprabulbar structures (Herlenius and Lagercrantz, 1999). In rhythmic medullary slices of mice, A2A agonists applied to inspiratory neurons do not affect rhythm. Similarly, A2A antagonists do not prevent the inhibitory actions of ADO (Mironov et al., 1999). In addition, the inhibitory actions of ADO in mouse medullary slices and island preparations are not affected by antagonizing GABA or glycine receptors (Vandam et al., 2008).

Most relevant to this study is the inconsistent description in the literature of a brainstem-delimited, A1R-mediated inhibition of inspiratory frequency. Comparison between studies is confounded by multiple factors including differences in: i) preparations (degree of reduction; brainstem spinal cord vs rhythmic slice); ii) species (mouse vs rat); iii) developmental stage, and; iv) method of drug application (specifically to the preBötC or bath application where it affects all regions of the preparation). Bath application of ADO agonists to inspiratory rhythm-generating brainstem spinal cord preparations from rat inhibits rhythm in some (Herlenius et al., 1997; Herlenius and Lagercrantz, 1999) but not all studies (Brockhaus and

Ballanyi, 2000; Funk et al., 2008b; Ruangkittisakul and Ballanyi, 2010). Developmental factors likely account for some discrepancies as the ADO inhibition of frequency described in the rat brainstem-spinal cord is prominent in fetal rats but disappears by P3 (Herlenius et al., 1997). Consistent with developmental changes are the observations in rhythmic slices from fetal but not postnatal rats that A1R antagonists enhance responses of preBötC networks to locally applied ATP and that local application of A1 antagonists into the preBötC increases rhythm (Huxtable et al., 2009).

Species differences are suggested by the observations in mice that A1R activation inhibits frequency in P4–14 slices (Mironov et al., 1999; Vandam et al., 2008) and P7 preBötC island preparations (Vandam et al., 2008), but not in brainstem-spinal cord preparations from rats older than P3 (Herlenius et al., 1997). However, the degree to which developmental or preparation-dependent factors account for apparent species difference is unclear. The A1 inhibition in rat disappears by P3 while in mice it is present between P4 and P14. Similarly problematic is that ADO effects have been tested on the brainstem-spinal cord preparation in rat but the medullary slice in mouse. By performing parallel experiments in the two species at similar stages of development using the same preparation and the same method of drug application, we show conclusively that the preBötC networks of neonatal mice and rat are differentially sensitive to A1R-mediated inhibition. Whereas in rats DPCPX has no effect on the ATP response (Huxtable et al., 2009), in mice local application of ATP in the preBötC only increased inspiratory frequency when applied in the presence of an A1R antagonist, DPCPX. It is possible that the tissue concentration of DPCPX produced in the initial experiments by local injection at 2 μ M was high enough to affect A2A and A2BRs. However, subsequent use of 0.1 μ M DPCPX (which would produce tissue levels of ~0.01 μ M; (Liu et al., 1990)) verified that block of A1Rs unmasks an ATP-mediated excitation. We cannot exclude the possibility that minor differences in the circuit elements contained within mouse and rat slices contribute to their differential responses to purinergic agents. However, we do not consider this to be a significant factor because drugs were locally injected directly

into the preBötC rather than bath-applied. In bath-application protocols, drugs can act at any locus within the slice, in which case differential drug responses could reflect differences in slice architecture. However, with local application into the preBötC, regions outside the preBötC are not exposed to the drug. Thus, minor differences in slice architecture should have minimal influence on drug responses. Slices were generated in reference to detailed mouse (Ruangkittisakul et al., 2011) and rat (Smith et al., 1991; Ruangkittisakul et al., 2006; Lorier et al., 2007) atlases so that the location of the preBötC relative to the rostral surface of the slice was similar between species. This facilitated application of drugs directly into the preBötC. In addition, responses to SP, ATP or MRS 2365 were mapped in each experiment to ensure drugs were locally injected into the preBötC.

In addition, because drugs were applied specifically into the preBötC, unmasking of an ATP-evoked frequency increase by DPCPX and the ADO-evoked frequency decrease show that activation of A1Rs in the preBötC is sufficient to inhibit rhythm. The brainstem site(s) responsible for the A1R-mediated inhibition of inspiratory frequency have not previously been identified because ADO or its agonists were always bath-applied. A reduction in the frequency of rhythmic bursts generated by preBötC islands and an inhibition of preBötC inspiratory neurons by A1Rs (via presynaptic inhibition of PSCs and postsynaptic hyperpolarization following inhibition of intracellular cAMP production and K_{ATP} channel activation) (Mironov et al., 1999) both suggested that A1Rs in the preBötC contribute to the ADO-mediated frequency inhibition. However, these data did not establish that activation of preBötC A1Rs is sufficient to slow frequency.

3.4.4 Differential ectonucleotidase expression

The differential sensitivity of mouse and rat preBötC networks to ATP may also reflect unique patterns of ectonucleotidase expression. There are multiple ectonucleotidase isoforms, each with different substrate affinities and end-products (Dunwiddie et al., 1997;

Zimmermann, 2000; Abbracchio et al., 2009). They also appear to be differentially distributed between and within discrete brain nuclei (Kukulski et al., 2004). Multiple isoforms with high activities are present in the medulla of adult rat (Langer et al., 2008). These data lack the spatial resolution required to define expression patterns within specific respiratory-related nuclei, but they clearly show that enzyme distribution is not uniform. Functionally, ectonucleotidases in the preBötC of rat are incredibly efficient at breaking down ATP and are significant determinants of preBötC ATP response kinetics. This is apparent in that ATP frequency responses closely follow ATP concentration profiles and that ATP responses are significantly prolonged when hydrolysis resistant-ATP analogues are used (Lorier et al., 2007; Funk et al., 2008a; Huxtable et al., 2009)(Fig 3.2). However, the significance of ectonucleotidase diversity and spatial heterogeneity for functioning networks, including preBötC inspiratory networks, remains unclear due to a lack of isoform-selective inhibitors and reliable information regarding the regional and cellular distribution of specific enzymes.

Our real-time PCR analysis of ectonucleotidase mRNA in preBötC tissue punches reveals the expression of multiple isoforms in the preBötC, and that the pattern varies among species. More importantly, the properties of the dominant isoform in the preBötC of mouse and rat match those predicted based on the respective ATP responses. For example, the ATP response in mice, which comprises a P2Y₁R excitation that is masked by an A1 inhibitory mechanism, predicts an enzyme complement that supports the rapid degradation of ATP to ADO. Consistent with this, TNAP, which degrades ATP all the way to ADO, is the dominant isoform in the mouse preBötC. In contrast, the potent excitatory response of rat preBötC networks to ATP predicts an enzyme complement that predisposes toward excitation. ENTPDase2 is the dominant transcript in the rat preBötC. It has an ~100-fold greater affinity for ATP than ADP and will cause ADP accumulation if the activity of enzymes that degrade ADP is low. This would most likely facilitate the excitatory effect of ATP because ADP is a more potent P2Y₁R agonist than ATP (Burnstock, 2006; von Kugelgen, 2006) that excites

preBötC networks (Lorier et al., 2007). An important caveat is that we report mRNA levels and these are not always indicative of protein levels. However, our observation that the properties of the most abundant transcripts match with the kinetics of network ATP responses in both mouse and rat suggests that transcript levels do reflect protein expression.

Based on the differential ADO sensitivity and ectonucleotidase expression in the preBötC of mouse and rat, the functional significance of ectonucleotidase activity for ATP signaling will also differ. In mouse, ectonucleotidases will not only reduce the P2Y₁-mediated excitation, they will also enhance the ADO-mediated inhibition. In contrast, greater ENTPDase 2 levels in rat will preferentially produce ADP and likely enhance or prolong the P2Y₁R-mediated excitation. Generation of ADO is not relevant since preBötC networks in rat are not sensitive to ADO (Fig 3.9). A full understanding of the role played by ectonucleotidases, however, will require use of preparations and stimuli that evoke endogenous release of ATP as well as analysis tools that provide increased spatial resolution to define at the cellular level the location of the various enzyme isoforms.

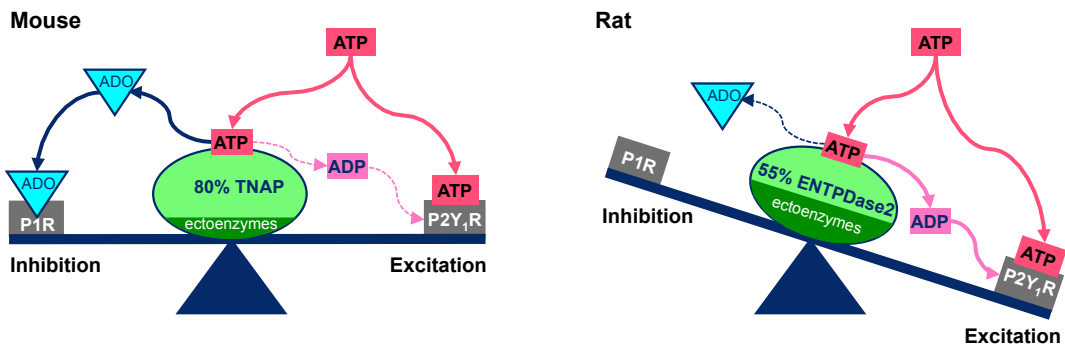


Figure 3.9 Schematic diagram of purinergic signaling in the preBötC illustrating that the balance between the excitatory effects of ATP at P2Y₁Rs and the inhibitory effects of ADO at A1Rs is tipped in favour of excitation in rats

Our data suggest that in mice, ATP alone does not affect rhythm because its P2Y₁R mediated excitatory action is balanced by an A1R-mediated inhibition that occurs due to the rapid degradation of ATP to ADO by TNAP, the predominant ectonucleotidase in the preBötC of mouse. In contrast, ATP is excitatory in the rat preBötC, likely reflecting that the predominant ectonucleotidase in rat, ENTPDase 2, preferentially produces ADP, which is excitatory at P2Y₁Rs. In addition, any ADO generated from the degradation of ATP is without consequence because the rat preBötC is not sensitive to the inhibitory actions of ADO.

3.4.5 Physiological significance

Hypoxia evokes ATP release within the VRC and preBötC where it attenuates the hypoxic respiratory depression (Gourine et al., 2005b). We therefore interpret our data in the context of the network response to hypoxia. From this perspective, our data define mechanisms through which ATP and its metabolites could act when they are released endogenously. The excitatory, P2Y₁R mechanism seen in mouse preBötC indicates that when ATP is released endogenously in response to hypoxia, or any other stimulus, it could excite preBötC networks (Gourine et al., 2005b). The lack of a frequency increase in response to exogenous ATP in mice does not exclude the possibility of a frequency increase in response to endogenous ATP because the time course of P2Y₁R activation, ATP degradation and A1R activation may differ. However, in mouse the ectonucleotidase complement favors ADO production and ADO directly inhibits preBötC networks, suggesting that the duration and magnitude of any endogenous ATP-evoked excitation is likely to be much smaller in the mouse compared to rat.

The surprising finding that preBötC networks in neonatal rat are not sensitive to ADO has several implications. It indicates that the hypoxic depression of breathing in rat (Mortola, 1996; Mayer et al., 2006) does not involve A1 receptor mechanisms in the preBötC. It also suggests that an A2A-mediated, GABAergic inhibition or an unknown, non-adenosinergic mechanism plays a more significant role in rat. These data are clinically relevant because ADO is implicated in the hypoxic depression of ventilation (Yan et al., 1995) and apnea of prematurity (AOP) (Bhatt-Mehta and Schumacher, 2003). Caffeine administration is the therapy of choice for AOP. Its efficacy as a respiratory stimulant is attributed to antagonism of A1 and A2A ADO receptors, however, a significant portion of premature infants do not respond to caffeine. This, combined with ongoing debate about potential long-term negative side effects of perinatal caffeine treatment on CNS development, including networks underlying respiratory control and sleep (Schmidt et al., 2007; Montandon et al., 2008),

suggest the need for alternate treatments. An ongoing clinical study shows that newborns treated with caffeine present no neuro-developmental disabilities in comparison to placebo-treated children (Schmidt et al., 2007; Schmidt et al., 2012). Neonatal caffeine administration provides clear short- and long-term health improvements, however the effects of this treatment on basic homeostatic functions such as respiratory regulation are unknown. Studies on rats indicate that caffeine treatment, especially during the perinatal period, alters adenosinergic neuromodulation of the respiratory control system, which raises important questions pertaining to the potential long-term effects of this treatment (Montandon et al., 2008). Our data also provide insight into basic mechanisms important in identifying drug targets such as strategies to enhance or extend P2Y₁ signaling actions through inhibition of ectonucleotidase activity. The presence of this mechanism in mice and rats, combined with a P2Y₁-like excitation of spinal locomotor CPGs in tadpole (Dale and Gilday, 1996; Brown and Dale, 2002) suggest it maybe a common excitatory mechanism in rhythmic networks.

In summary, our analysis of preBötC networks in neonatal mouse and rat further confirms the sensitivity of this vital network to P2Y₁R-mediated excitation. In addition, species variability in ATP responses emphasize that ATP signaling must be viewed as a three-part signaling system because differences in individual components dramatically alter overall network responses. These data also suggest that there may be significant therapeutic potential in developing methods that alter the ATP-ADO balance to favour the excitatory actions of ATP over the inhibitory actions of ADO (either by enhancing ATP release, ATP actions, minimizing ATP breakdown or inhibiting the actions of ADO). Species differences also emphasize that manipulation of ATP signaling in humans to treat CNS disorders of breathing requires that this three-part system be explored further in higher mammals, including primates and humans.

3.5 References

Abbracchio MP, Burnstock G, Verkhratsky A, Zimmermann H (2009) Purinergic signalling in the nervous system: an overview. *Trends Neurosci* 32:19-29.

Abbracchio MP, Boeynaems JM, Barnard EA, Boyer JL, Kennedy C, Miras-Portugal MT, King BF, Gachet C, Jacobson KA, Weisman GA, Burnstock G (2003) Characterization of the UDP-glucose receptor (re-named here the P2Y14 receptor) adds diversity to the P2Y receptor family. *Trends Pharmacol Sci* 24:52-55.

Ballanyi K (2004) Neuromodulation of the perinatal respiratory network. *Current Neuropharmacology* 2:221-243.

Bhatt-Mehta V, Schumacher RE (2003) Treatment of apnea of prematurity. *Paediatr Drugs* 5:195-210.

Bissonnette JM, Hohimer AR, Knopp SJ (1991) The effect of centrally administered adenosine on fetal breathing movements. *Respir Physiol* 84:273-285.

Bissonnette JM, Hohimer AR, Chao CR, Knopp SJ, Notoroberto NF (1990) Theophylline stimulates fetal breathing movements during hypoxia. *Pediatr Res* 28:83-86.

Brockhaus J, Ballanyi K (2000) Anticonvulsant A(1) receptor-mediated adenosine action on neuronal networks in the brainstem-spinal cord of newborn rats. *Neuroscience* 96:359-371.

Brown P, Dale N (2002) Modulation of K⁽⁺⁾ currents in *Xenopus* spinal neurons by p2y receptors: a role for ATP and ADP in motor pattern generation. *J Physiol* 540:843-850.

Burnstock G (2006) Historical review: ATP as a neurotransmitter. *Trends Pharmacol Sci* 27:166-176.

- Burr D, Sinclair JD (1988) The effect of adenosine on respiratory chemosensitivity in the awake rat. *Respir Physiol* 72:47-57.
- Dale N, Gilday D (1996) Regulation of rhythmic movements by purinergic neurotransmitters in frog embryos. *Nature* 383:259-263.
- Donnelly-Roberts D, McGaraughty S, Shieh CC, Honore P, Jarvis MF (2008) Painful purinergic receptors. *J Pharmacol Exp Ther* 324:409-415.
- Dunwiddie TV, Diao L, Proctor WR (1997) Adenine nucleotides undergo rapid, quantitative conversion to adenosine in the extracellular space in rat hippocampus. *J Neurosci* 17:7673-7682.
- Eldridge FL, Millhorn DE, Kiley JP (1984) Respiratory effects of a long-acting analog of adenosine. *Brain Res* 301:273-280.
- Eldridge FL, Millhorn DE, Kiley JP (1985) Antagonism by theophylline of respiratory inhibition induced by adenosine. *J Appl Physiol* 59:1428-1433.
- Feldman JL, Del Negro CA (2006) Looking for inspiration: new perspectives on respiratory rhythm. *Nat Rev Neurosci* 7:232-242.
- Fuller RW, Maxwell DL, Conradson TB, Dixon CM, Barnes PJ (1987) Circulatory and respiratory effects of infused adenosine in conscious man. *Br J Clin Pharmacol* 24:309-317.
- Funk GD, Huxtable AG, Lorier AR (2008a) ATP in central respiratory control: A three-part signaling system. *Respir Physiol Neurobiol*.
- Funk GD, Huxtable AG, Lorier AR (2008b) ATP in central respiratory control: a three-part signaling system. *Respir Physiol Neurobiol* 164:131-142.

Gourine AV (2005) On the peripheral and central chemoreception and control of breathing: an emerging role of ATP. *J Physiol* 568:715-724.

Gourine AV, Atkinson L, Deuchars J, Spyer KM (2003) Purinergic signalling in the medullary mechanisms of respiratory control in the rat: respiratory neurones express the P2X2 receptor subunit. *J Physiol* 552:197-211.

Gourine AV, Llaudet E, Dale N, Spyer KM (2005a) ATP is a mediator of chemosensory transduction in the central nervous system. *Nature* 436:108-111.

Gourine AV, Llaudet E, Dale N, Spyer KM (2005b) Release of ATP in the ventral medulla during hypoxia in rats: role in hypoxic ventilatory response. *J Neurosci* 25:1211-1218.

Gourine AV, Kasymov V, Marina N, Tang F, Figueiredo MF, Lane S, Teschemacher AG, Spyer KM, Deisseroth K, Kasparov S (2010) Astrocytes control breathing through pH-dependent release of ATP. *Science* 329:571-575.

Gray PA, Rekling JC, Bocchiaro CM, Feldman JL (1999) Modulation of respiratory frequency by peptidergic input to rhythmogenic neurons in the preBotzinger complex. *Science* 286:1566-1568.

Gray PA, Janczewski WA, Mellen N, McCrimmon DR, Feldman JL (2001) Normal breathing requires preBotzinger complex neurokinin-1 receptor-expressing neurons. *Nat Neurosci* 4:927-930.

Griffiths TL, Warren SJ, Chant AD, Holgate ST (1990) Ventilatory effects of hypoxia and adenosine infusion in patients after bilateral carotid endarterectomy. *Clin Sci (Lond)* 78:25-31.

- Griffiths TL, Christie JM, Parsons ST, Holgate ST (1997) The effect of dipyridamole and theophylline on hypercapnic ventilatory responses: the role of adenosine. *Eur Respir J* 10:156-160.
- Guyenet PG, Wang H (2001) Pre-Botzinger neurons with preinspiratory discharges "in vivo" express NK1 receptors in the rat. *J Neurophysiol* 86:438-446.
- Herlenius E, Lagercrantz H (1999) Adenosinergic modulation of respiratory neurones in the neonatal rat brainstem in vitro. *J Physiol* 518 (Pt 1):159-172.
- Herlenius E, Lagercrantz H, Yamamoto Y (1997) Adenosine modulates inspiratory neurons and the respiratory pattern in the brainstem of neonatal rats. *Pediatr Res* 42:46-53.
- Huxtable AG, Zwicker JD, Poon BY, Pagliardini S, Vrouwe SQ, Greer JJ, Funk GD (2009) Tripartite purinergic modulation of central respiratory networks during perinatal development: the influence of ATP, ectonucleotidases, and ATP metabolites. *J Neurosci* 29:14713-14725.
- Huxtable AG, Zwicker JD, Alvares TS, Ruangkittisakul A, Fang X, Hahn LB, Posse de Chaves E, Baker GB, Ballanyi K, Funk GD (2010) Glia contribute to the purinergic modulation of inspiratory rhythm-generating networks. *J Neurosci* 30:3947-3958.
- Johnson SM, Smith JC, Feldman JL (1996) Modulation of respiratory rhythm in vitro: role of Gi/o protein-mediated mechanisms. *J Appl Physiol* 80:2120-2133.
- King BF (2007) Novel P2X7 receptor antagonists ease the pain. *Br J Pharmacol* 151:565-567.
- Klotz KN (2000) Adenosine receptors and their ligands. *Naunyn Schmiedebergs Arch Pharmacol* 362:382-391.

- Koos BJ, Matsuda K (1990) Fetal breathing, sleep state, and cardiovascular responses to adenosine in sheep. *J Appl Physiol* 68:489-495.
- Koos BJ, Chau A (1998) Fetal cardiovascular and breathing responses to an adenosine A_{2a} receptor agonist in sheep. *Am J Physiol* 274:R152-159.
- Koos BJ, Kawasaki Y, Kim YH, Bohorquez F (2005) Adenosine A_{2A}-receptor blockade abolishes the roll-off respiratory response to hypoxia in awake lambs. *Am J Physiol Regul Integr Comp Physiol* 288:R1185-1194.
- Kowaluk EA, Bhagwat SS, Jarvis MF (1998) Adenosine kinase inhibitors. *Curr Pharm Des* 4:403-416.
- Kukulski F, Sevigny J, Komoszynski M (2004) Comparative hydrolysis of extracellular adenine nucleotides and adenosine in synaptic membranes from porcine brain cortex, hippocampus, cerebellum and medulla oblongata. *Brain Res* 1030:49-56.
- Lagercrantz H, Yamamoto Y, Fredholm BB, Prabhakar NR, von Euler C (1984) Adenosine analogues depress ventilation in rabbit neonates. Theophylline stimulation of respiration via adenosine receptors? *Pediatr Res* 18:387-390.
- Lambrecht G (2000) Agonists and antagonists acting at P2X receptors: selectivity profiles and functional implications. *Naunyn Schmiedebergs Arch Pharmacol* 362:340-350.
- Langer D, Hammer K, Koszalka P, Schrader J, Robson S, Zimmermann H (2008) Distribution of ectonucleotidases in the rodent brain revisited. *Cell Tissue Res* 334:199-217.
- Lieske SP, Thoby-Brisson M, Telkamp P, Ramirez JM (2000) Reconfiguration of the neural network controlling multiple breathing patterns: eupnea, sighs and gasps [see comment]. *Nat Neurosci* 3:600-607.

- Liu G, Feldman JL, Smith JC (1990) Excitatory amino acid-mediated transmission of inspiratory drive to phrenic motoneurons. *J Neurophysiol* 64:423-436.
- Lorier AR, Lipski J, Housley GD, Greer JJ, Funk GD (2008) ATP sensitivity of preBotzinger complex neurones in neonatal rat in vitro: mechanism underlying a P2 receptor-mediated increase in inspiratory frequency. *J Physiol* 586:1429-1446.
- Lorier AR, Peebles K, Brosenitsch T, Robinson DM, Housley GD, Funk GD (2004) P2 receptors modulate respiratory rhythm but do not contribute to central CO₂ sensitivity in vitro. *Respir Physiol Neurobiol* 142:27-42.
- Lorier AR, Huxtable AG, Robinson DM, Lipski J, Housley GD, Funk GD (2007) P2Y1 receptor modulation of the pre-Botzinger complex inspiratory rhythm generating network in vitro. *J Neurosci* 27:993-1005.
- Mayer CA, Haxhiu MA, Martin RJ, Wilson CG (2006) Adenosine A2A receptors mediate GABAergic inhibition of respiration in immature rats. *J Appl Physiol* 100:91-97.
- Mironov SL, Langohr K, Richter DW (1999) A1 adenosine receptors modulate respiratory activity of the neonatal mouse via the cAMP-mediated signaling pathway. *J Neurophysiol* 81:247-255.
- Montandon G, Kinkead R, Bairam A (2008) Adenosinergic modulation of respiratory activity: Developmental plasticity induced by perinatal caffeine administration. *Respir Physiol Neurobiol*.
- Mortola JP (1996) Ventilatory responses to hypoxia in mammals. In: *In Tissue Oxygen Deprevention* (Haddad GGAL, G., ed), pp 433-477. New York, NY: Marcel Dekker.
- Moss IR (2000) Respiratory responses to single and episodic hypoxia during development: mechanisms of adaptation. *Respir Physiol* 121:185-197.

- North RA (2002) Molecular physiology of P2X receptors. *Physiol Rev* 82:1013-1067.
- Pace RW, Del Negro CA (2008) AMPA and metabotropic glutamate receptors cooperatively generate inspiratory-like depolarization in mouse respiratory neurons in vitro. *Eur J Neurosci* 28:2434-2442.
- Pace RW, Mackay DD, Feldman JL, Del Negro CA (2007) Inspiratory bursts in the preBotzinger complex depend on a calcium-activated non-specific cation current linked to glutamate receptors in neonatal mice. *J Physiol* 582:113-125.
- Pagliardini S, Ren J, Greer JJ (2003) Ontogeny of the pre-Botzinger complex in perinatal rats. *J Neurosci* 23:9575-9584.
- Pagliardini S, Adachi T, Ren J, Funk GD, Greer JJ (2005) Fluorescent tagging of rhythmically active respiratory neurons within the pre-Botzinger complex of rat medullary slice preparations. *J Neurosci* 25:2591-2596.
- Ramirez JM, Telkamp P, Elsen FP, Quellmalz UJ, Richter DW (1997) Respiratory rhythm generation in mammals: synaptic and membrane properties. *Respir Physiol* 110:71-85.
- Reid PG, Watt AH, Penny WJ, Newby AC, Smith AP, Routledge PA (1991) Plasma adenosine concentrations during adenosine-induced respiratory stimulation in man. *Eur J Clin Pharmacol* 40:175-180.
- Ruangkittisakul A, Ballanyi K (2010) Methylxanthine reversal of opioid-evoked inspiratory depression via phosphodiesterase-4 blockade. *Respir Physiol Neurobiol* 172:94-105.
- Ruangkittisakul A, Panaitescu B, Ballanyi K (2011) K(+) and Ca(2)(+) dependence of inspiratory-related rhythm in novel "calibrated" mouse brainstem slices. *Respir Physiol Neurobiol* 175:37-48.

- Ruangkittisakul A, Schwarzacher SW, Secchia L, Poon BY, Ma Y, Funk GD, Ballanyi K (2006) High sensitivity to neuromodulator-activated signaling pathways at physiological [K+] of confocally imaged respiratory center neurons in on-line-calibrated newborn rat brainstem slices. *J Neurosci* 26:11870-11880.
- Runold M, Lagercrantz H, Prabhakar NR, Fredholm BB (1989) Role of adenosine in hypoxic ventilatory depression. *J Appl Physiol* 67:541-546.
- Sak K, Illes P (2005) Neuronal and glial cell lines as model systems for studying P2Y receptor pharmacology. *Neurochem Int* 47:401-412.
- Schmidt B, Roberts RS, Davis P, Doyle LW, Barrington KJ, Ohlsson A, Solimano A, Tin W (2007) Long-term effects of caffeine therapy for apnea of prematurity. *N Engl J Med* 357:1893-1902.
- Schmidt B, Anderson PJ, Doyle LW, Dewey D, Grunau RE, Asztalos EV, Davis PG, Tin W, Moddemann D, Solimano A, Ohlsson A, Barrington KJ, Roberts RS (2012) Survival without disability to age 5 years after neonatal caffeine therapy for apnea of prematurity. *JAMA* 307:275-282.
- Schmidt C, Bellingham MC, Richter DW (1995) Adenosinergic modulation of respiratory neurones and hypoxic responses in the anaesthetized cat. *J Physiol* 483 (Pt 3):769-781.
- Smith JC, Ellenberger HH, Ballanyi K, Richter DW, Feldman JL (1991) Pre-Botzinger complex: a brainstem region that may generate respiratory rhythm in mammals. *Science* 254:726-729.

- Soto F, Lambrecht G, Nickel P, Stuhmer W, Busch AE (1999) Antagonistic properties of the suramin analogue NF023 at heterologously expressed P2X receptors. *Neuropharmacology* 38:141-149.
- Thomas T, Ralevic V, Bardini M, Burnstock G, Spyer KM (2001) Evidence for the involvement of purinergic signalling in the control of respiration. *Neuroscience* 107:481-490.
- Vandam RJ, Shields EJ, Kelty JD (2008) Rhythm generation by the pre-Botzinger complex in medullary slice and island preparations: effects of adenosine A(1) receptor activation. *BMC Neurosci* 9:95.
- von Kugelgen I (2006) Pharmacological profiles of cloned mammalian P2Y-receptor subtypes. *Pharmacology & therapeutics* 110:415-432.
- von Kugelgen I, Wetter A (2000) Molecular pharmacology of P2Y-receptors. *Naunyn Schmiedebergs Arch Pharmacol* 362:310-323.
- Wang G, Zhou P, Repucci MA, Golanov EV, Reis DJ (2001) Specific actions of cyanide on membrane potential and voltage-gated ion currents in rostral ventrolateral medulla neurons in rat brainstem slices. *Neurosci Lett* 309:125-129.
- Wilson CG, Martin RJ, Jaber M, Abu-Shaweeesh J, Jafri A, Haxhiu MA, Zaidi S (2004) Adenosine A2A receptors interact with GABAergic pathways to modulate respiration in neonatal piglets. *Respir Physiol Neurobiol* 141:201-211.
- Yamamoto M, Nishimura M, Kobayashi S, Akiyama Y, Miyamoto K, Kawakami Y (1994) Role of endogenous adenosine in hypoxic ventilatory response in humans: a study with dipyridamole. *J Appl Physiol* 76:196-203.

Yan S, Laferriere A, Zhang C, Moss IR (1995) Microdialyzed adenosine in nucleus tractus solitarii and ventilatory response to hypoxia in piglets. *J Appl Physiol* 79:405-410.

Zimmermann H (2000) Extracellular metabolism of ATP and other nucleotides. *Naunyn Schmiedebergs Arch Pharmacol* 362:299-309.

Chapter 4: Exogenous and endogenous purinergic modulation of central respiratory networks *in vivo*

Zwicker JD, Gourine AV, Funk GD

I performed all experimental design, experiments and data analysis in this chapter. Plethysmography experiments were performed in Dr. AV Gourine's lab. Dr. GD Funk oversaw all aspects of the study. Overall, my contribution was 100% of the total.

Dr. S. Pagliardini aided in teaching me how to record from anesthetized adult rat and inject locally into the preBötC

Dr. A. Gourine and Dr. N Marina aided in carotid body denervation of anesthetized adult rat

4.1 Introduction

The hypoxic ventilatory response is biphasic, consisting of an initial increase in ventilation, followed by a secondary depression that is life threatening in premature infants (Moss, 2000; Waters and Gozal, 2003). While in adults ventilation remains above baseline levels during this secondary depression, in premature and most neonatal mammals ventilation decreases below baseline and may remain below baseline after returning to normoxia (Mortola et al., 1989; Mortola, 1996). The initial increase in ventilation is primarily mediated by the peripheral carotid body chemoreceptors (Gourine, 2005; Kumar, 2007; Lahiri et al., 2007). Type I glomus cells in the carotid body detect reductions in PO₂ and release transmitters which activate sensory terminals of the carotid sinus nerve. The carotid sinus nerve synapses in the NTS (Guyenet et al., 2010) and through subsequent synaptic relays, evokes graded cardiorespiratory reflexes, including increased ventilation. There is also some evidence for a central contribution to the hypoxia-evoked increase in ventilation. In some species (rat (Cardenas and Zapata, 1983; Martin-Body et al., 1985), cat (Miller and Tenney, 1975), dog (Davenport et al., 1947), goat (Davenport et al., 1947), pony (Bisgard et al., 1980)) there is a residual ventilatory response to acute hypoxia following carotid body denervation that may reflect the actions of other peripheral carotid chemoreceptors (i.e. aortic bodies) or direct central actions of hypoxia.

The secondary depression of ventilation is primarily mediated centrally, although the depressive effects of hypoxia on metabolism early in development contribute to the ventilatory depression in premature and neonatal mammals (Mortola et al., 1989). This central mechanism is not completely understood (for review see (Bissonnette, 2000)). It may involve actions of GABA at unknown sites. GABAergic neurons inhibit respiratory networks via GABA_ARs and during hypoxia ADO may act on its A2aR in the VRC to excite these GABAergic neurons and evoke respiratory depression (Wilson et al., 2004; Mayer et al., 2006). However this mechanism is not detectable in reduced preparations (Herlenius et al.,

1997; Mironov et al., 1999).

The reduction of the secondary hypoxic ventilatory depression by ADO antagonists (Runold et al., 1989; Bissonnette et al., 1990; Koos and Matsuda, 1990; Yan et al., 1995; Bissonnette, 2000; Koos et al., 2005) also implicates ADO in this ventilatory depression. However, there are significant species differences in the sensitivity of this depression to ADO antagonists (reviewed in (Ballanyi, 2004)). While the specific neurotransmitters or modulators involved remain unclear, recent data suggest that ATP plays an important role in shaping the hypoxic ventilatory depression. The use of ATP biosensors in adult anesthetized rats and horizontal slices of the adult rat medulla has revealed that ATP is released from the ventral respiratory column, including the preBötC, during hypoxia (Gourine et al., 2005b). This ATP release begins after the initial increase in ventilation and peaks during the secondary depression. The timing of the ATP release, combined with the observation that the magnitude of the ventilatory depression is increased when the P2R antagonist PPADS is applied to the ventral medullary surface, suggest that endogenously-released ATP attenuates the secondary hypoxic ventilatory depression (Gourine et al., 2005a). The strength of this conclusion, however, is limited, first by concerns about the specificity of the ATP biosensors in accurately detecting ATP release. In addition, although PPADS was used at a relatively low concentration in these experiments, there is the potential for nonselective actions, for example at glutamate receptors (Motin and Bennett, 1995; Nakazawa et al., 1995; Lambrecht, 2000).

Given these limitations and the lack of selective pharmacological tools to manipulate P2R signaling, the purpose of this study is to further test the role of ATP in shaping the hypoxic ventilatory response by increasing levels of ectonucleotidase activity in brainstem regions where ATP is proposed to mediate its excitatory actions. I injected bilaterally into the preBötC of adult rats a lentiviral vector encoding the enzyme, transmembrane prostatic acid phosphatase (TMPAP, degrades ATP to ADO) and GFP, under the control of the EF1alpha promoter, which drives expression in both neurons and glia. Injections were targeted to the

preBötC because, even though ATP appears to be released from the VRC in adult rats, *in vitro* data indicate that the excitatory actions of ATP on frequency are highest in the preBötC. Following 21–24 days to allow for significant TMPAP expression, the hypoxic ventilatory response of the TMPAP-injected animals was compared to controls (injected with lentiviral vector containing only GFP) both before and after carotid body denervation (to focus on the secondary, centrally-mediated phase of the hypoxic ventilatory response). The main finding is that increased expression of TMPAP (as suggested by increased GFP expression) within the preBötC in carotid body denervated rats is associated with an increased secondary hypoxic depression of both V_T and V_E . Injection of a P2Y₁R agonist or ADO into the preBötC *in vivo* further revealed that the preBötC network is excited by P2Y₁R activation but insensitive to ADOR activation, indicating that the greater hypoxic respiratory depression in the TMPAP rats is due to loss of an endogenous, excitatory ATP action rather than the addition of an inhibitory mechanism subsequent to ATP degradation. These findings suggest that the release of ATP in the preBötC during hypoxia acts through a P2Y₁R mechanism to attenuate the hypoxia-induced respiratory depression.

4.2 Methods

All the experiments were performed in accordance with the European Commission Directive 86/609/EEC (European Convention for the Protection of Vertebrate Animals used for Experimental and Other Scientific Purposes), the UK Home Office (Scientific Procedures) Act (1986), or in accordance with the guidelines of the Canadian Council on Animal Care and were approved by the University of Alberta Animal Ethics Committee with project approval from the University College London, and University of Alberta.

4.2.1 Virus injection

The lentiviral-vector encoding the Transmembrane Prostatic Acid Phosphatase

(TMPAP) employs an elongation factor 1-alpha (EF1 α) promoter to drive the expression of TMPAP, an enzyme that functions as an ectonucleotidase. In order to visualize expression, TMPAP is fused to EGFP. The plasmid SW-EF1a-TMPAP-EGFP was cloned into the LVV. Titres of LVV-SW-EF1a-TMPAP-EGFP and the control virus LVV-SW-EF1a-EGFP were between 1×10^9 and 1×10^{10} plaque forming units. Viral concentration and titration were performed as described in detail previously (Coleman et al., 2003)

4.2.2 *In vivo* gene transfer

A separate cohort of rats was used for the TMPAP virus injection experiments. TMPAP injected rats were compared to GFP control injected rats. Adult, male Sprague Dawley rats (~ 200 g) with a normal phenotype were anesthetized with mixture of ketamine (60 mg kg $^{-1}$; i.m.) and medetomidine (250 μ g kg $^{-1}$, i.m.). and positioned in a stereotaxic frame with bregma 5 mm below lambda and either the lentivirus LVV-SW-EF1a-TMPAP-EGFP(0.25μ L $n = 8$) or LVV-SW-EF1a-EGFP (0.25μ L $n = 8$) were pressure injected into the preBötC bilaterally through a sharp glass pipette (40 μ m tip diameter). The injection pipette was left in place for 5 min after each injection to minimize backflow of virus up the electrode track. Coordinates were as follows (in mm): 0.9 rostral, 2.0 lateral, and 2.8 ventral to the obex. Anesthesia was reversed with atipemazole (1 mg kg $^{-1}$). Rats recovered for 21 – 24 days with food and water *ad libitum* before plethysmography experiments.

4.2.3 Whole body plethysmography

Three weeks after *in vivo* gene transfer, respiratory rate (f, breaths min $^{-1}$) and tidal volume (V_T , relative to control) in conscious, freely moving SD rats were measured by whole-body plethysmography as described in detail previously (Rong et al., 2003). All experiments were performed at room temperature (22 – 24 °C). In brief, the rat was weighed and then placed in a Plexiglas recording chamber (~ 1100 ml) that was flushed continuously with a mixture of

79% nitrogen and 21% oxygen (unless otherwise required by the protocol) at a rate of ~1 L min⁻¹. Concentrations of CO₂ in the chamber were monitored on-line using a fast-response O₂/CO₂ monitor (Morgan Medical). The animals were allowed at least 10 min to acclimatize to the chamber environment at normoxia/normocapnia (21% O₂, 79% N₂, and <0.3% CO₂). After measuring baseline ventilation in normoxia, the hypoxic ventilatory response was measured by lowering the O₂ concentration in the inspired air to 10% for 5 min then 7.5% for 2 min followed by a 5 min recovery period in normoxia/normocapnia.

In a separate series of experiments, the ventilatory response to hypercapnia was measured by increasing the level of CO₂ in the inspired air to 3 and then 6% for 5 min sequentially followed by a 5 min recovery period in normoxia/normocapnia. The hypercapnic and hypoxic responses were measured one day apart with the hypercapnic treatment occurring first. This testing paradigm was repeated one day after carotid sinus denervation.

Two days after completion of both the hypoxia and hypercapnia experiments, the rats (~320g) were anaesthetised with a mixture of ketamine (60 mg kg⁻¹; i.m.) and medetomidine (250 µg kg⁻¹, i.m.) and the carotid sinus and aortic nerves were sectioned to eliminate inputs from the peripheral chemoreceptors and arterial baroreceptors. Hypoxic and hypercapnic ventilatory responses were then repeated (a day later) with the following minor adjustments to the gas exposure protocols. Carotid body denervation was verified by the lack of an abrupt increase in ventilation in response to hypoxia. The animals were allowed at least 10 min to acclimatize to the chamber environment at normoxia/normocapnia (21% O₂, 79% N₂, and <0.3% CO₂). After measurements of baseline ventilation were made in conditions of normoxia, hypoxia was induced by lowering the O₂ concentration in the inspired air down to a level of 15% for 2 min then 10% for 3 min then 7.5% for 2.5 min followed by a 5 min recovery at normoxia. Similarly, in separate experiments, hypercapnia was induced by titrating CO₂ into the respiratory mixture up to a level of 3 or 6% for 5 min at each CO₂ level.

4.2.4 MRS 2365/ADO injection experiments

Adult male Sprague Dawley rats (200–300 g) were used for acute experiments. Rats were initially anesthetized in isoflurane (1%, 1 L/min in air) while the femoral vein was cannulated and urethane (1.5–1.7 g/kg body weight) was gradually delivered to induce permanent and irreversible anesthesia. Additional doses of anesthesia were delivered as necessary to maintain the level of anesthesia but was rarely needed. The trachea was cannulated and respiratory flow was detected with a pneumotachograph connected to a transducer to measure airflow (GM Instruments). Coupled EMG wire electrodes (Cooner Wire) were inserted into the genioglossal (GG) and diaphragm (DIA) muscles. Wires were connected to amplifiers (Differential AC amplifier model 1700, A-M systems) and activity was sampled at 2–4 kHz (Powerlab 16SP; AD Instruments). To eliminate confounding effects induced by stimulation of vagal reflexes, rats were vagotomized by resecting a portion of the vagus nerve (2 mm) at mid-cervical level. Body temperature was kept constant at $37 \pm 1^\circ\text{C}$ with a servo-controlled heating pad (Harvard Apparatus). The rats were then placed in a stereotaxic frame with bregma 5 mm below lambda. MRS 2365 or ADO (1 mM or 500 μM ; 200 nl/side; Tocris and Sigma-Aldrich) made in HEPES-buffered solution (HBS; 137 mM NaCl, 5.4 mM KCl, 0.25 mM Na₂HPO₄, 0.44 mM KH₂PO₄, 1.3 mM CaCl₂, 1.0 mM MgSO₄, 4.2 mM NaHCO₃, 10 mM HEPES; pH 7.4–7.45) ($n = 4$) were pressure injected through a sharp glass pipette (40 μm tip diameter) into the preBötC. Coordinates were as follows (in mm): 0.9 rostral, 2.0 lateral, and 2.8 ventral to obex. Additional injections (along the rostrocaudal and mediolateral axes) were performed to identify the extent of the regions responsive to drug application. Fluorescent beads (0.2 μm diameter, 0.2% solution; Invitrogen) were added to the injected solution for subsequent localization of the injection site.

4.2.5 Histology

At the end of each experiment, rats were transcardially perfused with 4% paraformaldehyde in phosphate buffer. The brains were collected, postfixed, and cryoprotected, and 50 µm brainstem transverse sections were cut. Serial sections were either directly mounted on slides, stained with cresyl violet, and coverslipped or immunoreacted for detection of specific neuronal markers. Immunohistochemistry was performed according to the following protocol. Free-floating sections were rinsed in PBS and incubated with 10% normal donkey antiserum (NDS) and 0.2% Triton X-100 in PBS for 60 min to reduce nonspecific staining and increase antibody penetration. Sections were incubated overnight with primary antibodies diluted in PBS containing 1% NDS and 0.2% Triton X-100. The following day, sections were washed in PBS, incubated with the specific secondary antibodies conjugated to the fluorescent probes (Cy3-conjugated donkey anti rabbit; Cy3-conjugated donkey anti-mouse; Jackson ImmunoResearch) diluted in PBS and 1% NDS for 2 h. Sections were further washed in PBS, mounted, and coverslipped with Fluorsave mounting medium (Millipore). The primary antibodies used for this study were as follows: Substance P Receptor (rabbit; 1:1000; Millipore), and to the neuronal marker NeuN (mouse; 1:500; Millipore). Slides were observed under a Leica DM5500 fluorescent microscope with a Hamamatsu digital camera connected with MetaMorph acquisition software. Images were acquired, exported in TIFF files, and Adobe Illustrator was used to prepare final figures and identify electrode placement coordinates.

4.2.6 Drugs

Adenosine ($A_{1,2,3}$ agonist, 500 µM microinjected) and DLH (DL-Homocysteic acid, 1mM) were obtained from Sigma-Aldrich. MRS 2365([(1*R*,2*R*,3*S*,4*R*,5*S*)-4-[6-amino-2-(methylthio)-9*H*purin-9-yl]-2,3-dihydroxybicyclo[3.1.0]hex-1-yl]methyl]diphosphoric acid

mono ester trisodium salt), P2Y₁R agonist, 1mM microinjected) was obtained from Tocris Bioscience.

MRS 2365 was prepared as a stock solution in aCSF and frozen in aliquots. DLH and ADO were made fresh on the day of the experiment. Drug microinjections were controlled by a picospritzer (Spritzer4 Pressure Micro-Injector, 18 psi). Consecutive agonist applications were separated by a minimum of 15 min. We did not systematically assess whether this was the minimum time interval required for consistent responses, but it was sufficient for reproducible responses.

4.2.7 Data analysis and statistics

For plethysmography experiments, the pressure signal was amplified, filtered, recorded, and analyzed off-line using Spike 2 software (Cambridge Electronic Design). We were interested in the hypoxic depression and therefore focused on this phase of the response by taking measurements of f and V_T during the last 2 min before exposure to the stimulus and during the 2 min period at the end of each stimulus, when breathing stabilized. Analysis was done on 2 min of the trace at the end of each hypoxic treatment. Hypoxia- or hypercapnia-induced changes in the f , V_T , and minute ventilation (V_E) ($f \times V_T$; relative to control) were averaged and expressed as means \pm SE.

In the experiments that involved injection of MRS 2365 or ADO, traces were recorded on a computer and analyzed using LabChart (AD Instruments) and Excel software. The absolute value of EMG signals was digitally integrated with a time constant of 0.1 s to calculate peak amplitude and time onset. The airflow signal measured via pneumotachography was high-pass filtered to eliminate DC shifts and slow drifts, and used to calculate respiratory rate, period, inspiratory (T_I) and expiratory (T_E) durations. After filtering, the flow signal was digitally integrated to obtain tidal volume (V_T) and minute ventilation (\dot{V}_E). T_I , T_E , V_T , \dot{V}_E , integrated peak amplitude of DIA_{EMG}, and GG_{EMG} during

the drug were compared with the average value during the 2 min control period that immediately preceded drug application. The maximum effect of a drug on T_L , T_E , V_T , \dot{V}_E , integrated peak amplitude of DIA_{EMG} , and GG_{EMG} was determined as the maximum (or minimum) value measured in the moving average (calculation based on the average of three consecutive bursts) during the first minute after injection. Parameters are reported relative to control (predrug or prestimulus) levels, as means \pm standard error of the mean (SEM). Statistical comparison of means was performed on raw data unless otherwise stated using GraphPad Prism version 4 (GraphPad Software Inc., La Jolla, CA, USA). Statistical comparison of relative data was performed only after verification of normality. Differences between means were identified using a Paired *t* test (two-tail distribution), one-way ANOVA with Dunnett's multiple comparison test or via two-way repeated measures ANOVA. All values are reported as means \pm SEM. Values of $P < 0.05$ were assumed significant.

4.3 Results

4.3.1 The hypoxic ventilatory response in control rats and those with TMPAP injections into the preBötC

Carotid body intact rats.

Representative plethysmographic recordings of ventilatory activity at rest and during increasing hypoxic conditions (5 min 10% and 2 min 7.5% O₂) in a control and a TMPAP injected, carotid body-intact rat are presented in Fig 4.1 A, B.

TMPAP had no significant effect on the hypoxic ventilatory response of carotid body-intact rats. After 10 min of normoxia, rats were exposed to 5 min 10% O₂ and 2 min 7.5% O₂ followed by a 5 min recovery period. Control rats responded to 10% and 7.5% O₂ with significant 1.32 \pm 0.18 and 1.44 \pm 0.11 fold increase in V_E respectively ($p < 0.01$). This increase was due entirely to significant 1.28 \pm 0.10 and 1.47 \pm 0.11 ($p < 0.01$) fold increases in V_T since f

was unaffected (1.01 ± 0.07 of normoxic levels in 10% and 0.99 ± 0.05 of normoxic levels in 7.5% O₂) (Fig 4.1 A,C, n=8, two-way repeated measures ANOVA with Bonferroni post test). The response of TMPAP-injected rats was similar to the control rats. Minute ventilation increased significantly in 10% and 7.5% O₂ to 1.53 ± 0.24 and 1.65 ± 0.17 (p<0.001) fold relative to control respectively, due to significant increases in V_T (1.35 ± 0.14 fold in 10% O₂ and 1.42 ± 0.10 fold in 7.5% O₂ p<0.001). 1.09 ± 0.09 and 1.15 ± 0.10 fold increases in f in 10% and 7.5% O₂ were not significant (p<0.01, Fig 4.1 B,C. n=8, two-way repeated measures ANOVA with Bonferroni post test). With the transition in recovery from 7.5% O₂ to normoxia, V_E, V_T and f all decreased significantly (p<0.001, p<0.001 and p<0.01 respectively). Thus, in the presence of carotid body feedback, increased TMPAP expression in the preBötC, and presumably increased ATP breakdown, is not enough to affect the hypoxic ventilatory response.

Carotid body denervated rats.

In order to focus just on the central component of the hypoxic ventilatory response when ATP is hypothesized to underlie an increase in ventilation that offsets the secondary depression, we repeated the hypoxic ventilatory response measurements after carotid body denervation. Representative plethysmographic recordings of ventilatory activity at rest and during increasing hypoxic conditions (2 min 15%, 3 min 10% and 2.5 min 7.5% O₂) in a control and a TMPAP injected, carotid body denervated rats are presented in Fig 4.2 A, B. Control, denervated rats showed dose-dependent increases in ventilation in response to graded hypoxia. There was no significant response to 15% O₂ but V_E increased to 2.28 ± 1.52 and 2.07 ± 0.49 fold greater than control in 10% and 7.5% O₂ respectively. This reflected significant increases in V_T of 1.76 ± 1.20 at 10% and 1.59 ± 0.22 fold at 7.5% O₂. Frequency did not change significantly and was 1.30 ± 1.21 and 1.27 ± 0.23 of control at 10 and 7.5% O₂ respectively (Fig 4.2 A,C, n=5, two-way repeated measures ANOVA with Bonferroni post test, P<0.001). In contrast, TMPAP rats exposed to 7.5% oxygen showed no significant change in f, V_T or V_E at any level of hypoxia. At 7.5% O₂, f, V_T or V_E were 0.90 ± 0.11 ,

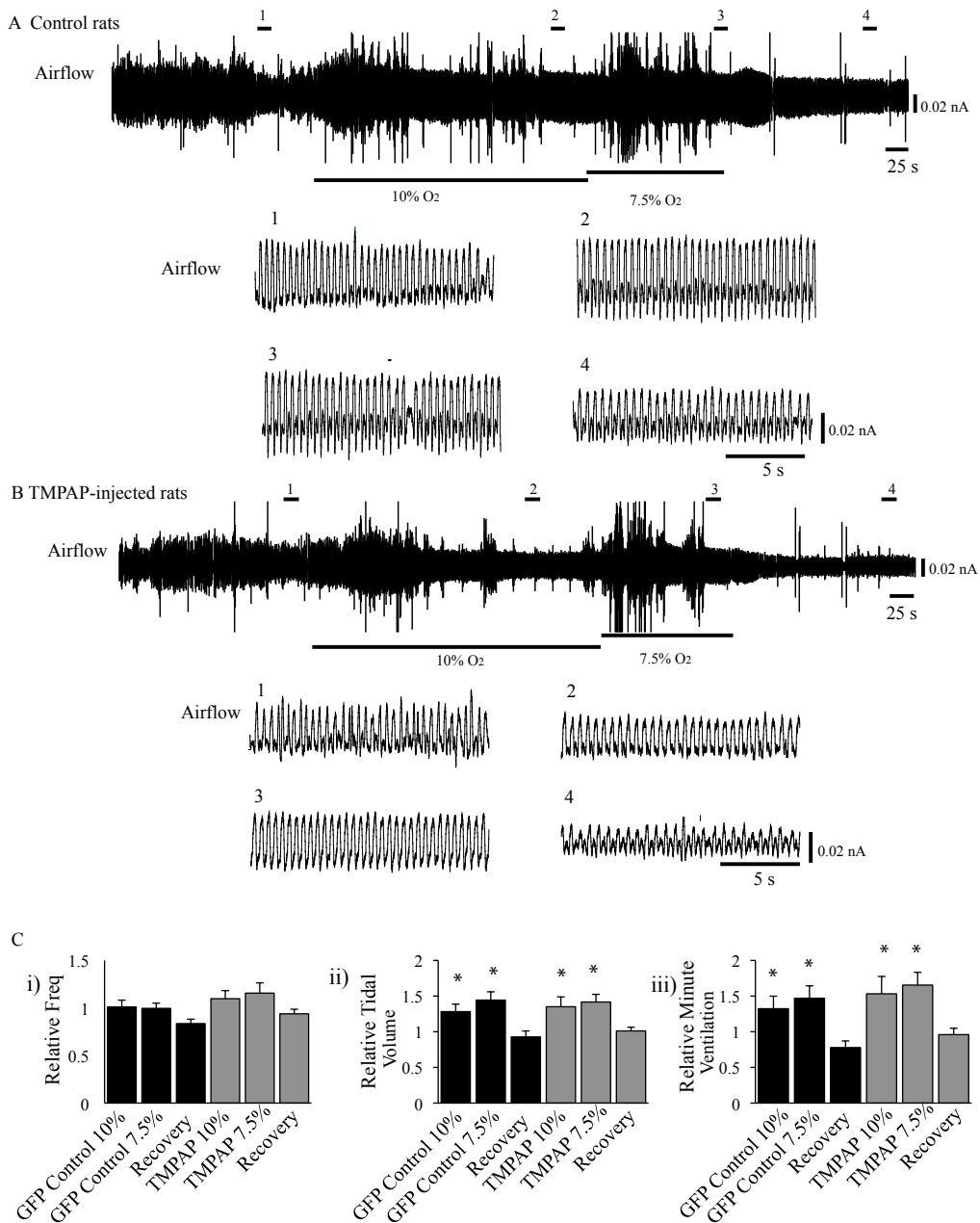
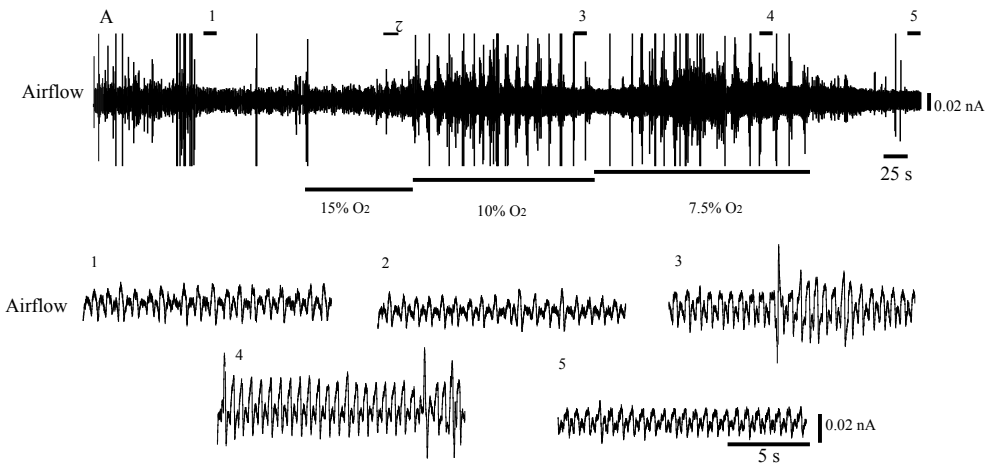


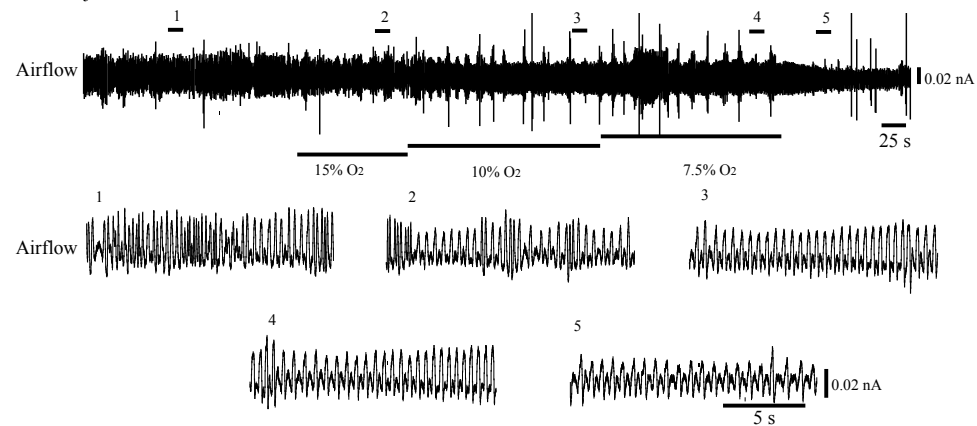
Figure 4.1 Effects of LVV-SW-EF1a-TMPAP-EGFP or LVV-SW-EF1a-EGFP lentivirus injection in the preBötC on the minute ventilation (V_E), tidal volume (V_T), and breathing frequency (f) responses to hypoxia in carotid body intact rats.

Ventilation was measured during normoxia (baseline) and following exposure to moderate hypoxia and then expressed relative to baseline levels. Representative plethysmographic recordings of ventilatory activity at rest and during increasing hypoxic conditions (10min control, 5 min 10%, 2 min 7.5% and 5 min recovery O₂) in a control (A, n=8) and a TMPAP (B, n=8) injected, carotid body-intact rat are presented. Graphs show changes in breathing frequency (C i), tidal volume (V_T, C ii) and minute ventilation (V_E, C iii) responses relative to baseline when exposed to hypoxia. Data are expressed as means ± SE. *Value significantly different from baseline ($P < 0.05$) n=8, two-way repeated measures ANOVA with Bonferroni post test.

A Control rats



B TMPAP-injected rats



C

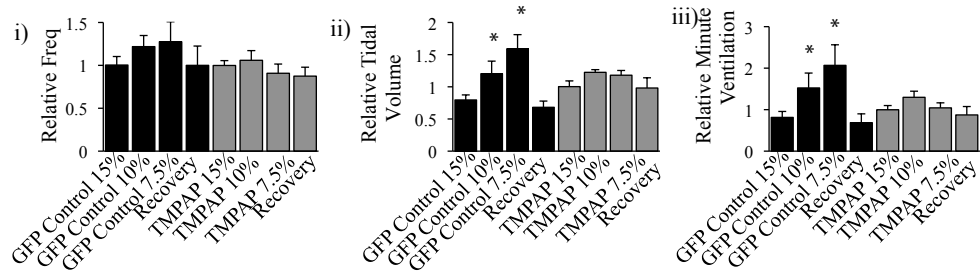


Figure 4.2 Effects of LVV-SW-EF1a-TMPAP-EGFP or LVV-SW-EF1a-EGFP lentivirus injection in the preBötC on the minute ventilation (V_E), tidal volume (V_T), and breathing frequency (f) responses to hypoxia in carotid body denervated rats.
Ventilation was measured during normoxia (baseline) and following exposure to moderate hypoxia and then expressed relative to baseline levels. Representative plethysmographic recordings of ventilatory activity at rest and during increasing hypoxic conditions (10min control, 2 min 15%, 3 min 10%, 2.5 min 7.5% and 5 min recovery O₂) in a control (A, n=5) and a TMPAP (B, n=7) injected, carotid body denervated rat are presented. Graphs show changes in breathing frequency (C i), tidal volume (V_T, C ii) and minute ventilation (V_E, C iii) responses relative to baseline when exposed to hypoxia. Data are expressed as means ± SE. *Value significantly different from baseline ($P < 0.05$), two-way repeated measures ANOVA with bonferroni post test.

1.18 ± 0.07 and 1.04 ± 0.12 of control values respectively (Fig 4.2 B,C, n=7, two-way repeated measures ANOVA with Bonferroni post test). The presence of an hypoxic ventilatory response in carotid body denervated control rats but not denervated TMPAP rats strongly suggests that ATP is released in hypoxia and underlies an increase in ventilation.

4.3.2 The hypercapnic ventilatory response in control rats and those with TMPAP injections into the preBötC

The TMPAP virus was injected into the preBötC because this is where ATP is thought to have a role in regulating the hypoxic ventilatory response. ATP also appears to play a role in the hypercapnic ventilatory response in the RTN (Mulkey et al., 2004), which is considerably rostral to the preBötC and should not be affected by TMPAP activity. We therefore compared the hypercapnic ventilatory response in control and TMPAP injected rats before and after carotid body denervation as a control to assess whether the actions of TMPAP in the preBötC were specific to the hypoxic ventilatory response or whether TMPAP reduced the responsiveness of the preBötC to excitatory drives in general.

Carotid body intact rats.

After 10 min in normoxia/normocapnia, rats were exposed sequentially to 5 min of 3% CO₂, 5 min of 6% CO₂ and 5min recovery (normoxia/normcapnia). Representative plethysmographic recordings of ventilatory activity at rest and during increasing hypercapnic conditions (5 min 3% and 3min 6% O₂) in a control and a TMPAP injected, carotid body-intact rat are presented in Fig 4.3 A, B.

TMPAP had no significant effect on the hypercapnic ventilatory response of carotid body-intact rats. After 10 min of normoxia/normocapnia, rats were exposed to 5 min 3% CO₂ and 5 min 6% CO₂ followed by a 5 min recovery period. Control rats did not respond significantly to 3% but had a significant response to 6% CO₂ with 1.07 ± 0.10 and 1.68 ± 0.20

(significant, $p<0.01$) fold increases in V_E respectively. This increase was due to 0.98 ± 0.06 and 1.11 ± 0.05 (significant, $p<0.01$) fold increases in f as changes in V_T weren't significant (1.09 ± 0.11 and 1.47 ± 0.16 fold increases) for 3% and 6% CO_2 respectively (Fig 4.3 A,C. $n=8$, two-way repeated measures ANOVA with Bonferroni post test). The response of TMPAP-injected rats was similar to the control rats. TMPAP rats did not respond significantly to 3% but had a significant response to 6% CO_2 with 1.42 ± 0.19 and 2.04 ± 0.30 ($p<0.001$) fold increase in V_E relative to control respectively. This increase was due to 1.28 ± 0.14 and 1.52 ± 0.21 (significant, $p<0.01$) fold increases in V_T and 1.15 ± 0.04 and 1.32 ± 0.21 (significant, $p<0.001$) fold increases in f for 3% and 6% CO_2 respectively (Fig 4.3 B,C. $n=8$, two-way repeated measures ANOVA with bonferroni post test). Responses of the control and TMPAP-injected animals were not significantly different, indicating that, as expected, expression of the TMPAP virus in the preBötC had no effect on the hypercapnic ventilatory response.

Carotid body denervated rats

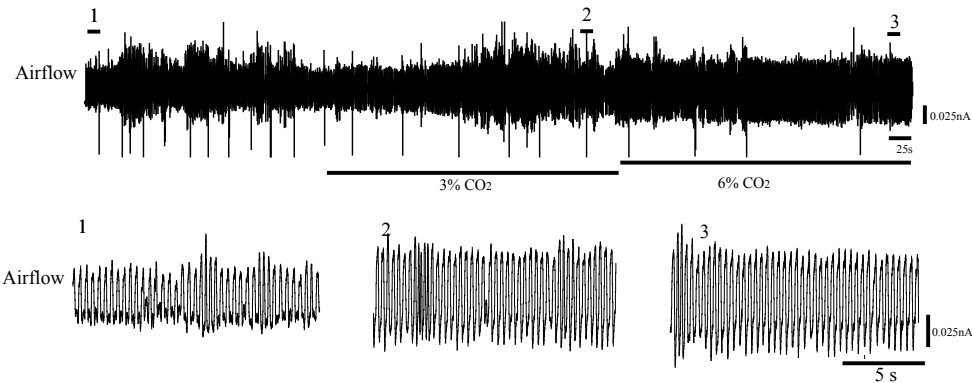
Representative plethysmographic recordings of ventilatory activity at rest and during increasing hypercapnic conditions (5 min 3% and 3min 6% O_2) in a control and a TMPAP injected, carotid body denervated rat are presented in Fig 4.4 A, B. TMPAP had no significant effect on the hypercapnic ventilatory response of carotid-body denervated rats. After 10 min of normoxia/normocapnia, rats were exposed to 5 min 3% CO_2 and 5 min 6% CO_2 followed by a 5 min recovery period. Control rats did not respond significantly to 3% but had a significant response to 6% CO_2 with 1.34 ± 0.19 and 1.85 ± 0.27 (significant, $p<0.05$) fold increases in V_E respectively. This increase was due to 1.16 ± 0.12 and 1.41 ± 0.10 (significant, $p<0.05$) fold increases in V_T and 1.13 ± 0.06 and 1.29 ± 0.10 (significant, $p<0.05$) fold increases in f for 3% and 6% CO_2 respectively (Fig 4.4 A,C. $n=5$, two-way repeated measures ANOVA with Bonferroni post test). The response of TMPAP-injected rats was similar to the control rats. TMPAP rats did not respond significantly to 3% but had a significant response to 6% CO_2 with 1.12 ± 0.11 and 2.21 ± 0.39 ($p<0.001$) fold increase in V_E .

relative to control respectively. This increase was due to 1.04 ± 0.07 and 1.45 ± 0.17 (significant, $p < 0.05$) fold increases in V_T and 1.06 ± 0.05 and 1.47 ± 0.19 (significant, $p < 0.05$) fold increases in f for 3% and 6% CO_2 respectively (Fig 4.4 A,C. $n=6$, two-way repeated measures ANOVA with Bonferroni post test). Again, the responses were similar in control and TMPAP-injected animals that had all undergone carotid body denervation. The specificity of the TMPAP effect on the hypoxic but not the hypercapnic ventilatory response suggests that the reduced hypoxic ventilatory response in TMPAP denervated animals reflects a direct action of ATP within the preBötC rather a general TMPAP mediated reduction in preBötC excitability.

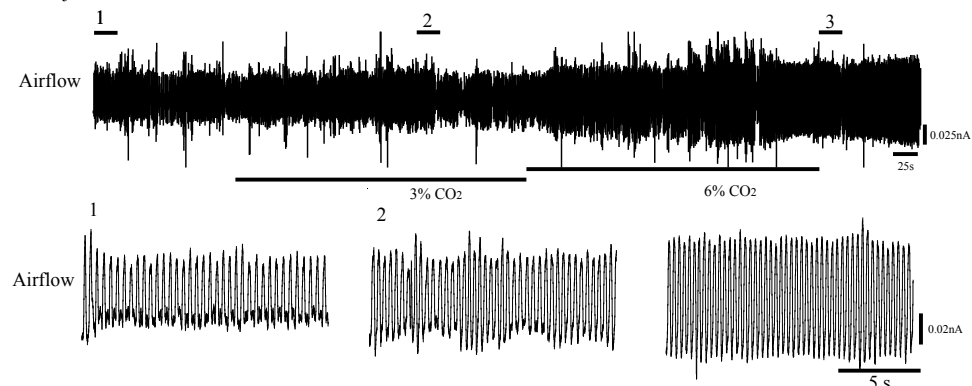
4.3.3 PreBötC of adult rat is directly sensitive to modulation by P2Y₁R

Our findings of reduced hypoxic ventilatory response in TMPAP-treated, denervated rats could be due to removal of an ATP-mediated excitatory effect or, through breakdown of ATP to adenosine, the addition of an ADO-mediated inhibition of preBötC networks. I hypothesize that it is the former based on *in vitro* data from neonatal rat that ATP in the preBötC potently increases frequency through a P2Y₁R mechanism (Lorier et al., 2007). I therefore tested the hypothesis that the excitatory effects of ATP via P2Y₁Rs persist into adulthood. I injected the P2Y₁R agonist MRS2365 (1mM, $n=8$) into the preBötC of adult, anesthetized, vagotomized rats while measuring respiratory airflow, DIA_{EMG} and GG_{EMG}. Consistent with the hypothesis, injection of MRS2365 (1mM, $n=8$) into the preBötC, triggered a 1.44 ± 0.09 fold increase in f ($p=0.0013$) and decrease in V_T to 0.60 ± 0.09 of control ($p=0.0054$) (Fig 4.5 A,C, paired t-test). Time course traces of a single injection (Fig 4.5 B) show an increase in f , a decrease in V_T , and stable V_E . The average time from drug onset to peak frequency increase and maximum V_T decrease was 36 ± 8.4 sec and 37.8 ± 15.1 sec, respectively. The simultaneous increase in f combined with the decrease in V_T , meant that there was no effect of MRS2365 injection on V_E . Injection of the P2Y₁R agonist

A Control rats



B TMPAP-injected rats



C

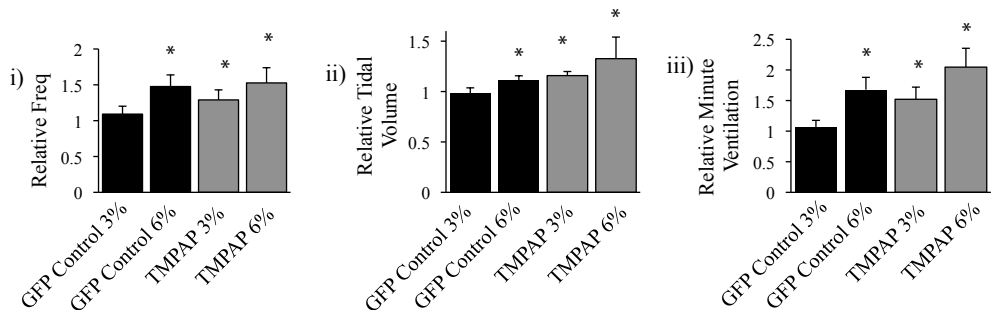


Figure 4.3 Effects of LVV-SW-EF1a-TMPAP-EGFP or LVV-SW-EF1a-EGFP lentivirus injection in the preBötC on the minute ventilation (V_E), tidal volume (V_T), and breathing frequency (f) responses to hypercapnia in carotid body intact rats.

Ventilation was measured during normoxia/normocapnia (baseline) and following exposure to moderate hypercapnia and then expressed relative to baseline levels. Representative plethysmographic recordings of ventilatory activity at rest and during increasing hypercapnic conditions (10min control, 5 min 3%, 5 min 6% CO_2) in a control (A, n=8) and a TMPAP (B, n=8) injected, carotid body-intact rat are presented. Graphs show changes in breathing frequency (C i), tidal volume (V_T , C ii) and minute ventilation (V_E , C iii) responses relative to baseline when exposed to hypercapnia. Data are expressed as means \pm SE. *Value significantly different from baseline ($p < 0.05$), two-way repeated measures ANOVA with Bonferroni post test.

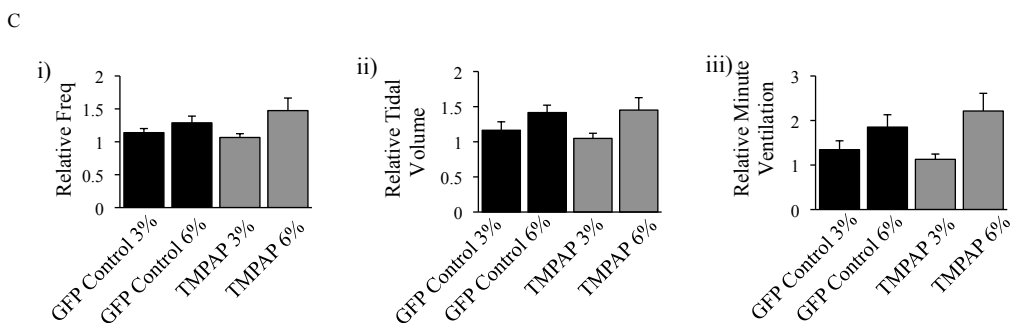
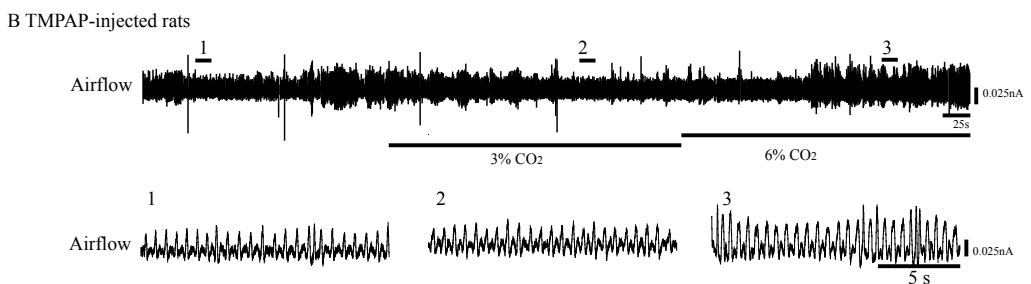
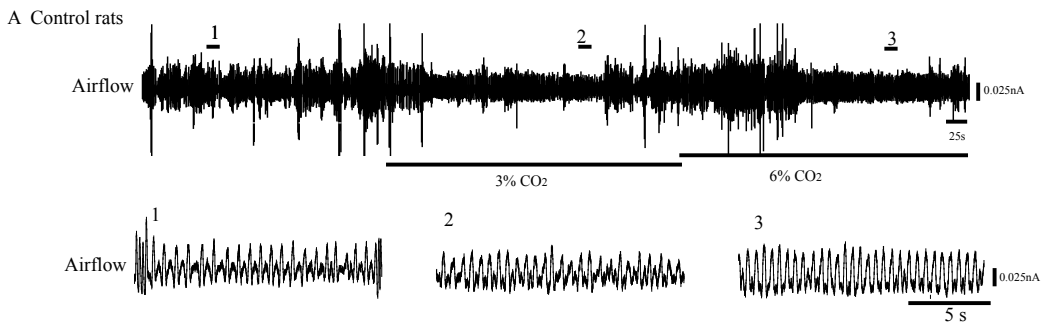


Figure 4.4 Effects of LVV-SW-EF1a-TMPAP-EGFP or LVV-SW-EF1a-EGFP lentivirus injection in the preBötC on the minute ventilation (V_E), tidal volume (V_T), and breathing frequency (f) responses to hypercapnia in carotid body denervated rats. Ventilation was measured during normoxia/normocapnia (baseline) and following exposure to moderate hypercapnia and then expressed relative to baseline levels. Representative plethysmographic recordings of ventilatory activity at rest and during increasing hypercapnic conditions (10min control, 5 min 3%, 5 min 6% CO₂) in a control (A, n=5) and a TMPAP (B, n=6) injected, carotid body denervated rat are presented. Graphs show changes in breathing frequency (C i), tidal volume (V_T, C ii) and minute ventilation (V_E, C iii) responses relative to baseline when exposed to hypercapnia. Data are expressed as means ± SE. *Value significantly different from baseline ($p < 0.05$), two-way repeated measures ANOVA with Bonferroni post test.

decreased both time of inspiration (T_i) to 0.87 ± 0.07 of control ($p=0.0313$) and time of expiration (T_e) to 0.63 ± 0.05 of control ($p<0.001$). MRS 2365 had no significant effect on duty cycle, T_i/T_{tot} which was 1.20 ± 0.10 relative to control ($n=8$, paired T test $p<0.05$). The peak amplitude of $\int DIA_{EMG}$ and $\int GG_{EMG}$ decreased to 0.60 ± 0.10 ($p=0.0049$) and 0.60 ± 0.05 ($p=0.0002$) of control, respectively. Burst area of $\int DIA_{EMG}$ and $\int GG_{EMG}$ decreased to 0.52 ± 0.09 ($p=0.0029$) and 0.32 ± 0.06 ($p<0.0001$) of control, respectively. Control saline injections into the same sites had no significant effects on f or V_T .

4.3.4 PreBötC of adult rat is not sensitive to modulation by ADO

The injection of MRS2365 into the preBötC indicates that ATP is likely to be excitatory in the adult rat preBötC through a P2Y₁R mechanism. This suggests that the reduced hypoxic ventilatory response in denervated, TMPAP-injected rats is due at least in part to the removal of ATP by TMPAP. However, it is still possible that the generation of ADO from TMPAP-hydrolyzed ATP contributes to the decreased V_T and V_E response of TMPAP-injected denervated rats. The preBötC of embryonic rat *in vitro* is sensitive to ADO-mediated inhibition (Herlenius et al., 2002; Huxtable et al., 2009) but this disappears in the early postnatal period (Herlenius et al., 1997; Herlenius and Lagercrantz, 1999; Herlenius et al., 2002; Zwicker et al., 2011). Consequently, I hypothesized that preBötC rhythm generating networks of adult rat are not sensitive to ADO-mediated inhibition. To test this, I stereotactically injected ADO (500 nl, 500 μ M) into the preBötC of adult anesthetized, vagotomized rats and recorded airflow, DIA_{EMG} and GG_{EMG} activity. Injection of ADO had no significant effect on ventilation, with a 1.09 ± 0.03 fold, 1.02 ± 0.01 fold and 1.09 ± 0.02 fold change in f , V_T and V_E , respectively (Fig 4.6 A, 4.7 D $n=7$, paired T test $P>0.05$). To

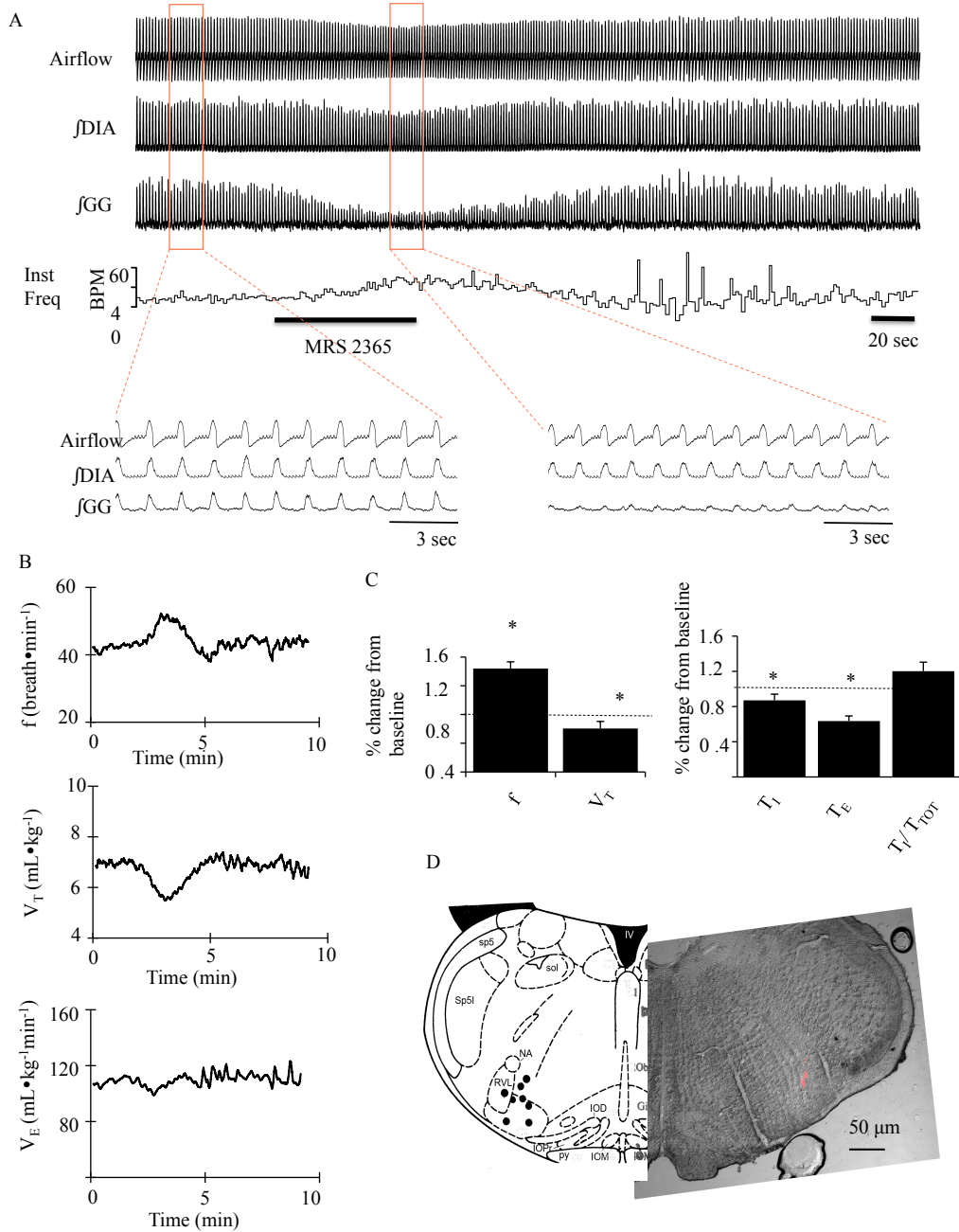


Figure 4.5 Activation of P2Y₁R in preBötC of adult rat *in vivo* with MRS 2365 (1 mM) evokes an increase in respiratory frequency (f) and a decrease in tidal volume (V_T)

(A) Airflow, diaphragm (DIA) and genioglossus (GG) EMG recordings show the response of an adult anesthetized vagotomized rat when stereotactically injecting MRS2365 into the preBötC. (B) Time course of f, V_T, and minute ventilation (V_E) for a single injection. (C) Group data illustrating the change in f, V_E, time of inspiration (T_i), time of expiration (T_e) and duty cycle (T_i / T_{tot}) relative to control (n=8)* values significantly different from predrug controls (paired T test p< 0.05). (D) Schematic showing 8 injection sites (left) and overlay of tissue section and injection site, marked with fluorescent microspheres (right). Inferior olive dorsal (IOD), inferior olive medial (IOM), inferior olive principal (IOP), 4th ventricle (IV), nucleus ambiguus (NA), pyramidal tract (PY), rostral ventrolateral medulla (RVL), spinal trigeminal tract (Sp5), spinal trigeminal interpolar (Sp5I), solitary tract (Sol).

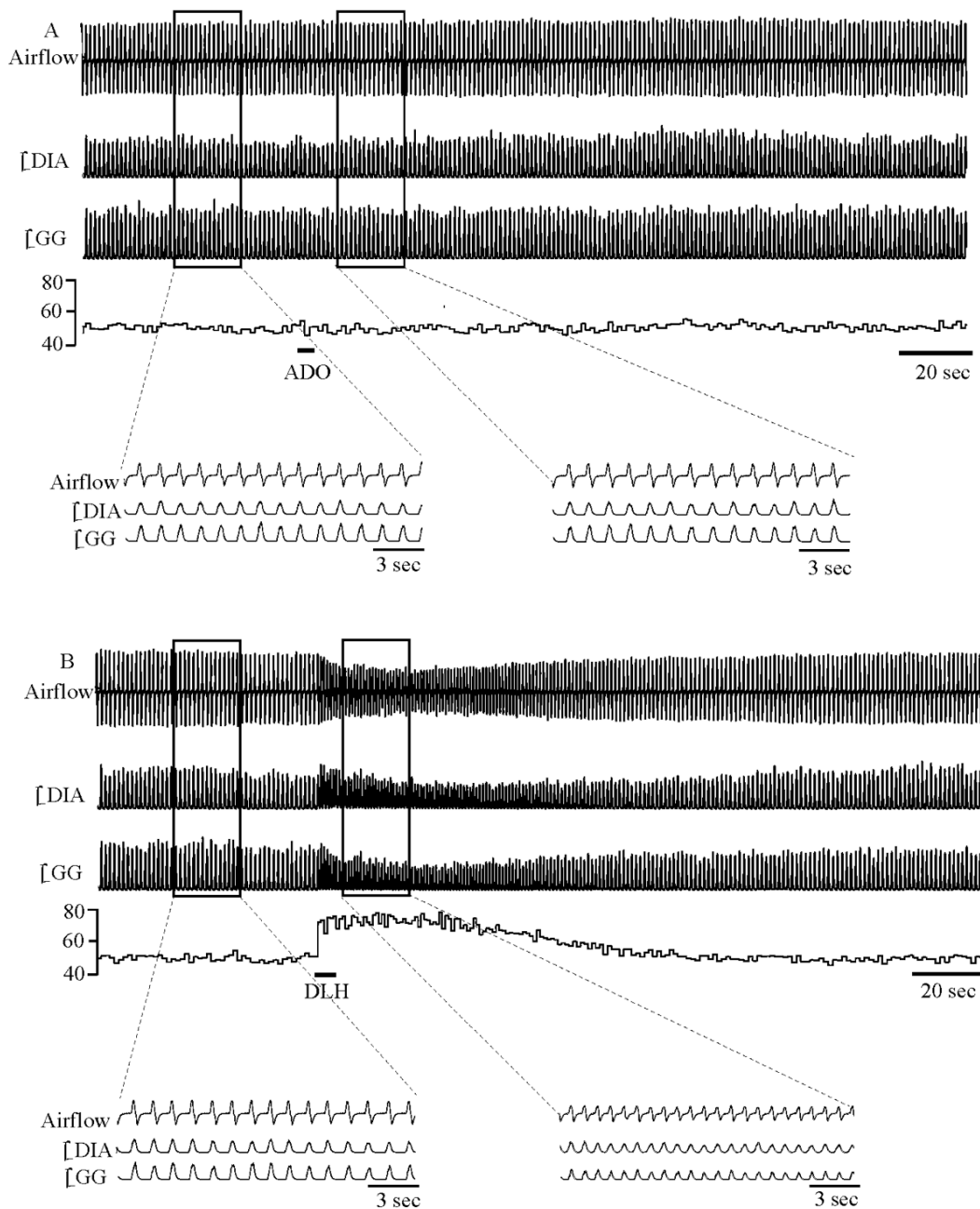


Figure 4.6 Activation of A1 R in preBötC of adult rat *in vivo* with ADO (500 μ M) evokes no effect on respiratory frequency (f) or tidal volume (V_T).

(A) Airflow, diaphragm (DIA) and genioglossus (GG) EMG recordings show the response of an adult anesthetized vagotomized rat when stereotactically injecting ADO into the preBötC.
 (B) Airflow, diaphragm (DIA) and genioglossus (GG) EMG recordings show the response of an adult anesthetized vagotomized rat when stereotactically injecting DLH (1mM) into the preBötC

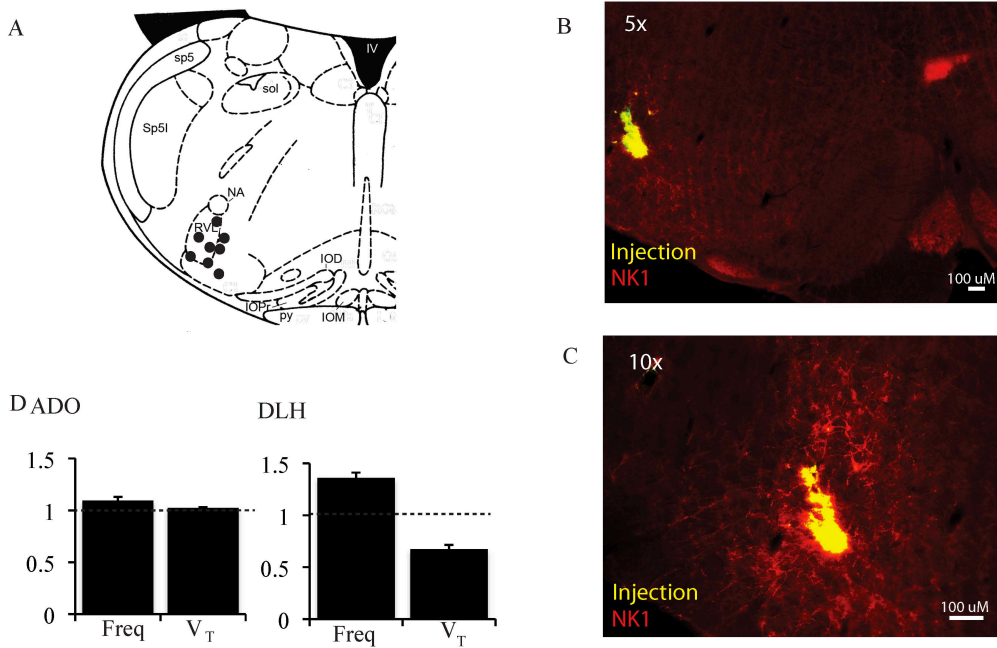


Figure 4.7 ADO (500 μ M) in the preBötC of adult rat *in vivo* has no effect on respiratory frequency (f) or tidal volume (V_T).

(A) Schematic showing 8 injection sites. Inferior olive dorsal (IOD), inferior olive medial (IOM), inferior olive principal (IOP), 4th ventricle (IV), nucleus ambiguus (NA), pyramidal tract (PY), rostral ventrolateral medulla (RVL), spinal trigeminal tract (Sp5), spinal trigeminal interpolar (Sp5I), solitary tract (Sol). B,C) Tissue section with injection site, marked with fluorescent microspheres (yellow). PreBötC neurons (NK1R⁺, red) are present in the region expressing LVV-SW-EF1a-TMPAP-EGFP lentivirus

(D) Group data illustrating the change in f and V_T relative to control (n=8)* values significantly different from predrug controls (paired T test P< 0.05). (D)

help establish that ADO injections were in the preBötC, we injected the excitatory amino acid dl-homocysteic acid (DLH) (1mM) into the preBötC 15 min after ADO injections. DLH injections into the preBötC caused a rapid respiratory response comprising a significant, 1.36 ± 0.05 fold ($p=0.004$) increase in f and a significant decrease in V_T to 0.67 ± 0.04 of control ($p=0.002$), suggesting that the injections were within the preBötC (Fig 4.6 B, 4.7 D, $n=5$, paired T test $p<0.05$).

4.3.5 ATP and ADO microinjection: histology

Microinjections of ATP and ADO into the preBötC included fluorescent beads for subsequent histological identification of all injection sites via analysis of $50 \mu\text{m}$ serial transverse sections through the medulla between the facial nucleus and obex. Injection sites were mapped onto schematics of serial cross sections based on their location relative to local landmarks (Paxinos and Watson, 2007). Injection sites were localized to a region extending only $150 \mu\text{m}$ in the rostrocaudal plane, the center of which was $\sim 800 \mu\text{m}$ caudal to the caudal end of the facial motor nucleus for both ATP and ADO injections (Fig. 4.5 D and 4.7 A,B,C, $n=8$ and 7 respectively). Sites were all ventral to the nucleus ambiguus, and overlapped with the location of the highest concentration of NK1R positive neurons (Fig 4.7 B,C), all of which suggest that the injection sites fell within the preBötC (Gray et al., 1999; Stornetta et al., 2003).

4.3.6 Viral injection: histology

In the interest of exploring our hypothesis that ATP signaling with the preBötC plays a critical role in the hypoxic ventilatory response, we focused our viral injections to transfect preBötC. We used a lentivirus coding for TMPAP that was fused with EGFP and driven by elongation factor 1-alpha (EF1 α) promoter LVV-SW-EF1a-TMPAP-EGFP (Zylka et al., 2008). After the TMPAP experiments, brains were isolated and processed for EGFP

expression pattern (indicative of TMPAP expression) and also NK1R immunoreactivity, which serves as a marker for the preBötC. 50 µm sections were examined under epiufluorescence and the distance of the rostral and caudal border of the fluorescence from the caudal border of facial nucleus was determined. The location of the ‘hotspot’ (peak) of fluorescence was also determined for each brainstem. The distribution of fluorescence was mapped out on reference sections based on the rat stereotaxic atlas (Paxinos and Watson, 2007).

NK1R immunolabeling extends beyond the preBötC so it was essential to examine serial sections for the region of most intense NK1R labeling. Based on histological examination of sections from injected rats, cells expressing EGFP (EGFP^+) were ventral and caudal to the semicompact division of nucleus ambiguus (Fig 4.8 B-E). The core of virus injection site (defined by the 50 µm section with the highest density of EGFP^+ cells) was 700–1,100 µm caudal to the caudal end of the facial motor nucleus (Fig 4.8 B-E). Outside this the core EFP^+ cell density rapidly decreased (Fig. 4.8 F-H) ($n = 16$). This viral injection hotspot overlapped with the location of the highest concentration of NK1R positive neurons (Fig 4.8 A-C) (Gray et al., 1999), suggesting that the injection site was targeted in the preBötC. More medially were only a few, if any, EGFP^+ cells. Expression spread along the ventral surface 400 µm both rostral and caudal to the preBötC injected hotspot. Aside from the injection site and this surrounding area, we did not observe EGFP^+ neurons anywhere in the brainstem. EGFP^+ -filled fibers extended along the ventral respiratory column into the Bötzinger complex (BötC) and preBötC. EGFP^+ -filled fibers projected only a few 100 µm dorsally and medially toward the hypoglossal nuclei. The presumptive origin of these fibers was EGFP^+ neurons at the injection site (Fig 4.8 B-E).

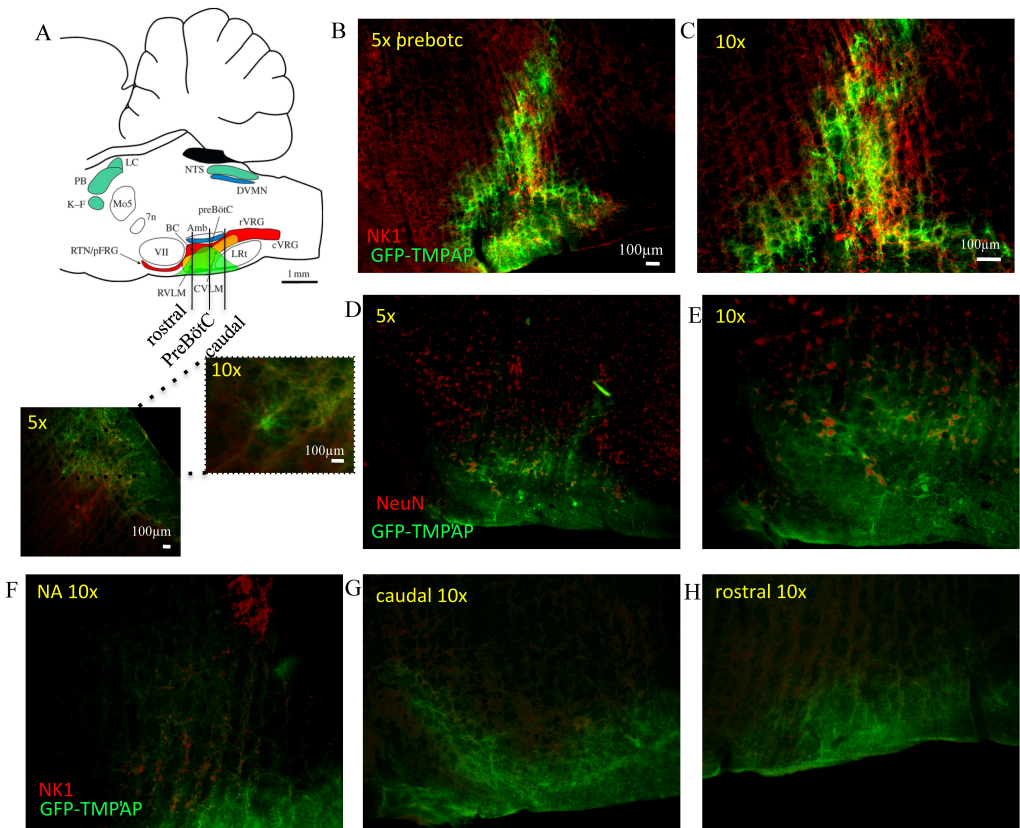


Figure 4.8 GFP expression 2 weeks after LVV-SW-EF1a-TMPAP-EGFP lentivirus injected in rat preBötC.

B–H, GFP (green, **B–H**), NK1R (red, **B,C,F,G,H**) and NeuN (red, **D, E**) expression in the ventrolateral medulla of LVV-SW-EF1a-TMPAP-EGFP lentivirus injected rats. **A**, Neuroanatomy of the brainstem cardiorespiratory control network. The diagram shows a sagittal view of the rat brainstem, indicating locations of the main groups of CNS neurons controlling respiratory, sympathetic and parasympathetic activities in mammals. VII, facial nucleus; Amb, nucleus ambiguus; BC, Bötzinger complex; cVRG, caudal ventral respiratory group; CVLM, caudal ventrolateral medulla; DVMN, dorsal vagal motonucleus; K–F, Kölliker–Fuse nucleus; LC, locus ceruleus; LRt, lateral reticular nucleus; Mo5, motor trigeminal nucleus; NTS, nucleus of the solitary tract; PB, parabrachial nucleus; preBötC, preBötzinger complex; RTN/pFRG, retrotrapezoid nucleus/parafacial respiratory group; rVRG, rostral ventral respiratory group; RVLM, rostral ventrolateral medulla (adapted from Spyra and Gourine, *Phil. Trans. R. Soc. B* 12 September 2009 vol. 364 no. 1529 2603–2610*I*). **B,C**, PreBötC neurons (NK1R^+) are present in the region expressing LVV-SW-EF1a-TMPAP-EGFP lentivirus. **F,G,H**, There is a marked reduction in GFP^+ neurons within the network of the ventrolateral medulla both caudal and rostral to the preBötC. **A–B**, GFP expression in cell bodies and fibers surrounding preBötC (green). **D–F**, EYFP expression in fibers in preBötC, BötC, hypoglossal nucleus (XII), and NTS (NA, nucleus ambiguus). **G–I**, Rstrocaudal distribution of $\text{EYFP}^+/\text{NeuN}^+$, $\text{EYFP}^+/\text{Phox2b}^+$, and $\text{EYFP}^+/\text{MN}^+$ double-labeled somata in relationship to caudal pole of the VIIIn ($n = 4$).

4.4 Discussion

My data provide compelling support of the existing hypothesis that ATP within the preBötC is an important mediator of the hypoxic ventilatory response (Gourine et al., 2005a). Data demonstrate that virally induced expression of the ectonucleotidase, TMPAP, in the preBötC of carotid body denervated adult rats *in vivo*, and the presumptive increase in ATP degradation, removes a steady-state, hypoxia-induced increase in ventilation. These data are completely consistent with the existing hypothesis that ATP release in the medulla attenuates the magnitude of the secondary hypoxic ventilatory depression (Gourine et al., 2005a). My data not only support this hypothesis, they also suggest that the excitatory actions of ATP *in vivo* are mediated at least in part within the preBötC via a P2Y₁R mechanism. This is the first study to use viral genetic approaches to manipulate ectonucleotidase activity in the CNS *in vivo* to demonstrate the physiological role of endogenous ATP in modulating neural network activity.

4.4.1 The role of ATP in the hypoxic ventilatory response

The hypothesis that ATP release in the medulla attenuates the magnitude of the secondary hypoxic ventilatory depression originated from a study that used ATP biosensors to demonstrate that during hypoxia ATP release is detected at the ventral surface of the medulla, and that its source corresponds to the ventral respiratory column (VRC), including the preBötC (Gourine et al., 2005a). The ATP release is delayed relative to the onset of the hypoxia-induced increase in ventilation, and it rises gradually as the hypoxic depression of breathing develops. This, combined with the observation that injection of that P2R antagonist PPADS into the ventrolateral medulla caused a greater hypoxic respiratory depression than control, underlies the above hypothesis (Gourine et al., 2005a).

The two major limitations of the study by Gourine *et al.* 2005 derive from concerns over the selectivity of ATP biosensors for ATP and of PPADS for P2Rs. The enzyme-based

ATP biosensor system used to monitor ATP concentration at the ventral medullary surface or on the surface of horizontal medullary sections consists of a platinum/iridium (Pt/Ir) microelectrode coated with a polymer containing two enzymes, glycerol kinase and glycerol-3-phosphate oxidase, that produce H₂O₂ in proportion to ATP concentration (Llaudet et al., 2003; Llaudet et al., 2005). The Pt/Ir microelectrode is polarized allowing amperometric detection of H₂O₂. A challenge is that these biosensors will generate current not only in response to ATP, but multiple electroactive species in the milieu. To control for this, a dual sensor-recording configuration is used where a null sensor lacking the enzymes is placed in the equivalent position as the ATP sensor on the other side of the medulla to monitor for nonspecific electro activity. The ATP-current is then taken as the difference between that recorded at the ATP and null sensors. ATP concentration is then established based on a calibration curve established at the beginning and end of the experiment and is referred to as the “difference current”. There are several assumptions with this measurement that require discussion. For the difference current to properly indicate ATP concentration, both the ATP and null sensors need to have identical sensitivity to non-ATP, electro active species throughout the experiment. In practice this is difficult to test. In addition, tissue on both sides of the brainstem underlying the null or ATP sensor would need to release the same electro active species at the same rate and distribution (such as monoamines etc.), which also may not be true. Finally, despite extensive efforts by the manufacturers of these sensors (Sarissa Probes, Coventry, UK) to demonstrate their ATP selectivity under non-biological conditions, purists are suspicious of sensor selectivity in living biological tissue because a direct test, i.e., the removal of ATP, cannot be done *in vitro* or *in vivo*.

The second limitation of the Gourine et al. (2005) study is that the P2 receptor antagonist PPADS (100 μM) was microinjected into the rostral part of the ventrolateral medulla to show that P2 receptor blockade augments the secondary hypoxic respiratory depression in rats. PPADS antagonizes P2X_{1,2,3,4,5,7} and P2Y_{1,4,6} receptors, however at higher concentrations (>10 μM) it also antagonizes glutamatergic transmission, inhibits

ectonucleotidase activity, inhibits IP₃-induced Ca²⁺ release, and has a variety of other non-specific effects (Motin and Bennett, 1995; Nakazawa et al., 1995; Lambrecht, 2000). Glutamate is essential for generation of respiratory rhythm and transmission of respiratory inputs to motoneurons (Funk et al., 1993). Therefore any reduction in respiratory activity associated with high concentrations of PPADs may not be indicative of endogenous activation of ATP receptors (Thomas et al., 1999). The concentration of 100 μM used by Gourine *et al.* (2005) for local injection should produce PPADS concentrations in the range of 10 μM in the tissue (due to rapid diffusion away from the pipette tip) and should minimally affect glutamatergic transmission. However, nonspecific actions cannot be excluded. Therefore, the data generated here through lentivirus-driven expression of TMPAP in the preBötC significantly strengthen the hypothesis that ATP signaling in the brainstem contributes to the hypoxic ventilatory response.

4.4.2 Validation of TMPAP as a model to study purinergic signaling

Given the limitations associated with sensors and P2R antagonists, I took an alternate viral genetics approach to examine the role of ATP and ATP receptors in the hypoxic ventilatory response. I used a lentiviral vector encoding TMPAP fused to EGFP for visualization. As the purpose of this experiment was to increase ectonucleotidase activity throughout the region of interest, the objective was to increase enzyme expression in as many cells as possible. The virus was therefore constructed so that TMPAP and EGFP expression was under the control of the EF1a promoter, which would drive expression in neurons and glia. Several control experiments carried out by our collaborator, Dr. Sergey Kasparov, have established the effectiveness of this viral vector. These controls have not yet been published, as the TMPAP-lentivirus is very new. Thus, they are described here. First, expression of LVV-SW-EF1a-TMPAP-EGFP is targeted to the plasma membrane in primary rat astrocyte cultures where it has access to extracellular ATP (Kasparov *et al.* unpublished findings).

Second, the ability of the virus to degrade extracellular ATP was tested in astrocyte cultures in which the propagation of mechanically evoked Ca^{2+} waves through the culture is dependent on signaling via extracellular ATP. Astrocyte cultures from cerebral cortex, cerebellum and brainstem of 2-days-old (P2) Wistar rats, were transduced with either LVV-SW-EF1a-TMPAP-EGFP or LVV-EF1a-EGFP and loaded with Rhod-2-AM to monitor intracellular Ca^{2+} [Ca^{2+}]_i. Astrocytes were mechanically stimulated with a patch pipette and changes in [Ca^{2+}]_i in the surrounding cells were assessed. A line was drawn from the mechanically stimulated cell to each cell that responded and an average distance of Ca^{2+} wave spread was calculated. Spread of the Ca^{2+} wave in TMPAP-EGFP expressing astrocyte cultures was reduced by 85% compared to EGFP expressing astrocytes. The addition of the P2Y₁ receptor antagonist MRS2179 (10 μM) also suppressed mechanically evoked Ca^{2+} waves, indicating that the waves are at least partially mediated by ATP acting through a P2Y₁R mechanism. These experiments show that transfection of astrocytes with the TMPAP-containing lentiviral vector greatly limits, but does not abolish, the diffusion of extracellular ATP between cultured astrocytes.

Although the TMPAP virus appears an effective tool for degrading extracellular ATP, additional caveats must be addressed. Injection of the TMPAP viral vector into the preBötC and viral infection of preBötC cells could alter baseline function of this important network, in which case altered hypoxia responsiveness might not reflect altered ATP signaling. This potential confounder was addressed in two ways. First, the control group in all cases comprised animals that were injected with an equivalent titre of viral vector containing only the cassette for EGFP, the reporter gene, and not TMPAP. This controlled for any effects that might be associated with lentiviral transfection of preBötC cells. Second, TMPAP inserts in the plasma membrane. Thus, it is possible that it will alter expression of other membrane proteins and the responsiveness of preBötC neurons to all inputs, not just those involving ATP signaling in the preBötC. Therefore, as a control to test whether TMPAP expression altered the sensitivity/responsiveness of the preBötC to all inputs, we compared CO_2

sensitivity of control and TMPAP-injected rats. Central CO₂ sensitivity is mediated by the actions of increased CO₂ or decreased pH on acid-sensitive neurons at several sites in the central nervous system including the caudal NTS and adjoining dorsal motor nucleus of the vagus, fastigial nucleus of the cerebellum, retrotrapezoid nucleus (RTN), rostroventrolateral medulla, medullary raphe and locus coeruleus (Nattie and Li, 2009). The output from these sites is hypothesized either to converge separately onto the central respiratory controller (the preBötC) (Nattie and Li, 2009; Dean and Putnam, 2010; Gargaglioni et al., 2010) or converge upstream of the preBötC in the RTN which sends an integrated, excitatory “CO₂” signal to the preBötC to drive breathing in proportion to the CO₂/pH stimulus (Guyenet et al., 2010). Regardless of which model is correct, the CO₂ response does not appear to involve the release of ATP in the preBötC or VRC (Gourine et al., 2005b; Gourine et al., 2010). The CO₂ response therefore provides a convenient stimulus to test whether TMPAP in the preBötC affects excitability in general, in which case the hypercapnic and hypoxic responses would be affected, or the hypoxic ventilatory response specifically.

An important point, however, is that ATP is involved in central chemoreception in the RTN. It is released from glia in response to reduced pH (increased CO₂) which increases the excitability of Phox2B-positive chemosensitive neurons, resulting in increased RTN output in response to CO₂ and a greater hypercapnic ventilatory response (Gourine et al., 2010). The validity of using the CO₂ sensitivity to determine whether TMPAP expression nonspecifically alters preBötC excitability therefore required that TMPAP expression not extend to the RTN. This was established via postmortem histological analysis of EGFP expression along the brainstem (Fig 4.8). Hypercapnic ventilatory responses in control and TMPAP animals were indistinguishable both before and after carotid body denervation. This series of control experiments suggests that the baseline physiology of preBötC cells was not dramatically affected by expression of the TMPAP virus. Thus, the presence of a hypoxia-evoked increase in ventilation in control-denervated rats but not TMPAP-injected, denervated rats supports the hypothesis that ATP-signaling in the preBötC contributes to the

hypoxic ventilatory response.

4.4.3 Effects of TMPAP on the hypoxic ventilatory response reflect loss of ATP excitation

The absence of a ventilatory response to hypoxia in carotid body denervated, TMPAP-injected rats along with its presence in denervated, control rats could reflect either the removal of an excitatory ATP mechanism or the addition of an inhibitory ADO mechanism subsequent to increased ATP degradation by TMPAP. *In vivo* microinjection data, however, clearly distinguished between these two possibilities. Local injection of MRS 2365 directly into the preBötC increased frequency, indicating that the preBötC in adult rats, like the preBötC of neonatal rats *in vitro* (Lorier et al., 2007; Huxtable et al., 2009), is excited by ATP through a P2Y₁R mechanism. In contrast, injection of ADO directly into the preBötC in anesthetized adult rats *in vivo* had no significant effect on ventilation, suggesting that the effects of TMPAP are due primarily to loss of an excitatory P2R-mediated mechanism.

There is little literature on the effects of ATP or ADO directly in the preBötC *in vivo*. ATP excites single medullary respiratory neurons *in vivo* and is excitatory when applied to the ventral medullary surface (Thomas and Spyer, 2000; Gourine et al., 2003; Gourine and Spyer, 2003). ATP evokes a 2–4 fold increase in inspiratory-related burst frequency in the preBötC of neonatal rats *in vitro* (Lorier et al., 2007; Huxtable et al., 2009; Huxtable et al., 2010; Zwicker et al., 2011). A P2Y₁R-mediated excitatory mechanism has been mapped specifically to the preBötC in neonatal rats *in vitro* (Lorier et al., 2007) and mice (Zwicker et al., 2011) and now in adult rats *in vivo*. Surprisingly, ATP has no effect on rhythm when injected into the preBötC networks of neonatal mouse *in vitro* (Zwicker et al., 2011). However, this actually reflects rapid degradation of ATP to adenosine and activation of a A1 inhibitory mechanism that is specific to mouse. The mouse preBötC is actually very sensitive to P2Y₁R activation; however, when ATP is applied this excitatory effect is obscured by the

ADO-mediated inhibition (Zwicker et al., 2011). The only other study to examine the effects on breathing of applying ATP in the ventral respiratory column reports that ATP causes apnea (Thomas et al., 2001), which is not consistent with all other studies demonstrating the excitatory effects of ATP on preBötC network (Lorier et al., 2007; Huxtable et al., 2009; Huxtable et al., 2010; Zwicker et al., 2011) and neuron (Lorier et al., 2007; Lorier et al., 2008) activity *in vitro* and *in vivo* (Thomas and Spyer, 2000; Gourine et al., 2003; Gourine and Spyer, 2003). This discrepancy may reflect that high concentrations of ATP (10 mM) were used (Thomas et al., 2001), which could overexcite neurons and cause depolarization block and apnea. 10 mM ATP in the preBötC *in vitro* causes apnea through this mechanism (Funk, unpublished observations). In addition, the sites of these ATP injections were not identified (Thomas et al., 2001). Injections were made at the site where a respiratory-related neuron was recorded but this could have been at sites along the ventral respiratory column where excitation inhibits rhythm, such as the Bötzinger Complex (Sun et al., 1992; Moraes et al., 2011). These data suggest that the production of apnea by ATP in the ventral respiratory column (Thomas et al., 2001) was mediated via actions outside the preBötC.

The effects on rhythm of ADO directly within the preBötC are also poorly investigated. However, the lack of an ADO effect following *in vivo* injection into the adult anesthetized rat preBötC is not surprising based on available *in vitro* data. In neonatal rat, bath administration of ADO or A1R agonists to the brainstem-spinal cord or rhythmic slice preparation evokes a theophylline-sensitive depression of ventilation *in vitro* in some (Herlenius and Lagercrantz, 1999; Herlenius et al., 2002; Wang et al., 2005) but not all cases (Brockhaus and Ballanyi, 2000; Ruangkittisakul and Ballanyi, 2010; Zwicker et al., 2011). These differences may be due to developmental and species differences. Species differences are suggested by the observations in mice that A1R activation inhibits frequency in P1–14 slices (Mironov et al., 1999; Vandam et al., 2008; Zwicker et al., 2011) and P7 preBötC island preparations (Vandam et al., 2008), but not in slices of P1–3 rats (Zwicker et al., 2011) or brainstem–spinal cord preparations from rats older than P3 (Herlenius et al., 1997).

Developmental changes in the ADO sensitivity of preBötC networks in rat is further supported by the finding that the excitatory actions of ATP are potentiated by ADO receptor antagonists in embryonic but not postnatal rat slices (Huxtable et al., 2009).

4.4.4 Significance of carotid-body denervation

The ventilatory response to hypoxia is biphasic, comprising an initial increase followed by a secondary depression during which ventilation falls to levels that remain greater than baseline in adult mammals including rats (Moss, 2000). In neonates, adenosine, serotonin, prostaglandin, GABA, opioids, catecholamines acting at α_2 -receptors, and other neuromodulators may all be involved in the depressing phase (Long and Lawson, 1984; Huang et al., 1994; Sugihara et al., 1994; Elnazir et al., 1996; Koos et al., 2005). The initial increase in ventilation is primarily attributed to the carotid body, however there is evidence for a central contribution as well. In rat there is an attenuated but residual ventilatory response to acute hypoxia following carotid body denervation (Cardenas and Zapata, 1983; Martin-Body et al., 1985), which may reflect some direct central actions of hypoxia. The secondary hypoxic ventilatory depression is thought to be mediated centrally and is associated with a decrease in V_E (Eden and Hanson, 1987). The fall in V_E is suggested to be attributed primarily to a decline in respiratory frequency in preterm human infants exposed to 15% oxygen (Rehan et al., 1996). However the degree of hypoxia may be important, as in neonatal rats exposed to 15% oxygen, the depressive phase is characterized by a decline in frequency, whereas at lower fractional oxygen concentration, V_T plays a larger role (Eden and Hanson, 1987). Our findings suggest a significant reduction in V_T is what accounts for the decrease in V_E in TMPAP animals secondary hypoxic ventilatory depression and this may be due to the lower fractional oxygen concentrations used within this study.

The purpose of the TMPAP experiments was to define specifically the effects of decreasing central ATP levels during hypoxia. Therefore, to increase the sensitivity of our

assay we eliminated the carotid bodies. Carotid body denervation is a means of removing peripheral chemoreceptor input so that the role of the central chemoreceptors can be studied. In our study the effects of TMPAP were only seen in carotid sinus denervated rats. Denervation was confirmed through visual inspection after removal of a section of nerve, and lack of an initial rapid increase in ventilation upon exposure to hypoxia. We can't exclude the possibility that denervation was not incomplete in some cases. However, we do not think this is a significant factor in the response of denervated TMPAP-injected and control rats to hypoxia, because this would require that the denervations were incomplete in only the TMPAP group but complete in the control group.

One interpretation of finding that TMPAP expression did not alter the hypoxic ventilatory response in intact animals is that peripheral chemoreceptor input plays a dominant role in determining the hypoxic ventilatory response, and the central effects of ATP are negligible in intact rats. However my data, combined with the observation that the P2R antagonist PPADS causes a greater hypoxic respiratory depression in intact animals suggest otherwise (Gourine et al., 2005a). In this study, TMPAP was expressed in the preBötC to increase ATP breakdown. The limitation is that the extent to which endogenous ATP levels are reduced by this manipulation is not known. It is unlikely that the increase in ATP evoked in the preBötC by hypoxia is completely arrested. First, ATP degradation is not instantaneous so there will be some time for endogenously released ATP to act. Second, TMPAP expression in the preBötC does not appear to be uniform based on EGFP distribution (Fig 4.8). Thus, ATP levels may still rise in some regions of the preBötC sufficiently that in carotid body intact, TMPAP rats, ATP may still cause an increase in ventilation, partially masking the greater secondary depression that is expected if ATP was removed completely. Application of PPADS to the ventral surface of the medulla clearly reveals a PPADS-sensitive, putative ATP mediated attenuation of the hypoxic respiratory depression (Gourine et al., 2005a). This may reflect that when applied in this manner, PPADS has greater access to the respiratory column, allowing a more complete block of the actions of ATP. In

denervated animals, in contrast, removal of the excitatory, carotid body mediated component of the hypoxic response, means that only the undefined depressive effect of hypoxia and the putative ATP-mediated excitatory mechanism are in operation. The presence of a ventilatory increase in control, denervated rats but not TMPAP, denervated rats suggests that ATP can overcome this secondary depressive effect. Lack of any ventilatory response in TMPAP, denervated animals suggests that any residual ATP-mediated excitation (evoked by unhydrolyzed ATP) is not sufficient to overcome the secondary hypoxic depressive mechanism and ventilation does not change.

In summary, use of a novel TMPAP viral vector to increase ectonucleotidase expression, and presumably ATP degradation, in the preBötC of adult rat *in vivo*, has provided indirect but strong evidence that ATP is released in the preBötC during hypoxia where it acts in part via P2Y₁R to offset the secondary hypoxic depression of breathing. These data confirm a physiological role for ATP-mediated purinergic signaling in the medullary mechanisms controlling respiratory activity, and suggest that during sustained hypoxia respiratory drive may partially depend on central ATP and its rate of breakdown by ectonucleotidases.

4.5 References

- Ballanyi K (2004) Neuromodulation of the perinatal respiratory network. Current Neuropharmacology 2:221-243.
- Bisgard GE, Forster HV, Klein JP (1980) Recovery of peripheral chemoreceptor function after denervation in ponies. J Appl Physiol 49:964-970.
- Bissonnette JM (2000) Mechanisms regulating hypoxic respiratory depression during fetal and postnatal life. Am J Physiol Regul Integr Comp Physiol 278:R1391-1400.

- Bissonnette JM, Hohimer AR, Chao CR, Knopp SJ, Notoroberto NF (1990) Theophylline stimulates fetal breathing movements during hypoxia. *Pediatr Res* 28:83-86.
- Brockhaus J, Ballanyi K (2000) Anticonvulsant A(1) receptor-mediated adenosine action on neuronal networks in the brainstem-spinal cord of newborn rats. *Neuroscience* 96:359-371.
- Cardenas H, Zapata P (1983) Ventilatory reflexes originated from carotid and extracarotid chemoreceptors in rats. *Am J Physiol* 244:R119-125.
- Coleman JE, Huentelman MJ, Kasparov S, Metcalfe BL, Paton JF, Katovich MJ, Semple-Rowland SL, Raizada MK (2003) Efficient large-scale production and concentration of HIV-1-based lentiviral vectors for use in vivo. *Physiol Genomics* 12:221-228.
- Davenport HW, Brewer G, et al. (1947) The respiratory responses to anoxemia of unanesthetized dogs with chronically denervated aortic and carotid chemoreceptors and their causes. *Am J Physiol* 148:406-416.
- Dean JB, Putnam RW (2010) The caudal solitary complex is a site of central CO₂ chemoreception and integration of multiple systems that regulate expired CO₂. *Respir Physiol Neurobiol* 173:274-287.
- Eden GJ, Hanson MA (1987) Maturation of the respiratory response to acute hypoxia in the newborn rat. *J Physiol* 392:1-9.
- Elnazir B, Marshall JM, Kumar P (1996) Postnatal development of the pattern of respiratory and cardiovascular response to systemic hypoxia in the piglet: the roles of adenosine. *J Physiol* 492 (Pt 2):573-585.

- Funk GD, Smith JC, Feldman JL (1993) Generation and transmission of respiratory oscillations in medullary slices: role of excitatory amino acids. *J Neurophysiol* 70:1497-1515.
- Gargaglioni LH, Hartzler LK, Putnam RW (2010) The locus coeruleus and central chemosensitivity. *Respir Physiol Neurobiol* 173:264-273.
- Gourine AV (2005) On the peripheral and central chemoreception and control of breathing: an emerging role of ATP. *J Physiol* 568:715-724.
- Gourine AV, Spyker KM (2003) Chemosensitivity of medullary respiratory neurones. A role for ionotropic P2X and GABA(A) receptors. *Adv Exp Med Biol* 536:375-387.
- Gourine AV, Atkinson L, Deuchars J, Spyker KM (2003) Purinergic signalling in the medullary mechanisms of respiratory control in the rat: respiratory neurones express the P2X2 receptor subunit. *J Physiol* 552:197-211.
- Gourine AV, Llaudet E, Dale N, Spyker KM (2005a) Release of ATP in the ventral medulla during hypoxia in rats: role in hypoxic ventilatory response. *J Neurosci* 25:1211-1218.
- Gourine AV, Llaudet E, Dale N, Spyker KM (2005b) ATP is a mediator of chemosensory transduction in the central nervous system. *Nature* 436:108-111.
- Gourine AV, Kasymov V, Marina N, Tang F, Figueiredo MF, Lane S, Teschemacher AG, Spyker KM, Deisseroth K, Kasparov S (2010) Astrocytes control breathing through pH-dependent release of ATP. *Science* 329:571-575.
- Gray PA, Rekling JC, Bocchiaro CM, Feldman JL (1999) Modulation of respiratory frequency by peptidergic input to rhythmogenic neurons in the preBotzinger complex. *Science* 286:1566-1568.

Guyenet PG, Stornetta RL, Bayliss DA (2010) Central respiratory chemoreception. *J Comp Neurol* 518:3883-3906.

Herlenius E, Lagercrantz H (1999) Adenosinergic modulation of respiratory neurones in the neonatal rat brainstem in vitro. *J Physiol* 518 (Pt 1):159-172.

Herlenius E, Lagercrantz H, Yamamoto Y (1997) Adenosine modulates inspiratory neurons and the respiratory pattern in the brainstem of neonatal rats. *Pediatr Res* 42:46-53.

Herlenius E, Aden U, Tang LQ, Lagercrantz H (2002) Perinatal respiratory control and its modulation by adenosine and caffeine in the rat. *Pediatr Res* 51:4-12.

Huang J, Sugihara C, Hehre D, Lin J, Bancalari E (1994) Effects of GABA receptor blockage on the respiratory response to hypoxia in sedated newborn piglets. *J Appl Physiol* 77:1006-1010.

Huxtable AG, Zwicker JD, Poon BY, Pagliardini S, Vrouwe SQ, Greer JJ, Funk GD (2009) Tripartite purinergic modulation of central respiratory networks during perinatal development: the influence of ATP, ectonucleotidases, and ATP metabolites. *J Neurosci* 29:14713-14725.

Huxtable AG, Zwicker JD, Alvares TS, Ruangkittisakul A, Fang X, Hahn LB, Posse de Chaves E, Baker GB, Ballanyi K, Funk GD (2010) Glia contribute to the purinergic modulation of inspiratory rhythm-generating networks. *J Neurosci* 30:3947-3958.

Koos BJ, Matsuda K (1990) Fetal breathing, sleep state, and cardiovascular responses to adenosine in sheep. *J Appl Physiol* 68:489-495.

Koos BJ, Kawasaki Y, Kim YH, Bohorquez F (2005) Adenosine A2A-receptor blockade abolishes the roll-off respiratory response to hypoxia in awake lambs. *Am J Physiol Regul Integr Comp Physiol* 288:R1185-1194.

- Kumar P (2007) Sensing hypoxia in the carotid body: from stimulus to response. *Essays Biochem* 43:43-60.
- Lahiri S, Mitchell CH, Reigada D, Roy A, Cherniack NS (2007) Purines, the carotid body and respiration. *Respir Physiol Neurobiol* 157:123-129.
- Lambrecht G (2000) Agonists and antagonists acting at P2X receptors: selectivity profiles and functional implications. *Naunyn Schmiedebergs Arch Pharmacol* 362:340-350.
- Llaudet E, Botting NP, Crayston JA, Dale N (2003) A three-enzyme microelectrode sensor for detecting purine release from central nervous system. *Biosens Bioelectron* 18:43-52.
- Llaudet E, Hatz S, Droniou M, Dale N (2005) Microelectrode biosensor for real-time measurement of ATP in biological tissue. *Anal Chem* 77:3267-3273.
- Long WA, Lawson EE (1984) Neurotransmitters and biphasic respiratory response to hypoxia. *J Appl Physiol* 57:213-222.
- Lorier AR, Lipski J, Housley GD, Greer JJ, Funk GD (2008) ATP sensitivity of preBotzinger complex neurones in neonatal rat in vitro: mechanism underlying a P2 receptor-mediated increase in inspiratory frequency. *J Physiol* 586:1429-1446.
- Lorier AR, Huxtable AG, Robinson DM, Lipski J, Housley GD, Funk GD (2007) P2Y1 receptor modulation of the pre-Botzinger complex inspiratory rhythm generating network in vitro. *J Neurosci* 27:993-1005.
- Martin-Body RL, Robson GJ, Sinclair JD (1985) Respiratory effects of sectioning the carotid sinus glossopharyngeal and abdominal vagal nerves in the awake rat. *J Physiol* 361:35-45.

- Mayer CA, Haxhiu MA, Martin RJ, Wilson CG (2006) Adenosine A_{2A} receptors mediate GABAergic inhibition of respiration in immature rats. *J Appl Physiol* 100:91-97.
- Miller MJ, Tenney SM (1975) Hypoxia-induced tachypnea in carotid-deafferented cats. *Respir Physiol* 23:31-39.
- Mironov SL, Langohr K, Richter DW (1999) A₁ adenosine receptors modulate respiratory activity of the neonatal mouse via the cAMP-mediated signaling pathway. *J Neurophysiol* 81:247-255.
- Moraes DJ, Bonagamba LG, Zoccal DB, Machado BH (2011) Modulation of respiratory responses to chemoreflex activation by L-glutamate and ATP in the rostral ventrolateral medulla of awake rats. *Am J Physiol Regul Integr Comp Physiol* 300:R1476-1486.
- Mortola JP (1996) Ventilatory responses to hypoxia in mammals. In: *In Tissue Oxygen Deprevention* (Haddad GGAL, G., ed), pp 433-477. New York, NY: Marcel Dekker.
- Mortola JP, Rezzonico R, Lanthier C (1989) Ventilation and oxygen consumption during acute hypoxia in newborn mammals: a comparative analysis. *Respir Physiol* 78:31-43.
- Moss IR (2000) Respiratory responses to single and episodic hypoxia during development: mechanisms of adaptation. *Respir Physiol* 121:185-197.
- Motin L, Bennett MR (1995) Effect of P₂-purinoceptor antagonists on glutamatergic transmission in the rat hippocampus. *Br J Pharmacol* 115:1276-1280.
- Mulkey DK, Stornetta RL, Weston MC, Simmons JR, Parker A, Bayliss DA, Guyenet PG (2004) Respiratory control by ventral surface chemoreceptor neurons in rats. *Nat Neurosci* 7:1360-1369.

Nakazawa K, Inoue K, Ito K, Koizumi S (1995) Inhibition by suramin and reactive blue 2 of GABA and glutamate receptor channels in rat hippocampal neurons. Naunyn Schmiedebergs Arch Pharmacol 351:202-208.

Nattie E, Li A (2009) Central chemoreception is a complex system function that involves multiple brain stem sites. J Appl Physiol 106:1464-1466.

Paxinos G, Watson C (2007) The Rat Brain in Stereotaxic Coordinates: Elsevier.

Rehan V, Haider AZ, Alvaro RE, Nowaczyk B, Cates DB, Kwiatkowski K, Rigatto H (1996) The biphasic ventilatory response to hypoxia in preterm infants is not due to a decrease in metabolism. Pediatr Pulmonol 22:287-294.

Rong W, Gourine AV, Cockayne DA, Xiang Z, Ford AP, Spyer KM, Burnstock G (2003) Pivotal role of nucleotide P2X2 receptor subunit of the ATP-gated ion channel mediating ventilatory responses to hypoxia. J Neurosci 23:11315-11321.

Ruangkittisakul A, Ballanyi K (2010) Methylxanthine reversal of opioid-evoked inspiratory depression via phosphodiesterase-4 blockade. Respir Physiol Neurobiol 172:94-105.

Runold M, Lagercrantz H, Prabhakar NR, Fredholm BB (1989) Role of adenosine in hypoxic ventilatory depression. J Appl Physiol 67:541-546.

Stornetta RL, Rosin DL, Wang H, Sevigny CP, Weston MC, Guyenet PG (2003) A group of glutamatergic interneurons expressing high levels of both neurokinin-1 receptors and somatostatin identifies the region of the pre-Botzinger complex. J Comp Neurol 455:499-512.

Sugihara C, Hehre D, Bancalari E (1994) Effect of dopamine on hypoxic ventilatory response of sedated piglets with intact and denervated carotid bodies. J Appl Physiol 77:285-289.

- Sun MK, Wahlestedt C, Reis DJ (1992) Action of externally applied ATP on rat reticulospinal vasomotor neurons. *Eur J Pharmacol* 224:93-96.
- Thomas T, Spyer KM (2000) ATP as a mediator of mammalian central CO₂ chemoreception. *J Physiol* 523 Pt 2:441-447.
- Thomas T, Ralevic V, Gadd CA, Spyer KM (1999) Central CO₂ chemoreception: a mechanism involving P2 purinoceptors localized in the ventrolateral medulla of the anaesthetized rat. *J Physiol* 517 (Pt 3):899-905.
- Thomas T, Ralevic V, Bardini M, Burnstock G, Spyer KM (2001) Evidence for the involvement of purinergic signalling in the control of respiration. *Neuroscience* 107:481-490.
- Vandam RJ, Shields EJ, Kelty JD (2008) Rhythm generation by the pre-Botzinger complex in medullary slice and island preparations: effects of adenosine A(1) receptor activation. *BMC Neurosci* 9:95.
- Wang JL, Wu ZH, Pan BX, Li J (2005) Adenosine A1 receptors modulate the discharge activities of inspiratory and biphasic expiratory neurons in the medial region of Nucleus Retrofacialis of neonatal rat in vitro. *Neurosci Lett* 379:27-31.
- Waters KA, Gozal D (2003) Responses to hypoxia during early development. *Respir Physiol Neurobiol* 136:115-129.
- Wilson CG, Martin RJ, Jaber M, Abu-Shaweeesh J, Jafri A, Haxhiu MA, Zaidi S (2004) Adenosine A2A receptors interact with GABAergic pathways to modulate respiration in neonatal piglets. *Respir Physiol Neurobiol* 141:201-211.
- Yan S, Laferriere A, Zhang C, Moss IR (1995) Microdialyzed adenosine in nucleus tractus solitarius and ventilatory response to hypoxia in piglets. *J Appl Physiol* 79:405-410.

Zwicker JD, Rajani V, Hahn LB, Funk GD Purinergic modulation of preBotzinger complex inspiratory rhythm in rodents: the interaction between ATP and adenosine. *J Physiol* 589:4583-4600.

Zwicker JD, Rajani V, Hahn LB, Funk GD (2011) Purinergic modulation of preBotzinger complex inspiratory rhythm in rodents: the interaction between ATP and adenosine. *J Physiol* 589:4583-4600.

Zylka MJ, Sowa NA, Taylor-Blake B, Twomey MA, Herrala A, Voikar V, Vihko P (2008) Prostatic acid phosphatase is an ectonucleotidase and suppresses pain by generating adenosine. *Neuron* 60:111-122.

Chapter 5: Microglia TLR4 signaling does not contribute to the opioid-induced depression of respiration

A version of this chapter has been prepared for submission to Journal of Applied Physiology:

Zwicker JD, Zhang Y, Ren J, Hutchinson MR, Rice KC, Watkins LR, Greer JJ, Funk GD

I performed all experiments and data analysis procedures except those listed below. I also contributed to all experimental design, article drafting and submission of the manuscript. Y Zhang performed and analyzed experiments associated with Fig 5.4, contributed relevant sections of text and participated in the final revision process. J Ren performed and analyzed experiments associated with Fig 5.5, contributed relevant sections of text and participated in the final revision process. MR Hutchinson and LR Watkins provided conceptual expertise and participated in the final revision process. KC Rice provided the (+)naloxone compound. GD Funk oversaw all aspects of the study, from conception to final publication. Overall, my contribution was ~75% of the total.

5.1 Introduction

The analgesic effects of opioids, which result from their activation of classical opioid receptors in the CNS, underlie their widespread clinical use. Unwanted actions include opioid tolerance, dependence, reward and perhaps most serious in acute terms is opioid-induced respiratory depression, which can be life threatening. This is particularly problematic in premature infants with immature respiratory networks and unstable breathing (Greer et al., 2006); it contributes significantly to the challenge of providing adequate pain control in the pediatric and adult population (Howard, 2003; Tibboel et al., 2005). Opioid-induced respiratory depression is counteracted clinically with opioid receptor antagonists (eg. (-)-naloxone), but this also counteracts analgesia. Thus, there is a need for pharmacological approaches to alleviate opioid-induced respiratory depression without loss of analgesia (Greer et al., 2006; Ren et al., 2006). Greater understanding of the mechanisms by which opioids depress breathing would greatly facilitate the development of such approaches.

Respiratory depression is primarily dependent on activation of μ -opioid receptors (Romberg et al., 2003), however, the location, cell type and cellular mechanism(s) are incompletely defined. The cellular mechanisms of μ -opioid receptor agonists have been shown to be both presynaptic (Ballanyi et al., 2010) and postsynaptic (Takeda et al., 2001; Lorier et al., 2008; Montandon et al., 2011). The direct actions of opioids on μ -opioid receptors expressed by respiratory neurons in a brainstem region critical for generating inspiratory rhythm, the preBötzinger complex (preBötC) (Ballanyi et al., 1997; Gray et al., 1999; Morin-Surun et al., 2001; Montandon et al., 2011), is considered a major contributor to this respiratory depression. However, recent data indicate that in addition to their action on classical opioid receptors, opioids also act by binding to toll-like-receptor 4 (TLR4) (Hutchinson et al., 2008b; Wang et al., 2012) which is expressed almost exclusively on non-neuronal cells such as glia (microglia and astrocytes) and endothelial cells (Watkins et al., 2009). Evidence has also been presented for opioid-induced TLR2-dependent microglial activation (Zhang et al.,

2011) and neuronal death (Li et al., 2010) and TLR9 for opioid-induced microglial apoptosis (He et al., 2011).

TLR4 is an innate immune pattern recognition receptor that is activated by pathogen associated molecular patterns (PAMPs), endogenous danger associated molecular patterns (DAMPs) and small molecule xenobiotics such as opioids (xenobiotic associated molecular patterns; XAMPs, (Hutchinson et al., 2012), leading to activation of microglia and astrocytes. Activated glia release a variety of compounds including proinflammatory cytokines (i.e.: TNF- α , IL-1 β , IL-18, BDNF, PGE₂, and nitric oxide), that in turn influence neuronal excitability and plasticity in a variety of neural networks including hippocampus (Curran and O'Connor, 2001), spinal cord (Zhou et al.; Coull et al., 2005; Liu et al., 2007; Kawasaki et al., 2008; Zhou et al., 2008; Li et al., 2009; Choi et al., 2010) and ventromedial medulla (Wei et al., 2008), by regulating gene transcription and translation. In addition, recent studies demonstrating TLR4 involvement in neurogenesis, and learning and memory in the absence of underlying infectious etiology suggest that TLR4 signaling can influence neural network activity independent of major inflammatory processes (Hanke and Kielian, 2011).

The net effect of opioids on CNS function will be determined by activation of classical opioid receptors and, at minimum, TLR4 on non-neuronal cells such as glia. Accumulating evidence suggests that opioid-induced, TLR4-mediated glial activation actively opposes opioid analgesia and contributes to many of the negative consequences of opioid exposure including tolerance, dependence and reward (Watkins et al., 2009; Hutchinson et al., 2010; Hutchinson et al., 2011; Hutchinson et al., 2012; Wang et al., 2012). Most relevant to this study is the recent demonstration in rats *in vivo* that the microglia attenuator, minocycline, reduced the opioid-induced depression of breathing (Hutchinson et al., 2008a). Such an action would require that microglial activation and TLR4 signaling affects neuronal excitability on a time scale (minutes) much faster than the translation- or transcription-

dependent mechanisms through which they are conventionally considered to affect neuronal/network excitability (hours). Morphine analgesia data presented in Hutchinson *et al.* (2008b) support the acute nature of the opioid-induced minocycline-sensitive microglial response. There is also precedence that many of the inflammatory cytokines released in response to TLR4 activation affect long-term potentiation of hippocampal synapses over relatively short time scales (20 min) (Curran and O'Connor, 2001). Moreover, if microglia and TLR4 signaling contribute to the respiratory depressant actions of opioids, stereoselective antagonism of opioid activation of TLR4 with (+) naloxone (which blocks TLR4 but not opioid receptors) could provide a pharmacological means of reducing the respiratory depressant actions of opioids without altering opioid-receptor dependent analgesia.

The objectives of this study were therefore to determine the contribution of activated glia or TLR4 signaling to the opioid-mediated depression of central respiratory networks and whether acute TLR4 activation can modulate respiratory network activity. We compared the effects on the opioid-induced respiratory depression of non-stereoselective opioid receptor antagonists ((-) naloxone, blocks both opioid receptors and TLR4) with stereoselective antagonists ((+) naloxone) and agents that inhibit microglial activation (minocycline). This was done both *in vitro* using rhythmically-active medullary slices, where opioid actions were limited to the preBötC or the medullary slice, and *in vivo* to reproduce the clinically-relevant setting in which opioids can act throughout the CNS to depress breathing.

5.2 Methods

All experiments were conducted in accordance with the guidelines of the Canadian Council on Animal Care and were approved by the University of Alberta Animal Ethics Committee.

5.2.1 Rhythmic medullary slices

Neonatal Sprague Dawley rats [postnatal day 0–4 (P0–P4)] were anesthetized through inhalation of isoflurane and decerebrated. The brainstem–spinal cord was then isolated in cold artificial CSF (aCSF) containing the following (in mM): 120 NaCl, 3 KCl, 1.0 CaCl₂, 2.0 MgSO₄, 26 NaHCO₃, 1.25 NaH₂PO₄, 20 D-glucose, equilibrated with 95% O₂/5% CO₂. The brainstem–spinal cord was pinned to a wax chuck, and serial 100–200 µm sections were cut in the rostral-to-caudal direction using a vibratome (VT1000S, Leica, Nussloch, Germany) and transilluminated to identify anatomical landmarks. The structure of the sub nuclei of the inferior olive was particularly useful in defining this boundary (Ruangkittisakul et al., 2010). One rhythmic, transverse, 700 µm-thick medullary slices was cut with the preBötC at the rostral surface of the slice, 0.35 mm caudal to the caudal aspect of the facial nucleus in rat (Smith et al., 1991; Ruangkittisakul et al., 2006; Lorier et al., 2007). Slices were pinned with the rostral surface up on Sylgard resin in a recording chamber (volume, 5 ml) and perfused with aCSF that was recirculated at a flow rate of 15 ml/min. The concentration of K⁺ in the aCSF ([K⁺]_e) was raised from 3 to 9 mM at least 30 min before the start of data collection. The majority of protocols in this study involved multiple interventions, and therefore required slices that produced stable inspiratory-related rhythm for extended periods (i.e., >5 h). Therefore, the [K⁺]_e was raised from 3 to 9 mM to produce prolonged, stable rhythm (Ruangkittisakul et al., 2010).

5.2.2 Electrophysiological recordings

Inspiratory activity was recorded, using glass suction electrodes (A-M Systems, Carlsborg, WA), from cut ends of XII (hypoglossal) nerve rootlets and directly from the ventrolateral surface of the slice. Surface field potentials were recorded using a four-axis manual manipulator to place a suction electrode (120 µm inside diameter) on the surface of the slice over the approximate region of the ventral respiratory cell column (Ramirez et al., 1997). The pipette was systematically moved in steps corresponding to one-half of the pipette

diameter until the most robust signal was detected. Signals were amplified, bandpass filtered (100 Hz to 3 kHz), full-wave rectified, integrated using a leaky integrator (τ = 25 or 50 ms), and displayed using Axoscope 9.2 (Molecular Devices, Union City, CA). Data were saved to computer using a Digidata 1322 A/D board and AxoScope 9.2 software (Molecular Devices) for off-line analysis. All recordings were conducted at room temperature (22–24°C).

5.2.3 Drugs and their application

Lipopolysaccharides from *Escherichia coli* (LPS) (TLR4 agonist, 200 ng/mL microinjected) and minocycline (microglia activation inhibitor, 0.5 μ M bath application or 45 mg/kg i.p.) were obtained from Sigma-Aldrich (Oakville, Ontario). LPS from *Rhodobacter sphaeroides* (LPS-RS) (TLR4 antagonist, 2000 ng/mL) was obtained from InvivoGen (San Diego, California). Fentanyl citrate (opioid agonist, 1 μ M bath-applied or 40 μ g/kg i.v.) was obtained from Sandoz, Boucherville, Quebec, Canada. (+) Naloxone (TLR4/MD2 antagonist, 10 μ M bath, 3-60 mg/kg i.v.) was kindly provided by Dr. K.C. Rice, Chemical Biology Research Branch, National Institute on Drug Abuse and National Institute on Alcohol Abuse and Alcoholism National Institutes of Health, Rockville, Maryland, USA. Drugs obtained from Tocris Bioscience included: [Sar⁹-Met(O₂)¹¹]-substance P (SP) (NK1R agonist, 1 μ M microinjected); DAMGO ([D-Ala², NMe-Phe⁴, Gly-ol⁵]-enkephalin), μ -opioid receptor agonist, 50 μ M microinjected, 0.5 μ M bath-applied); (-) naloxone ((5 α)-4,5-epoxy-3,14-dihydro-17-(2-propenyl)morphinan-6-one hydrochloride), opioid antagonist, 0.5 μ M bath-applied, 0.6 mg/kg IV)).

Drugs were prepared as stock solutions in aCSF and frozen in aliquots. Exceptions were DAMGO, (+) and (-) naloxone, which were made fresh on the day of the experiment. The final concentration of K⁺ in the drug solutions was matched to that of the aCSF. In slice preparations, drugs were unilaterally applied locally to the preBötC via triple-barreled pipettes (5–6 μ m outer diameter per barrel) pulled from borosilicate glass capillaries (World

Precision Instruments, Sarasota, FL). Care was taken to ensure that the outer tip diameter was within this range because fluorescent imaging (40x objective) of Lucifer yellow-filled triple-barreled pipettes established that pipettes in this range do not leak, but they do leak if tip diameter exceeds 6.5 μ m. Drug microinjections were controlled by a programmable stimulator (Master-8; A.M.P.I. Instruments Jerusalem, Israel) connected to a picospritzer (Spritzer4 Pressure Micro-Injector, Bioscience Tools (San Diego, CA), ~18 psi). Consecutive agonist applications were separated by a minimum of 15 min. We did not systematically assess whether this was the minimum time interval required for consistent responses, but it was sufficient for reproducible responses. The concentrations of drugs used in the present study should not be directly compared with those in experiments in which similar agents are applied in the bath or directly to isolated cells. The concentration of drug decreases exponentially with distance from the pipette tip, and previous experiments with this preparation have established that drug concentration in the pipette must be ~10-fold greater than the bath-applied concentration to produce similar effects (Liu et al., 1990).

The drug injection site was established as described previously (Lorier et al., 2007; Huxtable et al., 2009; Huxtable et al., 2010; Zwicker et al., 2011). Briefly, we first used the location of the VRC suction electrode as an approximate reference in the transverse plane to the region of most intense respiratory activity. The response to SP (1 μ M, 10 s) at this site was recorded. The drug pipette was then systematically moved in the dorsoventral and mediolateral directions until SP evoked a frequency increase that occurred within the first breath following drug onset and was at least two-fold greater than baseline. Based on these criteria and the established sensitivity of preBötC networks to SP (Johnson et al., 1996; Gray et al., 1999; Lorier et al., 2007; Huxtable et al., 2009; Huxtable et al., 2010) we are confident that positive injections sites were in the preBötC. Once the preBötC was located, and depending on the specific experiment, LPS, LPS-RS or DAMGO was microinjected into the same site. Control injections of aCSF were without effect.

Minocycline treatment. In one experimental series, minocycline was bath-applied at

0.5 µM immediately after DAMGO (50 µM, 10s) was injected in the preBötC and allowed 40 min to take effect before the second local application of DAMGO (Tikka et al., 2001; Nutile-McMenemy et al., 2007). In a second series, neonates were injected i.p with minocycline (45 mg/kg) 18 hours, and again 1 hour prior the isolation of the rhythmic medullary slice (Yrjanheikki et al., 1999; Teng et al., 2004; Osikowicz et al., 2009).

5.2.4 Plethysmographic recording

Measurements were made from adult male Sprague-Dawley rats (300–370 g). A tail vein was cannulated for i.v. infusion of drugs. Rats were anesthetized with isoflurane (3%) in an induction chamber and maintained under isoflurane (2%) anesthesia during tail vein cannulation (P10 size tubing). Animals were then placed within a whole-body, plexiglass plethysmograph (2000 ml volume) modified to allow exteriorization of the tail for drug infusion (KD Scientific infusion pump, Holliston MA). The plethysmograph had inflow and outflow ports for the continuous delivery of a steady flow of fresh air and removal of expired carbon dioxide. Fresh room air is then circulated through the chamber for 3 minutes prior to the fentanyl infusion to reduce residual isoflurane to minimum from the chamber. Pressure changes were recorded with a pressure transducer (model DP 103, Validyne, Northridge, CA), signal conditioner (CD-15, Validyne, Northridge, CA) and an analogue-digital board (Digidata 1322) and Axoscope software (Molecular Devices, Sunnyvale, California, USA). Our plethysmographic recording setup is effective for studying respiratory frequency (f). However, it is not suitable for precise quantification of tidal volume but rather changes relative to control values (i.e. pre- and post-drug delivery). The physical principle underlying whole-body plethysmography is the detection of pressure changes in the chamber resulting from the heating and humidification of inspired gas. However, tidal volume (V_T , ml.gram⁻¹) measurement may also be influenced by gas compression effects related to the airway resistance. Because of these limitations, whole-body plethysmography only provides semi-

quantitative measurements of V_T and detection of changes relative to control state (before drug). Therefore, relative value (to control), but not absolute value for V_T is provided.

5.2.5 Data analysis and statistics

For *in vitro* experiments, the effects of a drug on frequency of integrated inspiratory bursts recorded via suction electrodes from XII nerve roots were assessed off-line using pClamp 9.2 (Clampfit) and Microsoft Excel software. Values of frequency during the drug were compared with the average value during the 2 min control period that immediately preceded drug application. The maximum effect of a drug on frequency was determined as the maximum (or minimum) value measured in the moving average of inspiratory frequency (calculation based on the average of three consecutive events) during the first minute after injection. The time course of the response was obtained by averaging data points in 30 sec bins for the control period immediately before drug application, in 30 sec bins for the first 2 min after the onset of drug application (5 min for minocycline treatment), and in 1 min bins for the remainder of the trial. Parameters are reported relative to control (predrug) levels, as mean \pm SE.

Unless otherwise stated, statistical comparison of means for *in vitro* and *in vivo* data was performed on raw data using GraphPad Prism version 4 (GraphPad Software, La Jolla, CA). Statistical comparison of relative data was performed only after verification of normality. Differences between means were identified using a one-way or two-way ANOVA with Bonferroni correction for multiple comparisons. Values of $p < 0.05$ were assumed significant.

5.3 Results

5.3.1 TLR antagonism does not affect the DAMGO-mediated respiratory inhibition *in vitro*

Sites that underlie the depressant actions of opioids on respiratory rhythm are not fully known, but recent data implicate the preBötC as a key player (Montandon et al., 2011) and suggest that TLR4, which are primarily expressed on microglia and can be activated by small molecule opioids such as morphine (Song and Zhao, 2001; Johnston et al., 2004; Hutchinson et al., 2008a), contribute to this respiratory depression. To test whether TLR4-mediated signaling contributes to the DAMGO-induced respiratory depression (Gray et al., 1999; Ruangkittisakul and Ballanyi, 2010), we compared the effects on frequency of locally-applying the μ -opioid agonist DAMGO (50 μ M, 10 sec) into the preBötC before and immediately after local preapplication of the TLR4 antagonist LPS-RS (2000 ng/mL; 90 sec). The injection site for DAMGO within the preBötC was established using the previously developed mapping protocol (Lorier et al., 2007; Huxtable et al., 2009; Huxtable et al., 2010) that is described briefly in the methods. It is based primarily on the functional criterion that in the rhythmic slice SP evokes its maximum effect on frequency when it activates NK1Rs in the preBötC (Johnson et al., 1996; Gray et al., 1999). When SP (1 μ M, 10 sec) was injected into the site of maximum sensitivity (i.e. the preBötC), it produced a rapid-onset, 2.80 ± 0.58 - fold increase in burst frequency that peaked within 10 sec of SP application and remained significantly greater than baseline frequency until 90 sec after drug onset ($n = 5$). As seen previously (Gray et al., 1999; Takeda et al., 2001; Lorier et al., 2007; Lorier et al., 2008; Ballanyi et al., 2010; Ruangkittisakul and Ballanyi, 2010) when applied alone DAMGO produced a significant reduction in frequency that reached a nadir at 0.32 ± 0.12 of the relative control baseline frequency ~ 1 min after drug onset (Fig 1A, $n = 5$; Two-way ANOVA, multiple comparison test with Bonferroni correction). Preapplication of LPS-RS had no significant effect on the DAMGO-induced decrease in frequency (Fig 1B, C; $n = 5$; Two-way ANOVA, multiple comparison test with Bonferroni correction). After LPS-RS, DAMGO depressed frequency to a nadir that was 0.65 ± 0.09 of the control value. The DAMGO-evoked inhibition of frequency was repeatable after a 15 min washout period when frequency fell to 0.49 ± 0.17 of control.

We next tested the efficacy of two naloxone isomers in antagonizing the DAMGO- and fentanyl-induced respiratory depression. Fentanyl was chosen here as previous data support that it is a TLR4 agonist, in addition to being an opioid agonist (Hutchinson et al., 2010). (-) Naloxone is used commonly in clinical situations to counteract the actions of opioids. It is a non-selective antagonist that acts at both μ -opioid receptors and TLR4. Thus, antagonism by (-) naloxone could reflect actions of the opioid agonist at either opioid receptors or TLR4. (+) Naloxone, on the other hand binds stereoselectively to TLR4 and is useful in discriminating between the actions of opioids at the two types of receptors. We therefore applied the μ -opioid receptor agonists DAMGO (0.5 μ M, n=7, Fig 2.A,C) or Fentanyl (1 μ M, n=5, Fig 2.B,D) to the aCSF perfusing rhythmically-active medullary slice preparations and tested the effects of bath-applying first (+) naloxone and then (-) naloxone on the respiratory depression. DAMGO and Fentanyl significantly reduced frequency to 0.32 ± 0.04 or 0.68 ± 0.06 relative to control, respectively. Following bath application of the TLR-selective antagonist, (+) naloxone (10 μ M), the frequency in DAMGO was 0.55 ± 0.04 of control while that in Fentanyl was 0.48 ± 0.10 of control; i.e. (+) naloxone had no significant effect on the opioid-induced respiratory depression. In contrast, subsequent addition of (-) naloxone (0.5 μ M) to the bath rapidly (within 2 min) and completely reversed the respiratory depression. Inspiratory frequency returned to 1.11 ± 0.16 or 1.33 ± 0.07 of control in DAMGO (Fig 2.A,C) and Fentanyl (Fig 2. B,D) treated slices, respectively (One-way ANOVA, multiple comparison test with Bonferroni correction).

5.3.2 Effects of LPS on preBötC rhythm

Although TLR4 activation does not appear to contribute to the DAMGO- or fentanyl-induced depression of inspiratory rhythm in the rhythmic slice, this does not exclude the possibility that acute activation of TLR is capable of influencing inspiratory rhythm generating networks. While TLR4 signaling through microglia to affect neuronal/network

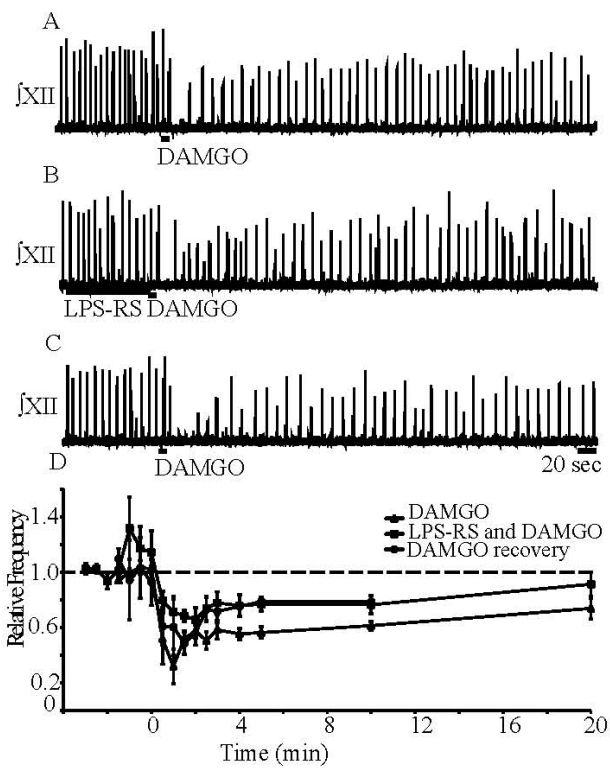


Figure 5.1 Preapplication of TLR4 antagonist LPS-RS has no effect on the DAMGO-mediated inhibition of frequency.

XII nerve (fXII) recordings showing opioid induced respiratory depression of rat rhythmic slice frequency to locally applied DAMGO (50 μ M, 10sec) in control (A)▲, after preapplication of TLR antagonist LPS-RS (2000ng/mL; 90sec)(B)■ and recovery (C)○. D) Group data illustrating the time course of the frequency response (relative to control; Rel Freq; n =5). * indicates significantly different from baseline. Values were not significantly different in the presence or absence of LPS-RS (Two-way ANOVA, multiple comparison test with Bonferroni correction).

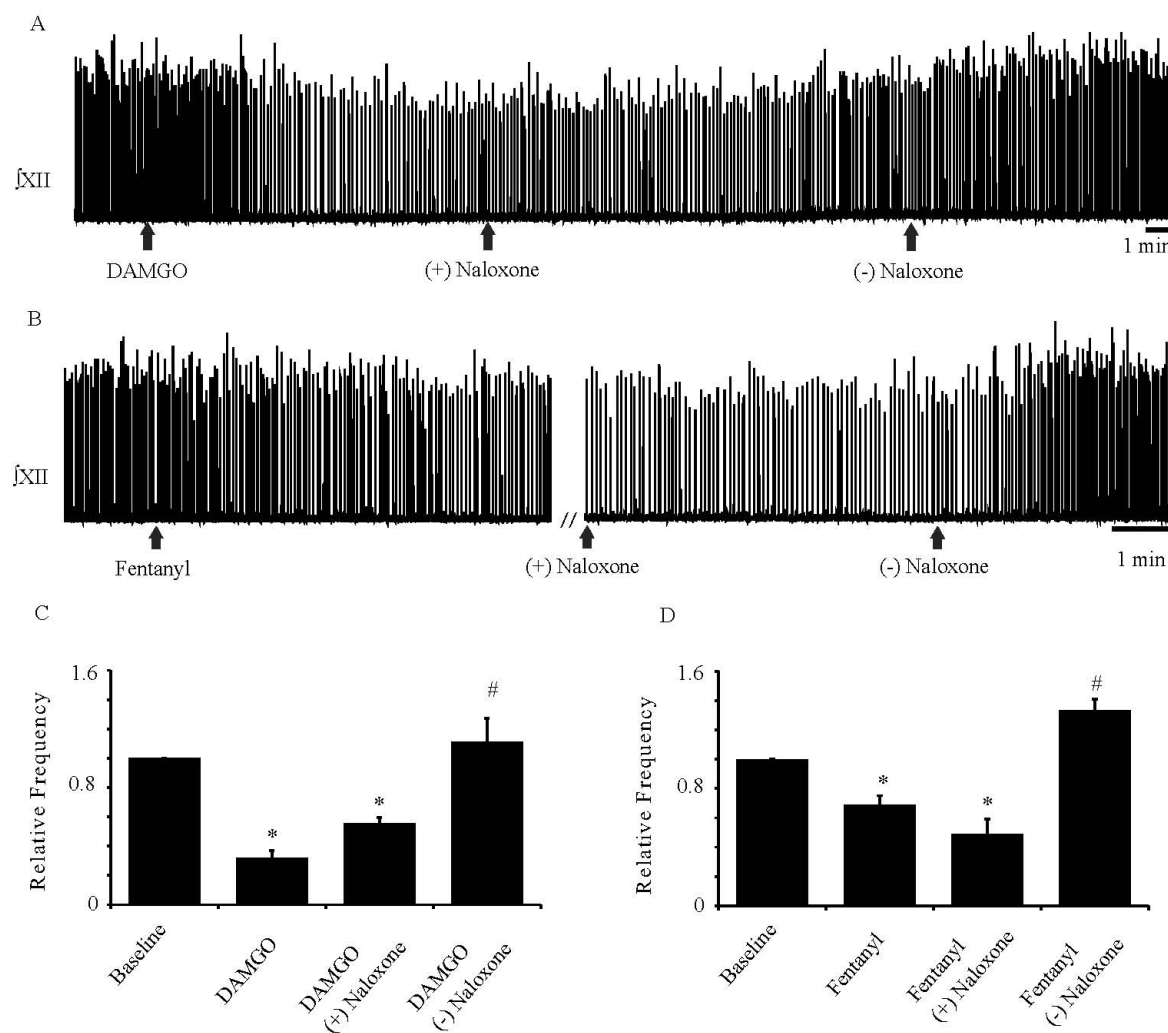


Figure 5.2 Bath application of the TLR4-selective antagonist, (+) naloxone, has no effect on the opioid-evoked depression of frequency.

XII nerve (jXII) recordings showing opioid-induced respiratory depression of rat rhythmic slice frequency evoked by bath application of DAMGO (0.5 μM, A) or Fentanyl (1 μM, B) under control conditions, and subsequent to bath application of the TLR-selective antagonist, (+) Naloxone (10 μM), and the classical μ-opioid receptor antagonist, (-) Naloxone (0.5 μM). Group data showing effects of (+)- and (-)-naloxone on the frequency depression (relative to control; Rel Freq) evoked by DAMGO (C n = 7) and Fentanyl (D, n = 5). * indicates significant difference from predrug control levels; # indicates significant difference from DAMGO or Fentanyl (One-way ANOVA, multiple comparison test with Bonferroni correction).

excitability is typically considered to operate on relatively long time scale (hrs) (Tanga et al., 2004), the hypothesis that microglia and TLR4 signaling contribute to the respiratory depressant actions of opioids (Hutchinson et al., 2008a) requires a mechanism of action that can occur within minutes. To test if TLR4 activation can directly modulate the activity of preBötC rhythm generating networks on this type of timescale, we locally applied LPS to the preBötC of rhythmically active medullary slices. The injection site for LPS within the preBötC was established using the previously described SP mapping protocol (Lorier et al., 2007; Huxtable et al., 2009). In these experiments, when SP (1 µM, 10 sec) was injected into the preBötC, it produced a rapid-onset, 2.07 ± 0.14 - fold increase in burst frequency that peaked within 10 sec of SP application and remained significantly greater than baseline frequency until 90 sec after drug onset (Fig 3 A, n = 4). Local injection of LPS (200 ng/mL, 10 sec) into the same site caused only small, statistically insignificant fluctuations in frequency (Fig 3 C, n=4, one-way ANOVA, multiple comparison test with Bonferroni correction).

5.3.3 Microglia and opioid-induced respiratory depression

The previous experiments exclude involvement of TLR4-mediated signaling in the opioid-induced respiratory depression and demonstrate that preBötC networks are insensitive to acute TLR4 activation. Microglia, however, may still play a role, as suggested by the demonstration that i.p. injection of minocycline attenuates a weak opioid-mediated depression in adult rats *in vivo* (Hutchinson et al., 2008a). To test the contribution of microglia in the DAMGO-mediated respiratory depression, we compared the effects on inspiratory frequency of locally applying DAMGO into the preBötC before and after bath application of minocycline in rhythmically active medullary slices of SD rats. The injection site for DAMGO within the preBötC was established using the previously described SP

mapping protocol. When SP (1 μ M, 10 sec) was injected into the preBötC it produced a rapid-onset, 2.42 ± 0.10 -fold increase in burst frequency ($n = 10$). Local injection of DAMGO (50 μ M, 10 sec) into the same site depressed inspiratory burst frequency to 0.51 ± 0.13 of control. Following 40 min of incubation in minocycline, DAMGO was reapplied into the same site where it similarly reduced frequency to 0.48 ± 0.06 of control; i.e. minocycline had no significant effect on the DAMGO-induced frequency depression (Fig 4, 0.5 μ M, $n=6$ Two-way ANOVA, multiple comparison test with Bonferroni correction).

Due to uncertainties about the time course required for minocycline to inhibit microglial activation and its efficacy when administered under *in vitro* conditions, we performed a second series of experiments in which minocycline was applied via i.p. injection (45 mg/kg, $n = 9$) to the neonatal rats 18 hours and again 1 hour prior to the generation of rhythmic medullary slices. We compared the frequency response to locally applied DAMGO (50 μ M, 10 sec) into the preBötC of slices from control and minocycline pretreated animals. In these experiments, SP evoked a 2.23 ± 0.13 and 2.51 ± 0.16 increase in control and minocycline treated slices. Both the time course and maximum effects of DAMGO on inspiratory frequency are shown for the two groups (Fig 4). DAMGO reduced frequency similarly to 0.51 ± 0.05 and 0.53 ± 0.03 in control and minocycline-treated slices respectively (Fig 4, Two-way ANOVA, multiple comparison test with Bonferroni correction).

5.3.4 (+) Naloxone, has no effect on the opioid-evoked depression of frequency *in vivo*
The previous data suggest that TLR4 signaling does not play a role in the DAMGO- or fentanyl-mediated depression of breathing. However, as all data are based on responses to local injection of opioid agonists into the preBötC or bath application to the medullary slice, these data do not exclude the possibility that microglia or TLR4 signaling contributes to the DAMGO- or fentanyl-induced respiratory depression through a region that is either outside the preBötC or not contained in the rhythmic slice. Certainly, under clinical conditions opioids are administered iv or orally where they can act throughout the CNS. Therefore, as a

final test of the hypothesis that TLR4 receptor signaling contributes to the fentanyl-mediated depression of respiration, we compared the abilities of (+) and (-) naloxone to reverse the respiratory depression produced by i.v. administration of fentanyl (40 µg/kg delivered over a 20 min period). The effects of fentanyl reached a stable level after ~8 min of infusion and remained stable throughout the infusion. Fentanyl markedly suppressed respiratory frequency (to 0.53 ± 0.09 of control) and tidal volume (to 0.42 ± 0.08 of control). Intravenous administration of (+) naloxone (3–60 mg/kg i.v.; n = 6) 10 min after onset of fentanyl administration had no effect on the fentanyl-induced respiratory depression (Fig. 5 A,B) as respiratory frequency and tidal volume were 0.55 ± 0.12 and 0.45 ± 0.10 of control, respectively. In contrast, intravenous administration of (-) naloxone (0.6 mg/kg i.v.; n = 6; in the presence of fentanyl) rapidly reversed the respiratory depression; respiratory frequency and tidal volume returned to 1.05 ± 0.07 and 0.94 ± 0.06 of control (pre-fentanyl) levels.

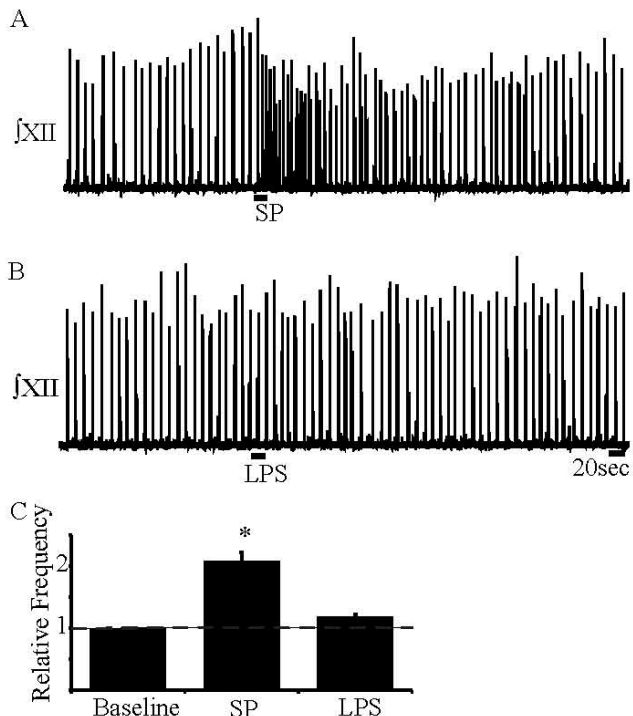


Figure 5.3 Local application of the TLR4 agonist LPS has no effect on respiratory frequency.

XII nerve (fXII) recordings showing a frequency increase in rat rhythmic slice with local application of SP (1 μM , 10sec, A) but not LPS (200ng/mL, 10sec, B). Group data illustrating the peak frequency (relative to control; Rel Freq) (C =4). (* , significantly different from baseline, one-way ANOVA, multiple comparison test with Bonferroni correction).

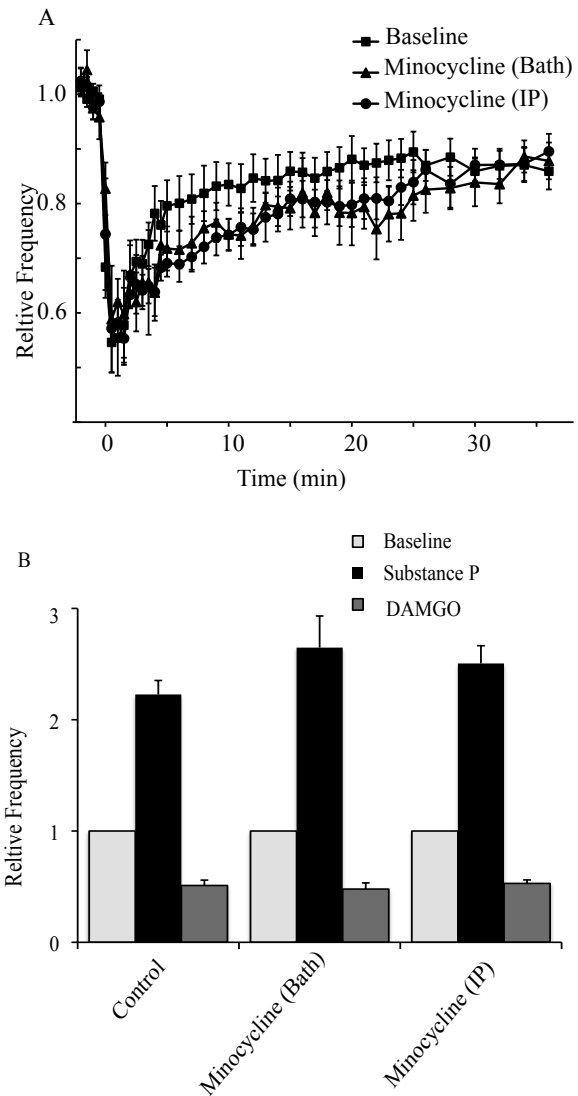


Figure 5.4 Microglia activation is not required for the opioid-induced respiratory depression .

Group data illustrating the time course of the frequency response (relative to control; Rel Freq) for XII nerve (XII) recordings showing opioid induced respiratory depression of rat rhythmic slice frequency to locally applied DAMGO □(50 μ M, 10sec) in control (n=10), after bath application of minocycline ▲ (500ng/ml, n=6) or i.p. injection of minocycline ○ (45mg/kg, n=9). Values were not significantly different in the presence or absence of either bath applied or pre-IP injected minocycline (Two-way ANOVA, multiple comparison test with Bonferroni correction). (B) Bar graph shows the average frequency changes (relative to control response) caused by local application of either SubP (1uM, 10s) or DAMGO (50 μ M, 10sec) of control, minocycline (bath) and minocycline (i.p.) group. There is no significant difference between either SubP- or DAMGO- induced fold changes in frequency of these three experimental groups before and after minocycline was administrated through the route of either bath or i.p. injection. (Two-way ANOVA, multiple comparisons test with Bonferroni correction).

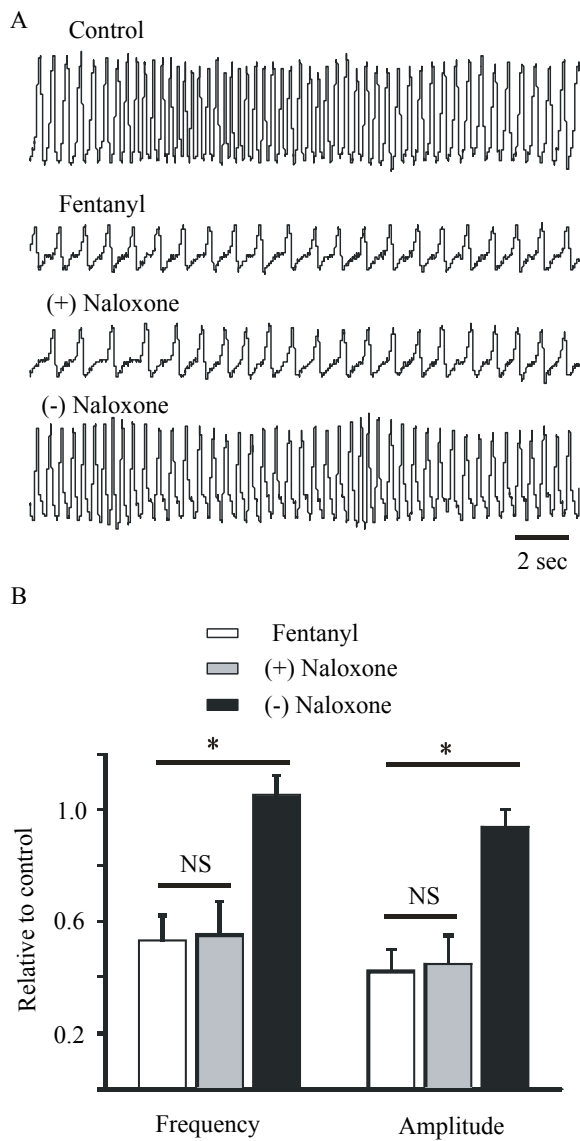


Figure 5.5 (-)-naloxone, but not (+)-naloxone counters fentanyl-induced depression of respiratory activity.

(A) Traces shown are whole-body plethysmographic measurements of the frequency and relative depth of breathing in an adult rat. Control: before fentanyl administration (top trace). Fentanyl (40 µg/kg IV over 20 min) caused a constant respiratory depression after 8 min administration (second trace). IV Injection of 60 mg/kg (+)-naloxone 10 min after fentanyl administration had no effect on the depression of respiratory frequency and amplitude (third trace). However, administration of (-)-naloxone (0.6 mg/kg, IV) instantly blocked the fentanyl-caused respiratory depression (bottom trace). (B) Population data ($n=6$) showing the relative effects (compared with control) of fentanyl, (+)-naloxone (3-60 mg/kg), and (-)-naloxone (in the continued presence of fentanyl) on amplitude and frequency of respiratory activity. Control values normalized to one. NS: $P > 0.05$, no significant difference; * $P < 0.001$, significant difference evaluated by an one way ANOVA with Tukey's post hoc correction (Sigmaplot 3.5, Systat Software, Chicago, IL).

5.4 Discussion

5.4.1 Neither TLR4 signaling nor microglia contribute to opioid respiratory depression

The vast majority of literature suggests that opioid-induced respiratory depression occurs via neuronal μ -opioid receptors. However, recent data suggest that glial activation opposes opioid analgesia and underlies many unwanted opioid side-effects including tolerance, dependence, reward and respiratory depression (Watkins et al., 2009; Hutchinson et al., 2011). Here we specifically examined this hypothesis that DAMGO and/or fentanyl act non-stereoselectively through TLR4 on microglia and contribute to respiratory depression (Hutchinson et al., 2008a). The reduced *in vitro* preparation enabled us to assess the role of microglia and proinflammatory signaling cascades in information processing within a functioning neural network. Ultimately, gaining an understanding of the mechanisms underlying the opioid-induced respiratory depression is essential for developing approaches to minimize the respiratory depression while maintaining opioid mediated analgesia. My data, however, convincingly demonstrate that the TLR4 signaling cascade is not involved in DAMGO- or fentanyl-induced respiratory depression. The failure with fentanyl is especially noteworthy given that prior literature supports that fentanyl is a TLR4 agonist (Hutchinson et al., 2010) whereas it is unknown whether or not DAMGO interacts directly with TLR4. *In vitro* injection of two TLR4 antagonists, LPS-RS and (+) naloxone had no effect on respiratory depression produced in the preBötC either by local or bath application of DAMGO or fentanyl. DAMGO and fentanyl both bind to the μ -opioid receptor. Thus, the observation that TLR4 inhibition with LPS-RS or (+)-naloxone had no effect on the respiratory depression while (-) naloxone completely reversed it, indicates that in this reduced preparation the respiratory depression is mediated by μ -opioid receptors. Similarly, (+) naloxone had no effect on the respiratory depression evoked by i.v. administration of fentanyl *in vivo*, while (-) naloxone rapidly and completely reversed it. Thus, under this

more clinically relevant condition where fentanyl can act throughout the CNS, TLR4 signaling did not contribute to the respiratory depression evoked by fentanyl.

A potential role for non-TLR4 microglial signaling mechanisms in the DAMGO- or fentanyl-mediated respiratory depression was also largely eliminated with our demonstration that the inhibitor of microglial activation, minocycline, had no effect on the ability of opioids to depress respiratory rhythm in tissues from neonatal rat. There is a possibility that the preBötC may not have microglia present at this stage of development or that gene expression of a large number of cytokines, chemokines and their receptors are not present on microglia during this stage of development (Schwarz et al., 2012). However, given that opioid-induced respiratory depression does occur in postnatal rats, the lack of microglia at this stage of development would further suggest that microglia are not involved in opioid-induced respiratory depression. The lack of an effect on the opioid-induced depression following 40 min bath application of minocycline could reflect insufficient time for minocycline to take effect or inability to arrest an activation process that may already been initiated during the slicing process itself (Watkins et al., 2009). However, opioid-induced depression was unaffected by i.p. injection of minocycline 18 and 1 hours prior to preparing the slice, addressing both concerns (Osikowicz et al., 2009). The specificity of minocycline as an inhibitor of microglial activation is also a potential concern. Indeed, since its initial use as an inhibitor of microglial activation (Yrjanheikki et al., 1998), the mechanisms underlying its inhibition of microglia remain unknown, but numerous additional effects have been documented, especially at the high concentrations used here (50 mg/kg). Minocycline has potent anti-inflammatory, immunomodulatory and neuroprotective actions. It can affect auto-reactive T lymphocytes by inhibiting antigen processing, inhibiting proliferation and production of cytokines and decreasing transmigration of T cells into the CNS (Kloppenburg et al., 1996; Kalish and Koujak, 2004; Nikodemova et al., 2007). Minocycline has also been found to be neuroprotective by inducing anti-apoptotic intracellular signaling pathways,

decreasing glutamate excitotoxicity, reducing oxygen radical release and NO-mediated neuronal destruction and sequestering excess Ca^{2+} (Wilkins et al., 2004; Maier et al., 2007; Mansson et al., 2007). It also limits iron deposition and modulates electron transport chain defects (Gutteridge, 1992; Teng et al., 2004).

Despite these caveats, the high concentration of minocycline and its potential non-specific actions are of minimal consequence in the context of this study because minocycline was without effect on the opioid-induced respiratory depression. The high concentration is in fact a strength of this study; the high concentration was selected to eliminate the possibility of a false negative result; i.e. that we would miss an effect of minocycline by using a subthreshold concentration. Thus, our data provide compelling evidence that microglial TLR4 activation does not contribute to the DAMGO or fentanyl-induced respiratory depression *in vitro*, however given our lack of positive control (confirming glia activation was inhibited by minocycline) we can't exclude the possibility that minocycline didn't inhibit microglia.

Data supporting microglial activation and TLR4 signaling in the negative side-effects of opioids are most compelling for opioid-induced reward (Narita et al., 2006; Terashvili et al., 2008; Hutchinson et al., 2012) dependence (Wu et al., 2008; Burns and Wang, 2010; Liu et al., 2010; Coller and Hutchinson, 2012) and withdrawal (Hutchinson et al., 2008a; Hutchinson et al., 2009; Hutchinson et al., 2010; Liu et al., 2010). Spinal cord microglia contribute to morphine tolerance (Raghavendra et al., 2004a); i.e., when, after chronic use, opioid levels must be increased progressively to maintain a constant level of analgesia. Chronic morphine administration activates microglia (Song and Zhao, 2001; Raghavendra et al., 2002) and microglial p38 MAP kinase (Liu et al., 2006), and upregulated spinal proinflammatory cytokines (Raghavendra et al., 2002; Johnston et al., 2004). Morphine tolerance is also slowed or reversed by inhibition of spinal proinflammatory cytokines (Raghavendra et al., 2002; Johnston et al., 2004) or knockout of IL-1 signaling (Shavit et al., 2005). Additionally, glial GLAST and GLT-1 glutamate transporter is downregulated in

spinal cord dorsal horn with chronic morphine administration (Mao et al., 2002; Tai et al., 2006). The downregulation of spinal glutamate transporters may contribute to the development of morphine tolerance. Of great interest is that TLR4 KO mice do not develop analgesic tolerance with chronic opioid administration (Liu et al., 2011). These data suggest that opioid tolerance may, in part, result from a TLR4-induced, glial-mediated increase in neuronal excitability, subsequent to elevations in glutamate and proinflammatory cytokines that oppose the actions of opioids.

Microglia also contribute to the development of morphine dependence (Raghavendra et al., 2002; Johnston et al., 2004; Raghavendra et al., 2004a). Morphine withdrawal-induced pain enhancement is blocked by drugs that block glial proinflammatory cytokine production and IL-1 receptor (Raghavendra et al., 2002; Johnston et al., 2004; Raghavendra et al., 2004a). Administration of AV411 (ibudilast), a blood brain barrier permeable glial activation inhibitor, with systemic chronic morphine maintains glial activation near basal levels (Leedeboer et al., 2007) and reduces brain-mediated withdrawal symptoms. Blocking TLR4 receptor with (+)-naloxone similarly attenuates withdrawal in rats (Hutchinson et al., 2010). In contrast, TLR4 KO mice display similar degrees of withdrawal behavior as their wild-type equivalent (Liu et al., 2011) implicating other neuroimmune pathways in opioid withdrawal.

Involvement of microglia or TLR4 signaling in the opioid-induced respiratory depression is least studied, but supported by the observation that the respiratory depression evoked in rats by subcutaneous administration of morphine (10 mg/kg; a known TLR4 agonist (Hutchinson et al., 2010)) was attenuated by pre-administration of minocycline via gavage 30 min prior to morphine (Hutchinson et al., 2008a). Close scrutiny of these data, however, reveals that the opioid-induced respiratory depression in this study was mediated by reductions in tidal volume and frequency, but the attenuation of the respiratory depression by minocycline-was achieved by reversing the reduction in tidal volume. The morphine-induced frequency reduction was not affected by minocycline. *In vivo*, the major effect on breathing of opioids in the brain is depression in respiratory frequency (Gray et al., 1999;

Manzke et al., 2003; Montandon et al., 2011). Effects on tidal volume can occur through actions on motoneurons (Hajiha et al, 2009) or premotoneurons (Lalley, 2003; Stucke et al., 2008; Montandon et al., 2011). Reductions in tidal volume are also attributed to opioid-induced reductions in lung, chest-wall or airway compliance (Scamman, 1983; Benvenga et al., 1992) via unknown mechanisms. Minocycline did not counteract the effects of opioids on frequency (Hutchinson et al., 2008a), suggesting that it did not reverse the central depressant effects of opioids on respiratory rhythm generating networks, but perhaps counteracted effects of opioids on premotor/motoneurons or the opioid-induced decrease in chest wall/lung compliance. Therefore, an alternative site of action for minocycline in these studies may warrant further investigation.

Our data are consistent with the majority of literature, which suggests that opioid-induced respiratory depression is primarily dependent on activation of μ -opioid receptors (Pattinson, 2008). Most compelling amongst this large database are genetic studies in which knockout mice lacking the μ -opioid receptor display no analgesia or respiratory depression with morphine, reinforcing clinical observations that analgesic and respiratory effects of opioids are strongly linked (Romberg et al., 2003). These data also suggest that it is unlikely to be any clinical potential in using TLR4-selective antagonists (such as (+) naloxone) in combination with opioids as a means of counteracting the respiratory depressant actions of opioids.

The CNS sites that mediate the opioid respiratory depression are not fully characterized. Several sites in the brain that have a direct or indirect influence on the respiratory network express μ -opioid receptors, including higher brains centers such as the insula, thalamus, anterior cingulate cortex, cerebellum, periaqueductal gray and prefrontal cortex (Baumgartner et al., 2006; Pattinson et al., 2009) that are all implicated in dyspnea in humans. μ -opioid receptors are also abundant throughout brainstem respiratory control centers (Wamsley, 1983; Xia and Haddad, 1991), which are believed to be the main areas underlying the respiratory depression. Our *in vitro* data, in which local application of

DAMGO or fentanyl into the preBötC reduces frequency, add to similar data supporting the view that opioid-sensitive neurons in the preBötC are a significant contributor to the respiratory depression (Ballanyi et al., 1997; Gray et al., 1999; Morin-Surun et al., 2001). Recent *in vivo* data also suggest, at least in rat, that the preBötC is a site contributing to respiratory depression (Montandon et al., 2011). To determine whether the preBötC is sensitive to opioids, the μ -opioid receptor agonists DAMGO or fentanyl were continuously applied unilaterally into the preBötC via reverse microdialysis in isoflurane-anesthetized adult rats resulting in sustained slowing of respiratory rate and increased ataxic breathing. The observation in the same study that bilateral administration of naloxone only into the preBötC, but not other regions, reversed the respiratory depression evoked by systemic administration of fentanyl, demonstrated in rats that the preBötC is an important mediator of the central respiratory depression. In contrast, in decerebrate dogs (Stucke et al., 2008; Mustapic et al., 2010) μ -opioid receptors appear to produce their depressive effects outside the pre-BötC region. Bilateral injections of naloxone in the pre-BötC or picoejections onto single preBötC neurons in dogs neither changes the depression in respiratory frequency nor affects neuronal discharge. In fact in dog, microinjection of DAMGO into the pre-BötC region increases respiratory rate. Nevertheless, intravenous naloxone reverses the respiratory depression. Bilateral injection of the μ -opioid receptor agonist DAMGO into the preBötC of awake goats also has no significant effect on respiratory rhythm or pattern during eupneic conditions (Krause et al., 2009). However identification of the preBötC was based on NK1 immuno and relative location from the nucleus ambiguus and the facial nucleus only and did not include mapping to identify the opioid sensitive “hotspot” as done by Montandon et al. 2011.

One possible explanation for the discrepancy of these effects *in vivo* is the difference in preparation. In preparations where the entire respiratory network is intact there would be greater capability for compensation by excitatory inputs into the preBötC for the presumed depressant effect of DAMGO on preBötC inspiratory neurons than in anesthetized

preparations with reduced drive to cortical regions. This would suggest that descending input from the cortex has an important role in opioid induced respiratory depression. However, work in decerebrate dogs showed no effect of opioids on the preBötC regulation of breathing (Mustapic et al., 2010) contradicting this theory. Alternatively, there may be species differences in the site mediating opioid induced respiratory depression. There are other sites in the brainstem that may be involved in mediating the mechanism opioid drugs use to suppress breathing (Xia and Haddad, 1991; Gray et al., 1999; Manzke et al., 2003; McCrimmon and Alheid, 2003; Lalley, 2006) and regulate the preBötC output. In dogs, the presence of dense μ -opioid receptors in the parabrachial nuclei of the pons and NTS suggest that these could be potential sites where systemic opioids could produce their effect on breathing rate (Mustapic et al., 2010). Although there may be several sites that express μ -opioid receptors and could influence the respiratory network, (Montandon et al., 2011) present strong evidence for the importance of the preBötC as the site of opioid inhibition. Bilateral microdialysis administration of naloxone in the preBötC hotspot (verified by NK1 expression) *in vivo*, completely prevented the inhibitory effects of systemic opioid administration. In contrast, experiments in dogs show no effects of opioids in the preBötC, were using single injections and may not have been targeting the NK1 preBötC hotspot (Stucke et al., 2008; Mustapic et al., 2010). The importance of targeting NK1R expressing neurons is clear. Cells in the preBötC co-label for NK1 and μ -opioid receptors (Gray et al., 1999) and mice missing tachykinin 1 gene (encodes precursor protein of NK1 ligand SP) showed reduced morphine induced respiratory depression (Bilkei-Gorzo et al., 2010). Conflicting findings *in vivo* may simply reflect the challenge of injecting targeting the discrete region of the preBötC. Give the recent findings in rat *in vivo*, the preBötC is clearly important in mediating the inhibitory effects of opioids on respiratory rhythm in rat. However, these findings need to be replicated in other animal models.

5.4.2 Acute TLR4 activation in the preBötC does not modulate rhythm

The effects of inflammatory cytokines on synaptic signaling and plasticity are evident in several neural networks. For example, in hippocampus the proinflammatory cytokine IL-18 impairs long-term potentiation 20 min after application and NMDAR signaling providing evidence of a direct neuromodulatory role for IL-18 in synaptic plasticity (Curran and O'Connor, 2001). Similarly, synaptic transmission in the spinal cord is powerfully regulated by microglial mediators, TNF- α (>2hrs incubation), IL-1 β (<2min incubation), and BDNF (<90min incubation), that enhance excitatory synaptic transmission, suppress inhibitory synaptic transmission (Coull et al., 2005; Kawasaki et al., 2008; Li et al., 2009) and induce spinal long-term potentiation (Liu et al., 2007; Zhou et al., 2008; Zhou et al., 2011)(via TNF- α and BDNF). Nerve injury induces TNF α , which stimulates AMPAR subunit phosphorylation and trafficking to the membrane (Choi et al., 2010) in dorsal horn neurons, and facilitates NMDA receptor phosphorylation in the rostral ventromedial medulla (Wei et al., 2008). These findings strengthen the view that glia-derived proinflammatory cytokines interact with excitatory amino acid receptors.

For microglial signaling to contribute to the morphine-induced respiratory depression (Hutchinson et al., 2008a), the proinflammatory mediators released from the morphine-activated, TLR4-microglial pathway would need to affect neuronal excitability on a relatively rapid time scale; i.e., in the order of minutes. It is well established that microglia play an important role in the long-term modulation of neural networks. TLR4 activation of microglia influences neuronal networks in several CNS pathologies including Alzheimer's disease (Minoretti et al., 2006; Tan et al., 2008), ischemic stroke (Caso et al., 2007; Abate et al., 2010) and chronic pain (Nicotra et al., 2012). For example, TLR-induced proinflammatory cytokines contribute to the initiation and maintenance of chronic pain states (Grace et al.,

2011). The slow timescale required for activation of these pathways, however, is not consistent with the rapid onset of the opioid-induced respiratory depression. The TLR4 transcriptional upregulation that occurs in the initiation of pathological pain and the TLR4 transcriptional events associated with acute inflammation occur within 4 h throughout the CNS including the lumbar spinal cord, brain stem and forebrain (Raghavendra et al., 2004b). In the hippocampus, inflammatory cytokines released in response to TLR4 activation inhibit long-term potentiation of hippocampal synapses over relatively short time scales (20 min), but these data do not take into account the time required from TLR4 activation to initiate cytokine release (Curran and O'Connor, 2001).

The activity of respiratory networks is also sensitive to inflammatory mediators. Systemic LPS injection alters breathing frequency and minute ventilation 24 hrs post injection in unanesthetized Lewis rats (Huxtable et al., 2011). Systemic LPS also decreases the hypoxic ventilatory response in a variety of animals (for review see (Huxtable et al., 2011)). These LPS-induced respiratory changes could reflect direct actions of inflammatory mediators on brainstem centers controlling frequency or indirect actions via sensory receptors that project to these rhythm-generating neurons. Some central involvement is supported by the observation in neonatal rats that intratracheal endotoxin increases expression of proinflammatory cytokines in the caudal nucleus tractus solitarius (NTS) and area postrema of the central respiratory network, and that these changes contribute to the blunting of the ventilatory response to hypoxia (Balan et al., 2011). However, the timescale is still in question. None of these effects appear to occur rapidly enough to support a role for inflammatory mediators in the opioid-induced respiratory depression. Our data are consistent with a slow time course. Microinjection of the TLR4 agonist LPS directly into the preBötC *in vitro* had no effect on respiratory rhythm. We are confident in the negative conclusion because injection of the NK1R agonist SP into the same site produced a robust frequency increase, confirming injection into the preBötC. Thus, while over long time scales it appears that LPS-induced inflammatory processes can modulate central respiratory network activity,

possibly playing a role in the adaptive/plastic changes that occur in respiratory control during chronic disease, LPS-sensitive pathways do not acutely influence the activity of preBötC networks.

In summary, our *in vitro* and *in vivo* data strongly suggest that the respiratory depression evoked by acute DAMGO administration does not involve TLR4 and acute fentanyl administration does not involve TLR4 or microglia. Whether chronic opioid activation of TLR4 signaling and microglia has longer-term effects on respiratory control is not known.

5.5 References

- Abate W, Alghaithy AA, Parton J, Jones KP, Jackson SK (2010) Surfactant lipids regulate LPS-induced interleukin-8 production in A549 lung epithelial cells by inhibiting translocation of TLR4 into lipid raft domains. *J Lipid Res* 51:334-344.
- Balan KV, Kc P, Hoxha Z, Mayer CA, Wilson CG, Martin RJ (2011) Vagal afferents modulate cytokine-mediated respiratory control at the neonatal medulla oblongata. *Respir Physiol Neurobiol* 178:458-464.
- Ballanyi K, Panaitescu B, Ruangkittisakul A (2010) Indirect opioid actions on inspiratory pre-Botzinger complex neurons in newborn rat brainstem slices. *Adv Exp Med Biol* 669:75-79.
- Ballanyi K, Lalley PM, Hoch B, Richter DW (1997) cAMP-dependent reversal of opioid- and prostaglandin-mediated depression of the isolated respiratory network in newborn rats. *J Physiol* 504 (Pt 1):127-134.
- Baumgartner U, Buchholz HG, Belosevich A, Magerl W, Siessmeier T, Rolke R, Hohnemann S, Piel M, Rosch F, Wester HJ, Henriksen G, Stoeter P, Bartenstein P,

- Treede RD, Schreckenberger M (2006) High opiate receptor binding potential in the human lateral pain system. *Neuroimage* 30:692-699.
- Benvenga MJ, Del Vecchio RA, Capacchione JF, Jerussi TP (1992) An in vivo alpha-2 assay reversal of opioid-induced muscular rigidity and neuroleptic-induced ptosis. *J Pharmacol Toxicol Methods* 27:45-50.
- Bilkei-Gorzo A, Berner J, Zimmermann J, Wickstrom R, Racz I, Zimmer A (2010) Increased morphine analgesia and reduced side effects in mice lacking the tac1 gene. *Br J Pharmacol* 160:1443-1452.
- Burns LH, Wang HY (2010) PTI-609: a novel analgesic that binds filamin A to control opioid signaling. *Recent patents on CNS drug discovery* 5:210-220.
- Caso JR, Pradillo JM, Hurtado O, Lorenzo P, Moro MA, Lizasoain I (2007) Toll-like receptor 4 is involved in brain damage and inflammation after experimental stroke. *Circulation* 115:1599-1608.
- Choi JI, Svensson CI, Koehrn FJ, Bhuskute A, Sorkin LS (2010) Peripheral inflammation induces tumor necrosis factor dependent AMPA receptor trafficking and Akt phosphorylation in spinal cord in addition to pain behavior. *Pain* 149:243-253.
- Coller JK, Hutchinson MR (2012) Implications of central immune signaling caused by drugs of abuse: mechanisms, mediators and new therapeutic approaches for prediction and treatment of drug dependence. *Pharmacology & therapeutics* 134:219-245.
- Coull JA, Beggs S, Boudreau D, Boivin D, Tsuda M, Inoue K, Gravel C, Salter MW, De Koninck Y (2005) BDNF from microglia causes the shift in neuronal anion gradient underlying neuropathic pain. *Nature* 438:1017-1021.

Curran B, O'Connor JJ (2001) The pro-inflammatory cytokine interleukin-1 β impairs long-term potentiation and NMDA receptor-mediated transmission in the rat hippocampus in vitro. *Neuroscience* 108:83-90.

Grace PM, Rolan PE, Hutchinson MR (2011) Peripheral immune contributions to the maintenance of central glial activation underlying neuropathic pain. *Brain Behav Immun* 25:1322-1332.

Gray PA, Rekling JC, Bocchiaro CM, Feldman JL (1999) Modulation of respiratory frequency by peptidergic input to rhythmogenic neurons in the preBotzinger complex. *Science* 286:1566-1568.

Greer JJ, Funk GD, Ballanyi K (2006) Preparing for the first breath: prenatal maturation of respiratory neural control. *J Physiol* 570:437-444.

Gutteridge JM (1992) Iron and oxygen radicals in brain. *Ann Neurol* 32 Suppl:S16-21.

Hanke ML, Kielian T (2011) Toll-like receptors in health and disease in the brain: mechanisms and therapeutic potential. *Clin Sci (Lond)* 121:367-387.

He L, Li H, Chen L, Miao J, Jiang Y, Zhang Y, Xiao Z, Hanley G, Li Y, Zhang X, LeSage G, Peng Y, Yin D (2011) Toll-like receptor 9 is required for opioid-induced microglia apoptosis. *PLoS One* 6:e18190.

Howard RF (2003) Current status of pain management in children. *JAMA* 290:2464-2469.

Hutchinson MR, Shavit Y, Grace PM, Rice KC, Maier SF, Watkins LR (2011) Exploring the neuroimmunopharmacology of opioids: an integrative review of mechanisms of central immune signaling and their implications for opioid analgesia. *Pharmacol Rev* 63:772-810.

- Hutchinson MR, Zhang Y, Brown K, Coats BD, Shridhar M, Sholar PW, Patel SJ, Crysdale NY, Harrison JA, Maier SF, Rice KC, Watkins LR (2008a) Non-stereoselective reversal of neuropathic pain by naloxone and naltrexone: involvement of toll-like receptor 4 (TLR4). *Eur J Neurosci* 28:20-29.
- Hutchinson MR, Northcutt AL, Chao LW, Kearney JJ, Zhang Y, Berkelhammer DL, Loram LC, Rozeske RR, Bland ST, Maier SF, Gleeson TT, Watkins LR (2008b) Minocycline suppresses morphine-induced respiratory depression, suppresses morphine-induced reward, and enhances systemic morphine-induced analgesia. *Brain Behav Immun* 22:1248-1256.
- Hutchinson MR, Lewis SS, Coats BD, Skyba DA, Crysdale NY, Berkelhammer DL, Brzeski A, Northcutt A, Vietz CM, Judd CM, Maier SF, Watkins LR, Johnson KW (2009) Reduction of opioid withdrawal and potentiation of acute opioid analgesia by systemic AV411 (ibudilast). *Brain Behav Immun* 23:240-250.
- Hutchinson MR et al. (2010) Evidence that opioids may have toll-like receptor 4 and MD-2 effects. *Brain Behav Immun* 24:83-95.
- Hutchinson MR et al. (2012) Opioid Activation of Toll-Like Receptor 4 Contributes to Drug Reinforcement. *J Neurosci* 32:in press.
- Huxtable AG, Zwicker JD, Poon BY, Pagliardini S, Vrouwe SQ, Greer JJ, Funk GD (2009) Tripartite purinergic modulation of central respiratory networks during perinatal development: the influence of ATP, ectonucleotidases, and ATP metabolites. *J Neurosci* 29:14713-14725.

Huxtable AG, Vinit S, Windelborn JA, Crader SM, Guenther CH, Watters JJ, Mitchell GS (2011) Systemic inflammation impairs respiratory chemoreflexes and plasticity. *Respir Physiol Neurobiol* 178:482-489.

Huxtable AG, Zwicker JD, Alvares TS, Ruangkittisakul A, Fang X, Hahn LB, Posse de Chaves E, Baker GB, Ballanyi K, Funk GD (2010) Glia contribute to the purinergic modulation of inspiratory rhythm-generating networks. *J Neurosci* 30:3947-3958.

Johnson SM, Smith JC, Feldman JL (1996) Modulation of respiratory rhythm in vitro: role of Gi/o protein-mediated mechanisms. *J Appl Physiol* 80:2120-2133.

Johnston IN, Milligan ED, Wieseler-Frank J, Frank MG, Zapata V, Campisi J, Langer S, Martin D, Green P, Fleshner M, Leinwand L, Maier SF, Watkins LR (2004) A role for proinflammatory cytokines and fractalkine in analgesia, tolerance, and subsequent pain facilitation induced by chronic intrathecal morphine. *J Neurosci* 24:7353-7365.

Kalish RS, Koujak S (2004) Minocycline inhibits antigen processing for presentation to human T cells: additive inhibition with chloroquine at therapeutic concentrations. *Clin Immunol* 113:270-277.

Kawasaki Y, Zhang L, Cheng JK, Ji RR (2008) Cytokine mechanisms of central sensitization: distinct and overlapping role of interleukin-1beta, interleukin-6, and tumor necrosis factor-alpha in regulating synaptic and neuronal activity in the superficial spinal cord. *J Neurosci* 28:5189-5194.

Kloppenburg M, Brinkman BM, de Rooij-Dijk HH, Miltenburg AM, Daha MR, Breedveld FC, Dijkmans BA, Verweij C (1996) The tetracycline derivative minocycline differentially affects cytokine production by monocytes and T lymphocytes. *Antimicrob Agents Chemother* 40:934-940.

- Krause KL, Neumueller SE, Marshall BD, Kiner T, Bonis JM, Pan LG, Qian B, Forster HV (2009) Micro-opioid receptor agonist injections into the presumed pre-Botzinger complex and the surrounding region of awake goats do not alter eupneic breathing. *J Appl Physiol* 107:1591-1599.
- Lalley PM (2003) Mu-opioid receptor agonist effects on medullary respiratory neurons in the cat: evidence for involvement in certain types of ventilatory disturbances. *Am J Physiol Regul Integr Comp Physiol* 285:R1287-1304.
- Lalley PM (2006) Opiate slowing of feline respiratory rhythm and effects on putative medullary phase-regulating neurons. *Am J Physiol Regul Integr Comp Physiol* 290:R1387-1396.
- Leedeboer A, Hutchinson MR, Watkins LR, Johnson KW (2007) Ibudilast (AV-411). A new class therapeutic candidate for neuropathic pain and opioid withdrawal syndromes. *Expert Opin Investig Drugs* 16:935-950.
- Li J, Xie W, Zhang JM, Baccei ML (2009) Peripheral nerve injury sensitizes neonatal dorsal horn neurons to tumor necrosis factor-alpha. *Mol Pain* 5:10.
- Li Y, Li H, Zhang Y, Sun X, Hanley GA, LeSage G, Zhang Y, Sun S, Peng Y, Yin D (2010) Toll-like receptor 2 is required for opioids-induced neuronal apoptosis. *Biochemical and biophysical research communications* 391:426-430.
- Liu G, Feldman JL, Smith JC (1990) Excitatory amino acid-mediated transmission of inspiratory drive to phrenic motoneurons. *J Neurophysiol* 64:423-436.
- Liu L, Coller JK, Watkins LR, Somogyi AA, Hutchinson MR (2011) Naloxone-precipitated morphine withdrawal behavior and brain IL-1beta expression: comparison of different mouse strains. *Brain Behav Immun* 25:1223-1232.

- Liu W, Wang CH, Cui Y, Mo LQ, Zhi JL, Sun SN, Wang YL, Yu HM, Zhao CM, Feng JQ, Chen PX (2006) Inhibition of neuronal nitric oxide synthase antagonizes morphine antinociceptive tolerance by decreasing activation of p38 MAPK in the spinal microglia. *Neurosci Lett* 410:174-177.
- Liu WT, Han Y, Liu YP, Song AA, Barnes B, Song XJ (2010) Spinal matrix metalloproteinase-9 contributes to physical dependence on morphine in mice. *J Neurosci* 30:7613-7623.
- Liu YL, Zhou LJ, Hu NW, Xu JT, Wu CY, Zhang T, Li YY, Liu XG (2007) Tumor necrosis factor-alpha induces long-term potentiation of C-fiber evoked field potentials in spinal dorsal horn in rats with nerve injury: the role of NF-kappa B, JNK and p38 MAPK. *Neuropharmacology* 52:708-715.
- Lorier AR, Lipski J, Housley GD, Greer JJ, Funk GD (2008) ATP sensitivity of preBotzinger complex neurones in neonatal rat in vitro: mechanism underlying a P2 receptor-mediated increase in inspiratory frequency. *J Physiol* 586:1429-1446.
- Lorier AR, Huxtable AG, Robinson DM, Lipski J, Housley GD, Funk GD (2007) P2Y1 receptor modulation of the pre-Botzinger complex inspiratory rhythm generating network in vitro. *J Neurosci* 27:993-1005.
- Maier K, Merkler D, Gerber J, Taheri N, Kuhnert AV, Williams SK, Neusch C, Bahr M, Diem R (2007) Multiple neuroprotective mechanisms of minocycline in autoimmune CNS inflammation. *Neurobiol Dis* 25:514-525.
- Mansson R, Hansson MJ, Morota S, Uchino H, Ekdahl CT, Elmer E (2007) Re-evaluation of mitochondrial permeability transition as a primary neuroprotective target of minocycline. *Neurobiol Dis* 25:198-205.

- Manzke T, Guenther U, Ponimaskin EG, Haller M, Dutschmann M, Schwarzacher S, Richter DW (2003) 5-HT₄(a) receptors avert opioid-induced breathing depression without loss of analgesia. *Science* 301:226-229.
- Mao J, Sung B, Ji RR, Lim G (2002) Chronic morphine induces downregulation of spinal glutamate transporters: implications in morphine tolerance and abnormal pain sensitivity. *J Neurosci* 22:8312-8323.
- McCrimmon DR, Alheid GF (2003) On the opiate trail of respiratory depression. *Am J Physiol Regul Integr Comp Physiol* 285:R1274-1275.
- Minoretti P, Gazzaruso C, Vito CD, Emanuele E, Bianchi M, Coen E, Reino M, Geroldi D (2006) Effect of the functional toll-like receptor 4 Asp299Gly polymorphism on susceptibility to late-onset Alzheimer's disease. *Neurosci Lett* 391:147-149.
- Montandon G, Qin W, Liu H, Ren J, Greer JJ, Horner RL (2011) PreBotzinger complex neurokinin-1 receptor-expressing neurons mediate opioid-induced respiratory depression. *J Neurosci* 31:1292-1301.
- Morin-Surun MP, Boudinot E, Dubois C, Matthes HW, Kieffer BL, Denavit-Saubie M, Champagnat J, Foutz AS (2001) Respiratory function in adult mice lacking the mu-opioid receptor: role of delta-receptors. *Eur J Neurosci* 13:1703-1710.
- Mustapic S, Radocaj T, Sanchez A, Dogas Z, Stucke AG, Hopp FA, Stuth EA, Zuperku EJ (2010) Clinically relevant infusion rates of mu-opioid agonist remifentanil cause bradypnea in decerebrate dogs but not via direct effects in the pre-Botzinger complex region. *J Neurophysiol* 103:409-418.
- Narita M, Miyatake M, Narita M, Shibasaki M, Shindo K, Nakamura A, Kuzumaki N, Nagumo Y, Suzuki T (2006) Direct evidence of astrocytic modulation in the

- development of rewarding effects induced by drugs of abuse.
Neuropsychopharmacology 31:2476-2488.
- Nicotra L, Loram LC, Watkins LR, Hutchinson MR (2012) Toll-like receptors in chronic pain. *Exp Neurol* 234:316-329.
- Nikodemova M, Watters JJ, Jackson SJ, Yang SK, Duncan ID (2007) Minocycline down-regulates MHC II expression in microglia and macrophages through inhibition of IRF-1 and protein kinase C (PKC) α/β II. *J Biol Chem* 282:15208-15216.
- Nutile-McMenemy N, Elfenbein A, Deleo JA (2007) Minocycline decreases in vitro microglial motility, β 1-integrin, and Kv1.3 channel expression. *J Neurochem* 103:2035-2046.
- Osikowicz M, Skup M, Mika J, Makuch W, Czarkowska-Bauch J, Przewlocka B (2009) Glial inhibitors influence the mRNA and protein levels of mGlu2/3, 5 and 7 receptors and potentiate the analgesic effects of their ligands in a mouse model of neuropathic pain. *Pain* 147:175-186.
- Pattinson KT (2008) Opioids and the control of respiration. *Br J Anaesth* 100:747-758.
- Pattinson KT, Governo RJ, MacIntosh BJ, Russell EC, Corfield DR, Tracey I, Wise RG (2009) Opioids depress cortical centers responsible for the volitional control of respiration. *J Neurosci* 29:8177-8186.
- Raghavendra V, Rutkowski MD, DeLeo JA (2002) The role of spinal neuroimmune activation in morphine tolerance/hyperalgesia in neuropathic and sham-operated rats. *J Neurosci* 22:9980-9989.

Raghavendra V, Tanga FY, DeLeo JA (2004a) Complete Freunds adjuvant-induced peripheral inflammation evokes glial activation and proinflammatory cytokine expression in the CNS. *Eur J Neurosci* 20:467-473.

Raghavendra V, Tanga FY, DeLeo JA (2004b) Attenuation of morphine tolerance, withdrawal-induced hyperalgesia, and associated spinal inflammatory immune responses by propentofylline in rats. *Neuropsychopharmacology* 29:327-334.

Ramirez JM, Telgkamp P, Elsen FP, Quellmalz UJ, Richter DW (1997) Respiratory rhythm generation in mammals: synaptic and membrane properties. *Respir Physiol* 110:71-85.

Ren J, Poon BY, Tang Y, Funk GD, Greer JJ (2006) Ampakines alleviate respiratory depression in rats. *Am J Respir Crit Care Med* 174:1384-1391.

Romberg R, Sarton E, Teppema L, Matthes HW, Kieffer BL, Dahan A (2003) Comparison of morphine-6-glucuronide and morphine on respiratory depressant and antinociceptive responses in wild type and mu-opioid receptor deficient mice. *Br J Anaesth* 91:862-870.

Ruangkittisakul A, Ballanyi K (2010) Methylxanthine reversal of opioid-evoked inspiratory depression via phosphodiesterase-4 blockade. *Respir Physiol Neurobiol* 172:94-105.

Ruangkittisakul A, Panaitescu B, Ballanyi K (2010) K(+) and Ca(2)(+) dependence of inspiratory-related rhythm in novel "calibrated" mouse brainstem slices. *Respir Physiol Neurobiol* 175:37-48.

Ruangkittisakul A, Schwarzacher SW, Secchia L, Poon BY, Ma Y, Funk GD, Ballanyi K (2006) High sensitivity to neuromodulator-activated signaling pathways at

- physiological [K+] of confocally imaged respiratory center neurons in on-line-calibrated newborn rat brainstem slices. *J Neurosci* 26:11870-11880.
- Scamman FL (1983) Fentanyl-O₂-N₂O rigidity and pulmonary compliance. *Anesth Analg* 62:332-334.
- Schwarz JM, Sholar PW, Bilbo SD (2012) Sex differences in microglial colonization of the developing rat brain. *J Neurochem* 120:948-963.
- Shavit Y, Wolf G, Goshen I, Livshits D, Yirmiya R (2005) Interleukin-1 antagonizes morphine analgesia and underlies morphine tolerance. *Pain* 115:50-59.
- Smith JC, Ellenberger HH, Ballanyi K, Richter DW, Feldman JL (1991) Pre-Botzinger complex: a brainstem region that may generate respiratory rhythm in mammals. *Science* 254:726-729.
- Song P, Zhao ZQ (2001) The involvement of glial cells in the development of morphine tolerance. *Neurosci Res* 39:281-286.
- Stucke AG, Zuperku EJ, Sanchez A, Tonkovic-Capin M, Tonkovic-Capin V, Mustapic S, Stuth EA (2008) Opioid receptors on bulbospinal respiratory neurons are not activated during neuronal depression by clinically relevant opioid concentrations. *J Neurophysiol* 100:2878-2888.
- Tai YH, Wang YH, Wang JJ, Tao PL, Tung CS, Wong CS (2006) Amitriptyline suppresses neuroinflammation and up-regulates glutamate transporters in morphine-tolerant rats. *Pain* 124:77-86.
- Takeda S, Eriksson LI, Yamamoto Y, Joensen H, Onimaru H, Lindahl SG (2001) Opioid action on respiratory neuron activity of the isolated respiratory network in newborn rats. *Anesthesiology* 95:740-749.

- Tan L, Schedl P, Song HJ, Garza D, Konsolaki M (2008) The Toll-->NFkappaB signaling pathway mediates the neuropathological effects of the human Alzheimer's Abeta42 polypeptide in Drosophila. *PLoS One* 3:e3966.
- Tanga FY, Raghavendra V, DeLeo JA (2004) Quantitative real-time RT-PCR assessment of spinal microglial and astrocytic activation markers in a rat model of neuropathic pain. *Neurochem Int* 45:397-407.
- Teng YD, Choi H, Onario RC, Zhu S, Desilets FC, Lan S, Woodard EJ, Snyder EY, Eichler ME, Friedlander RM (2004) Minocycline inhibits contusion-triggered mitochondrial cytochrome c release and mitigates functional deficits after spinal cord injury. *Proc Natl Acad Sci U S A* 101:3071-3076.
- Terashvili M, Wu HE, Schwasinger ET, Hung KC, Hong JS, Tseng LF (2008) (+)-Morphine attenuates the (-)-morphine-produced conditioned place preference and the mu-opioid receptor-mediated dopamine increase in the posterior nucleus accumbens of the rat. *Eur J Pharmacol* 587:147-154.
- Tibboel D, Anand KJ, van den Anker JN (2005) The pharmacological treatment of neonatal pain. *Semin Fetal Neonatal Med* 10:195-205.
- Tikka T, Fiebich BL, Goldsteins G, Keinanen R, Koistinaho J (2001) Minocycline, a tetracycline derivative, is neuroprotective against excitotoxicity by inhibiting activation and proliferation of microglia. *J Neurosci* 21:2580-2588.
- Wamsley JK (1983) Opioid receptors: autoradiography. *Pharmacol Rev* 35:69-83.
- Wang X, Loram LC, Ramos K, de Jesus AJ, Thomas J, Cheng K, Reddy A, Somogyi AA, Hutchinson MR, Watkins LR, Yin H (2012) Morphine activates neuroinflammation in a manner parallel to endotoxin. *Proc Natl Acad Sci U S A* 109:6325-6330.

Watkins LR, Hutchinson MR, Rice KC, Maier SF (2009) The "toll" of opioid-induced glial activation: improving the clinical efficacy of opioids by targeting glia. *Trends Pharmacol Sci* 30:581-591.

Wei F, Guo W, Zou S, Ren K, Dubner R (2008) Supraspinal glial-neuronal interactions contribute to descending pain facilitation. *J Neurosci* 28:10482-10495.

Wilkins A, Nikodemova M, Compston A, Duncan I (2004) Minocycline attenuates nitric oxide-mediated neuronal and axonal destruction in vitro. *Neuron Glia Biol* 1:297-305.

Wu N, Lu XQ, Yan HT, Su RB, Wang JF, Liu Y, Hu G, Li J (2008) Aquaporin 4 deficiency modulates morphine pharmacological actions. *Neurosci Lett* 448:221-225.

Xia Y, Haddad GG (1991) Ontogeny and distribution of opioid receptors in the rat brainstem. *Brain Res* 549:181-193.

Yrjanheikki J, Keinanen R, Pellikka M, Hokfelt T, Koistinaho J (1998) Tetracyclines inhibit microglial activation and are neuroprotective in global brain ischemia. *Proc Natl Acad Sci U S A* 95:15769-15774.

Yrjanheikki J, Tikka T, Keinanen R, Goldsteins G, Chan PH, Koistinaho J (1999) A tetracycline derivative, minocycline, reduces inflammation and protects against focal cerebral ischemia with a wide therapeutic window. *Proc Natl Acad Sci U S A* 96:13496-13500.

Zhang Y, Li H, Li Y, Sun X, Zhu M, Hanley G, Lesage G, Yin D (2011) Essential role of toll-like receptor 2 in morphine-induced microglia activation in mice. *Neurosci Lett* 489:43-47.

Zhou LJ, Zhong Y, Ren WJ, Li YY, Zhang T, Liu XG (2008) BDNF induces late-phase LTP of C-fiber evoked field potentials in rat spinal dorsal horn. *Exp Neurol* 212:507-514.

Zhou LJ, Yang T, Wei X, Liu Y, Xin WJ, Chen Y, Pang RP, Zang Y, Li YY, Liu XG Brain-derived neurotrophic factor contributes to spinal long-term potentiation and mechanical hypersensitivity by activation of spinal microglia in rat. *Brain Behav Immun* 25:322-334.

Zhou LJ, Yang T, Wei X, Liu Y, Xin WJ, Chen Y, Pang RP, Zang Y, Li YY, Liu XG (2011) Brain-derived neurotrophic factor contributes to spinal long-term potentiation and mechanical hypersensitivity by activation of spinal microglia in rat. *Brain Behav Immun* 25:322-334.

Zwicker JD, Rajani V, Hahn LB, Funk GD (2011) Purinergic modulation of preBotzinger complex inspiratory rhythm in rodents: the interaction between ATP and adenosine. *J Physiol* 589:4583-4600.

Chapter 6: General Discussion

6.1 Introduction

Ventilation is regulated by the brainstem motor network, which maintains homeostatic control of arterial oxygen, CO₂ and pH at physiological levels. The brainstem neural network must remain highly dynamic and adaptable to maintain these homeostatic levels and this is achieved, in part, through its modulation by a variety of neurotransmitters. A greater understanding of the mechanisms through which these neuromodulators and associated signaling cascades impact respiratory network behavior is needed. These neuromodulatory systems are implicated in breathing-related central nervous system disorders such as central and obstructive sleep apnea and apnea of prematurity (Martin et al., 2004) and a better understanding of these mechanisms will result in advancements in pharmacological therapies. In this context, the objective of my thesis research has been to explore the significance of the 3-part purinergic signaling system for preBötC networks in rodents using rhythmically active medullary slices from rats and mice, primary cultures of preBötC glia, and anesthetized adult rats. Increasing support is evident for the involvement of ATP in neuronal and glial communication (Butt, 2011; Koles et al., 2011) and I have identified that glia may have an important role in the purinergic modulation of the preBötC inspiratory rhythm generating network. The dynamics of this purinergic modulation is dependent on expression of P2 and P1 receptors within the network, as well as the ectonucleotidases that degrade ATP into ADO. The balance of this modulation is different between species and throughout development. This modulatory system is important for maintaining homeostasis, as evident in the important role of ATP in offsetting the secondary hypoxic ventilatory depression *in vivo* (Gourine et al., 2005). However, we are only starting to understand the impact of purinergic signaling, likely mediated at least in part by glia cells, in central inspiratory control. This understanding will be critical for advancements in understanding pathology affecting the preBötC. It is also important to consider the function other glia cells, particularly microglia, might have in inflammatory processes within the preBötC as this is a

critical, yet unexplored area. In this discussion I will address the importance of glia in the purinergic modulation of the preBötC inspiratory rhythm generating network and the advancements needed *in vivo* to further our understanding of complex physiological processes such as the hypoxic ventilatory response.

6.2 Purinergic modulation of the central respiratory network by glia

Gone are the days when glia were thought to be simply the ‘glue’ or support cells of the CNS. There are now numerous studies showing that glia have an active role in communication throughout the CNS (reviewed in (Deitmer et al., 1998; Allen and Barres, 2005; Fiacco and McCarthy, 2006; Barres, 2008). Functional roles for glia cells have been established including myelination, immune response, ion and transmitter homeostasis, as well as active participation in synaptic plasticity and neuronal excitability illustrating their diversity and significance (Mulkey et al., 2010; Deitmer et al., 1998; Allen and Barres, 2005; Fiacco and McCarthy, 2006; Barres, 2008). While classification has varied based on cell location or morphology, it seems that classification of glial cells and their subpopulations based on more functional roles may be a better categorization of this diverse cell population. As such, glia can be classified into four subpopulations: microglia, oligodendrocytes, polydendrocytes and astrocytes, with each category distinguished based on function, immunoreactivity and electrophysiology (see recent review for criteria (Mulkey et al., 2010; Deitmer et al., 1998; Allen and Barres, 2005; Fiacco and McCarthy, 2006; Barres, 2008). Oligodendrocytes are myelin producing cells and polydendrocytes are NG2-expressing, glial precursor cells present throughout life (Nishiyama et al., 2009). Astrocytes are the largest class of glial cells and can be divided further based on location into protoplasmic and fibrous astrocytes in the gray and white matter respectively. These cells are highly associated with the surrounding vasculature with fine processes surrounding blood vessels as well as neurons and synapses. Two types of astrocytes have been identified within

the preBötC, however, functional roles remains unclear (Grass et al., 2004). In contrast, microglia are immunocompetent cells of the central nervous system. In their “resting” state microglia interact with other cells in the CNS and respond to a variety of physiological signals. They can be activated by injury/toxicity, and once activated, microglia undergo morphological changes, upregulate P2X and P2Y receptors and secrete high levels of pro-inflammatory cytokines. In this thesis, I have looked at both astrocytes and microglia and their influence on the central respiratory network under specific conditions. A better understanding of these cells and how they modulate the central respiratory network will advance our current understanding of the neural control of breathing. Additionally, understanding how glia modulate the respiratory network will shed light on the potential roles for these cells throughout the CNS in health and disease states.

The aim of Chapter II was to assess the hypothesis that glial cells contribute to the frequency increase evoked by ATP in the preBötC. We were specifically interested in determining if glia cells in the preBötC region of the medulla have properties that would enable them to mediate ATP-evoked modulation of the central inspiratory network. Glial cells (presumably astrocytes) play a significant role in the P2Y₁R-mediated frequency increase that is evoked by ATP in the preBötC. We have found that in neonatal rat *in vitro*, agents that disrupt glial function dramatically reduce the frequency increase evoked by ATP in the preBötC without affecting the neuronally mediated SP response. Like glia in many other brain regions (Verkhratsky et al., 2009; Halassa and Haydon, 2010; Koles et al., 2011), preBötC glia express P2Y₁R (Huxtable et al., 2010). We have also established that glia cells are sensitive to ATP, as preBötC astrocytes in slices and in primary culture respond to ATP with increased Ca²⁺ through a P2Y₁R mechanism. These cultured primary preBötC astrocyte respond to ATP by releasing glutamate.

With these findings we have developed our working hypothesis that ATP acts through P2Y₁R on both neurons and glia to activate second messenger cascades that increase intracellular calcium and release glutamate. This glutamate release then excites preBötC

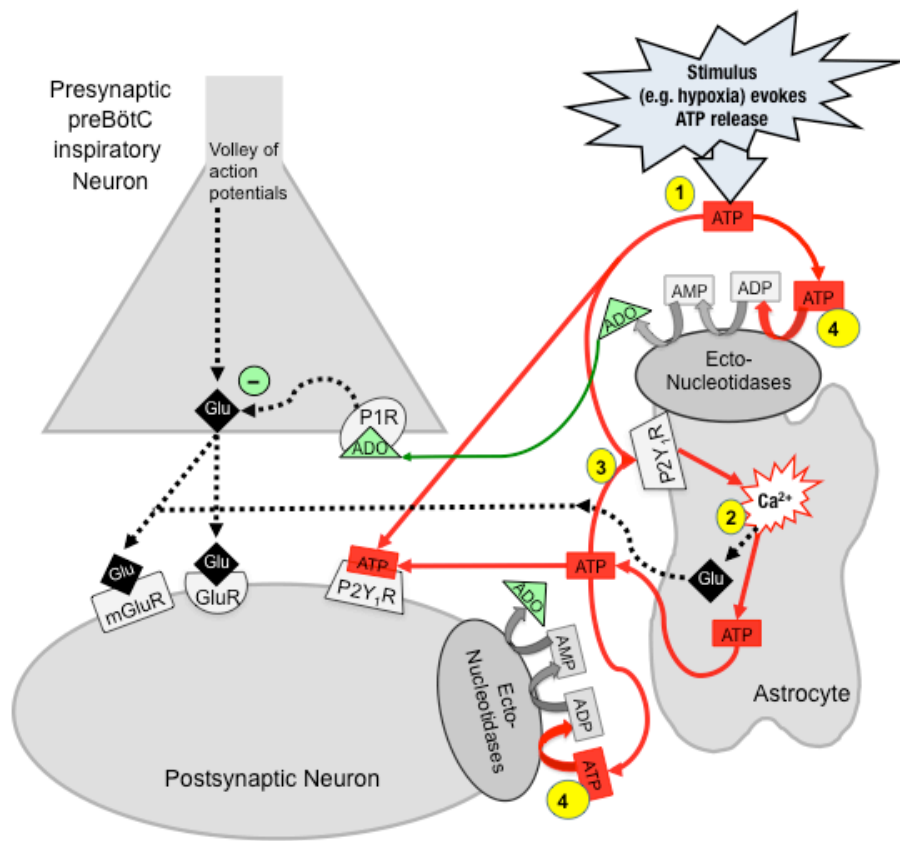


Figure 6.1 Schematic illustrating the mechanisms through which purinergic signaling is hypothesized to modulate activity at the glutamatergic inspiratory synapse and contribute to the hypoxic ventilatory response.

- 1) Hypoxia evokes ATP release, directly activating P2Y₁Rs on neurons and astrocytes.
- 2) $[\text{Ca}^{2+}]$ in the astrocyte increases, causing glutamate and ATP release, which indirectly excite neurons.
- 3) ATP also acts in an autocrine/paracrine manner to enhance gliotransmitter release.
- 4) ATP is degraded by ectonucleotidases, producing ADP (which activates P2Y₁Rs, not shown) and adenosine (ADO), which acts on presynaptic P1Rs to inhibit glutamate release.

inspiratory neurons, ultimately producing an increase in frequency (Fig 6.1). However there still remain several areas where more research is needed. The specific second messenger pathways involved in the increase in Ca^{2+} still needs to be resolved. Glia cells express a large number of G protein coupled receptors (GPCR)(Porter and McCarthy, 1997; Deitmer et al., 1998; Verkhratsky and Steinhauser, 2000), which upon activation result in Ca^{2+} mobilization. GPCR binding will evoke Ca^{2+} oscillations in glia networks, which modulates neuronal networks through gliotransmitter release (Deitmer et al., 1998; Fiacco and McCarthy, 2006; Haydon and Carmignoto, 2006; Santello et al., 2012) highlighting the important role of GPCR and Ca^{2+} in neuron-glia communication. The most common second messenger cascade underlying increases in intracellular Ca^{2+} in astrocytes (in culture and slices *in vitro*) is the phospholipase C (PLC)/ inositol 1,4,5-triphosphate (IP3) pathway, which ultimately causes Ca^{2+} release from the endoplasmic reticulum (Agulhon, 2008), and in some cases, gliotransmitter release. Little is known about the role of glial GPCR in modulating neuronal excitability in functioning CNS neural networks. This reflects the challenge of selectively blocking glial GPCR *in situ* or *in vitro*, as glia and neurons release some of the same neuromodulators and express the same receptors (Porter and McCarthy, 1997; Deitmer et al., 1998; Verkhratsky and Steinhauser, 2000). In primary astrocyte cultures we have found that ATP acts via PLC/IP3 to release Ca^{2+} from intracellular stores (Zwicker et al. unpublished findings). While cultured glia offer several advantages for exploring mechanisms of signal transduction without the confounding influences of neurons, one drawback is that like most cells, the pattern of gene and protein expression in glia can change when grown in culture. Some genes that are not expressed *in vivo* can be expressed in culture; the reverse is also true (Wilhelm et al., 2004; Cahoy et al., 2008). Thus, the role of the PLC/IP3 second messenger cascade, most specifically whether this second messenger pathways underlies the frequency increase evoked by ATP in the preBötC, needs to be explored in more intact preparations.

Based on this thesis and previous work (Gourine et al., 2005; Gourine et al. 2010), there is strong evidence that ATP contributes to the modulation of the central inspiratory

network, specifically within the VRC and preBötC. Whether glutamate contributes to the ATP-evoked increase in frequency remains unclear. The transmitters/modulators most commonly released from glia are glutamate, ATP and D-serine (reviewed in (Agulhon, 2008). Glutamate is the main transmitter underlying fast excitatory synaptic transmission between neurons within respiratory networks (Greer et al., 1991; Funk et al., 1993). ATP-evoked glutamate release occurs in cultured hippocampal astrocytes (Coco et al., 2003) and increases in intracellular Ca^{2+} cause glutamate release in cultured astrocytes (Araque et al., 2000; Bezzi and Volterra, 2001; Pasti et al., 2001). ATP-evoked ATP release can help propagate intracellular Ca^{2+} waves or activate receptors on neighboring neurons or glia cells (Coco et al., 2003). D-serine, in contrast is an allosteric modulator of the NMDA subtype of glutamate receptor that acts at the glycine-binding site to potentiate NMDA currents. In the preBötC, glutamate evokes a dramatic increase in frequency (Funk et al., 1993), as does ATP (Lorier et al., 2007). D-serine has minimal effect (Funk GD, unpublished observations). Thus, if preBötC glia respond to ATP by releasing glutamate or ATP, this would contribute to the frequency increase caused by ATP in the preBötC and would be a plausible explanation for our findings. However, it remains to be determined how the glutamate (or other gliotransmitters) is released and whether this release is Ca^{2+} -dependant.

Glia can release neuroactive agents via a variety of mechanisms including through connexin hemichannels (Ye et al., 2003), volume-regulated anion channels (Kimelberg et al., 1990), reversal of transporters (Szatkowski et al., 1990) and diffusion through ionotropic purinergic receptors, like P2X7 (Duan et al., 2003). However, in the context of controlling network excitability, the Ca^{2+} -dependent release mechanisms are of more interest because they can be activated by chemical signals from other cells and therefore may be involved in the two-way communication between neurons and glia. Consequently, the most likely physiological mode of glutamate release is Ca^{2+} -dependent. Of the Ca^{2+} -dependent mechanisms, a regulated exocytotic vesicular mechanism is most likely (Fiacco and McCarthy, 2006). In culture, glia express a number of vesicular associated proteins. These

proteins are localized preferentially in glial processes and upon a Ca^{2+} increase fuse with the plasma membrane (Bezzi et al., 2004). Novel optogenetic approaches that allow selective stimulation of preBötC astrocytes in *in vitro* and *in vivo* models offer a possible way forward, as recently demonstrated in studies examining the role of astrocytes in central respiratory chemosensitivity (Gourine et al., 2010). Not only will optogenetic approaches enable the selective stimulation of astrocytes in a neural network, but also ultimately the development of viral vectors that can selectively inhibit glia cells will shed new light on the role of these cells within a neural network.

In the context of the above findings, there remain some key questions involving the function of glia in the CNS. One area in need of development is to understand the physiological significance of glia heterogeneity. There is a need for a better understanding of the morphology, development, metabolism, physiology, pathology and most importantly functional heterogeneity among glia cells (for review see (Zhang and Barres, 2010)). Currently, our understanding of glia in the central inspiratory network, along with the majority of work in the CNS, derives from cultured glia *in vitro*. A culture technique that maintains *in vivo* gene expression, or ultimately tools for the selective labeling and manipulation of specific subsets of glia enabling the study of glia heterogeneity *in vivo* is needed. Our work specifically characterized primary astrocyte cultures from the preBötC, however as mentioned earlier, there is a great need for understanding what glia cells from all the subpopulations do in the preBötC and the CNS.

With the use of pharmacology we were able to explore one hypothesized role of microglia in inflammatory processes in the preBötC. Inflammation has profound effects on important neural functions, such as synaptic transmission and plasticity (Di Filippo et al., 2008). However, the impact of inflammation on the neural control of breathing is virtually unknown. In Chapter V we examined the effect of microglia inhibitors on opioid-induced respiratory depression. We found that microglia aren't involved in opioid-induced respiratory depression, however this doesn't exclude the possibility and likelihood that microglia have

an important role in other aspects of the neural control of breathing. For example, changes in inspiratory drive occur at the level of the brainstem very soon after exposure to endotoxin or local microinjection of a pro-inflammatory cytokine (Gresham et al., 2011), however we need to understand the early, acute inflammatory response and how it alters respiratory control immediately following induction of inflammation. In chapter V, I describe experiments where I injected the inflammatory mediator LPS directly into the preBötC and saw no effect. These experiments highlight the need for a better understanding of the time course over which the pro-inflammatory cytokines act on central inspiratory networks. Inflammation impacts neural function in the nervous system such as synaptic transmission and plasticity(Di Filippo et al., 2008; Huxtable et al., 2011), neuropathic pain mechanisms (Watkins et al., 2007; Abbadie et al., 2009) and opioid tolerance, dependence and reward (Watkins et al., 2009). There is a high incidence of inflammatory activity in CNS disorders (Lehnardt, 2010) and more information about the mechanism and time course by which inflammation impairs the neural control of breathing, will potentially shed light on some of these disorders. Unfortunately at this point, little is known about the role played by microglia in systemic and/or neural disorders, let alone what role they play in respiratory-related regions of the CNS.

Another critical aspect to better understanding the function of astrocytes in the CNS is understanding the tripartite synapse and the bidirectional communication that occurs between neurons and astrocytes. In chapter II I have shown that primary astrocyte cultures from the preBötC have P2Y₁ GPCR that activate increases in Ca²⁺. It is clear that astrocytes in culture, *in situ* and *in vivo* in several regions of the brain, express a wide variety of GPCRs that affect a diverse set of signaling cascades, some of which cause increases in astrocytic Ca²⁺ (Porter and McCarthy, 1995; Beck et al., 2004; Agulhon, 2008). However, the physiological role of this GPCR and the subsequent Ca²⁺ increase remains unclear. Reports in the early 1990s first described the phenomena of astrocytes responding to external stimuli with increases in intracellular Ca²⁺ and more importantly that they transmit this signal to

adjacent astrocytes as an intracellular Ca^{2+} wave (ICW) (Cornell-Bell et al., 1990; Charles et al., 1991). These findings revolutionized the way we look at astrocytes in the CNS and sparked further research showing that neuron activity can trigger these Ca^{2+} waves (Dani et al., 1992), and in turn these waves can modulate neuronal activity (Dani et al., 1992; Nedergaard, 1994; Parpura et al., 1994; Kang et al., 1998; Parri et al., 2001). These ICWs are thought to be transmitted through cells by Ca^{2+} mobilizing second messenger cascades that use a combination of gap junctions (Finkbeiner, 1992; Nedergaard, 1994) or P2X7 receptors (Suadicani et al., 2006) and regeneration *de novo* via exocytosis of ATP which activates neighboring cells and helps propagate the ICW (Guthrie et al., 1999; Fumagalli et al., 2003). While it is clear these waves occur *in vitro*, there is controversy over whether these ICW occur *in vivo* and under what physiological and pathological situations these ICW are transmitted to the syncytium (for reviews see (Butt et al., 2004; Scemes and Giaume, 2006; Agulhon, 2008)). Understanding the importance of Ca^{2+} signaling in astrocytes will be critical for interpreting the physiological relevance of astrocyte culture studies (such as our data in chapter II).

One step in better understanding these Ca^{2+} waves will be advancements in the knowledge of the mechanism of gliotransmission within the tripartite synapse and how this modulates both neurons and glia *in vivo*. As mentioned previously, several mechanisms of gliotransmitter release have been described under a variety of reduced experimental conditions. There is much speculation about the significance of each pathway but clarification is required regarding the specific conditions and stimuli important for different types of release. Controversy surrounds the actual role of gliotransmission in modulating synaptic transmission and neuronal excitability.

In astrocyte-neuron co-cultures Ca^{2+} was determined to be necessary and sufficient for gliotransmission to occur (Araque et al., 1999; Parpura and Haydon, 2000) and astrocytes *in situ* were shown to express G_q -coupled metabotropic receptors that could be activated by neurons, evoking gliotransmission (Volterra and Meldolesi, 2005; Halassa et al., 2007;

Henneberger et al., 2010). While findings *in vitro* suggest that gliotransmission occurs, recent work questions the Ca^{2+} -dependency of gliotransmission. Due to the challenge of selectively stimulating glial GPCR *in vivo*, transgenic tools were developed to selectively stimulate or eliminate astrocytic G_q GPCR-mediated Ca^{2+} elevations (Agulhon et al., 2010). This study suggested that astrocyte Ca^{2+} elevations are not sufficient for gliotransmission as the selective stimulation or blocking of G_q GPCR-mediated Ca^{2+} elevations in astrocytes failed to produce changes in neuronal excitatory synaptic activity indicative of gliotransmission. These findings have questioned if the proposed mechanism of gliotransmission is physiologically relevant in healthy brain tissue (reviewed in (Hamilton and Attwell, 2010; Kirchhoff, 2010)). However, the lack of graded inhibition or stimulation of astrocytes with this method has raised questions as to the physiological applicability of these findings as well. Another transgenic mouse model developed selectively expresses dnSNARE only in astrocytes, presumably interfering with exocytosis (Halassa et al., 2009). This mouse model allowed the regulation of the glial source of ADO and findings indicate that astrocytes may contribute to sleep homeostasis. This would suggest that astrocytes can contribute via gliotransmission to circuits underlying behavior. Given the conflicting findings, there remain many unanswered questions regarding gliotransmission. Whether Ca^{2+} elevations alone are sufficient for gliotransmitter release by astrocytes remains to be determined. Due to the tiny size of fine astrocyte processes surrounding synapses, the relevant Ca^{2+} elevations involved in gliotransmission may be too small, too fast, and too local to detect using available Ca^{2+} indicators and two-photon imaging methods (Rusakov et al., 2011), but this remains to be determined. Propagating ICW waves between astrocytes indicating release of gliotransmitters have not been substantiated in healthy brain tissue but are evident in neuropathologies such as epilepsy, stroke and Alzheimer's Disease (for review see (Nedergaard et al., 2010)). However it remains to be resolved if gliotransmission is Ca^{2+} dependent as recent reviews discuss findings both for (Zorec et al., 2012) and against (Agulhon et al., 2012) this theory. To add further complexity to the debate, new findings suggest that in addition to Ca^{2+} , other

signaling molecules produced by activated microglia and reactive astrocytes may be important for gliotransmission (Agulhon et al., 2012). Activation of microglia using a proinflammatory TLR4 ligand LPS, evokes a rapid (minutes) increase in the frequency of excitatory synaptic events in acute hippocampal slices (Pascual et al., 2012). The proposed mechanism included the release of ATP by microglia to activate metabotropic P2Y₁R receptors on astrocytes, triggering glutamate release from astrocytes to modulate synaptic mGluRs. Given that inflammatory processes can transform astrocytes into competent gliotransmitter releasing cells, inflammatory processes need to be considered when addressing the role of Ca²⁺ in gliotransmission. This could implicate astrocytes as potential targets for therapy of neurological disorders as well as neuroinflammatory and neurodegenerative disease. The development of optogenetic tools for selectively activating and ultimately inhibiting GPCR mediated Ca²⁺ increases in astrocytes (Gourine et al., 2010; Figueiredo et al., 2011) will help elucidate the significance of gliotransmission within the CNS. Overall, future work that better characterizes the heterogeneity of glia throughout the CNS and the significance of Ca²⁺ mediated communication and subsequent gliotransmission *in vivo*, will greatly illuminate how the nervous system develops, how neuronal circuits function, and how neurological disorders can be treated.

6.3 Purinergic modulation maintains homeostasis in the hypoxic ventilatory response

The hypoxic ventilatory response is biphasic, comprising an initial increase followed by a secondary depression. Chapter IV describes the important role ATP plays in shaping the secondary hypoxic ventilatory depression within the preBötC. For the first time, we have shown that the secondary hypoxic ventilatory depression is attenuated, in part, by the excitatory actions of ATP on P2Y₁R, specifically within the preBötC. We now know that while the actions of ATP within the preBötC contribute to this homeostatic reflex *in vivo*, ADO doesn't seem to have any role in the adult rat preBötC. These findings support previous

data also showing, via ATP sensors and application of the imperfect P2R antagonist PPADS, that the release of ATP in the ventrolateral medulla (VLM) attenuates the secondary hypoxic respiratory depression (Gourine et al., 2005). Given the limitations of this earlier study associated with the sensors and potential nonspecific actions of PPADS, manipulation of endogenous ATP signaling via viral injection of TMPAP into the preBötC represents an important advance. These data, combined with previous data (Gourine et al 2005) strongly support a role for purinergic signaling in the hypoxic ventilatory responses. While this technique is a powerful tool for examining the role of endogenous ATP in specific regions of the brain, it also illustrates the importance of considering purinergic signaling in the larger context of a three-part signaling system, as it is the actions of ATP in combination with its rate of breakdown, and the actions of the breakdown products that shape the dynamics of the hypoxic ventilatory response. By increasing TMPAP expression, and presumably the rate of ATP degradation, I have shown that the rate of ATP breakdown helps determine the duration of the P2Y₁R excitatory response and consequently the degree to which ATP offsets the secondary hypoxic depression. As identified in Chapter II, in addition to receptor expression, the key factor in establishing the dynamics of the interaction between P2 and P1 receptor signaling is the level and type of ectonucleotidase activity expressed within the preBötC. In turn, the breakdown of ATP will increase extracellular ADO. In adult rats *in vivo* ADO doesn't have any effect on the preBötC. However, ADO may be a factor in shaping response kinetics in the newborn rat and newborn and adult mouse where ADO is inhibitory within the preBötC.

Our findings within the central inspiratory network are important and relevant to purinergic modulation in other regions of the CNS. The selective P2R antagonists available limit current understanding of purinergic signaling in the brain, and advancements in these pharmacological tools will be an asset to advancement of the field. P2R-mediated signaling occurs at all levels of CNS organization (Burnstock, 2007) and is involved in both neuron-neuron, neuron-glia and glia-glia signaling (Abbracchio et al., 2009). A role for ATP in CNS

control of autonomic function has now been established and our findings, along with others, suggest that neuron-glia interactions are important in this modulation (Tsuda et al., 2000; James and Butt, 2002; Gourine et al., 2010). Given these recent findings in the respiratory network it is important that research examining the purinergic system within other areas of the CNS consider the how the balance between agonists (ATP and ADP vs ADO) established by diverse ectonucleotidases along with heterogeneous P2 and P1 receptor expression patterns interact to influence excitability and network function.

It now appears that the hypoxic ventilatory depression is countered by a central delayed response linked to ATP release and its action on the central inspiratory network (Gourine et al., 2005). Given this, combined with my findings in Chapter II that glia contribute to the purinergic modulation of inspiratory rhythm generating networks (Huxtable et al., 2010), it seems reasonable to hypothesize that glia contribute to the ATP modulation of the secondary hypoxic ventilatory depression. While our study in Chapter IV has further established the importance of ATP within the preBötC *in vivo* in this response, available transgenic tools did not allow me to discern whether these effects were mediated by neurons or glia. The use of novel viral vectors with a promoter specific to glia will help elucidate the precise cell types involved in this homeostatic response. Most important will be the development of methods to inhibit glial function. However, at present there is insufficient information on how glia influence network function to specifically interfere with their activity. Given the lack of understanding surrounding the role of glia cells in functioning neural networks *in vivo* discussed previously, the demonstration of glia producing gliotransmitters that modulate the hypoxic ventilatory response *in vivo* would be a significant advance.

Direct evidence that glia and gliotransmission play an active role in complex behaviors is limited. In the context of breathing, glia on the ventral surface of the medulla at the level of the RTN appear to act as CO₂ chemosensors that contribute to central CO₂ respiratory sensitivity (Gourine, 2005; Gourine et al., 2010). Two discrete transduction

mechanisms have been proposed. In the first, a fall in pH evokes an increase in intracellular Ca^{2+} , which evokes exocytotic release of astrocytic ATP (Gourine, 2005; Gourine et al., 2010), activating P2YRs on Phox2B chemosensitive neurons (Mulkey et al., 2006). The resultant membrane depolarization increases Phox2B neuron output which increases excitatory drive to the preBötC and increases ventilatory output (Bochorishvili et al., 2012). Selective activation of channel rhodopsin-2-expressing astrocytes in the RTN has confirmed parts of this hypothesis; photoactivated astrocytes release ATP via a Ca^{2+} -dependent, exocytotic mechanism, excite Phox2B neurons and increase respiratory output (Gourine et al., 2010). In the second mechanism of ATP release, CO_2 sensitive connexin-26 hemichannels expressed in the membrane of ventral surface astrocytes, again at the RTN, open in response to elevated CO_2 releasing ATP which again is proposed to activate chemosensitive RTN neurons (Huckstepp et al., 2010a; Huckstepp et al., 2010b). These data, combined with evidence presented in this thesis that glia and ATP signaling participate in the hypoxic ventilatory response, strongly suggest that glia and purinergic signaling are important in the homeostatic control of breathing.

Several key questions remain in understanding glia in the context of chemoreception. The acid sensing mechanism by which ventral surface astrocytes detect changes in pH occurs through a Ca^{2+} dependent exocytosis mechanism (Gourine et al., 2010). The application of a similar technique within the hypoxia sensitive region of the brainstem, would help determine if glia are involved in the ATP-mediated attenuation of the hypoxic ventilatory depression as hypothesized (Huxtable et al., 2010). However, the hypoxia sensitive regions are between 400 and 800 μm from the surface of the brainstem, which provides some practical challenges that need to be overcome for optogenetic stimulation.

Our research has identified an important role for the three-part purinergic signaling system in modulating the homeostatic hypoxic ventilatory response of the central inspiratory network. Future research will need to consider the differences in this modulatory system

across different species. Ultimately, these species differences emphasize that manipulation of ATP signaling in humans to treat CNS disorders of breathing requires that each component of the three-part system be explored further in higher mammals, including primates and humans. Although recent years have brought tremendous progress in characterization of the preBötC in experimental animals, the identification of the preBötC has remained elusive in the human brain until recently. Functional and structural magnetic resonance imaging techniques, optimized for the human brainstem, identified respiratory activity in response to CO₂ stimuli in the dorsal rostral pons (representing the Kölliker-Fuse/parabrachial (KF/PB) nuclei and locus coeruleus), the inferior ventral pons and the dorsal and lateral medulla (Pattinson et al., 2009). The authors suggest that these areas of activation in the human correspond to respiratory nuclei identified in rodent studies. Anatomical analogies between experimental animals and the human preBötC are difficult due to both the enlargement of the human inferior olive and subsequent rearrangement of other areas within the ventrolateral medulla as well as the strong interconnectivity in the reticular formation which makes the histological localization of respiratory nuclei difficult (Schwarzacher et al., 2011). However, in 2011, Schwarzacher *et al.* identified the human preBötC using three complementary approaches including: (i) comparison of distinct cytoarchitectonic characteristics (Schwarzacher et al., 1995; Ruangkittisakul et al., 2006) of neighbouring nuclei and fiber tracts within the medulla oblongata between experimental mammals and humans; (ii) immunocytochemical staining of pre-Bötzinger complex neurons in human brain sections based on data from laboratory animals (Gray et al., 1999; Stornetta et al., 2003); and (iii) systematic comparison between brainstems of normal human individuals and of patients suffering from neurodegenerative diseases associated with the occurrence of breathing deficits (Schwarzacher et al., 2011). This is the first study to localize the human preBötC in the ventrolateral area of the medulla at the rostrocaudal level of +9mm from obex. The anatomical coordinates and properties of the human preBötC reported in this study open the possibility for pathological investigation of central respiratory neurological diseases affecting

the preBötC. Insights gained from animal models can now be compared to specific human neuropathology, which will ultimately result in advancements in scientific and clinical understanding of human central inspiratory networks.

The data in chapters III and IV suggest that there may be significant therapeutic potential in developing methods that alter the ATP-ADO balance to favor the excitatory actions of ATP over the inhibitory actions of ADO. Our findings suggest that strategies to enhance or extend P2Y₁R signaling actions in the preBötC would help offset the secondary hypoxic ventilatory depression. Enhancing endogenous ATP release, potentiating ATP actions, minimizing ATP breakdown or inhibiting the actions of ADO could achieve this. Given the influence of purinergic modulation on preBötC network activity, a better understanding of purinergic modulation in the human preBötC is needed. With the identification of the human preBötC, insights gained in animal models that are amenable to experimental manipulations can now be compared with specific human neuropathology. ADO is implicated in the hypoxic ventilatory depression of ventilation of piglets (Yan et al., 1995) and apnea of prematurity(Bhatt-Mehta and Schumacher, 2003; Martin et al., 2004; Schmidt, 2005; Schmidt et al., 2006). Given the proposed role for endogenously released ATP in counteracting the secondary depression of the hypoxic ventilatory response and ADO in producing this depression, it is possible that postnatal changes in the effects of ATP, its breakdown products, or ectonucleotidase activity contribute to the developmental decrease in the magnitude of the secondary hypoxic ventilatory depression. Greater sensitivity of fetal preparations to ADO (Herlenius et al., 2002) is hypothesized to be a factor in the greater sensitivity of premature mammals hypoxic ventilatory depression. This also has implications for apnea of prematurity as a premature, ADO-sensitive respiratory network is thought to contribute to respiratory instability in premature babies (Barrington and Finer, 1991). We know that the ability for ATP to modulate respiratory rhythm is constant between E19 and P0-P4 in rat (Huxtable et al., 2009; Zwicker et al., 2011) but not postnatal mouse (Zwicker

et al., 2011). An endogenous adenosinergic inhibitory tone in the rVRG/preBötC has been reported in fetal but not postnatal rat preparations (Huxtable et al., 2009; Zwicker et al., 2011) suggesting that the inhibitory action of ATP metabolites is strongest in fetal stages (Herlenius et al., 2002; Huxtable et al., 2009). However, the inhibitory actions of ADO in the preBötC network of postnatal mice (Zwicker et al., 2011) emphasize that preBötC network sensitivity to ADO varies both between species and with development. Ultimately a better understanding of ADO sensitivity in preBötC of premature infants is needed. Additionally, understanding the significance of ectonucleotidase diversity for ATP signaling in respiratory networks and brain function is essential for the development of better therapeutic strategies. We know that developmentally, the ability of preBötC tissue to produce phosphate from ATP (reflecting increased enzyme activity or a shift to isoforms that generate more phosphate per ATP) increases between E17 and P0–P4 in rats (Huxtable et al., 2009). Ectonucleotidase isoform expression also differs between postnatal rats and mice further highlighting the need to understand the developmental and regional distribution of ectonucleotidases in premature human infants. The current treatment for apnea of prematurity is administration of the A1 and A2A ADORs antagonist caffeine (Hascoet et al., 2000; Bhatt-Mehta and Schumacher, 2003; Schmidt, 2005; Schmidt et al., 2006). However ~ 20% of premature infants do not respond to caffeine and there are ongoing concerns surrounding the negative side effects perinatal caffeine treatment may have on CNS development of neural networks controlling sleep and respiratory control (Schmidt et al., 2007; Montandon et al., 2008; Schmidt et al., 2012). Consequently there is a great need for a better understanding of the three-part, purinergic signaling mechanism in the context of human development.

6.4 Conclusions

Purinergic modulation has an important role in the rhythmic bursting central inspiratory network, providing dynamic adaptability important for the maintenance of homeostasis under a variety of environmental and developmental conditions. This thesis identifies the purinergic system as a three-part modulator of preBötC network activity that involves stimulation by ATP, rapid breakdown by ectonucleotidases and the inhibitory actions of ADO. The balance of this system helps determine the excitability of central inspiratory network. Differential expression of receptors and ectonucleotidases between brain regions, between species and between different stages of development will determine the balance of the three-part purinergic modulation. While purinergic modulation of respiratory frequency was thought to primarily act neuronally, this thesis presents findings implicating glia in the purinergic modulation of the tripartite synapse. Furthermore, it extends data from *in vitro* preparations and helps establish a role for purinergic modulation *in vivo*.

Chemosensitive reflexes are a key integrative property of the central inspiratory network. This thesis identifies the important role purinergic modulation plays in the hypoxic ventilatory response in the preBötC and the maintenance of breathing homeostasis. It lays the foundation for future research involving the role of glia within the hypoxic ventilatory response and other physiological behaviors within the CNS. Unraveling the mechanisms of purinergic modulation is an ongoing challenge that will have great implications for understanding hypoxic ventilatory depression in the context of developing pharmacological therapies for conditions such as apnea of prematurity. It is also important that the balance of the entire three-part purinergic modulatory system is considered, as the delicate balance of this system will have implications in other regions of the CNS. Ultimately, gaining a better understanding of respiratory system modulation is critical for clinical advancements in central respiratory network dysfunction.

6.5 References

- Abbadie C, Bhangoo S, De Koninck Y, Malcangio M, Melik-Parsadaniantz S, White FA (2009) Chemokines and pain mechanisms. *Brain Res Rev* 60:125-134.
- Abbracchio MP, Burnstock G, Verkhratsky A, Zimmermann H (2009) Purinergic signalling in the nervous system: an overview. *Trends Neurosci* 32:19-29.
- Agulhon C, Fiacco TA, McCarthy KD (2010) Hippocampal short- and long-term plasticity are not modulated by astrocyte Ca²⁺ signaling. *Science* 327:1250-1254.
- Agulhon C, Sun MY, Murphy T, Myers T, Lauderdale K, Fiacco TA (2012) Calcium Signaling and Gliotransmission in Normal vs. Reactive Astrocytes. *Frontiers in pharmacology* 3:139.
- Agulhon C, Petracic J., McMullen, A.B., Sweger, E.J., Minton, S.K., Taves, S.R., Casper, K.B., Fiacco, T.A., McCarthy, K.D. (2008) What is the role of astrocyte calcium in neurophysiology? *Neuron* 59:932-946.
- Allen NJ, Barres BA (2005) Signaling between glia and neurons: focus on synaptic plasticity. *Curr Opin Neurobiol* 15:542-548.
- Araque A, Sanzgiri RP, Parpura V, Haydon PG (1999) Astrocyte-induced modulation of synaptic transmission. *Can J Physiol Pharmacol* 77:699-706.
- Araque A, Li N, Doyle RT, Haydon PG (2000) SNARE protein-dependent glutamate release from astrocytes. *J Neurosci* 20:666-673.
- Barres BA (2008) The mystery and magic of glia: a perspective on their roles in health and disease. *Neuron* 60:430-440.
- Barrington K, Finer N (1991) The natural history of the appearance of apnea of prematurity. *Pediatr Res* 29:372-375.

- Beck A, Nieden RZ, Schneider HP, Deitmer JW (2004) Calcium release from intracellular stores in rodent astrocytes and neurons *in situ*. *Cell Calcium* 35:47-58.
- Bezzi P, Volterra A (2001) A neuron-glia signalling network in the active brain. *Curr Opin Neurobiol* 11:387-394.
- Bezzi P, Gunderson V, Galbete JL, Seifert G, Steinhauser C, Pilati E, Volterra A (2004) Astrocytes contain a vesicular compartment that is competent for regulated exocytosis of glutamate. *Nat Neurosci* 7:613-620.
- Bhatt-Mehta V, Schumacher RE (2003) Treatment of apnea of prematurity. *Paediatr Drugs* 5:195-210.
- Bochorishvili G, Stornetta RL, Coates MB, Guyenet PG (2012) Pre-Botzinger complex receives glutamatergic innervation from galaninergic and other retrotrapezoid nucleus neurons. *J Comp Neurol* 520:1047-1061.
- Burnstock G (2007) Physiology and pathophysiology of purinergic neurotransmission. *Physiol Rev* 87:659-797.
- Butt AM (2011) ATP: a ubiquitous gliotransmitter integrating neuron-glia networks. *Seminars in cell & developmental biology* 22:205-213.
- Butt AM, Pugh M, Hubbard P, James G (2004) Functions of optic nerve glia: axoglial signalling in physiology and pathology. *Eye (Lond)* 18:1110-1121.
- Cahoy JD, Emery B, Kaushal A, Foo LC, Zamanian JL, Christopherson KS, Xing Y, Lubischer JL, Krieg PA, Krupenko SA, Thompson WJ, Barres BA (2008) A transcriptome database for astrocytes, neurons, and oligodendrocytes: a new resource for understanding brain development and function. *J Neurosci* 28:264-278.

- Charles AC, Merrill JE, Dirksen ER, Sanderson MJ (1991) Intercellular signaling in glial cells: calcium waves and oscillations in response to mechanical stimulation and glutamate. *Neuron* 6:983-992.
- Coco S, Calegari F, Pravettoni E, Pozzi D, Taverna E, Rosa P, Matteoli M, Verderio C (2003) Storage and release of ATP from astrocytes in culture. *J Biol Chem* 278:1354-1362.
- Cornell-Bell AH, Finkbeiner SM, Cooper MS, Smith SJ (1990) Glutamate induces calcium waves in cultured astrocytes: long-range glial signaling. *Science* 247:470-473.
- Dani JW, Chernjavsky A, Smith SJ (1992) Neuronal activity triggers calcium waves in hippocampal astrocyte networks. *Neuron* 8:429-440.
- Deitmer JW, Verkhratsky AJ, Lohr C (1998) Calcium signalling in glial cells. *Cell Calcium* 24:405-416.
- Di Filippo M, Sarchielli P, Picconi B, Calabresi P (2008) Neuroinflammation and synaptic plasticity: theoretical basis for a novel, immune-centred, therapeutic approach to neurological disorders. *Trends Pharmacol Sci* 29:402-412.
- Duan S, Anderson CM, Keung EC, Chen Y, Swanson RA (2003) P2X7 receptor-mediated release of excitatory amino acids from astrocytes. *J Neurosci* 23:1320-1328.
- Fiacco TA, McCarthy KD (2006) Astrocyte calcium elevations: properties, propagation, and effects on brain signaling. *Glia* 54:676-690.
- Figueiredo M, Lane S, Tang F, Liu BH, Hewinson J, Marina N, Kasymov V, Souslova EA, Chudakov DM, Gourine AV, Teschemacher AG, Kasparov S (2011) Optogenetic experimentation on astrocytes. *Exp Physiol* 96:40-50.
- Finkbeiner S (1992) Calcium waves in astrocytes-filling in the gaps. *Neuron* 8:1101-1108.

- Fumagalli M, Brambilla R, D'Ambrosi N, Volonte C, Matteoli M, Verderio C, Abbracchio MP (2003) Nucleotide-mediated calcium signaling in rat cortical astrocytes: Role of P2X and P2Y receptors. *Glia* 43:218-203.
- Funk GD, Smith JC, Feldman JL (1993) Generation and transmission of respiratory oscillations in medullary slices: role of excitatory amino acids. *J Neurophysiol* 70:1497-1515.
- Gourine AV (2005) On the peripheral and central chemoreception and control of breathing: an emerging role of ATP. *J Physiol* 568:715-724.
- Gourine AV, Llaudet E, Dale N, Spyer KM (2005) Release of ATP in the ventral medulla during hypoxia in rats: role in hypoxic ventilatory response. *J Neurosci* 25:1211-1218.
- Gourine AV, Kasymov V, Marina N, Tang F, Figueiredo MF, Lane S, Teschemacher AG, Spyer KM, Deisseroth K, Kasparov S (2010) Astrocytes control breathing through pH-dependent release of ATP. *Science* 329:571-575.
- Grass D, Pawlowski PG, Hirrlinger J, Papadopoulos N, Richter DW, Kirchhoff F, Hulsmann S (2004) Diversity of functional astroglial properties in the respiratory network. *J Neurosci* 24:1358-1365.
- Gray PA, Rekling JC, Bocchiaro CM, Feldman JL (1999) Modulation of respiratory frequency by peptidergic input to rhythmogenic neurons in the preBotzinger complex. *Science* 286:1566-1568.
- Greer JJ, Smith JC, Feldman JL (1991) Role of excitatory amino acids in the generation and transmission of respiratory drive in neonatal rat. *J Physiol* 437:727-749.

- Gresham K, Boyer B, Mayer C, Foglyano R, Martin R, Wilson CG (2011) Airway inflammation and central respiratory control: results from in vivo and in vitro neonatal rat. *Respir Physiol Neurobiol* 178:414-421.
- Guthrie PB, Knappenberger J, Segal M, Bennett MV, Charles AC, Kater SB (1999) ATP released from astrocytes mediates glial calcium waves. *J Neurosci* 19:520-528.
- Halassa MM, Haydon PG (2010) Integrated brain circuits: astrocytic networks modulate neuronal activity and behavior. *Annu Rev Physiol* 72:335-355.
- Halassa MM, Fellin T, Haydon PG (2007) The tripartite synapse: roles for gliotransmission in health and disease. *Trends in molecular medicine* 13:54-63.
- Halassa MM, Florian C, Fellin T, Munoz JR, Lee SY, Abel T, Haydon PG, Frank MG (2009) Astrocytic modulation of sleep homeostasis and cognitive consequences of sleep loss. *Neuron* 61:213-219.
- Hamilton NB, Attwell D (2010) Do astrocytes really exocytose neurotransmitters? *Nat Rev Neurosci* 11:227-238.
- Hascoet JM, Hamon I, Boutroy MJ (2000) Risks and benefits of therapies for apnoea in premature infants. *Drug Saf* 23:363-379.
- Haydon PG, Carmignoto G (2006) Astrocyte control of synaptic transmission and neurovascular coupling. *Physiol Rev* 86:1009-1031.
- Henneberger C, Papouin T, Oliet SH, Rusakov DA (2010) Long-term potentiation depends on release of D-serine from astrocytes. *Nature* 463:232-236.
- Herlenius E, Aden U, Tang LQ, Lagercrantz H (2002) Perinatal respiratory control and its modulation by adenosine and caffeine in the rat. *Pediatr Res* 51:4-12.

Huckstepp RT, Eason R, Sachdev A, Dale N (2010a) CO₂-dependent opening of connexin 26 and related beta connexins. *J Physiol* 588:3921-3931.

Huckstepp RT, id Bihi R, Eason R, Spyer KM, Dicke N, Willecke K, Marina N, Gourine AV, Dale N (2010b) Connexin hemichannel-mediated CO₂-dependent release of ATP in the medulla oblongata contributes to central respiratory chemosensitivity. *J Physiol* 588:3901-3920.

Huxtable AG, Zwicker JD, Poon BY, Pagliardini S, Vrouwe SQ, Greer JJ, Funk GD (2009) Tripartite purinergic modulation of central respiratory networks during perinatal development: the influence of ATP, ectonucleotidases, and ATP metabolites. *J Neurosci* 29:14713-14725.

Huxtable AG, Vinit S, Windelborn JA, Crader SM, Guenther CH, Watters JJ, Mitchell GS (2011) Systemic inflammation impairs respiratory chemoreflexes and plasticity. *Respir Physiol Neurobiol* 178:482-489.

Huxtable AG, Zwicker JD, Alvares TS, Ruangkittisakul A, Fang X, Hahn LB, Posse de Chaves E, Baker GB, Ballanyi K, Funk GD (2010) Glia contribute to the purinergic modulation of inspiratory rhythm-generating networks. *J Neurosci* 30:3947-3958.

James G, Butt AM (2002) P2Y and P2X purinoceptor mediated Ca²⁺ signalling in glial cell pathology in the central nervous system. *Eur J Pharmacol* 447:247-260.

Kang J, Jiang L, Goldman SA, Nedergaard M (1998) Astrocyte-mediated potentiation of inhibitory synaptic transmission. *Nat Neurosci* 1:683-692.

Kimelberg HK, Goderie SK, Higman S, Pang S, Waniewski RA (1990) Swelling-induced release of glutamate, aspartate, and taurine from astrocyte cultures. *J Neurosci* 10:1583-1591.

- Kirchhoff F (2010) Neuroscience. Questionable calcium. *Science* 327:1212-1213.
- Koles L, Leichsenring A, Rubini P, Illes P (2011) P2 receptor signaling in neurons and glial cells of the central nervous system. *Adv Pharmacol* 61:441-493.
- Lehnardt S (2010) Innate immunity and neuroinflammation in the CNS: the role of microglia in Toll-like receptor-mediated neuronal injury. *Glia* 58:253-263.
- Lorier AR, Huxtable AG, Robinson DM, Lipski J, Housley GD, Funk GD (2007) P2Y1 receptor modulation of the pre-Botzinger complex inspiratory rhythm generating network in vitro. *J Neurosci* 27:993-1005.
- Martin RJ, Abu-Shaweeesh JM, Baird TM (2004) Apnoea of prematurity. *Paediatric respiratory reviews* 5 Suppl A:S377-382.
- Montandon G, Kinkead R, Bairam A (2008) Adenosinergic modulation of respiratory activity: Developmental plasticity induced by perinatal caffeine administration. *Respir Physiol Neurobiol.*
- Mulkey DK, Wenker IC, Kreneisz O (2010) Current ideas on central chemoreception by neurons and glial cells in the retrotrapezoid nucleus. *J Appl Physiol* 108:1433-1439.
- Mulkey DK, Mistry AM, Guyenet PG, Bayliss DA (2006) Purinergic P2 receptors modulate excitability but do not mediate pH sensitivity of RTN respiratory chemoreceptors. *J Neurosci* 26:7230-7233.
- Nedergaard M (1994) Direct signaling from astrocytes to neurons in cultures of mammalian brain cells. *Science* 263:1768-1771.
- Nedergaard M, Rodriguez JJ, Verkhratsky A (2010) Glial calcium and diseases of the nervous system. *Cell Calcium* 47:140-149.

- Nishiyama A, Komitova M, Suzuki R, Zhu X (2009) Polydendrocytes (NG2 cells): multifunctional cells with lineage plasticity. *Nat Rev Neurosci* 10:9-22.
- Parpura V, Haydon PG (2000) Physiological astrocytic calcium levels stimulate glutamate release to modulate adjacent neurons. *Proc Natl Acad Sci U S A* 97:8629-8634.
- Parpura V, Basarsky TA, Liu F, Jeftinija K, Jeftinija S, Haydon PG (1994) Glutamate-mediated astrocyte-neuron signalling. *Nature* 369:744-747.
- Parri HR, Gould TM, Crunelli V (2001) Spontaneous astrocytic Ca²⁺ oscillations in situ drive NMDAR-mediated neuronal excitation. *Nat Neurosci* 4:803-812.
- Pascual O, Ben Achour S, Rostaing P, Triller A, Bessis A (2012) Microglia activation triggers astrocyte-mediated modulation of excitatory neurotransmission. *Proc Natl Acad Sci U S A* 109:E197-205.
- Pasti L, Zonta M, Pozzan T, Vicini S, Carmignoto G (2001) Cytosolic calcium oscillations in astrocytes may regulate exocytotic release of glutamate. *J Neurosci* 21:477-484.
- Pattinson KT, Mitsis GD, Harvey AK, Jbabdi S, Dirckx S, Mayhew SD, Rogers R, Tracey I, Wise RG (2009) Determination of the human brainstem respiratory control network and its cortical connections in vivo using functional and structural imaging. *Neuroimage* 44:295-305.
- Porter JT, McCarthy KD (1995) GFAP-positive hippocampal astrocytes in situ respond to glutamatergic neuroligands with increases in [Ca²⁺]i. *Glia* 13:101-112.
- Porter JT, McCarthy KD (1997) Astrocytic neurotransmitter receptors in situ and in vivo. *Prog Neurobiol* 51:439-455.
- Ruangkittisakul A, Schwarzacher SW, Secchia L, Poon BY, Ma Y, Funk GD, Ballanyi K (2006) High sensitivity to neuromodulator-activated signaling pathways at

- physiological [K+] of confocally imaged respiratory center neurons in on-line-calibrated newborn rat brainstem slices. *J Neurosci* 26:11870-11880.
- Rusakov DA, Zheng K, Henneberger C (2011) Astrocytes as regulators of synaptic function: a quest for the Ca²⁺ master key. *The Neuroscientist : a review journal bringing neurobiology, neurology and psychiatry* 17:513-523.
- Santello M, Cali C, Bezzi P (2012) Gliotransmission and the tripartite synapse. *Adv Exp Med Biol* 970:307-331.
- Scemes E, Giaume C (2006) Astrocyte calcium waves: what they are and what they do. *Glia* 54:716-725.
- Schmidt B (2005) Methylxanthine therapy for apnea of prematurity: evaluation of treatment benefits and risks at age 5 years in the international Caffeine for Apnea of Prematurity (CAP) trial. *Biology of the neonate* 88:208-213.
- Schmidt B, Roberts RS, Davis P, Doyle LW, Barrington KJ, Ohlsson A, Solimano A, Tin W (2006) Caffeine therapy for apnea of prematurity. *N Engl J Med* 354:2112-2121.
- Schmidt B, Roberts RS, Davis P, Doyle LW, Barrington KJ, Ohlsson A, Solimano A, Tin W (2007) Long-term effects of caffeine therapy for apnea of prematurity. *N Engl J Med* 357:1893-1902.
- Schmidt B, Anderson PJ, Doyle LW, Dewey D, Grunau RE, Asztalos EV, Davis PG, Tin W, Moddemann D, Solimano A, Ohlsson A, Barrington KJ, Roberts RS (2012) Survival without disability to age 5 years after neonatal caffeine therapy for apnea of prematurity. *JAMA* 307:275-282.
- Schwarzacher SW, Smith JC, Richter DW (1995) Pre-Botzinger complex in the cat. *J Neurophysiol* 73:1452-1461.

Schwarzacher SW, Rub U, Deller T (2011) Neuroanatomical characteristics of the human pre-Botzinger complex and its involvement in neurodegenerative brainstem diseases. *Brain* 134:24-35.

Stornetta RL, Rosin DL, Wang H, Sevigny CP, Weston MC, Guyenet PG (2003) A group of glutamatergic interneurons expressing high levels of both neurokinin-1 receptors and somatostatin identifies the region of the pre-Botzinger complex. *J Comp Neurol* 455:499-512.

Suadicani SO, Brosnan CF, Scemes E (2006) P2X7 receptors mediate ATP release and amplification of astrocytic intercellular Ca²⁺ signaling. *J Neurosci* 26:1378-1385.

Szatkowski M, Barbour B, Attwell D (1990) Non-vesicular release of glutamate from glial cells by reversed electrogenic glutamate uptake. *Nature* 348:443-446.

Tsuda M, Koizumi S, Kita A, Shigemoto Y, Ueno S, Inoue K (2000) Mechanical allodynia caused by intraplantar injection of P2X receptor agonist in rats: involvement of heteromeric P2X2/3 receptor signaling in capsaicin-insensitive primary afferent neurons. *J Neurosci* 20:RC90.

Verkhratsky A, Steinhauser C (2000) Ion channels in glial cells. *Brain Res Brain Res Rev* 32:380-412.

Verkhratsky A, Krishtal OA, Burnstock G (2009) Purinoceptors on neuroglia. *Mol Neurobiol* 39:190-208.

Volterra A, Meldolesi J (2005) Astrocytes, from brain glue to communication elements: the revolution continues. *Nat Rev Neurosci* 6:626-640.

Watkins LR, Hutchinson MR, Milligan ED, Maier SF (2007) "Listening" and "talking" to neurons: implications of immune activation for pain control and increasing the efficacy of opioids. *Brain Res Rev* 56:148-169.

Watkins LR, Hutchinson MR, Rice KC, Maier SF (2009) The "toll" of opioid-induced glial activation: improving the clinical efficacy of opioids by targeting glia. *Trends Pharmacol Sci* 30:581-591.

Wilhelm A, Volknandt W, Langer D, Nolte C, Kettenmann H, Zimmermann H (2004) Localization of SNARE proteins and secretory organelle proteins in astrocytes in vitro and in situ. *Neurosci Res* 48:249-257.

Yan S, Laferriere A, Zhang C, Moss IR (1995) Microdialyzed adenosine in nucleus tractus solitarius and ventilatory response to hypoxia in piglets. *J Appl Physiol* 79:405-410.

Ye ZC, Wyeth MS, Baltan-Tekkok S, Ransom BR (2003) Functional hemichannels in astrocytes: a novel mechanism of glutamate release. *J Neurosci* 23:3588-3596.

Zhang Y, Barres BA (2010) Astrocyte heterogeneity: an underappreciated topic in neurobiology. *Curr Opin Neurobiol* 20:588-594.

Zorec R, Araque A, Carmignoto G, Haydon PG, Verkhratsky A, Parpura V (2012) Astroglial excitability and gliotransmission: an appraisal of Ca²⁺ as a signalling route. *ASN neuro* 4.

Zwicker JD, Rajani V, Hahn LB, Funk GD (2011) Purinergic modulation of preBotzinger complex inspiratory rhythm in rodents: the interaction between ATP and adenosine. *J Physiol* 589:4583-4600.